INTRODUCTION TO BIOPHOTONICS

INTRODUCTION TO BIOPHOTONICS

Paras N. Prasad

WILEY-INTERSCIENCE

A JOHN WILEY & SONS, INC., PUBLICATION

Published by John Wiley & Sons, Inc., Hoboken, New Jersey.
Published simultaneously in Canada.

Library of Congress Cataloging-in-Publication Data:

Prasad, Paras N.
Introduction to biophotonics / Paras N. Prasad.
p. cm.
ISBN 0-471-28770-9 (cloth)
1. Photobiology. 2. Photonics. 3. Biosensors. 4. Nanotechnology. I. Title.
QH515.P73 2003
571.4′55—dc21

2003000578

Printed in the United States of America

10 9 8 7 6 5 4 3 2 1

SUMMARY OF CONTENTS

1. Introduction
2. Fundamentals of Light and Matter
3. Basics of Biology
4. Fundamentals of Light-Matter Interactions
5. Principles of Lasers, Current Laser Technology and Nonlinear Optics
6. Photobiology
7. Bioimaging: Principles and Techniques
8. Bioimaging: Applications
9. Optical Biosensors
10. Microarray Technology for Genomics and Proteomics
11. Flow Cytometry
12. Light-Activated Therapy: Photodynamic Therapy
13. Tissue Engineering with Light
14. Laser Tweezers and Laser Scissors
15. Nanotechnology for Biophotonics: Bionanophotonics
16. Biomaterials for Photonics

CONTENTS

Preface xv

Acknowlegments xvii

1. Introduction 1

1.1 Biophotonics—A New Frontier 1
1.2 An Invitation to Multidisciplinary Education, Training, and Research 2
1.3 Opportunities for Both Basic Research and Biotechnology Development 4
1.4 Scope of this Book 5

2. Fundamentals of Light and Matter 11

2.1 Nature of Light 12
2.1.1 Dual Character of Light 12
2.1.2 Propagation of Light as Waves 14
2.1.3 Coherence of Light 17
2.1.4 Light as Photon Particles 19
2.1.5 Optical Activity and Birefringence 20
2.1.6 Different Light Sources 21
2.2 Quantized States of Matter 21
2.2.1 Introductory Concepts 21
2.2.2 Quantized States of Atoms 24
2.2.3 Quantized States of Molecules: Partitioning of Molecular Energies 27
2.2.4 Electronic States of a Molecule 29
2.2.5 Bonding in Organic Molecules 35
2.2.6 Conjugated Organic Molecules 37
2.2.7 Vibrational States of a Molecule 39
2.3 Intermolecular Effects 41
2.4 Three-Dimensional Structures and Stereoisomers 43
Highlights of the Chapter 46
References 48

3. Basics of Biology **50**

3.1 Introductory Concepts 51
3.2 Cellular Structure 52
3.3 Various Types of Cells 58
3.4 Chemical Building Blocks 60
3.5 Interactions Determining Three-Dimensional Structures of Biopolymers 68
3.6 Other Important Cellular Components 72
3.7 Cellular Processes 73
3.8 Protein Classification and Function 82
3.9 Organization of Cells into Tissues 85
3.10 Types of Tissues and Their Functions 87
3.11 Tumors and Cancers 88
Highlights of the Chapter 89
References 91

4. Fundamentals of Light-Matter Interactions **92**

4.1 Interactions Between Light and a Molecule 93
4.1.1. Nature of Interactions 93
4.1.2. Einstein's Model of Absorption and Emission 95
4.2 Interaction of Light with a Bulk Matter 97
4.3 Fate of Excited State 99
4.4 Various Types of Spectroscopy 102
4.5 Electronic Absorption Spectroscopy 105
4.6 Electronic Luminescence Spectroscopy 109
4.7 Vibrational Spectroscopy 113
4.8 Spectroscopy Utilizing Optical Activity of Chiral Media 117
4.9 Fluorescence Correlation Spectroscopy (FCS) 122
Highlights of the Chapter 124
References 127

5. Principles of Lasers, Current Laser Technology, and Nonlinear Optics **129**

5.1 Principles of Lasers 130
5.1.1 Lasers: A New Light Source 130
5.1.2 Principles of Laser Action 131
5.1.3 Classification of Lasers 135
5.1.4 Some Important Lasers for Biophotonics 139
5.2 Current Laser Technologies 139
5.3 Quantitative Description of Light: Radiometry 142
5.4 Nonlinear Optical Processes with Intense Laser Beam 143
5.4.1 Mechanism of Nonlinear Optical Processes 143

5.4.2 Frequency Conversion by a Second-Order Nonlinear Optical Process 145
5.4.3 Symmetry Requirement for a Second-Order Process 146
5.4.4 Frequency Conversion by a Third-Order Nonlinear Optical Process 148
5.4.5 Multiphoton Absorption 149
5.5 Time-Resolved Studies 152
5.6 Laser Safety 154
Highlights of the Chapter 156
References 157

6. Photobiology 159

6.1 Photobiology—At the Core of Biophotonics 160
6.2 Interaction of Light with Cells 160
6.2.1 Light Absorption in Cells 161
6.2.2 Light-Induced Cellular Processes 163
6.2.3 Photochemistry Induced by Exogenous Photosensitizers 167
6.3 Interaction of Light with Tissues 168
6.4 Photoprocesses in Biopolymers 175
6.4.1 The Human Eye and Vision 176
6.4.2 Photosynthesis 181
6.5 *In Vivo* Photoexcitation 186
6.5.1 Free-Space Propagation 186
6.5.2 Optical Fiber Delivery System 187
6.5.3 Articulated Arm Delivery 189
6.5.4 Hollow Tube Waveguides 190
6.6 *In Vivo* Spectroscopy 190
6.7 Optical Biopsy 191
6.8 Single-Molecule Detection 195
Highlights of the Chapter 197
References 199

7. Bioimaging: Principles and Techniques 203

7.1 Bioimaging: An Important Biomedical Tool 205
7.2 An Overview of Optical Imaging 206
7.3 Transmission Microscopy 209
7.3.1 Simple Microscope 209
7.3.2 Compound Microscope 210
7.3.3 Kohler Illumination 212
7.3.4 Numerical Aperture and Resolution 214

7.3.5 Optical Aberrations and Different Types of Objectives 215
7.3.6 Phase Contrast Microscopy 216
7.3.7 Dark-Field Microscopy 216
7.3.8 Differential Interference Contrast Microscopy (DIC) 217
7.4 Fluorescence Microscopy 219
7.5 Scanning Microscopy 220
7.6 Inverted and Upright Microscopes 221
7.7 Confocal Microscopy 221
7.8 Multiphoton Microscopy 223
7.9 Optical Coherence Tomography 225
7.10 Total Internal Reflection Fluorescence Microscopy 228
7.11 Near-Field Optical Microscopy 232
7.12 Spectral and Time-Resolved Imaging 234
7.12.1 Spectral Imaging 235
7.12.2 Bandpass Filters 235
7.12.3 Excitation Wavelength Selection 236
7.12.4 Acousto-Optic Tunable Filters 236
7.12.5 Localized Spectroscopy 237
7.13 Fluorescence Resonance Energy Transfer (FRET) Imaging 237
7.14 Fluorescence Lifetime Imaging Microscopy (FLIM) 238
7.15 Nonlinear Optical Imaging 240
7.15.1 Second-Harmonic Microscopy 241
7.15.2 Third-Harmonic Microscopy 243
7.15.3 Coherent Anti-Stokes Raman Scattering (CARS) Microscopy 243
7.16 Future Directions of Optical Bioimaging 245
7.16.1 Multifunctional Imaging 245
7.16.2 4Pi Imaging 245
7.16.3 Combination Microscopes 246
7.16.4 Miniaturized Microscopes 246
7.17 Some Commercial Sources of Imaging Instruments 246
Highlights of the Chapter 246
References 249

8. Bioimaging: Applications 255

8.1 Fluorophores as Bioimaging Probes 256
8.1.1 Endogenous Fluorophores 256
8.1.2 Exogenous Fluorophores 257
8.1.3 Organometallic Complex Fluorophores 264
8.1.4 Near-IR and IR Fluorophore 265

8.1.5 Two-Photon Fluorophores 265
8.1.6 Inorganic Nanoparticles 269
8.2 Green Fluorescent Protein 269
8.3 Imaging of Organelles 271
8.4 Imaging of Microbes 273
8.4.1 Confocal Microscopy 273
8.4.2 Near-Field Imaging 274
8.5 Cellular Imaging 276
8.5.1 Probing Cellular Ionic Environment 276
8.5.2 Intracellular pH Measurements 277
8.5.3 Optical Tracking of Drug-Cell Interactions 279
8.5.4 Imaging of Nucleic Acids 281
8.5.5 Cellular Interactions Probed by FRET/FLIM Imaging 287
8.6 Tissue Imaging 289
8.7 *In Vivo* Imaging 294
8.8 Future Directions 301
8.9 Commercially Available Optical Imaging Accessories 303
Highlights of the Chapter 303
References 306

9. Optical Biosensors 311

9.1 Biosensors: An Introduction 312
9.2 Principles of Optical Biosensing 314
9.2.1 Biorecognition 314
9.2.2 Optical Transduction 316
9.2.3 Fluorescence Sensing 317
9.2.4 Fluorescence Energy Transfer Sensors 317
9.2.5 Molecular Beacons 320
9.2.6 Optical Geometries of Biosensing 321
9.3 Support for and Immobilization of Biorecognition Elements 323
9.3.1 Immobilization 323
9.4 Fiber-Optic Biosensors 327
9.5 Planar Waveguide Biosensors 331
9.6 Evanescent Wave Biosensors 334
9.7 Interferometric Biosensors 338
9.8 Surface Plasmon Resonance Biosensors 339
9.9 Some Recent Novel Sensing Methods 343
9.10 Future Directions 347
9.11 Commercially Available Biosensors 349
Highlights of the Chapter 349
References 352

10. Microarray Technology for Genomics and Proteomics **357**

10.1 Microarrays, Tools for Rapid Multiplex Analysis 358
10.2 DNA Microarray Technology 363
10.2.1 Spotted Arrays 363
10.2.2 Oligonucleotide Arrays 366
10.2.3 Other Microarray Technologies 367
10.3 Protein Microarray Technology 368
10.4 Cell Microarray Technology 375
10.5 Tissue Microarray Technology 379
10.6 Some Examples of Application of Microarrays 379
10.7 Future Directions 382
10.8 Companies Producing Microarrays 383
Highlights of the Chapter 384
References 386

11. Flow Cytometry **390**

11.1 A Clinical, Biodetection, and Research Tool 391
11.2 Basics of Flow Cytometry 394
11.2.1 Basic Steps 394
11.2.2 The Components of a Flow Cytometer 395
11.2.3 Optical Response 403
11.3 Fluorochromes for Flow Cytometry 405
11.4 Data Manipulation and Presentation 408
11.5 Selected Examples of Applications 415
11.5.1 Immunophenotyping 415
11.5.2 DNA Analysis 418
11.6 Future Directions 423
11.7 Commercial Flow Cytometry 426
Highlights of the Chapter 426
References 430

12. Light-Activated Therapy: Photodynamic Therapy **433**

12.1 Photodynamic Therapy: Basic Principles 434
12.2 Photosensitizers for Photodynamic Therapy 437
12.2.1 Porphyrin Derivatives 438
12.2.2 Chlorins and Bacteriochlorins 440
12.2.3 Benzoporphyrin Derivatives 441
12.2.4 5-Aminolaevulinic Acid (ALA) 442
12.2.5 Texaphyrins 443
12.2.6 Phthalocyanines and Naphthalocyanines 443
12.2.7 Cationic Photosensitizers 445
12.2.8 Dendritic Photosensitizers 445

12.3 Applications of Photodynamic Therapy 447
12.4 Mechanism of Photodynamic Action 450
12.5 Light Irradiation for Photodynamic Therapy 453
12.5.1 Light Source 453
12.5.2 Laser Dosimetry 454
12.5.3 Light Delivery 455
12.6 Two-Photon Photodynamic Therapy 455
12.7 Current Research and Future Directions 457
Highlights of the Chapter 460
References 461

13. Tissue Engineering with Light 464

13.1 Tissue Engineering and Light Activation 465
13.2 Laser Tissue Contouring and Restructuring 467
13.3 Laser Tissue Welding 472
13.4 Laser Tissue Regeneration 475
13.5 Femtolaser Surgery 476
13.6 Future Directions 478
Highlights of the Chapter 479
References 480

14. Laser Tweezers and Laser Scissors 482

14.1 New Biological Tools for Micromanipulation by Light 483
14.2 Principle of Laser Tweezer Action 487
14.3 Design of a Laser Tweezer 490
14.4 Optical Trapping Using Non-Gaussian Beams 495
14.5 Dynamic Holographic Optical Tweezers 496
14.6 Laser Scissors 499
14.6.1 Laser Pressure Catapulting (LPC) 500
14.6.2 Laser Capture Microdissection (LCM) 502
14.7 Selected Examples of Applications 502
14.7.1 Manipulation of Single DNA Molecules 502
14.7.2 Molecular Motors 506
14.7.3 Protein–Protein Interactions 507
14.7.4 Laser Microbeams for Genomics and Proteomics 509
14.7.5 Laser Manipulation in Plant Biology 510
14.7.6 Laser Micromanipulation for Reproduction Medicine 511
14.8 Future Directions 512
14.8.1 Technology of Laser Manipulation 513
14.8.2 Single Molecule Biofunctions 513
14.9 Commercially Available Laser Microtools 514

Highlights of the Chapter 514
References 516

15. Nanotechnology for Biophotonics: Bionanophotonics 520

15.1 The Interface of Bioscience, Nanotechnology, and Photonics 521
15.2 Nanochemistry 523
15.3 Semiconductor Quantum Dots for Bioimaging 528
15.4 Metallic Nanoparticles and Nanorods for Biosensing 532
15.5 Up-Converting Nanophores 532
15.6 PEBBLE Nanosensors for *In Vitro* Bioanalysis 536
15.7 Nanoclinics for Optical Diagnostics and Targeted Therapy 537
15.8 Future Directions 539
Highlights of the Chapter 541
References 543

16. Biomaterials for Photonics 545

16.1 Photonics and Biomaterials 545
16.2 Bioderived Materials 548
16.3 Bioinspired Materials 559
16.4 Biotemplates 560
16.5 Bacteria as Biosynthesizers for Photonic Polymers 564
16.6 Future Directions 567
Highlights of the Chapter 568
References 569

Index 573

Preface

Biophotonics deals with interactions between light and biological matter. It is an exciting frontier which involves a fusion of photonics and biology. It offers great hope for the early detection of diseases and for new modalities of light-guided and light-activated therapies. Also, biology is advancing photonics, since biomaterials are showing promise in the development of new photonic media for technological applications.

Biophotonics creates many opportunities for chemists, physicists, engineers, health professionals and biomedical researchers. Also, producing trained healthcare personnel and new generations of researchers in biophotonics is of the utmost importance to keep up with the increasing worldwide demands.

Although several books and journals exist that cover selective aspects of biophotonics, there is a void for a monograph that provides a unified synthesis of this subject. This book provides such an overview of biophotonics which is intended for multidisciplinary readership. The objective is to provide a basic knowledge of a broad range of topics so that individuals in all disciplines can rapidly acquire the minimal necessary background for research and development in biophotonics. The author intends that this book serve both as a textbook for education and training as well as a reference book that aids research and development of those areas integrating light, photonics and biological systems. Another aim of the book is to stimulate the interest of researchers and healthcare professionals and to foster collaboration through multidisciplinary programs.

This book encompasses the fundamentals and various applications involving the integration of light, photonics and biology into biophotonics. Each chapter begins with an introduction describing what a reader will find in that chapter. Each chapter ends with highlights which are basically the take home message and may serve as a review of the materials presented.

In each of the chapters, a description of future directions of research and development is also provided, as well as a brief discussion of the current status, identifying some of areas of future opportunities. A few of the existing commercial sources of instrumentation and supplies relevant to the content of many of the applications chapters (7 and higher) are listed in the respective chapters.

In order to author a book such as this, which covers a very broad range of topics, I received help from a large number of individuals at the Institute for

Lasers, Photonics and Biophotonics and from elsewhere. This help has consisted of gathering technical content, making illustrations, providing critiques and preparing the manuscript. A separate Acknowledgement recognizes these individuals.

Here I would like to acknowledge the individuals whose broad-based support has been of paramount value in completing the book. I wish to express my sincere gratitude to my wife, Nadia Shahram who has been a constant source of inspiration, providing support and encouragement for this project, in spite of her own very busy professional schedule. I am also indebted to our daughters, Melanie and Natasha, for showing their understanding by sacrificing their quality time with me.

I express my sincere appreciation to my colleague, Professor Stanley Bruckenstein, for his endless support and encouragement. I thank Dr. E.J. Bergey for his valuable general support and technical help in bio-related areas. Valuable help was provided by Dr. Haridas Pudavar and it is very much appreciated. I owe thanks to my administrative assistant, Ms. Margie Weber, for assuming responsibility for many of the non-critical administrative issues at the Institute. Finally, I thank Ms. Barbara Raff, whose clerical help in manuscript preparation was invaluable.

Paras N. Prasad
Buffalo, NY

ACKNOWLEDGMENTS

Technical Contents:

Dr. E. James Bergey, Dr. Ryszard Burzynski, Dr. Aliaksandr Kachynski, Dr. Andrey Kuzmin, Dr. Paul Markowicz, Dr. Tymish Ohulchanskyy, Dr. Haridas Pudavar, Dr. Marek Samoc, Professor Brenda Spangler, Professor Carlton Stewart

Technical Illustrations and References:

Professor J.M.J. Frechet, Mr. Christopher Friend, Dr. Jeffrey Kingsbury, Professor R. Kopelman, Dr. Tzu Chau Lin, Mr. Emmanuel Nishanth, Mr. Hanifi Tiryaki, Dr. Indrajit Roy, Dr. Kaushik RoyChoudhury, Dr. Yudhisthira Sahoo, Dr. Yuzchen Shen, Professor Hiro Suga, Dr. Richard Vaia, Dr. Jeffrey Winiarz, Mr. QingDong Zheng, Mr. Gen Xu

Chapter Critiques:

Professor Frank Bright, Professor Stanley Bruckenstein, Professor Allan Cadenhead, Mr. Martin Casstevens, Dr. Joseph Cusker, Professor Michael Detty, Professor Sarah Gaffen, Professor Margaret Hollingsworth, Dr. David James, Mr. William Kirkey, Dr. Joydeep Lahiri, Dr. Raymond Lanzafame, Professor Antonia Monteiro, Dr. Janet Morgan, Dr. Allan Oseroff, Dr. Ammasi Periasamy, Dr. Anthony Prezyna, Dr. David Rodman, Professor Malcolm Slaughter, Professor Joseph J. Tufariello, Professor Charles Spangler

Manuscript Preparation:

Cindy Hennessey, Michelle Murray, Kristen Pfaff, Barbara Raff, Patricia Randall, Theresa Skurzewski, Marjorie Weber

CHAPTER 1

Introduction

1.1 BIOPHOTONICS—A NEW FRONTIER

We live in an era of technological revolutions that continue to impact our lives and constantly redefine the breadth of our social interactions. The past century has witnessed many technological breakthroughs, one of which is photonics. Photonics utilizes photons instead of electrons to transmit, process, and store information and thus provides a tremendous gain in capacity and speed in information technology. Photonics is an all-encompassing light-based optical technology that is being hailed as the dominant technology for this new millennium. The invention of lasers, a concentrated source of monochromatic and highly directed light, has revolutionized photonics. Since the demonstration of the first laser in 1960, laser light has touched all aspects of our lives, from home entertainment, to high-capacity information storage, to fiber-optic telecommunications, thus opening up numerous opportunities for photonics.

A new extension of photonics is biophotonics, which involves a fusion of photonics and biology. Biophotonics deals with interaction between light and biological matter. A general introduction to biophotonics is illustrated in Figure 1.1.

The use of photonics for optical diagnostics, as well as for light-activated and light-guided therapy, will have a major impact on health care. This is not surprising since Nature has used biophotonics as a basic principle of life from the beginning. Harnessing photons to achieve photosynthesis and conversion of photons through a series of complex steps to create vision are the best examples of biophotonics at work. Conversely, biology is also advancing photonics, since biomaterials are showing promise as new photonic media for technological applications.

As an increasingly aging world population presents unique health problems, biophotonics offers great hope for the early detection of diseases and for new modalities of light-guided and light-activated therapies. Lasers have already made a significant impact on general, plastic, and cosmetic surgeries. Two popular examples of cosmetic surgeries utilizing lasers are skin resurfacing

Introduction to Biophotonics, by Paras N. Prasad
ISBN: 0-471-28770-9

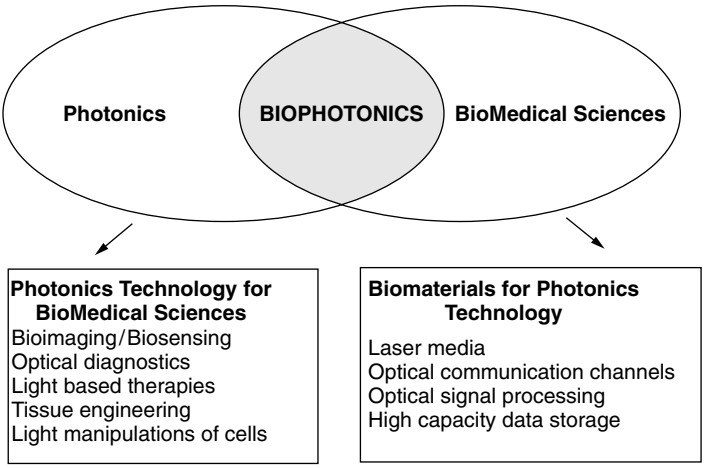

Figure 1.1. Biophotonics as defined by the fusion of photonics and biomedical sciences. The two broad aspects of biophotonics are also identified.

(most commonly known as wrinkle removal) and hair removal. Laser technology also allows one to administer a burst of ultrashort laser pulses that have shown promise for use in tissue engineering. Furthermore, biophotonics may produce retinal implants for restoring vision by reverse engineering Nature's methods.

This book provides an introduction to the exciting new field of biophotonics and is intended for multidisciplinary readership. The book focuses on its potential benefits to medicine. An overview of biophotonics for health care applications is presented in Figure 1.2. It illustrates the scope of biophotonics through multidisciplinary comprehensive research and development possibilities. The focus of the book is on optical probing, diagnostics, and light-activated therapies. However, biophotonics in a broad sense also includes the use of biology for photonics technology, such as biomaterials and development of bioinspired materials as photonic media. These topics are also briefly covered in this book.

1.2 AN INVITATION TO MULTIDISCIPLINARY EDUCATION, TRAINING, AND RESEARCH

In the 21st century, major technological breakthroughs are more likely to occur at the interfaces of disciplines. Biophotonics integrates four major technologies: lasers, photonics, nanotechnology, and biotechnology. Fusion of these technologies truly offers a new dimension for both diagnostics and therapy. Biophotonics creates many opportunities for chemists, physicists, engineers, physicians, dentists, health-care personnel, and biomedical researchers. The

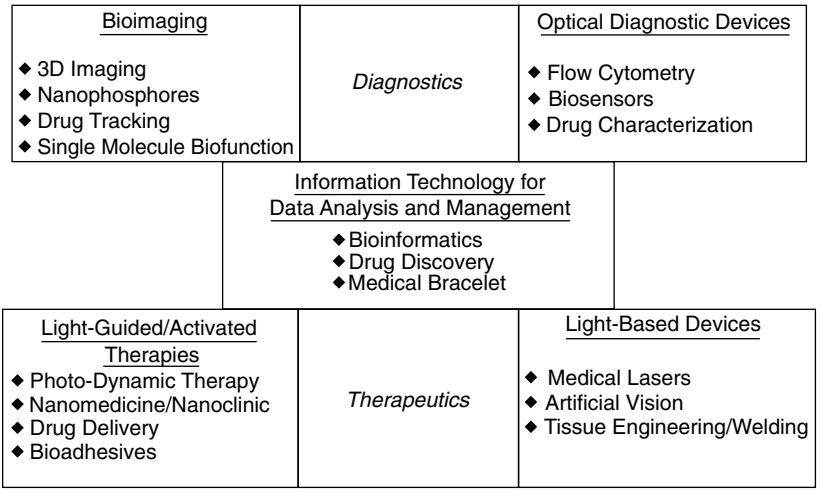

Figure 1.2. The comprehensive multidisciplinary scope of biophotonics for health care.

need for new materials and technologies to provide early detection of diseases, to produce more effective targeted therapies, and to restore impaired biological functions is constantly increasing. The world we live in has become more complex and increasingly dependent upon advanced technologies.

The benefits of lasers to health care are well recognized, even by the general population. Many light-based and spectroscopic techniques are already currently being used as optical probes in clinical laboratories as well as in medical and other health-care practices. Photodynamic therapy, which uses light to treat cancer and has a great potential for growth, is now being practiced.

Producing trained health-care personnel and new generations of researchers in biophotonics is of the utmost importance to keep up with the increasing worldwide demands. Undergraduate and graduate research training programs are needed to develop a skilled workforce and a future generation of researchers respectively for a rapidly growing biotechnology industrial sector. The number of conferences being organized in this field are rapidly increasing, as are the education and training programs at various institutions worldwide. The NSF sponsored integrative graduate education and training program (IGERT) on biophotonics at the University at Buffalo's Institute for Lasers, Photonics, and Biophotonics is a prime example of this trend. This IGERT program is developing multiple interdepartmental courses to provide the needed multidisciplinary education.

A monthly journal, *Biophotonics International*, has emerged as a major reference source. In the areas of research and development, many disciplines can contribute individually as well as collaboratively. Multidisciplinary interactions create unique opportunities that open new doors for the development and application of new technologies.

The author intends that this book serve both as a textbook for education and training as well as a reference book aiding research and development. An aim of the book is to stimulate the interest of researchers and to foster collaboration through multidisciplinary programs. This can lead to the creation of a common language among researchers of widely varying background. The inability to communicate effectively is a major hurdle in establishing any interdisciplinary program.

1.3 OPPORTUNITIES FOR BOTH BASIC RESEARCH AND BIOTECHNOLOGY DEVELOPMENT

Biophotonics offers tremendous opportunities for both biotechnology development and fundamental research. From a technological perspective, biophotonics, as described above, integrates four major technologies: lasers, photonics, nanotechnology, and biotechnology. These technologies have already established themselves in the global marketplace, collectively generating hundreds of billions of dollars per year. Biophotonics also impacts a wide range of industries including biotechnology companies, health care organizations (hospitals, clinics, and medical diagnostic laboratories), medical instrument suppliers, and pharmaceutical manufacturers, as well as those dealing with information technology and optical telecommunication. In the future, biophotonics will have a major impact both in generating new technologies and in offering huge commercial rewards worldwide.

Biophotonics offers challenging opportunities for researchers. A fundamental understanding of the light activation of biomolecules and bioassemblies, and the subsequent photoinduced processes, is a fundamental requirement in designing new probes and drug delivery systems. Also, an understanding of multiphoton processes utilizing ultrashort laser pulses is a necessity both for developing new probes and creating new modalities of light-activated therapy. Some of the opportunities, categorized by discipline, are listed below:

Chemists

- Development of new fluorescent tags
- Chemical probes for analyte detection and biosensing
- Nanoclinics for targeted therapy
- Nanochemistries for materials probes and nanodevices
- New structures for optical activation

Physicists

- Photoprocesses in biomolecules and bioassemblies
- New physical principles for imaging and biosensing

- Single-molecule biophysics
- Nonlinear optical processes for diagnostics and therapy

Engineers

- Efficient and compact integration of new generation lasers, delivery systems, detectors
- Device miniaturization, automation, and robotic control
- New approaches to noninvasive or minimally invasive light activation
- Optical engineering for *in vivo* imaging and optical biopsies
- Nanotechnologies for targeted detection and activation
- Optical BioMEMS (micro-electro-mechanical systems) and their nanoscale analogues.

Biomedical Researchers

- Bioimaging to probe molecular, cellular, and tissue functions
- Optical signature for early detection of infectious diseases and cancers
- Dynamic imaging for physiological response to therapy and drug delivery
- Cellular mechanisms of drug action
- Toxicity of photoactivatable materials
- Biocompatibility of implants and probes

Clinicians

- *In vivo* imaging studies using human subjects
- Development of optical *in vivo* probes for infections and cancers
- *In vivo* optical biopsy and optical mammography
- Tissue welding, contouring, and regeneration
- Real-time monitoring of drug delivery and action
- Long-term clinical studies of side effects

The opportunities for future research and development in a specific biophotonics area are provided in the respective chapter covering that area.

1.4 SCOPE OF THIS BOOK

This book is intended as an introduction to biophotonics, not as an in-depth and exhaustive treatise of this field. The objective is to provide a basic knowledge of a broad range of topics so that even a newcomer can rapidly acquire the minimal necessary background for research and development.

Although several books and journals exist that cover selective aspects of biophotonics, there is a clear need for a monograph that provides a unified synthesis of this subject. The need for such a book as this became apparent while teaching this topic as an interdisciplinary course available to students in many departments at the University at Buffalo. While offering tutorial courses at several professional society conferences such as BIOS of SPIE, the need became even more apparent. The makeup of the registrants for these tutorial courses has been multidisciplinary. Over the years, participants in these courses have constantly emphasized the need for a comprehensive and multidisciplinary text in this field.

The book is written with the following readership in mind:

- Researchers working in the area; it will provide useful information for them in areas outside their expertise and serve as a reference source.
- Newcomers or researchers interested in exploring opportunities in this field; it will provide for them an appreciation and working knowledge of this field in a relatively short time.
- Educators who provide training and tutorial courses at universities as well as at various professional society meetings; it will serve them as a textbook that elucidates basic principles of existing knowledge and multidisciplinary approaches.

This book encompasses the fundamentals and various applications of biophotonics. Chapters 1 through 6 cover the fundamentals intended to provide the reader with background, which may be helpful in understanding biophotonics applications covered in subsequent chapters. Chapters 7 through 11 illustrate the use of light for optical diagnostics. Chapters 12 and 13 provide examples of light-based therapy and treatment. Chapters 14 and 15 present specialized topics dealing with micromanipulation of biological objects by light and the infusion of nanotechnology into biophotonics. Chapter 16 discusses the other aspect of biophotonics—that is, the use of biomaterials for photonics technology (see Figure 1.1).

Each chapter begins with an introduction describing what a reader will find in that chapter. In the case of Chapters 1–6, the introductory section also provides a guide to which parts may be skipped by a reader familiar with the content or less inclined to go through details. Each chapter ends with highlights of the material covered in it. The highlights are basically the take home message from the chapter and may serve as a review of the materials presented in the chapter. For an instructor, the highlights may be useful in the preparation of lecture notes or power point presentations. For researchers who may want to get a cursory glimpse, the highlights will provide a summary of what the chapter has covered.

In each of the chapters dealing with applications (Chapters 7–16), a description of future directions of research and development is also provided, along with a brief discussion of current status and the identification of some areas

of future opportunities. Each of these application chapters also lists commercial sources of instrumentation and suppliers relevant to the content of the chapter. This list may be useful to a researcher new to this area and interested in acquiring the necessary equipment and supplies or to a researcher interested in upgrading an existing facility.

The book is organized to be adapted for various levels of teaching. Chapters 2–6 can be covered partly or completely, depending on the depth and length of the course and its intended audience. Chapters 7–13 are the various applications of photonics to life sciences and are somewhat interrelated. Chapters 14–16 can be optional, because they deal with specialized topics and do not necessarily require the detailed contents of preceding chapters. Chapters 8–16 are, to a great degree, independent of each other, which allows considerable freedom in the choice of areas to be covered in a course.

Chapter 2 begins with a discussion of the fundamentals of light and matter at a basic level, emphasizing concepts and avoiding mathematical details. For those readers with little exposure to the subject, the materials of this chapter will assist them in grasping the concepts. For those readers already familiar with the subject, the chapter will serve as a condensed review. The dual nature of light as electromagnetic waves and photon particles is described, along with manifestations derived from them. The section on matter introduces a simplified quantum description of atoms, molecules, and the nature of chemical bonding. The description of Π-bonding and the effect of conjugation are provided. The geometric effect derived from the shapes of molecules, along with intermolecular effects, is also covered.

Chapter 3 focuses on building a molecular understanding of biological structures and their relation to biological functions. It provides the basics of biology and introduces the necessary terminology and concepts of biology used in this book. The chapter is written primarily for those unfamiliar with biological concepts, or those wishing to refresh their background in this subject. The chapter describes the chemical makeup of a biological cell and the different organelles. The various cellular functions are also discussed. Then, assembling of cells to form a tissue structure is described, along with the nature of extracellular components in a tissue. The chapter ends with a brief description of tumors and cancers.

Various aspects of light and matter, which form the fundamental basis for biophotonics, are addressed in Chapter 4. This chapter, written for a multidisciplinary readership with varied backgrounds, provides knowledge of the necessary tools of optical interactions utilized in biophotonics applications. These are covered in Chapters 7–16. The emphasis again is on introducing concepts and terminologies, avoiding complex theoretical details. Various spectroscopic techniques useful for biology are covered.

Chapter 5 describes the principle of laser action, relying on simple diagrammatic descriptions. The various steps involved and components used in laser operation are briefly explained. The present status of the laser technology, useful for biophotonics, is described. The chapter also introduces

the concepts of nonlinear optical interactions that take place under the action of an intense laser beam. These nonlinear optical interactions are increasingly recognized as useful for biophotonics. The chapter also provides a brief discussion of laser safety.

Chapter 6 discusses photobiology—that is, the interactions of various molecular, cellular, and tissue components with light. Light-induced radiative and nonradiative processes are described, along with a discussion of the photochemical processes at both the cellular and tissue levels. As important examples of biophotonics in Nature, the processes of vision and photosynthesis are presented. A fascinating topic in photobiology is *in vivo* photoexcitation in live specimens, which has opened up the new area of optical biopsy. Another exciting new area is the use of optical techniques to probe interactions and dynamics at the single-cell/single-biomolecule level.

Chapter 7 describes the basic principles and techniques used for optical bioimaging, a major thrust area of biophotonics applications. Although ultrasonic imaging and MRI are well established in the biomedical field, optical imaging offers a complementary approach. For example, it allows multidimensional imaging (multicolor, three-dimensional, time-resolved) and also covers application to all biological organisms, from microbes to humans. Topics discussed include spectral imaging, fluorescence resonance energy transfer (FRET), and lifetime imaging. Newer nonlinear optical imaging methods utilizing multiphoton absorption, harmonic generation, and coherent anti-Stokes scattering (CARS) are also presented. Various types of microscopies described in this chapter include differential interference contrast (DIC), confocal, two-photon laser scanning, optical coherence tomography (OCT), total internal reflection fluorescence (TIRF), and near-field microscopy (NSOM or SNOM).

Chapter 8 provides examples of the wide usage of optical bioimaging to investigate structures and functions of cells and tissues and also to profile diseases at cellular, tissue, and *in vivo* specimen levels. This chapter also discusses the various fluorophores used for fluorescence imaging. Cellular imaging to probe structures and functions of viruses, bacteria, and eukaryotic cells are presented. Then imaging at the tissue level is presented. Finally, *in vivo* imaging, for example optical mammography is discussed.

Chapter 9 on biosensors describes the basic optical principles and the various techniques utilized in biosensing. Biosensors are of especially great interest right now. They are important in combating the constant health danger posed by new strands of microbial organisms and spread of infectious diseases, by characterizing them rapidly. They will be effective tools in the worldwide struggle against chemical and bioterriosm. Chapter 9 provides a detailed coverage of the various existing optical biosensors and ongoing activities given in the literature. The biosensors covered in this chapter are fiber-optic biosensors, planar waveguide biosensors, evanescent wave biosensors, interferometric biosensors, and surface plasmon resonance biosensors. Some novel sensing methods are also described.

Chapter 10 covers microarray technology. It is a natural extension of biosensing. Microarray technology utilizes a micropatterned array of biosensing capture agents for rapid and simultaneous probing of a large number of DNA, proteins, cells, or tissue fragments. It provides a powerful tool for high-throughput, rapid analysis of a large number of samples. This capability has been of significant value in advancing the fields of genomics, proteomics, and bioinformatics, which are at the forefront of modern structural biology, molecular profiling of diseases, and drug discovery. Biophotonics has played an important role in the development of microarray technology, since optical methods are commonly used for detection and readout of microarrays. Four types of microarrays are covered here: DNA microarrays, protein microarrays, cell microarrays, and tissue microarrays.

Chapter 11 introduces the flow cytometer, an optical diagnostic device that currently is used in research and clinical laboratories for disease profiling by measuring the physical and/or chemical characteristics of cells. Flow cytometry is also suitable for rapid and sensitive screening of potential sources of deliberate contamination, an increasing source of concern in bioterrorism. Flow cytometer is also emerging as a powerful technique for agricultural research and livestock development. The chapter describes the steps involved in flow cytometry. The various components of a flow cytometer are described. Methods of data collection, analysis, and display are also discussed.

Chapters 12 and 13 treat the use of light for therapy and treatment, an important area of biophotonics. These chapters provide examples of the use of light for therapy and medical procedures. Chapter 12 covers light-activated therapy, specifically the use of light to activate an administered photosensitizer that causes the destruction of cancer or treats a diseased tissue. This procedure is called *photodynamic therapy* (PDT) and constitutes a multidisciplinary area that has witnessed considerable global growth. Treatment of certain types of cancer using photodynamic therapy is already approved in the United States by the Food and Drug Administration as well as by equivalent agencies in other countries. Therefore, this chapter can be useful not only for researchers but also for clinicians and practicing oncologists. Applications of photodynamic therapy to areas other than cancer—for example, to age-related macular degeneration—are also discussed.

Lasers have emerged as powerful tools for tissue engineering. Chapter 13 discusses tissue engineering with light, utilizing various types of light–tissue interactions. Chapter 13 also has sufficient medical focus to be useful to medical practitioners as well. The chapter covers three main types of laser-based tissue engineering: (i) tissue contouring and restructuring, (ii) tissue welding, and (iii) tissue regeneration. Specific examples of tissue contouring and restructuring are chosen from dermatology and ophthalmology. The section on laser welding of tissues discusses how lasers are used to join tissues. Laser tissue regeneration is a relatively new area; recent work suggests that laser treatment can effect tissue regeneration to repair tissue damage due to an injury. A major impetus to the area of laser-based tissue engineering has

been provided by developments in femtosecond laser technology, giving rise to the emergence of "femtolaser surgery."

Chapter 14 covers the usage of a laser beam as a tool for micromanipulation of biological specimens. Two types of laser micromanipulation discussed are laser tweezers for optical trapping and laser scissors for microdissection. The principle of laser optical trapping using a laser is explained. Chapter 14 also provides a detailed discussion of the design of a laser tweezer for the benefit of readers interested in building their own laser tweezers. The use of pulsed laser beam for microdissection of a tissue is discussed. The applications covered are both fundamental, such as in the studies of single molecular biofunction, and applied, such as for reproductive medicine and in plant breeding.

Chapter 15 covers the subject of bionanophotonics, the merging of biomedical science and technology and nanophotonics. Nanophotonics is an emerging field that describes nanoscale optical science and technology. Specifically, this chapter discusses the use of nanoparticles for optical bioimaging, optical diagnostics and light guided and activated therapy. The chapter includes the use of a nanoparticles platform for intracellular diagnostics and targeted drug delivery. Specifically discussed are (a) the PEBBLE nanosensors approach for monitoring intracellular activities and (b) the nanoclinic approach with carrier groups to target specific biological sites for diagnostics and external activation of therapy.

Chapter 16 describes the application of biomaterials to photonics-based information technology, which utilizes light–matter interactions for information processing, transmission, data storage, and display. The continued development of photonics technology is crucially dependent on the availability of suitable optical materials. Biomaterials are emerging as an important class of materials for a variety of photonics applications. The various types of biomaterials being investigated for photonics are presented. Examples of photonics applications discussed in this chapter include efficient harvesting of solar energy, low-threshold lasing, high-density data storage, and efficient optical switching and filtering.

The author hopes that this book will inspire new ideas and stimulate new directions in biophotonics.

CHAPTER 4

Fundamentals of Light–Matter Interactions

Biophotonics involves interaction of light with biological matter. Therefore, an understanding of light–matter interactions provides the fundamental basis for biophotonics. This chapter, written for multidisciplinary readership with varied backgrounds, provides knowledge of the necessary tools of optical interactions utilized in biophotonics applications which are covered in Chapters 7–16. The emphasis again is on introducing concepts and terminologies without getting into complex theoretical details.

The interaction of light at the molecular level, producing absorption, spontaneous emission, stimulated emission, and Raman scattering, is described. Then interaction at the bulk level, producing absorption, refraction, reflection, and scattering during the propagation of light through a bulk sample, is introduced. The various photophysical and photochemical processes produced in the excited state that is generated by light absorption are discussed.

A major branch of interaction between light and matter is spectroscopy, which involves the study of a transition between quantized levels. As discussed in Chapter 2, the quantized levels of biological interests are electronic and vibrational. The various spectroscopic approaches are then introduced and discussed in relation to their utilities in biological investigation.

Another major area of light–matter interaction is light emission, which can be either (a) intrinsic due to a biomaterial or (b) extrinsic due to an added molecule. This emission is utilized in a number of applications such as bioimaging (Chapters 7 and 8), biosensors (Chapter 9), microarray technology (Chapter 10), and flow cytometry (Chapter 11). The concepts of fluorescence emission and its associated properties are introduced here, providing the necessary backgrounds for these subsequent chapters.

Many biological molecules are chiral, a type of stereoisomers defined in Chapter 2. An active area of spectroscopy is the differences in interaction of a chiral molecule with left and right circularly polarized light. This difference in interactions as probed by electronic, vibrational, and Raman spectroscopy

Introduction to Biophotonics, by Paras N. Prasad
ISBN: 0-471-28770-9

and utilized to investigate conformation and dynamics of biopolymers is discussed. Another technique presented is fluorescence correlation spectroscopy, which is useful for the study of diffusion and association of biopolymers.

For further reading on the topics covered here, some general references suggested here are:

Atkins and dePaula (2002): General introduction to light-matter interaction and spectroscopy

Sauer (1995): Broad coverage of spectroscopic techniques to biochemistry

Lakowicz (1999): Coverage of various aspects of fluorescence spectroscopy

Chalmers and Griffiths (2002): Vibrational spectroscopy and its application to biology, pharmaceutics, and agriculture

Griffiths and deHaseth (1986): Principles and applications of Fourier transform infrared spectroscopy

4.1 INTERACTIONS BETWEEN LIGHT AND A MOLECULE

4.1.1 Nature of Interactions

As described in Section 2.1, light is an electromagnetic radiation consisting of oscillating electric and magnetic fields. Biological systems are molecular media. For such a medium the interaction with light can be described by the electronic polarization of a molecule subjected to an electric field. This approach is also referred to as the *electric dipole* (or simply *dipole*) *approximation*.

The linear field response, which is defined by linear dependence of the dipole moment on the electric field, gives the total molecular dipole as

$$\mu_T = -er = \mu + \alpha\varepsilon(\nu') \tag{4.1}$$

In the above equation, μ_T is the total electronic dipole moment vector given by the product of the electronic charge e and its position r. The term μ is the permanent dipole term in the absence of any field, and the term $\alpha\varepsilon(\nu')$ is the electric-field-induced dipole moment, μ_{in}, describing the polarization of the electronic cloud of a molecule in the field. In the case of polarization due to the oscillating electric field $\varepsilon(\nu')$ of light, the induced polarization is characterized by the dynamic polarizability term α, which is a second rank tensor that relates the directions of two vectors, the electric field ε and, as in this case, the resulting dipole, μ_{in}.

The dipolar interaction V between the molecule and a radiation field $\varepsilon(\nu)$ can be described as

$$V = \varepsilon(\nu)\mu + \varepsilon(\nu)\alpha\varepsilon(\nu') \tag{4.2}$$

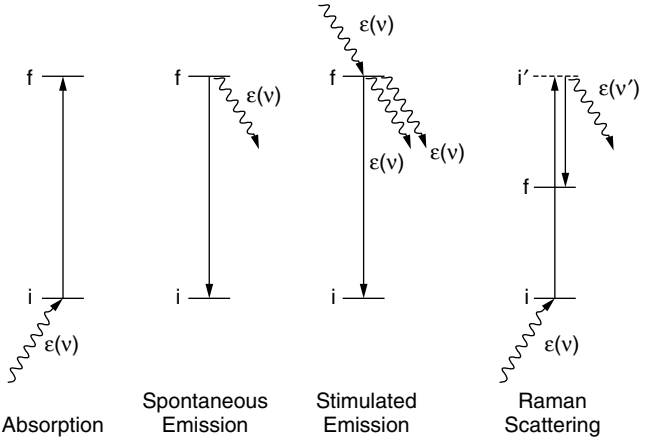

Figure 4.1. Schematics of various light–molecule interaction processes.

The first term in equation (4.2) describes interaction with a photon field of frequency ν leading to the phenomenon of absorption and emission of a photon by the molecule. The second term represents inelastic scattering, Raman scattering, where a photon of frequency ν is scattered inelastically (with a change in energy) by a molecule creating a photon of a different frequency ν′ and exchanging the energy difference with the molecule. The energy diagrams in Figure 4.1 describe these processes. The absorption process describes the transition from a quantized lower energy initial level, *i*, to a higher energy level, *f*, with the energy gap between them matching the photon energy. For electronic absorption, generally the initial electronic level *i* is the ground state (the lowest electronic level). If the initial level is an excited level, the resulting absorption is called an *excited state absorption*. The spontaneous emission process describes the return of the molecule from the excited state, *f*, to its lower energy state, *i*, by emission of a photon of energy corresponding to the energy gap between the two levels. The stimulated emission is a process of emission triggered by an incident photon of an energy corresponding to the energy gap between *i* and *f*. In the absence of an incident photon of same energy, there can be no stimulated emission, but only spontaneous emission.

The Raman scattering describes a process that is a single-step scattering of a photon of energy $h\nu$, being scattered into another photon of energy $h\nu'$, the difference $h(\nu - \nu')$ corresponding to the energy gap $\Delta E = E_f - E_i$. In the schematics shown in Figure 4.1, the scattered photon of energy $h\nu'$ is of lower energy than the incident photon ($h\nu$), depositing the energy difference $h(\nu - \nu')$ in the molecule to produce an excited state *f*. This process is called *Stokes Raman scattering*, which is normally studied in Raman spectroscopy. The case where $h\nu'$ is higher than $h\nu$ represents anti-Stokes Raman scattering. Very often Raman scattering is described by the photon ε(ν) taking the molecule to a virtual intermediate level, *i*′ (as shown in Figure 4.1), from which the

molecule emits a photon $\varepsilon(\nu')$ to end up in the final state f. This level, i', is generally not a real level (no energy level exists at this energy value). If i' is a real level, then the scattering process is considerably enhanced and the process is called *resonance Raman scattering*.

As we shall see later, the absorption and emission processes are exhibited by both the electronic and vibrational states of a molecule. They also are exhibited by the quantized electronic states of atoms. However, the Raman scattering processes of significance involve vibrational states of a molecule or a molecular aggregate.

4.1.2 Einstein's Model of Absorption and Emission

The Einstein model is often used to describe the absorption and emission processes (Atkins and dePaula, 2002). In this model, the absorption process from a lower energy state i to a higher energy state f is described by a transition rate W^{abs} which is proportional both to the number of molecules, N_{i}, present in state i and to the density of photons ρ. Hence

$$W^{\text{abs}} = B_{if} N_i \rho \tag{4.2a}$$

where B the proportionality constant is called the *Einstein's coefficient* and the subscripts i and f simply designate that the coefficient is for states i and f.

The stimulated emission, which also requires a photon to trigger it, is also given by a similar expression for its rate, $W_{\text{st}}^{\text{emi}}$:

$$W_{\text{st}}^{\text{emi}} = B_{if} N_f \rho \tag{4.2b}$$

This rate is proportional both to the number N_f in the excited state f from where emission originates and to the density of photons present. The proportionality constant is the same coefficient B_{if}.

The spontaneous emission rate, however, is only proportional to the number, N_f, of molecules in the excited state f because this process does not require triggering by another photon. Hence,

$$W_{\text{sp}}^{\text{emi}} = A_{if} N_f \tag{4.2c}$$

where A_{if} is called the *Einstein's coefficient of spontaneous emission*.

The total emission rate is then given by

$$W_{\text{st}}^{\text{emi}} + W_{\text{sp}}^{\text{emi}} = N_f (A_{if} + B_{if} \rho) \tag{4.2d}$$

The net absorption of a photon is given as

$$W_{\text{net}}^{\text{abs}} = B_{if} N_i \rho - N_f (A_{if} + B_{if} \rho) \tag{4.3}$$

In the presence of stimulated emission, this process dominates over the spontaneous emission, which can then be ignored. Hence, the absorption rate of equation (4.3) becomes

$$W_{\text{net}}^{\text{abs}} = B_{if}N_i\rho - B_{if}N_f\rho = (N_i - N_f)B_{if}\rho \tag{4.4}$$

A net absorption process takes place when this rate is positive: in other words, when $N_i > N_f$. This situation, when the lower energy state, i, has more molecules than the higher energy state, f, is called *normal population condition*.

In the case where $N_f > N_i$ the net absorption rate of equation (4.4) will have a negative sign, implying that a net stimulated emission rather than a net absorption will occur under these conditions. This net stimulated emission rate is given as

$$W_{\text{net}}^{\text{emi}} = (N_f - N_i)B_{if}\rho \tag{4.5}$$

The situation $N_f > N_i$ for the stimulated emission where more molecules are in the higher energy (excited) state than in the ground state is called the *population inversion condition*. This population inversion is one of the conditions to achieve laser action as discussed in Chapter 5.

The quantum mechanical description of these processes provides a formal theoretical foundation for them. Quantum mechanical formulation of a transition from state i to state f is described by a quantity called the *transition dipole moment*, μ_{if}, which connects states i and f through charge/electron redistribution (hence, dipole interaction). This transition dipole moment, μ_{if}, is evaluated as an integral using standard quantum mechanical procedures described in Levine (2000).

Quantum mechanics also provides expressions relating the coefficients of stimulated absorption and emissions with the transition dipole moments as

$$B_{if} = 4\pi^2 \frac{|\mu_{if}|^2}{6\varepsilon_0 h^2} \tag{4.6}$$

$$A_{if} = \left(\frac{8\pi h\nu^3}{c^3}\right)B_{if} \tag{4.7}$$

The term ε_o is the dielectric constant of the medium. Therefore, the strength of a transition from state i to state f is proportional to the square of the transition dipole moment. Similarly, the coefficient of spontaneous emission, A_{if}, being related to B_{if} can be calculated from μ_{if}. Here, c = speed of light, and ν is the frequency of light.

Although, in order to quantify the strength of a transition, one needs to evaluate the transition dipole moment, one can often get qualitative information about it whether a transition is dipole-allowed ($\mu_{if} \neq 0$) or dipole-

forbidden ($\mu_{if} = 0$), based on symmetry consideration of orbitals i and f (whether atomic or molecular). For example, for a molecular system with an inversion symmetry i (discussed in Chapter 2), the Laporte rule provides the following guidance:

(i) A transition from a g state (overall wave function symmetric, g, under inversion, as described in Chapter 2) to a u state or a u state to a g state is dipole-allowed ($\mu_{if} \neq 0$).
(ii) A transition from a g state to another g state or from a u state to another u state is dipole-forbidden ($\mu_{if} = 0$).

While (ii) of this simple rule always holds, (i) is not strictly true. One needs to consider the overall representations of the energy states i and f under the point group symmetry of the molecule to determine if a transition between i and f is allowed.

4.2 INTERACTION OF LIGHT WITH A BULK MATTER

Interaction of light with a bulk matter such as a molecular aggregate with a size scale comparable to or larger than the wavelength produces new manifestations such as reflection, refraction, and scattering, in addition to the absorption process. These manifestations also play an important role in understanding the interaction of a biological bulk specimen such as a tissue with light. The interaction of light with biological tissues is discussed in detail in Chapter 6, for which the materials presented here form the basis.

The bulk property is derived from an average sum of the corresponding molecular properties. Again, in the linear response theory (only linear term in electric field ε), one considers the bulk polarization P of a bulk medium induced by the external electric field ε (such as that due to light of frequency ν) and given as (Prasad and Williams, 1991)

$$P(\nu) = \chi^{(1)}(\nu) \cdot \varepsilon(\nu) \tag{4.8}$$

P for bulk is analogous to ($\mu_T - \mu$) of equation (4.1), describing the dipole moment per volume induced by an electric field ε. The proportionality constant $\chi^{(1)}$, called *linear optical susceptibility*, is a second rank tensor that relates the vector P with another vector ε.

As described in Chapter 2, Section 2.1.2, the optical response of a medium with respect to propagation of light through it is described by a refractive index, n, which determines the phase as well as the velocity of propagation. It is related to the linear susceptibility $\chi^{(1)}$ by the relation

$$n^2(\nu) = 1 + 4\pi\chi^{(1)}(\nu) \tag{4.9}$$

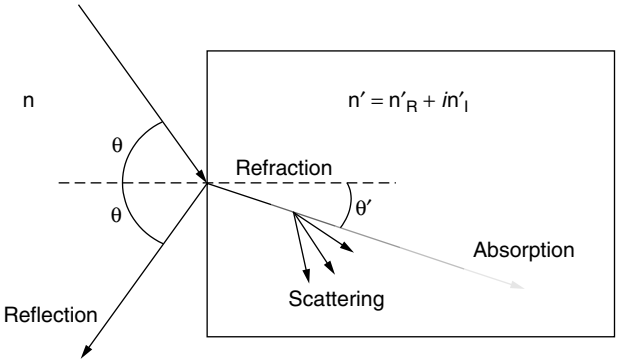

Figure 4.2. Propagation of a light ray from one medium (air) to a medium of interest (a biological tissue).

The refractive index n at frequencies corresponding to the gap between the two states of a medium (near a resonance) becomes a complex quantity given as

$$n = n_R + in_I \tag{4.10}$$

The real part, n_R, determines the refraction and scattering, while the imaginary part, n_I, describes the absorption of light in a medium.

Figure 4.2 represents the various processes when light enters from one medium (such as air) into another bulk medium of interest. The reflection from an interface between the two bulk media (air and tissue, for example) and refraction (change of angle of propagation when entering from one medium to another) are governed by principles called *Fresnel's law* (Feynman et al., 1963) and their relative strengths are determined by the relative values of their refractive indices.

In propagation from air ($n \approx 1$) to a tissue of refractive index n', the reflectance, R (ratio of the reflected to the incidence intensities of light), is given as (in the case of normal incidence)

$$R = \left(\frac{n'_R - 1}{n'_R + 1} \right)^2 \tag{4.11}$$

Equation (4.11) is useful in calculating reflections from various tissues.

In general, the reflectance is dependent also on the polarization of light and the angle of incidence. The two polarizations often used are s, where the polarization of light is perpendicular to the plane of incidence, and p, where the polarization is parallel to the plane of incidence.

The refraction behavior is given by Snell's law:

$$n \sin\theta = n' \sin\theta' \tag{4.12}$$

The scattering behavior is more complex. It will be discussed in the section on light–tissue interactions in Chapter 6.

4.3 FATE OF EXCITED STATE

This section discusses the processes that can take place following an excitation created by light absorption, which takes a molecule to an excited state. These processes can be radiative, where a photon is emitted (emission) to bring the molecule back to the ground state. They can be nonradiative, where the excited-state energy is dissipated as a heat or in producing a chemical reaction (photochemistry). The return to the ground state may also involve a combination of both. The nonradiative processes producing heat involve crossing from one electronic level to another of lower energy, with the excess energy converting to vibrational energy by an interaction called *electronic–vibrational state coupling*. Subsequently, the excess vibrational energy is converted to heat by coupling to translation (this process is called *vibrational relaxation*). These processes are schematically represented in Table 4.1. In this table the star sign, such as in A*, signifies that A is in the excited state. The processes of

TABLE 4.1. Schematic Representation of Processes Involved in Electronic Excitation

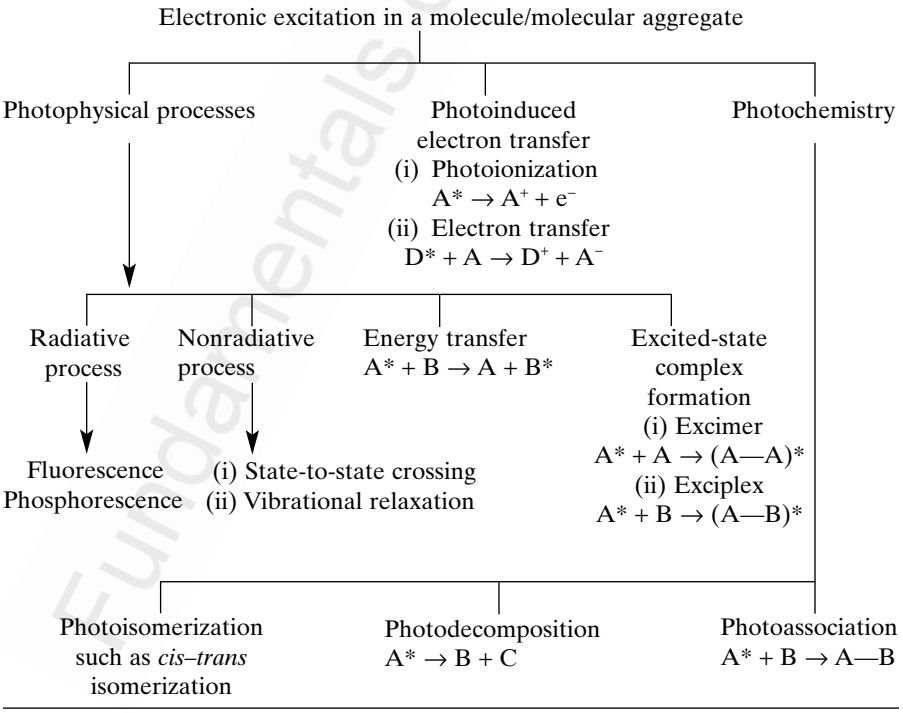

energy transfer and excited-state complex formation occur only when more than one molecule are interacting. Therefore, for such processes a minimum size molecular aggregate is a dimer (A_2) or a bimolecular (AB) unit. An excimer [an excited-state dimer, (A–A)*] or an exciplex [an excited-state complex, (A–B)*] may return to the ground state radiatively (by emitting light) or nonradiatively. An example of excimer formation is provided by an aromatic dye, pyrene, which shows a broad structureless fluorescence peaked at ~500 nm, well shifted to the red from the emission (at ~390 nm) of the single pyrene molecule. In biological fluid media, the excimer formation is diffusion-controlled. Therefore, excimer emission (such as from the pyrene dye) has been used to study diffusion coefficient (a quantity defining the diffusion rate) in membranes.

Exciplexes are excited-state complexes formed between two different molecules (or molecular units), A and B, when one of them (e.g., A) is excited (designated as A* in Table 4.1). Exciplexes can form between aromatic molecules, such as naphthalene and dimethylaniline. Just like in the case of an excimer, the resulting emission from the exciplex (A–B*) is red-shifted, compared to that from A*. Of biological interest has been the exciplex formation between a metalloporphyrin and a nucleic acid or an oligonucliotide, which can provide structural information on the microenvironment of the metalloporphyrin (Mojzes et al., 1993; Kruglik et al., 2001). Exciplex formation has been studied for double-stranded polynucleotides and natural DNA having regular double-helix structures.

The photochemical processes, listed under photochemistry in Table 4.1, are of considerable significance to biology, because they occur in biological materials with important consequences. These processes in biological materials are discussed in detail in Chapter 6, "Photobiology," with specific examples provided there.

The state-to-state crossing and the various possible radiative and nonradiative processes in an organic structure are often represented by the so-called Jablonski diagram shown in Figure 4.3. In this diagram, the radiative processes are represented by a straight arrow, whereas nonradiative processes (also sometimes referred to as *radiationless transition*) are represented by a wiggly arrow.

The ground state of most molecules (organics in particular) involves paired electrons; therefore, their total spin $S = 0$ and the spin multiplicity $2S + 1 = 1$. These are singlet states and, in the order of increasing energy from the ground-state, singlets are labeled S_0, S_1, S_2, and so on. An exception is the common form of O_2, where the ground-state is a triplet with the spin $S = 1$ and the spin multiplicity $2S + 1 = 3$. Therefore, the ground state of oxygen is T_0. This case is not represented in Figure 4.3, which only depicts the case of molecules with a singlet ground state, S_0. For molecules whose ground states are S_0, the excitation of an electron from a paired electron pair to an excited state can produce either a state where the two electrons are still paired (like S_1) or where the two electrons are unpaired (a triplet, T state). The excited

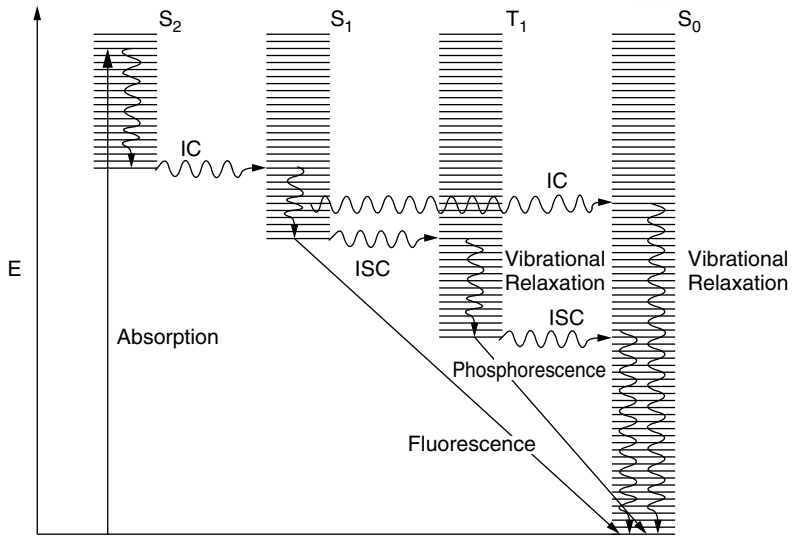

Figure 4.3. The Jablonski diagram describing the possible fates of excitation.

triplet configurations are labeled as T_1, T_2, and so on, in order of increasing energies.

Quantum mechanical considerations show that for the excitation to the same orbital state, the energy of the excited triplet state (say T_1 state) is lower than that of its corresponding singlet state (S_1 in this case). In Figure 4.3 the possibilities for the fate of an excitation to a higher singlet S_2 manifold are described. The horizontal closely spaced lines represent the vibrational levels. Suppose the excitation is to an electronic level, S_2. A nonradiative crossing from the S_2 state to S_1 is generally the dominant mechanism. Only very few molecules (e.g., azulene), show emission (radiative decay) from S_2. This crossing between two electronic states of the same spin multiplicity (such as from S_2 to S_1) is called *internal conversion* (IC). This IC process is then followed by a rapid vibrational relaxation where the excess vibrational energy is dissipated into heat, the molecule now ending up at the lowest, zero-point vibration level ($v = 0$, see Chapter 2 on vibration) of the S_1 electronic state. From here, it can return to the ground electronic state S_0 by emitting a photon (radiatively). This emission from a state (S_1) to another state (S_0) of same spin multiplicity is called *fluorescence* and is spin-allowed (observes the rule of no change of spin value). It, therefore, has a short lifetime of emission, generally in the nanoseconds (10^{-9}-sec) range. Alternatively, the excitation may cross from S_1 to T_1 by another nonradiative process called *intersystem crossing* (ISC) between two states of different spin. This crossing (change) of spin violates the rule of no change of electron spin during a change of electronic state and is thus called a *spin-forbidden transition*. This spin violation (or occurrence of a spin-forbidden transition) is promoted by spin–orbit coupling, described in

Chapter 2, which relaxes the spin property by mixing with an orbital character. Followed by a rapid vibrational relaxation, the excitation ends in the zero-point vibrational level of the T_1 state. A radiative process of emission from here leading to S_0 is spin-forbidden and is called *phosphorescence*. Again, the spin-violation occurs because of spin–orbit coupling (Chapter 2). This is a weaker emission process and, therefore, has a long lifetime. Some of the phosphorescence lifetimes are in seconds. Many photochemical processes originate from this type of long-lived triplet state. Heavy metals, molecular oxygen (having a triplet ground state), paramagnetic molecules, and heavy atoms such as iodine increase the intersystem crossing rate, thus reducing the fluorescence and enhancing the process taking place from the excited triplet state.

Finally, there can also be a nonradiative intersystem crossing from T_1 to S_0.

4.4 VARIOUS TYPES OF SPECTROSCOPY

Spectroscopy deals with characterization and applications of transition between two quantized states of an atom, a molecule, or an aggregate. A description of the nature of interactions and various spectroscopic transitions has already been presented in Section 4.1.

The various spectroscopic transitions and methods useful for biophotonics are described in Table 4.2. Electronic transitions are not efficiently excited by a Raman process. A vibrational excitation generally decays by a nonradiative process and, therefore, exhibits no fluorescence; exceptions are small molecules such as CO_2.

A spectrum is a plot of the output intensity of light exiting a medium as a function of its frequency (or wavelength). For absorption, a broad band light source generally is used, and its transmission (and hence, attenuation or absorption) is obtained as a function of frequency or wavelength. For an emission or a Raman process, the medium is excited at a specific wavelength (called *excitation wavelength*), and the emitted or scattered radiation intensity is monitored as a function of wavelength.

Two types of spectrometers are used for obtaining the spectral information on the intensity distribution as a function of wavelength:

- *Conventional Spectrometers*. In this case a dispersive element such a prism or a diffraction grating separates light with different frequencies into different spatial directions. The intensities of spatially dispersed radiation of different wavelengths may be obtained by using a multielement array detector where each array detects radiation of a narrow spectral range centered at a specific frequency. This type of spectrometer allowing simultaneous detection of lights of all wavelengths is also referred to as a *spectrograph*. Alternatively, one may scan the angle of a diffraction grating (or a prism) so that at a given angle only a narrowly defined wave-

TABLE 4.2. The Various Spectroscopies Useful for Biophotonics

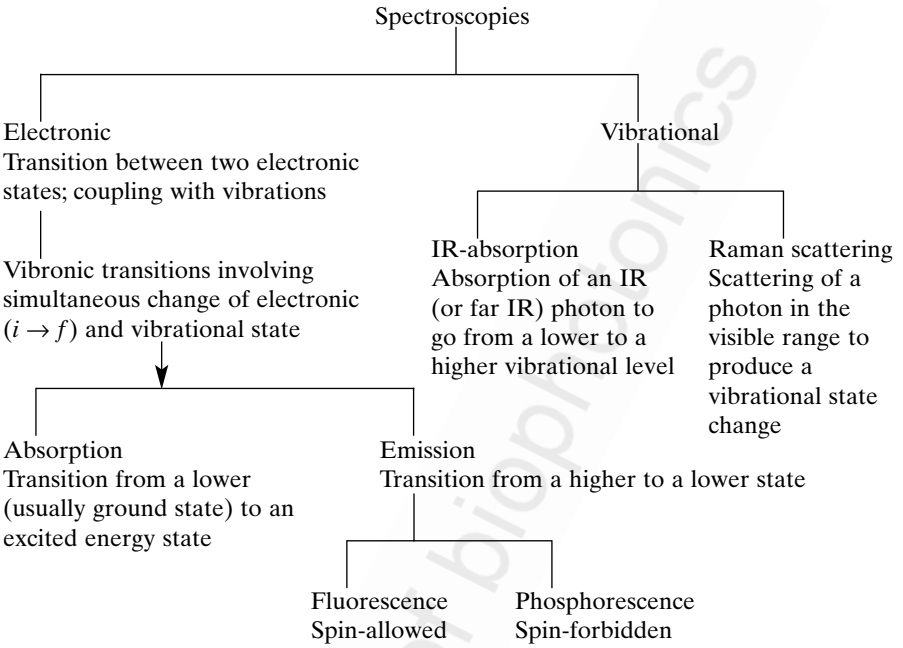

length region passes through as narrow aperture (a slit) to impinge on the photodetector.

- *Fourier Transform Spectrometers*. Most modern IR-absorption spectrometers employ this technique and hence are often called FT–IR spectrometers (FT is the abbreviation for Fourier transform). Here, instead of using a dispersive element, such as a diffraction grating or a prism to disperse the different frequencies, the information on intensity distribution as a function of frequency is obtained by using an optical device called a *Michelson interferometer*. In a Michelson interferometer, the beam from a broad-band light source (infrared light source in the case of FT–IR) is split into two beams by a beam splitter, with one beam going to a fixed mirror and the other incident on a movable mirror. After reflection from the two mirrors, the beams recombine at the beam splitter and then pass through the sample. This arrangement is shown in Figure 4.4. Depending on the relative positions of the two mirrors, the beams can constructively or destructively interfere for various frequencies. The plot of the interference intensity, called the *interferogram*, as a function of the position of the movable mirror, is related to the intensity of light as a function of frequency by a mathematical relation called *Fourier transform*. Thus, by performing a Fourier transform with the help of a computer, one can obtain

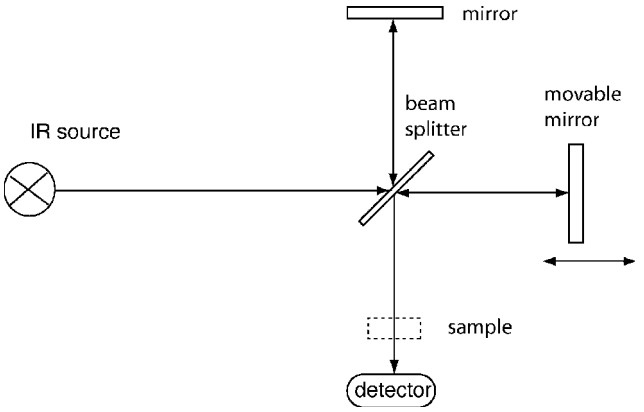

Figure 4.4. Schematics of Michaelson interferometer.

the plot of intensity versus. the frequency of light, which gives the spectrum. For more details of this technique, the reader is referred to the book by Griffiths and deHaseth (1986). A major advantage of the Fourier transform method is that one can monitor the entire spectrum continuously with a good sensitivity. Recently, FT–Raman spectrometers have also become commercially available (Chase and Robert, 1994; Lasema, 1996). In this case, a near-IR monochromatic source, such as the beam at 1064 nm from a CW Nd: YAG laser, is used to generate the Raman spectra. This laser is described in Chapter 5. The same Fourier transform technique using a Michelson interferometer is used for FT–Raman spectroscopy.

Spectral transition from a quantized state *i* (initial) to another quantized state *f* (final) does not occur at one (monochromatic) frequency ν (or wavelength λ). There is a spread of frequency ν of transition, called the *linewidth*, which is quantified by the term $\Delta\nu$ and is often defined as the width (spread of frequency) of a spectroscopic transition at half of the maximum value (also called full width at half maximum, or FWHM). The width corresponds to the broadening of a spectroscopic transition, also known as *line broadening*. There are two mechanisms of line broadening:

1. Inhomogeneous broadening caused by a statistical distribution of the same type of molecule or biopolymer among energetically inequivalent environment. For example, the biopolymer molecules may be distributed at various sites with different local structures, and thus interactions, producing a distribution of their site energies. This type of statistical broadening gives rise to a Gaussian distribution of the intensity, also called a *Gaussian lineshape*.
2. Homogeneous broadening due to the limited lifetime of the states involved in the transition. Here the frequency (energy) spread is caused by the condition imposed by the Heisenberg's uncertainty principle that

a finite lifetime (uncertainty in time) produces a corresponding uncertainty in energy (frequency), the products of their uncertainty being equal to the Planck's constant.

4.5 ELECTRONIC ABSORPTION SPECTROSCOPY

Electronic absorption is often used for a quantitative analysis of a sample (Tinoco et al., 1978). The basic absorption process uses a linear absorption of light from a conventional lamp (e.g., a Xe lamp), which provides a continuous distribution of the electromagnetic radiation from UV to near IR. The spectrometer used for this purpose is often called a *UV-visible spectrometer*, and it measures linear electronic absorption. This linear absorption is defined by the Beer–Lambert's law, according to which the attenuation of an incident beam of intensity I_o at frequency ν is described by an exponential decay whereby the output intensity I is given as

$$I(\nu) = I_0 e^{-k(\nu)bc} = I_0(\nu)10^{-\varepsilon(\nu)bc} \tag{4.13}$$

The more frequently used coefficient ε(ν) expressed in L (liters) mol^{-1} cm^{-1}, rather than the coefficient k, is called the molar extinction coefficient at frequency ν; c is the molar concentration (mol/L). This ε should not be confused with ε used in 4.1.1 and 4.2. This concentration c is not to be confused with the term c used earlier to represent the speed of light in vacuum. The term b (in cm) is the optical path length defined by the length of the absorbing medium through which the light travels. This situation is illustrated by Figure 4.5. In terms of the photon picture, a linear absorption process involves the absorption of a single linear photon by a molecule to excite an electron from a lower (ground) level to an excited level.

Other terms used to describe absorption or attenuation are

$$\text{Absorbance:} \quad A(\nu) = \log_{10}\left(\frac{I_0(\nu)}{I(\nu)}\right) = \varepsilon(\nu)bc$$

$$(\therefore \quad \text{A more familiar, simpler equation } A = \varepsilon(\nu)bc) \tag{4.14}$$

$$\text{Transmittance:} \quad T(\nu) = \frac{I(\nu)}{I_0(\nu)}$$

$$\text{Optical density (OD)} = \log_{10}(1/T)$$

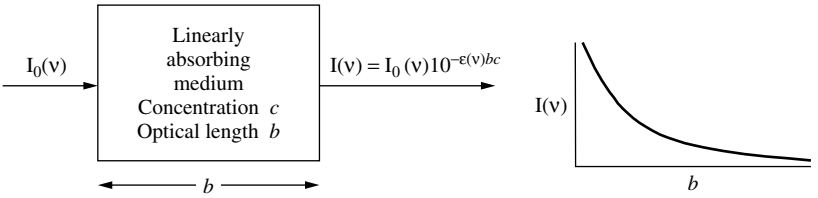

Figure 4.5. A linear absorption process.

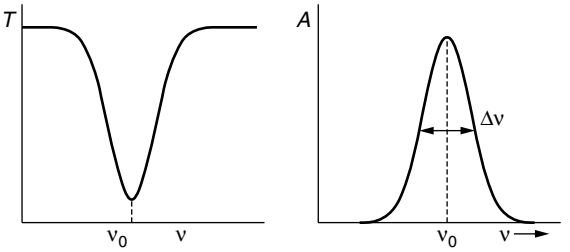

Figure 4.6. Absorption spectra in two different representations, obtainable on most commercial spectrometers.

The terms transmittance and optical density consider intensity losses due to both absorption and scattering when light travels through a medium. If the dominant contribution is due to absorption, then $OD = A$.

A typical absorption spectrum is exhibited as a plot of either T versus ν (or λ) or A versus ν. Typical absorption curves are shown in Figure 4.6. In the case of transmission, a continuous output from a lamp (or any broadband light source) shows a dip at the absorption frequency, ν. In the case of absorption, a peak appears at the absorption frequency ν_o. $\Delta\nu$, the full width at half maximum (FWHM), defines the width (frequency spread) of an absorption band (transition) at half of the maximum absorbance for the band.

The absorption spectra can be used to identify a molecular unit called a *chromophore* where an electron being excited is primarily localized. The transition in a chromophore produces absorption at a specific frequency (or frequency range). This absorption frequency can be dependent on the environment of the chromophore. Therefore, from the shift of the absorption band one can also probe the interactions in which the chromophore or the chromophore containing bioassemblies may be involved. Quantitatively, knowing the molar extinction coefficient $\varepsilon(\nu)$ at frequency ν for an identified chromophore, one can obtain the number density (concentration) of the chromophore.

In the case where a bioassembly (biological medium) may contain many absorbing chromophores of known molar excitation coefficients, the absorbance A is measured at a number of frequencies to obtain the concentrations of various chromophores.

Types of Electronic Transitions. The various electronic transitions encountered in a bioassembly are listed here (Atkins and de Paula, 2002):

(a) σ–σ^* *Transitions*. They involve the promotion of an electron from a bonding σ orbital to an antibonding σ^* orbital. The required energy for

this transition is large. For example, methane which only consists of C–H σ bonds exhibits a σ–σ* transition at 125 nm. These transitions, being of high energy (vacuum u.v.), are not suitable as spectroscopic probes of biomolecules.

(b) *d–d Transitions*. These transitions are encountered in an organometallic biomolecule involving a transition metal complex with organic ligands. Examples are hemoglobin involving Fe or a porphyrin involving Mn or Zn. The *d–d* transitions involve the excitation of an electron from one *d* orbital of the transition metal atom to another *d* level, the splitting between the *d* orbitals being determined by the surrounding ligands. The rare-earth complexes, also used for probing and imaging biological structures, involve transitions of *f* electrons in rare-earth ions (e.g., Eu^{3+}). The molar extinction coefficient ε for these transitions are low.

(c) π–π* *Transitions*. Associated with double bonds (e.g., C=C or C=O) or a conjugated structural unit, they involve the promotion of an electron from a bonding π orbital to an antibonding π* orbital. This absorption is often also represented as a ππ* transition. An important example of this type of transition is provided by the absorption in the 11-*cis*-retinal chromophore in eye which forms the basis of the photochemical mechanism of vision. These transitions are relatively strong, with the molar extinction coefficients ε being between 1000 to 10,000 $L\,mol^{-1}\,cm^{-1}$.

(d) *n*–π* *Transition*. It involves the excitation of an electron from a nonbonding orbital to an empty π* orbital. An example is the excitation of an electron of the electron pair in the outer nonbonding orbital of oxygen in a >C=O group to the π* MO of the C=O double bond. This absorption is also represented as an *n*π* transition. These are weak transitions (symmetry forbidden) with molar extinction coefficients in the range of 10 to 100 $L\,mol^{-1}\,cm^{-1}$.

(e) *Charge Transfer Transition.* This transition, giving rise to a charge transfer band, involves the excitation of an electron from the highest occupied orbital centered on one atom (or a group) to the lowest unoccupied orbital centered on another atom or a group. In the case of an organometallic molecule involving a transition element, a *d*π* transition promoting a *d* electron of the metal to an empty π* orbital of the ligand is called a metal-to-ligand charge-transfer transition (MLCT). The reverse π*d* or *nd* transition indicating a photoinduced charge transfer from the ligand to the metal is called the ligand-to-metal charge-transfer transition (LMCT).

Another type of charge transfer transition involves an asymmetric molecule containing both an electron donor and an electron acceptor. These transitions also occur where two neighboring molecules are involved, one of them of donor type, the other of acceptor type. Here a charge-transfer band

describes the transition to an excited state where there is an additional charge transfer from the electron donor to the electron acceptor producing an increase in the permanent dipole moment (i.e., the excited state is more ionic). Sometimes, a reverse process also occurs by which the dipole moment is reduced in the excited state. The molar extinction coefficients of the charge-transfer transitions can be quite large (greater than $10{,}000\,\mathrm{L\,mol^{-1}\,cm^{-1}}$).

A molecular specie, particularly a biomolecule, can exhibit a complex absorption spectra consisting of many absorption bands due to the various types of spectroscopic transitions discussed above.

A class of biological molecules, called *macrocycles*, which consist of a large-size π-electron-rich fused ring with a considerable delocalization of the π electrons, exhibits a number of π–π* transitions, because there are many π and π* orbitals (discussed in Chapter 2). An important example is a porphyrin such as the heme group in hemoglobin. The absorption spectra of porphyrins exhibit an intense π–π* transition in blue region at 400 nm which is called the "Soret band." In addition, there are a series of weaker π–π* transitions in the region, 450–650 nm which are called "Q bands." Chlorophyll *a*, discussed in Chapters 3 and 6, is a porphyrin derivative. Its absorption spectrum is shown in Figure 4.7. The absorption at 650 nm is responsible for the green color of chlorophyll, as the absorption in the red (650 nm) produces a green transmitted or scattered light (complementary color). Another examples is HPPH, a

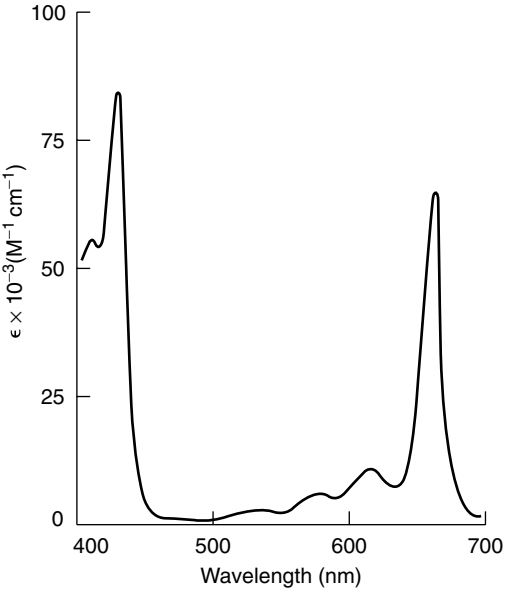

Figure 4.7. Absorption spectrum of chlorophyll *a* in ether. (Reproduced with permission from Goodwin and Mercer, 1972.)

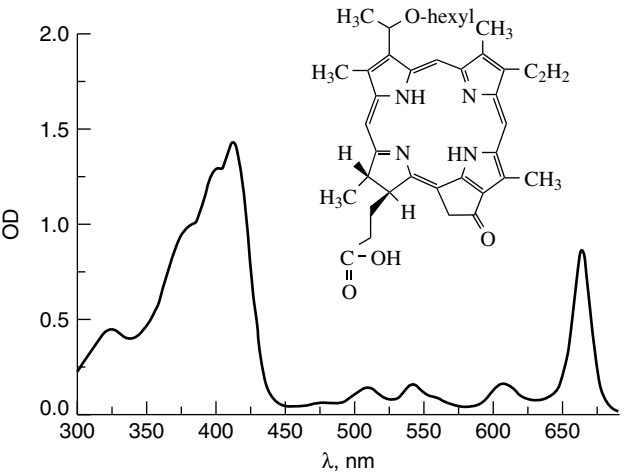

Figure 4.8. Absorption spectrum of HPPH (2-divinyl-2-(1-hexyloxyethyl)pyropheophorbide), a drug for photodynamic therapy. Water solution, $C = 22\,\mu M$.

porphrin based drug which is used in photodynamic therapy discussed in Chapter 12. The absorption spectrum of HPPH is shown in Figure 4.8.

4.6 ELECTRONIC LUMINESCENCE SPECTROSCOPY

Luminescence spectroscopy deals with emission associated with a transition from an excited electronic state to a lower state (generally the ground state) (Lakowicz, 1999; Lakowicz, 1991–2000). Biological molecules at room temperature exhibit fluorescence. Phosphorescence from a triplet excited state to the singlet ground state is rarely observed at room temperature. One-photon absorption produces a fluorescence band that is red-shifted (to a lower energy). This shift between the peak of the absorption band and that of the fluorescence band is called *Stokes shift*. The amount of Stokes shift is a measure of the relaxation process occurring in the excited state, populated by absorption. The difference in the energy of the absorbed photon and that of the emitted photon corresponds to the energy loss due to nonradiative processes. The Stokes shift may arise from environmental effect as well as from a change in the geometry of the emitting excited state. Figure 4.9 shows the absorption and the emission spectra of fluorescein, a commonly used dye.

Although fluorescence measurements are more sophisticated than an absorption (transmission) experiment, they provide a wealth of the information about the structure, interaction, and dynamics in a bioassembly. Also, fluorescence imaging is the dominant optical bioimaging technique for biophotonics.

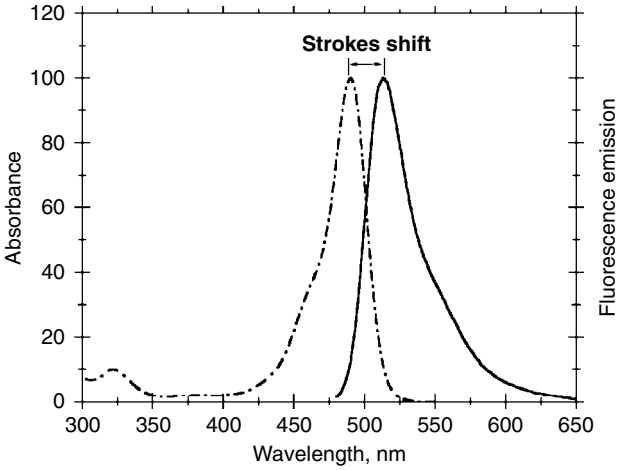

Figure 4.9. Absorption and fluorescence spectra of fluorescein in buffer (pH 9.0).

The fluorescence spectroscopy includes the study of the following features to probe the interaction and dynamics:

- Fluorescence spectra
- Fluorescence excitation spectra
- Fluorescence lifetime
- Fluorescence quantum efficiency
- Fluorescence depolarization

The fluorescence spectrum is obtained by exciting the molecules in a medium using a conventional lamp (a xenon lamp or a mercury xenon lamp). For excitation, a wavelength range corresponding to the absorption band is selected by a broad-band cutoff filter that only allows light at frequencies higher than that of emission. The fluorescence spectrum comprised of the fluorescence intensity as a function of frequency is obtained in a fluorescence spectrometer which includes a dispersive element (grating). Lasers are often used as a convenient and powerful source for one-photon excited fluorescence in which case it is called *laser-induced fluorescence* (LIF).

The fluorescence excitation spectra (sometimes simply referred to as *excitation spectra*) give information on the absorption (excitation) to the state that produces maximum fluorescence. Here the total fluorescence or fluorescence at the maximum frequency is monitored and the excitation frequency of a lamp or a tunable laser source is scanned to obtain the excitation spectrum. A maximum in the excitation spectrum corresponds to the frequency of a photon, where absorption produces maximum fluorescence.

Fluorescence lifetime represents the decay of fluorescence intensity. A simple fluorescence decay is exponential (first-order kinetics) involving a rate constant k which describes the decay of the fluorescence intensity I as $I = I_o e^{-kt}$ where I_o is the fluorescence intensity at the start of fluorescence (at $t = 0$). This behavior is called a *single exponential decay*. The rate constant k has two contributions, a radiative decay constant k_r characterized by a radiative lifetime τ_r and a nonradiative decay constant k_{nr}, characterized by a nonradiative lifetime τ_{nr}. Thus:

$$k = k_r + k_{nr} = \frac{1}{\tau_r} + \frac{1}{\tau_{nr}} = \frac{1}{\tau}$$
$$I = I_0 e^{-t/\tau} \tag{4.15}$$

From experimental measurements and fit of the decay to a single exponential, one obtains the overall fluorescence lifetime τ.

The radiative lifetime τ_r is inversely proportional to the strength of the transition dipole moment. It can be shown that it is related to the maximum extinction coefficient, $\varepsilon_{max}(\nu)$, of the absorption to the emitting state as follows:

$$\tau_r = \frac{10^{-4}}{\varepsilon_{max}(\nu)} \quad \text{sec} \tag{4.16}$$

In this equation, $\varepsilon_{max}(\nu)$ is in the unit of $\text{L mol}^{-1}\,\text{cm}^{-1}$.

Two methods of measurement of fluorescence lifetimes are:

(a) *Time Domain Measurement.* Here a short pulse, generally from a pulse laser source, excites the fluorescence, and decay of fluorescence is measured. The fluorescence lifetimes are generally in the range of nanoseconds to hundreds of picoseconds. For nanosecond decay, one utilizes a fast scope or a boxcar technique, whereas for lifetimes in hundreds of picoseconds, one utilizes a streak camera.

(b) *Phase Modulation Measurement.* This method utilizes a modulated excitation source (a lamp or a mode-locked laser, the latter of which is discussed in Chapter 5) and is based on the principle that a finite fluorescence lifetime causes the fluorescence waveform to be phase-shifted by an amount φ with respect to the waveform of the exciting light. This phase shift φ is related to the lifetime by the following equation:

$$\tan\varphi = \omega\tau \tag{4.17}$$

where ω is the modulation frequency (rate of modulation of exciting light). Therefore, from a measurement of the phase shift using a phase-sensitive detector (a lock-in amplifier), one can obtain the fluorescence lifetime τ. Several companies now sell instruments for phase-modulation lifetime measurements.

A rapidly growing field in photobiology is time-resolved fluorescence spectroscopy. Here the entire fluorescence spectrum is obtained as a function of time to monitor a spectral change induced by any dynamic change in the local configuration of the fluorescent unit called *fluorophore* or *fluorochrome*.

A nonexponential decay or a multiexponential decay (fit into a weighted sum of a number of exponentials) represents more complicated decay kinetics of the excited states. Some of the processes are (i) decay of the excited states through a number of channels (to different lower states), (ii) bimolecular decay involving interaction between two molecules, (iii) diffusion-controlled decay, and (iv) Förster energy transfer from an excitation donor molecular unit (the molecule absorbing the photon) to an excitation acceptor (the molecule which accepts the excitation and then may emit). Förster energy transfer is efficient when the emission spectrum of the donor molecule overlaps with the absorption spectrum of the acceptor molecule. With a significant overlap, the energy transfer is also called a *resonance energy transfer* and the fluorescence from the acceptor molecule is also called *fluorescence resonance energy transfer* (FRET). FRET has also found useful application for bioimaging, as discussed in Chapters 7 and 8 on bioimaging.

The rate of energy-transfer under a dipole–dipole transfer mechanism is inversely proportional to the sixth power of their separation. This dependence of energy transfer has been used to determine distance of separation between the excitation donor and acceptor sites and their mobilities.

The fluorescence quantum efficiency (also called *quantum yield*) Φ is defined as

$$\Phi = \frac{\tau_{\text{nr}}}{\tau_{\text{nr}} + \tau_r} = \frac{\kappa_r}{\kappa_r + \kappa_{\text{nr}}} \tag{4.18}$$

The quantum yield is a quantitative measure of the ratio of the number of photons emitted to the number of photons absorbed. In the absence of any nonradiative decay, the quantum yield Φ equals 1; that is, the excited state decays only by a radiative (fluorescence) process. This is the case producing the most efficient fluorescence; therefore, ideal fluorophores to be used as fluorescent probes should have a quantum yield as close as possible to 1. Fluorescence efficiency (quantum yield) serves as an excellent probe for the environment surrounding a fluorophore in a bioassembly.

Fluorescence depolarization is a measure of the loss of polarization of fluorescence by a number of dynamic effects such as rotation of the fluorophore. The polarization P of fluorescence is defined as

$$P = \frac{(I_{\parallel} - I_{\perp})}{(I_{\parallel} + I_{\perp})} \tag{4.19}$$

Another quantity also representing polarization of fluorescence is called *fluorescence emission* anisotropy, defined as $r = (I_{\parallel} - I_{\perp})/(I_{\parallel} + 2I_{\perp})$. Here $I_{\parallel}$ and $I_{\perp}$

are the fluorescence intensities polarized parallel and perpendicular to the polarization of excitation light.

The polarization ratio is determined by the relative orientation of the transition dipole moment (a vector) connecting the emitting excited state to the ground state (also called *emission dipole*) and the transition dipole moment connecting the ground state to the absorbing excited state (also called *absorption dipole*). For a randomly oriented rigid medium (molecular not being able to change the orientation) averaging over all possible molecular orientation yields $P = +1/2$ for the case when absorption (excitation) and emission dipoles are parallel, and $P = -1/3$ for the case when they are perpendicular to each other. A significant reduction in the magnitude of P indicates fluorescence depolarization. Therefore, a study of P or r for a fluorophore attached to a biopolymer or a biomembrane can provide information about the rotational mobility of its microenvironment. The P and r measurements are also used to measure rotational diffusion of molecules in biological systems such as membranes and cytosols (the biological systems are described in Chapter 3).

4.7 VIBRATIONAL SPECTROSCOPY

Vibrational spectroscopy comprises IR spectroscopy and Raman spectroscopy (Chalmers and Griffiths, 2002). In IR spectroscopy, the absorption of an IR (or far IR) photon produces a change in vibrational levels. The selection rule for a vibrational transition using a harmonic oscillator model discussed above is $\Delta v = 1$ for any vibrational mode. Overtone ($\Delta v > 1$) absorption is possible, but it is much weaker. The overtone absorption in water is, however, important in some wavelength ranges (i.e., ~$1.9\mu_m$.) The IR absorption spectrum consists of a series of $\Delta v = 1$ vibrational transitions for different vibrational modes of a molecule. For most vibrations, it involves an absorption from a $v = 0$ (zero-point vibrational level) to a $v = 1$ level. However, some low-frequency vibrations can be thermally populated, leading to absorption starting from $v \neq 0$. These are called *hot bands*. For a truly harmonic vibrational mode, all vibrational spacings between adjacent levels are equal and, therefore, all $\Delta v = 1$ transition will be at the same IR frequency. However, anharmonic interactions make the spacings change; therefore, different $\Delta v = 1$ transitions occur at different IR frequencies. The anharmonic effect has been discussed in Chapter 2.

The strength of an IR transition for a vibrational mode (described by a normal coordinate that consists of a vibrational displacement pattern) is determined by the dipole moment (μ) derivative $d\mu/dQ_k$, where Q_k is the normal coordinate for vibrational mode k. The normal mode of vibration (displacement) producing the largest change in the dipole moment exhibits the strongest vibrational transition in IR (most intense band in the IR spectra). For a molecule with an inversion symmetry, only u-type vibrational modes are excited by IR absorption.

In Raman spectroscopy, a photon of frequency in the visible spectral range (generally of an argon-ion laser line of wavelength 488 nm or 514.5 nm) is scattered to a shifted frequency light, the difference in energy being the vibrational energy (Farrano and Nakamoto, 1994). If the frequency of the scattered photon is lower than that of the incident photon, a vibrational transition from a lower level to a higher level is induced. This process is called *Stokes Raman scattering*, and the corresponding peaks in the Raman spectra are called *Stokes Raman lines*. If the scattered photon is of higher frequency than the frequency of the incident photon, a transition from a thermally populated higher vibrational level to a lower level is induced, giving rise to what is known as *anti-Stokes lines*.

As discussed in Section 4.1.1, Raman scattering is derived from the polarizability term, α. The strength of the Raman transition for a vibrational mode (normal mode) with normal coordinate Q_k is determined by the polarizability derivative $d\alpha/dQ_K$. The larger the derivative (the larger the change in the polarizability due to the vibrational displacement of the normal mode), the stronger is the Raman transition due to this normal mode of vibration.

The efficiency of Raman scattering is weak: Typically, one out of 10^5 photons is scattered to produce a frequency-shifted photon. For this reason, one uses a laser source (a source of high photon density), which provides a monochromatic excitation laser at frequency ν_o. The intensity of scattered photon frequency is plotted as a function of frequency shift ($\nu_o - \nu$). The different peaks correspond to Raman excitations of various vibrations of frequency $\nu_R = (\nu_o - \nu)$. Thus, one obtains a vibrational spectrum.

For a centrosymmetric molecule with an inversion symmetry, only *g*-type vibrational modes are excited by Raman scattering. Therefore, for a centrosymmetric molecule, there is a mutual exclusion between the vibrational modes that are Raman active (*g*-type) and those that are IR-active (*u*-type).

The $\Delta v = 1$ transition gives rise to what are called *fundamental bands*, while $\Delta v > 1$ are called *vibrational overtones*. Also, Raman scattering can excite a combination of two vibrational modes. This type of coupled transitions gives rise to what are called *combination bands*.

IR spectroscopy (more routinely now in the form of FT–IR spectroscopy) and Raman spectroscopy are used as complementary techniques to provide information on various vibrational transitions or vibrational bands. These vibrational bands provide a detailed fingerprint of different bonds, functional groups, and conformations of molecules, biopolymers, and even microorganisms. Even though vibrational transitions are considerably weaker than the electronic transitions, they are much richer in structures (a large number of vibrational modes and corresponding bands, well resolved in the spectra) compared to room-temperature electronic spectra (whether absorption or fluorescence), which are relatively featureless. Therefore, vibrational spectroscopy has found wide application in structural characterization of biological materials and in probing interaction dynamics (Table 4.3) (Stuart, 1997; Thomas, 1999). As examples of illustrations of vibrational spectra of molecules of

TABLE 4.3. Representative Vibrational Frequencies of Some Bonds

Hydroxyl (OH)	3610–3640 cm^{-1}
Amines (NH)	3300–3500 cm^{-1}
Aromatic rings (CH)	3000–3100 cm^{-1}
Alkenes (CH)	3020–3080 cm^{-1}
Alkanes (CH)	2850–2960 cm^{-1}
Triple bonds (C≡C)	2500–1900 cm^{-1}
Double bonds (C=C)	1900–1500 cm^{-1}

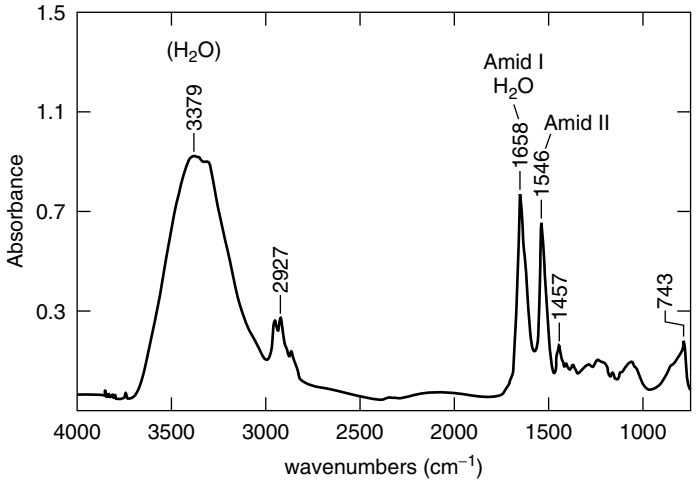

Figure 4.10. Typical IR absorption spectrum of hydrated protein film, in this case intrinsic cell membrane protein bacteriorhodopsin. (Reproduced with permission from Elsevier Science; Colthup et al., 1990.)

biological interested, presented here are the IR spectra of a protein, bacteriorhodopsin, and the Raman spectra of insulin (Figures 4.10 and 4.11).

As discussed above, Raman spectroscopy is not as sensitive as IR spectroscopy because of the relative inefficiency of Raman scattering. Furthermore, if the sample exhibits any intrinsic fluorescence (also called *autofluorescence*, which is discussed in Chapter 6), the fluorescence signal is many orders of magnitude higher than that of Raman. Therefore, the fluorescence background can overwhelm the Raman bands, limiting the utility of Raman spectroscopy. However, Raman spectroscopy offers a number of distinct advantages over the IR spectroscopy for vibrational analysis and probing; some of them are as follows:

- Ability to obtain vibrational spectra in an aqueous medium, because water shows very weak Raman scattering. On the other hand, IR absorp-

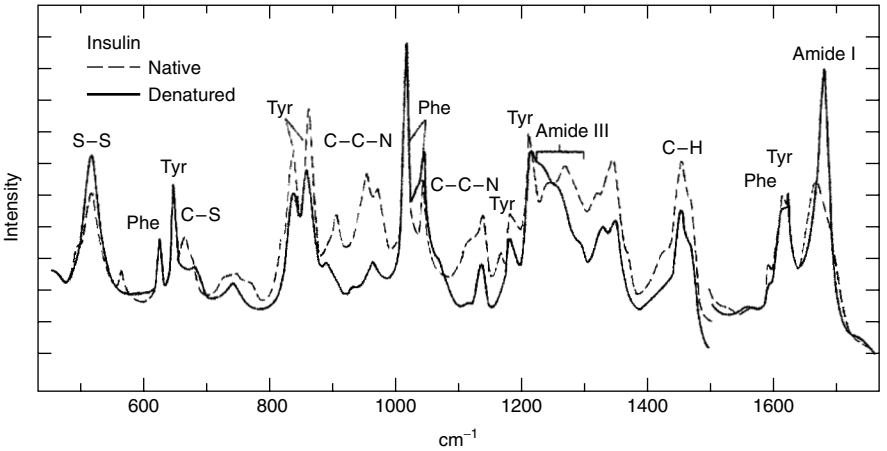

Figure 4.11. Raman spectra of native and denatured insulin in the solid state. (Reproduced with permission from Elsevier Science; Yu et al., 1972.)

tion by water is very strong, which overwhelms absorption by other cellular constituents.

- Ability to use samples in their natural form, (liquid, solid, gels). No special sample preparation is needed.
- Ability to focus the visible wavelength laser excitation source to a micron size spot. This allows one to obtain Raman spectra of microsize dimensions such as a single cell.
- Ability to selectively probe a specific chemical segment or subcellular component. This goal is achieved by resonantly enhancing the Raman scattering from the desired chemical unit by using an excitation frequency close to its absorption band.

The last point is illustrated by the selective enhancement of the Raman bands due to the β-carotene structural unit in the photosynthetic protein (Ghanotakis et al., 1989), by using the 488-nm excitation wavelength, which is close to the absorption band of β-carotene. The resonance-enhanced Raman spectrum is compared with the ordinary Raman spectrum in Figure 4.12.

A growing field is ultraviolet resonance Raman spectroscopy, whereby the excitation provided around 230–250 nm resonantly enhances the bands due to the aromatic residues of proteins. The UV resonance Raman spectroscopy has been used to derive specific interactions concerning the noncovalent interactions (such as hydrogen bonding) of important aromatic residues, tyrosine and tryptophan (Chi and Asher, 1998).

Another method of enhancement of Raman transitions is provided by surface-enhanced Raman spectroscopy (Lasema, 1996). Surface-enhanced Raman spectroscopy refers to the method where the intensity of the Raman

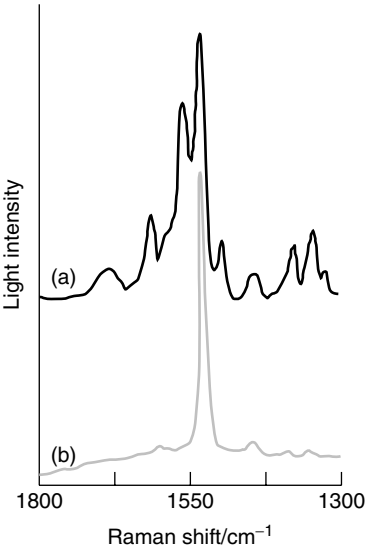

Figure 4.12. (a) The Raman spectra of photosynthetic protein obtained using 407-nm excitation and exhibiting Raman bands of both chlorophyll *a* and β-carotene; (b) resonantly enhanced Raman spectra, obtained with 488-nm excitation, showing the bands of β-carotene. (Reproduced with permission from Ghanotakis et al., 1989.)

vibrational transitions of a molecule is enhanced by deposition of molecules on the surface of a microscopically rough metal, metal colloids, and metal nanoparticles. The enhancement is by several orders of magnitude. The metals providing the largest enhancement are silver and gold and have been used to increase the Raman spectroscopic sensitivity for the study of molecules and biopolymers such as proteins.

4.8 SPECTROSCOPY UTILIZING OPTICAL ACTIVITY OF CHIRAL MEDIA

As discussed in Chapter 2, optically active chiral media consist of structures such as those containing an asymmetric carbon (chiral center) or a helical structure (such as in protein and DNA). These media interact differently with right- and left-circularly polarized light. One manifestation, already discussed in Chapter 2, is rotation of plane of polarization of a linearly polarized light as it propagates through a chiral medium. This effect results from a difference in the phase velocities due to different refractive indices for right- and left-circularly polarized light. As a linearly polarized light can be considered as composed of right- and left-circularly polarized light with equal amplitudes, this difference in phase velocity creates a phase difference between the right- and left-circularly polarized components, which amounts to rotation of the

plane of polarization. The variation of optical rotation as a function of wavelength is called *optical rotary dispersion* (ORD).

Spectroscopic response of a chiral medium also shows differences in interaction with left- and right-circularly polarized light. The three spectroscopic effects discussed here are circular dichroism (CD), vibrational circular dichroism (VCD), and Raman optical activity (ROA). These effects provide valuable spectroscopic probes for structure, interactions, and functions of chiral biological matter. These three spectroscopic methods utilizing chirality are discussed here.

Circular Dichroism (CD). Circular dichroism refers to the difference in the absorption of left- and right-circularly polarized light to create an electronic transition (Berova et al., 2000). In other words, the extinction coefficient ε (or the absorbance A) of equation (4.13) for an electronic transition (electronic band) are different for the left and right circular polarizations. This is to be expected from optical principles. As shown in equation (4.10), the real part of the refractive index gives rise to phase information (propagation, refraction, etc.). A change in the real part of refractive index, from left- to right-circularly polarized light, determines optical rotary strength and its dispersion. The imaginary part of the refractive index represents absorption. The corresponding change in the imaginary part of the refractive index determines circular dichroism. The change in the real part of the refractive index produces a corresponding change in the imaginary part of the refractive index because the two are related by a well-known equation called *Kronig–Kramers transformation*. Thus, ORD, which gives optical rotation as a function of wavelength, and CD are related.

The CD spectra are typically measured as the difference in the absorbance of a molecule for the left- and right-circularly polarized light for varying wavelength λ (or wavenumber ν) as

$$\Delta A(\lambda) = A_{\mathrm{L}}(\lambda) - A_{\mathrm{R}}(\lambda) \tag{4.19a}$$

Here A_L is the absorbance for the left-circularly polarized light and A_R is the absorbance for the right-circularly polarized light. The CD spectra are also frequently expressed as the difference in the molar extinction coefficient defined as

$$\Delta\varepsilon(\lambda) = \varepsilon_{\mathrm{L}}(\lambda) - \varepsilon_{\mathrm{R}}(\lambda) \tag{4.19b}$$

Based on this definition, the unit used for representing circular dichroism is molar circular dichroism, also called delta epsilon in $\mathrm{L\,mol^{-1}\,cm^{-1}}$. Another unit used for CD is mean residue ellipticity in degree $\mathrm{cm^2\,dmol^{-1}}$. The ellipticity unit is derived from the conceptual visualization that two equal amplitudes of opposite circular polarization (left and right) form a linearly polarized light. If the material exhibits circular dichroism—that is, left- and-right circularly polarized

lights are absorbed to a different extent—then their amplitudes (contributions) will not be the same, resulting in an elliptical behavior of the distribution of electric field. The ellipticity is quantified as the tangent of the ratio of the two elliptical axes (perpendicular contributions) called minor and major.

Circular dichroism spectroscopy has been used for a number of applications in structural biology. Some of them are as follows:

- Determination if a protein is folded and thus of its secondary and tertiary structure
- Comparison of structures of proteins obtained from different sources or structures of different mutants of the same protein
- Study of conformational stability of a protein under various environmental perturbations (temperature, pH, buffer composition, addition of stabilizers and excipients)
- Determination of the effect of protein–protein interactions on the protein conformation

The application of circular dichroism to biology is illustrated here with the example of identification of secondary and tertiary structures of proteins. The far-UV spectral region (190–250 nm) is representative of the peptide bond. Thus, the CD spectra in this region arise if the peptide bond is in a regular, folded environment, thus providing information on the secondary structure of a protein. Figure 4.13 compares the CD spectra of different conformations: alpha helix, beta sheet, and random coil structures of poly-lysine.

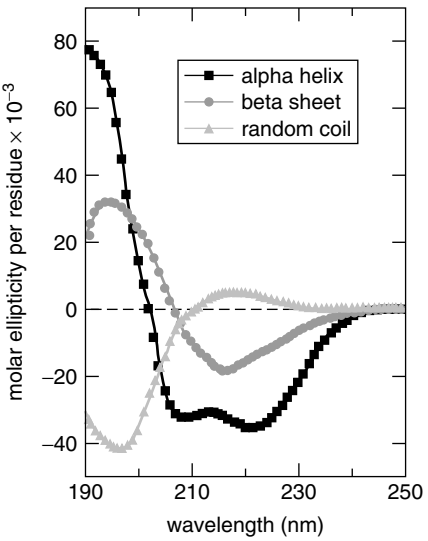

Figure 4.13. CD spectra of the three conformations of poly-lysine. (Reproduced with permission from http://www.ap-lab.com/circular_dichroism.htm.)

The appropriate fraction of each structure present in any protein can be obtained by fitting its far-UV CD spectrum as a weighted sum of reference spectra for each structure.

The CD spectra of proteins in the near-UV spectral region of 250–350 nm are characteristics of aromatic amino acids and disulfide bonds. The CD signal in this region, therefore, is a sensitive probe of the overall tertiary structure of a protein. For example, the presence of a significant CD signal in the near-UV region indicates that the protein is folded into a well-defined structure. Thus, the near-UV CD spectra can be used as a sensitive probe for any change in the tertiary structure due to protein–protein interactions or any external perturbation such as changes in the solvent.

Vibrational Circular Dichroism (VCD). Just like the electronic transitions discussed above giving rise to CD, vibrational transitions also exhibit optical activity in their response to left- versus right-circularly polarized light (Berova et al., 2000). The general term for optical activity of vibrational transitions is vibrational optical activity (VOA). The vibrational circular dichroism (VCD) is one type of VOA which specifically refers to the difference in vibrational spectrum of a molecule for left- versus right-circularly polarized light as obtained by using the IR spectroscopic technique discussed above (Nafie et al., 2002). It is, therefore, an extension of CD spectroscopy from UV–visible (electronic transitions) to near-IR and IR (vibrational transitions).

Dramatic progress in the instrumentation has lead now to the availability of a VOA spectrometer from a number of commercial sources, which makes it possible for a nonspecialist in this field to use VCD for a variety of applications. For example, a dedicated FT–IR spectrometer is available from Biomen-Bio Tools of Quebec, Canada. This instrument is constructed on one optical platform that includes the interferometer (for FT–IR) and all the VCD optical components. The advantage of VCD over the UV–visible CD (due to electronic absorption) is derived from the rich structural sensitivity of IR spectroscopy due to a large number of vibrational transitions representing the various vibrations (vibrational modes) of a molecule. An important application of VCD is the determination of absolute three-dimensional configuration of a biomolecule. This determination utilizes a comparison of the experimentally measured VCD spectrum to that theoretically calculated. If there is a good correlation of the bands and their signs, then the theoretical absolute configuration corresponds to that of the unknown sample. The theoretical VCD spectra can be calculated using accurate *ab initio* methods, introduced briefly in Chapter 2 (Nafie et al., 2002). Figure 4.14 provides an example of the correlation between the experimental and the calculated IR spectra and the corresponding VCD spectra of (+) *trans*-pinene (Nafie et al., 2002). The molecule α-pinene is routinely used as a standard for VCD because it has a strong VCD signal., it can be sampled in high concentration as a neat (pure) liquid and has a rigid stereoconfiguration due to its fused ring structure. According to the convention, a positive VCD band corresponds with the case

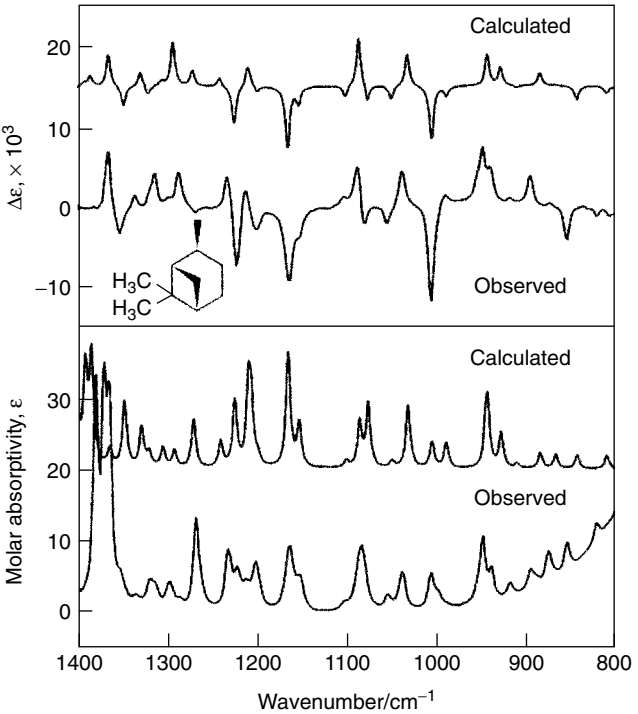

Figure 4.14. Comparison of the experimental and theoretically calculated IR spectra and the corresponding VCD spectra of (+) *trans*-pinene under conditions of neat liquid using a sample pathlength of 55 µm. (Reproduced with permission from Nafie et al., 2002.)

where the left-circularly polarized light is absorbed more than the right-circularly polarized light.

Proteins exhibit strong VCD in the amide vibrational band regions of the IR spectrum (Keiderling, 1994). VCD can be used to study the secondary structures of peptides and proteins, as well as the conformations of nucleic acids and sugars. The chirality in nucleic acids is derived from the sugar-phosphate backbone. The VCD technique is particularly sensitive to the base stacking regions between 1750 and 1550 cm^{-1} (Wang and Keiderling, 1992).

VCD is also emerging as an important tool for pharmaceutical research (Dukor and Nafie, 2000). VCD can be used to determine the optical purity of manufactured drugs and to characterize a biologically active enantiomeric form of a particular drug.

Raman Optical Activity (ROA). The definition of Raman optical activity (ROA) is more complex than that of VCD, because a Raman transition, as discussed above, involves the polarization characteristics of both the incident beam and the frequency shifted Raman scattered beam. The original form of

ROA, sometimes also called as incident circular polarization (ICP)ROA is defined as the difference in the intensity of Raman scattering, measured using right- and left-circularly polarized incident light (Barron et al., 2002; Nafie and Freedman, 2001). Hence, the convention used for (ICP)ROA is opposite (right minus left) to that used for VCD where the difference is measured between left-and right-circularly polarized light (left minus right for VCD). (ICP)ROA is commonly used for studying ROA spectra. Other forms of ROA involve changing the polarization state of the scattered radiation between the right-circularly polarized and the left-circularly polarized states. Another variable in the ROA is the scattering angle; nearly all current ROA measurements are carried out using a backscattering geometry which minimizes the interference due to high background scattering from the solvent and any residual fluorescence.

Like VCD, ROA probes the effect of chirality on vibrational transitions. As discussed above, IR spectra and Raman spectra can provide complementary information on the vibrational bands and thus can be used as fingerprints for a molecular structure and its conformation. Similarly, VCD and ROA are complementary techniques to study vibrational optical activity and use it to determine secondary and tertiary structure of biopolymers, study protein folding, elucidate the conformation of nucleic acids and sugars, and determine the optical purity of a pharmaceutical compound. However, due to the lower sensitivity of the available Raman techniques compared to that of FT–IR spectroscopy, ROA has not been used as widely as VCD. Thus, no commercial ROA instrument is available at the time of writing of this book.

Despite its lower sensitivity compared to VCD, ROA provides some distinct advantages. These advantages are derived from those of Raman over IR as discussed above. A primary one is the use of H_2O and D_2O as excellent solvents for Raman studies of biopolymers. An important application of ROA has been in fold determination, which is of special importance in post-genome structural biology. ROA can be used to discriminate between extended helix (as in the coat proteins of filamentous bacteriophases), the globin fold (as in the serum albumins), and the helix bundle (as in tobacco mosaic virus). As a sufficiently large set of protein reference spectra becomes available, ROA may become a routine technique for reliable determination of protein fold. ROA can also be useful for the study of non-native protein states such as molten globules and native states containing mobile regions.

4.9 FLUORESCENCE CORRELATION SPECTROSCOPY (FCS)

The contents of this section are derived from the following website: **www.probes.com/handbook/boxes/1571.html**. This website provides a very lucid description of the method of fluorescence correlation spectroscopy. Another suggested reference is a review by Thompson (1991).

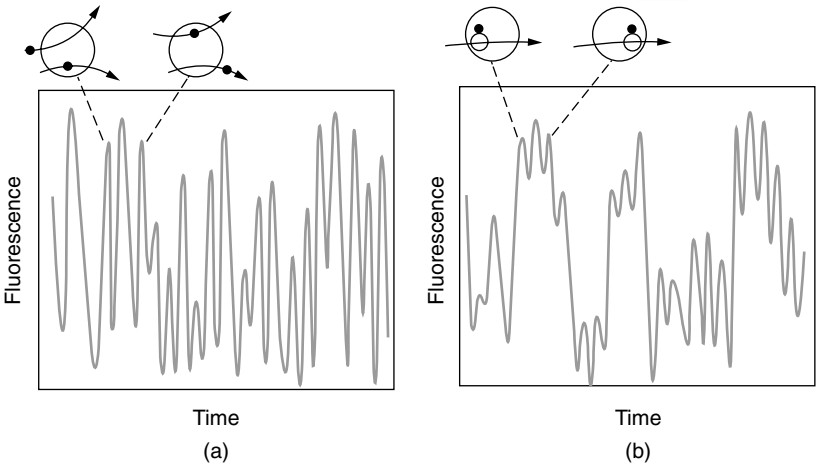

Figure 4.15. (a) Fluorescence intensity fluctuations caused by diffusion of small molecules; (b) fluorescence intensity fluctuations caused by diffusion of less mobile biopolymers. (Reproduced with permission from the highlighted website.)

In fluorescence correlation spectroscopy, often abbreviated as FCS, spontaneous fluorescence intensity fluctuations in a microscopic volume consisting of only a small number of molecules is monitored as a function of time. The volume typically sampled is about 10^{-15} L (or a femtoliter) compared to that of 0.1–1.0 mL or even larger, typically sampled by conventional fluorescence spectroscopy. The fluorescence intensity fluctuations measured by FCS relates to dynamical processes occurring in the interrogation volume. These dynamical processes can be due to changes in the number of fluorescing molecules due to their diffusion in and out of the microscopic volume sampled. They can also represent a change in the fluorescence quantum yield due to processes occurring in the interrogation volume.

Fluctuations caused by diffusion of molecules depend on their size. Rapidly diffusing small molecules produce rapid intensity fluctuations as shown in Figure 4.15a. In contrast, large molecules and biopolymers such as proteins or protein bound ligands exhibit slowly fluctuating patterns of bursts of fluorescence, as shown in Figure 4.15b. Quantitatively, the fluorescence intensity fluctuation is characterized by a function $G(\tau)$, called the *autocorrelation function*, which correlates the fluctuation $\delta F(t)$ in fluorescence intensity at time t with that $[\delta F(t + \tau)]$ at time $(t + \tau)$, where τ is a variable time interval., averaged over all data points in the time series. Thus, $G(\tau)$ is defined as

$$G(\tau) = \frac{< \delta F(t) \cdot \delta F(t+\tau) >}{< F(t) >^2} \tag{4.19c}$$

The brackets in this expression represent the average over all data points at different times t.

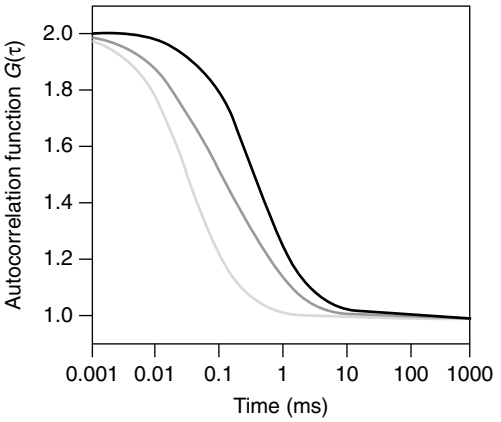

Figure 4.16. Simulated FCS autocorrelation functions representing a free ligand and a corresponding bound ligand. The intermediate curve represents a mixture. (Reproduced with permission from the above highlighted website.)

A typical autocorrelation function $G(\tau)$ plotted as a function of time interval τ is represented in Figure 4.16 for a free ligand (low molecular weight) which can diffuse faster and a bound ligand which diffuse slower. The initial amplitude of the autocorrelation function is inversely proportional to the number of molecules in the sampled volume. The decay of the autocorrelation function is fast for a free ligand and relatively slow for a bound ligand. Thus, the decay behavior of $G(\tau)$ provides information on the diffusion rates of the fluorescing species.

FCS is an excellent probe for monitoring biomolecular association and dissociation processes. With the recent progress of increase of detection sensitivity for fluorescence to the limit of single molecule detection, FCS has emerged as a valuable tool to investigate a variety of biological processes such as protein–protein interactions, binding equilibria for drugs, and clustering of membrane bound receptors. Another extension of FCS is dual color cross-correlation, which measures the cross-correlation of the time-dependent fluorescence intensities of two different dyes fluorescing at different wavelengths (Schwiller et al., 1997). This method has the advantage that cross-correlated fluorescence is only generated by molecules or biopolymers fluorescently labelled (chemically attached) with both dyes, allowing quantitation of interacting dyes.

HIGHLIGHTS OF THE CHAPTER

- Light–matter interactions involve four types of energy exchange between them: (i) absorption of a photon, (ii) spontaneous emission of a photon, (iii) stimulated emission of a photon, and (iv) Raman scattering.

- The absorption of a photon leads to a transition (jump) from a quantized lower energy state of a molecule (or atom), often called the *ground state*, to its higher state, often called an *excited state*.
- The spontaneous emission of a photon brings back the molecule (or atom) from its excited state to a lower energy state.
- Stimulated emission of a photon occurs when there is a population inversion—that is, more molecules (or atoms) are in the excited state than in the ground state. The stimulated emission requires triggering by (thus the presence of) another photon of same frequency.
- Raman scattering produces photons of energy (frequency) different from the energy (frequency) of the incident photon; the difference in energy is either deposited in a molecule to create an excited state, usually a vibrationally excited state (in a Stokes process), or taken away from a vibrationally excited molecule (in an anti-Stokes process).
- The processes of absorption, spontaneous emission, and stimulated emission are phenomenologically described by Einstein's model.
- Quantum mechanically, the strength of a transition between two energy states is characterized by the magnitude of a quantity called the transition dipole moment, which connects the two states through charge redistribution.
- The Lapote rule provides a qualitative guide if a transition between two states is dipole allowed (i.e., the transition dipole moment has nonzero value) and will occur with great probability (strength) or whether it is dipole forbidden (i.e., the transition dipole moment has a zero value) and may only be weakly manifested because of other interactions.
- Interaction of light with bulk matter is described in terms of the process of reflection, refraction, scattering, and absorption and is determined by the refractive index properties of the bulk and the surrounding medium.
- An excited energy state may dispose of the excess (excitation) energy by a photophysical process, by a photoinduced electron transfer process, or by performing a photochemical process.
- The various photophysical processes are (i) radiative, in which the excess energy is emitted as a photon (spontaneous and stimulated emission); (ii) nonradiative, in which the excess energy is dissipated as heat; (iii) energy transfer in which the excess energy is transferred to another neighboring molecule, and (iv) excited state complex formation (association) between neighboring molecules.
- The various radiative and nonradiative processes in an organic molecule are often described by the so-called Jablonski diagram.
- A nonradiative transition between two electronic states of same spin being spin-allowed (spin conserving) is called the process of *internal conversion*, and that between two states of different spin occurs by a spin-forbidden (and thus weak) process of *intersystem crossing*.

- The emission from a higher electronic state to a lower electronic state of same spin (spin conserving) is called *fluorescence* and is much stronger than that of the process of phosphorescence, which is between two states of different spin.
- Spectroscopy is a branch of light interactions which deals with the study of dependence of light absorption or emission on the wavelength of light; the plot of the strength of the transition as a function of wavelength is called the *spectrum*.
- Electronic absorption spectroscopy dealing with absorption between two electronic states is quantitatively expressed by Beer–Lambert's law under ordinary light intensity consideration. Here only one photon absorption per molecule occurs at a time (hence, linear absorption).
- Electronic fluorescence spectroscopy allows for a multiparameter analysis using its emission spectra (emission as a function of wavelength), excitation spectra (strength of emission as a function of excitation wavelength), lifetime of emission (decay of emission), and the polarization characteristics of the emitted light.
- Vibrational spectroscopy gives information on the vibrational frequencies (energies) associated with different chemical bonds and associated bond angles. These vibrational frequencies are used as a detailed chemical fingerprint for various bonds, bond angles, and chemical units and, thus, for identification of molecules.
- The two types of vibrational spectroscopy are (a) IR, which involves absorption of an IR photon to create vibrational transition, and (b) Raman, where a Raman scattering process generates a vibrational excitation.
- IR is more sensitive than Raman and is often used to get detailed structural information on organic molecules in solid or liquid or nonaqueous forms.
- For biological samples, often in an aqueous environment, Raman spectroscopy is more useful because water produces only weak Raman scattering but has very strong IR transitions.
- Resonance Raman spectroscopy offers the prospect of selectively exciting the vibrations of a particular molecular unit by choosing the incident wavelength at which this unit absorbs.
- Circular dichroism, referring to the difference in the electronic absorption of left- and right-circularly polarized light in a chiral structure, is very useful for determining the secondary and tertiary structures, and interactions of a biopolymer.
- Vibrational circular dichroism refers to the difference in IR vibrational spectra of a chiral molecule for left- versus right-circularly polarized light. It is useful for determining absolute three-dimensional configuration of a biopolymer.

- Raman optical activity is the difference in the Raman scattering of a chiral molecule using the right- and left-circularly polarized incident light.
- Fluorescence correlation spectroscopy measures the correlation between fluorescence intensities at two different times, from a microscopic volume containing only a small number of molecules. It provides information on fluorescent intensity fluctuation due to processes such as molecular diffusion and protein–ligand association.

REFERENCES

Atkins, P., and dePaula, J., *Physical Chemistry*, 7th edition, W.H. Freeman, New York, 2002.

Barron, L. D., Hecht, L., Blanch, E. W., and Bell, A. F., Solution, Structure and Dynamics of Biomolecules from Raman Optical Activity, *Prog. Biophys. Mol. Biol.* **73**, 1–49 (2000).

Berova, N., Nakanishi, K., and Woody, R. W., eds., *Circular Dichroism: Principles and Applications*, 2nd edition, Wiley-VCH, New York, 2000.

Chalmers, J. M.. and Griffiths, P. R., *Handbook of Vibrational Spectroscopy*, Vol. 5, *Applications in Life, Pharmaceutical and Natural Sciences*, Wiley Milan, Italy, 2002.

Chase, D. B., and Robert, J. F., eds., *Fourier Transform Raman Spectroscopy: From Concept to Experiment*, Academic Press, San Diego, 1994.

Chi, Z., and Asher, S. A., UV Raman Determination of the Environment and Solvent Exposure of Tyr and Trp Residues, *J. Phys. Chem. B*. **102**, 9595–9602 (1998).

Colthup, N. B., Daly, L. H., and Wiberly, S. E., *Introduction to Infrared and Raman Spectroscopy*, Academic Press, Boston, 1990.

Dukor, R. K., and Nafie, L. A., Vibrational Optical Activity of Pharmaceuticals and Biomolecule, in R. A. Meyers, ed., *Encyclopedia of Analytical Chemistry*, John Wiley & Sons, Chichester, 2000, pp. 662–676.

Farrano, J. R., and Nakamoto, K., *Introductory Raman Spectroscopy*, Academic Press, San Diego, 1994.

Feynman, R. P., Leighton, R. B., and Sands, M., *The Feynman Lectures on Physics*, Vol. 1, Addison-Wesley, Reading, MA, 1963.

Ghanotakis, D. F., dePaula, J. C., Demetriou, D. M., Bowlby, N. R., Petersen, J., Babcock, G. T., and Yocum, C. F., Isolation and Characterization of the 47 kDa Protein and the D1, D2, Cytochrome B-559 Complex, *Biochim. Biophys. Acta* **974**, 44–53 (1989).

Goodwin, T. W., and Mercer, E. I., *Introduction to Plant Biochemistry*, Pergamon Press, New York, 1972.

Griffiths, P. R., and deHaseth, J. A., *Fourier Transform Infrared Spectrometry*, John Wiley & Sons, New York, 1986.

Keiderling, T. A., Vibrational Circular Dichroism Spectroscopy of Peptides and Proteins, in K. Nakanishi, N. D. Berova, and R. W. Woody, eds., *Circular Dichroism Principles*, Wiley-VCH, New York, 1994, pp. 497–521.

Kruglik, S. G., Mojzes, P., Mizutani, Y., Mizutani, Y., Kitagawa, T., and Turpin, P.-Y., Time-Resolved Resonance Raman Study of the Exciplex Formed Between Excited Cu-Porphyrin and DNA, *J. Phys. Chem. B* **105**, 5018–5031 (2001).

Lakowicz, J. R., *Principals of Flouresence Spectometry*, Kluwer/Plenum, New York, 1999.

Lakowicz, J. R., ed., *Topics in Fluorescence Spectroscopy,* Vol. 1 (1991), Vol. 2 (1991), Vol. 3 (1992), Vol. 4 (1994), Vol. 5 (1997), Vol. 6 (2000), Plenum, New York.

Lasema, J. J., ed., *Modern Techniques in Raman Spectroscopy*, John Wiley & Sons, New York, 1996.

Levine, I. N., *Quantum Chemistry*, 5th edition, Prentice-Hall, Upper Saddle River, NJ, 2000.

Mojzes, P., Chinsky, L., and Turpin, P.-Y., Interaction of Electronically Excited Copper (II) Porphyrin with Oligonucleotides and Polynucleotides—Exciplex Building Process by Photoinitiated Axial Ligation of Porphyrin to Thymine and Uracil Residues, *J. Phys. Chem. B* **97**, 4841–4847 (1993).

Nafie, L. A., Dukor, R. K., and Freedman, T. B., Vibrational Circular Dichroism, in J. M. Chalmers and P. R. Griffiths, eds., *Handbook of Vibrational Spectroscopy*, Vol. 1, John Wiley & Sons, Chichester, 2002, pp. 731–744.

Nafie, L. A., and Freedman, T. B., Biological and Pharmaceutical Applications of Vibrational Optical Activity, in H. U. Gremlich and B. Yan, eds., *Infrared and Raman Spectroscopy of Biological Materials*, Marcel Dekker, New York, 2001, pp. 15–54.

Prasad, P. N., and Williams, D. J., *Introduction to Non-Linear Optical Effects in Molecules and Polymers*, John Wiley & Sons, New York, 1991.

Sauer, K., Biochemical Spectroscopy, *Methods in Enzymology*, Vol. 246, Academic Press, San Diego, 1995.

Schwiller, P., Meyer-Almes, F. J., Rigler, R., Dual-Color Fluroescence Cross-Correlation Spectroscopy for Multicomponent Differential Analysis in Solution, *Biophys. J.* **72**, 1878–1886 (1997).

Stuart, B., *Biological Applications of Infrared Spectroscopy*, John Wiley & Sons, New York, 1997.

Thomas, G. J., Jr., Raman Spectroscopy of Protein and Nucleic Assemblies, *Annu. Rev. Biophys. Biomol. Struct*. **28**, 1–27 (1999).

Thompson, N. L., Fluorescence Correlation Spectroscopy, in J. R. Lakowicz, ed., *Topics in Florescence Spectroscopy*, Vol. 1, Kluwer/Plenum, New York, 1991.

Tinoco, I., Jr., Sauer, K., and Wang, J. C., *Physical Chemistry, Principles and Applications in Biological Sciences*, Prentice-Hall, Englewood Cliffs, NJ, 1978.

Wang, L., and Keiderling, T. A., Vibrational Circular Dichroism Studies of the A-to-B Conformational Transition in DNA, *Biochemistry* **31**, 10265–10271 (1992).

Yu, N. T., Liu, C. S., and O'Shea, D. C., Lasar Raman Spectroscopy and the Confirmation of Insulin and Proinsulin, *J. Mol. Biol*. **70**, 117–132 (1972).

CHAPTER 6

Photobiology

This chapter covers the topic of photobiology, which deals with the interaction of light with biological matter. Thus, it is a natural extension of Chapter 4, which discussed the interaction of light with matter in general. The topic of photobiology, hence, forms the core of biophotonics, which utilizes interactions of light with biological specimens. This chapter utilizes a number of concepts, optical processes, and techniques already covered in Chapters 2–5.

This chapter discusses the interactions of various molecular, cellular, and tissue components with light. The various light-induced radiative and nonradiative processes are described, along with a discussion of the various photochemical processes. Photochemistry in cells and tissues can also be initiated by externally added exogenous substances, often called *photosensitizers*, which form the basis for photodynamic therapy, a topic Covered in Chapter 12.

The various types of scattering processes occurring in a tissue are covered. These processes, together with light absorption, determine the penetration of light of a given wavelength into a particular type of tissue. Methods of measurement of optical reflection, absorption, and scattering properties of a tissue are introduced. Some important manifestations of nonradiative processes in a tissue, used for a number of biophotonics applications such as laser tissue engineering (covered in Chapter 13) and laser microdissection (covered in Chapter 14), are thermal, photoablation, plasma-induced ablation, and photodisruption. These processes are defined.

Photoprocesses occurring in biopolymers play a major role in biological functions. Examples are the processes of vision and of photosynthesis. These processes are also covered.

An emerging area of biophotonics is *in vivo* imaging and spectroscopy for optical diagnosis. This topic is covered, along with the various methods of light delivery for *in vivo* photoexcitation. Another exciting *in vivo* biophotonics area is that of optical biopsy to detect the early stages of cancer. This topic is covered as well.

Finally, the chapter concludes with the coverage of single molecule detection. Understanding of structure and functions at the single biomolecule and

Introduction to Biophotonics, by Paras N. Prasad
ISBN: 0-471-28770-9

bioassembly levels is a major thrust of molecular and structural biology. The use of novel optical techniques allows one to probe processes at the single molecule level.

For supplementary reading on the contents of this chapter, suggested books are:

Grossweiner and Smith (1989): A general reference on photobiology
Niemz (1996): A comprehensive coverage of laser–tissue interactions

6.1 PHOTOBIOLOGY—AT THE CORE OF BIOPHOTONICS

Photobiology deals with the interaction of light with living organisms, from cellular specimens, to sectional tissues, to *in vivo* live specimens. Therefore, it deals with interactions of light with matter ranging in size scale from ~100 nm (viruses) to macro-objects (live organisms). It is an area that still offers many challenges in understanding the nature of light-induced processes. Chapter 4 dealt with the interaction of light with matter. The concepts developed in that chapter are of direct relevance to the topics discussed here, providing the basic foundation for them. However, the interaction of light and biological media, whether individual cells or tissues, is much more complex, often introducing a chain of events. The interactions can induce physical, thermal, mechanical, and chemical effects, as well as a combination of them. These interactions form the basis for the use of light for optical diagnostics and light-induced therapy as well as for medical procedures, which are discussed in subsequent chapters. These light-induced processes are mostly initiated by linear absorption of light. However, under intense field using a short laser pulse, one can induce nonlinear optical processes. For example, one can observe second-harmonic generation (SHG) from the surface of a cell membrane. Also, two-photon absorption can be induced in many chromophores. Here we discuss only the linear optical absorption. Table 6.1 lists various absorbing biological components.

6.2 INTERACTION OF LIGHT WITH CELLS

Biological cells span the size scale from submicron dimensions to over 20 μm. Therefore, they can be smaller than the wavelength of light or much larger. Interaction with light can lead to both scattering and absorption. Of particular interest in this regard is the Rayleigh scattering where even the subcellular components, organelles, can be a scattering center. Rayleigh scattering is dependent on three parameters: (i) the size of the scattering centers (cells or organelles), (ii) the refractive index mismatch (difference) between a scattering center and the surrounding medium, and (iii) the wavelength of light. The Rayleigh scattering is inversely proportional to the fourth power of wavelength. Therefore, a blue light (shorter wavelength) will be more scattered than a red light. Therefore, on the basis of scattering alone as the optical loss mech-

TABLE 6.1. Various Molecular, Cellular, and Tissue Components that Interact with Light

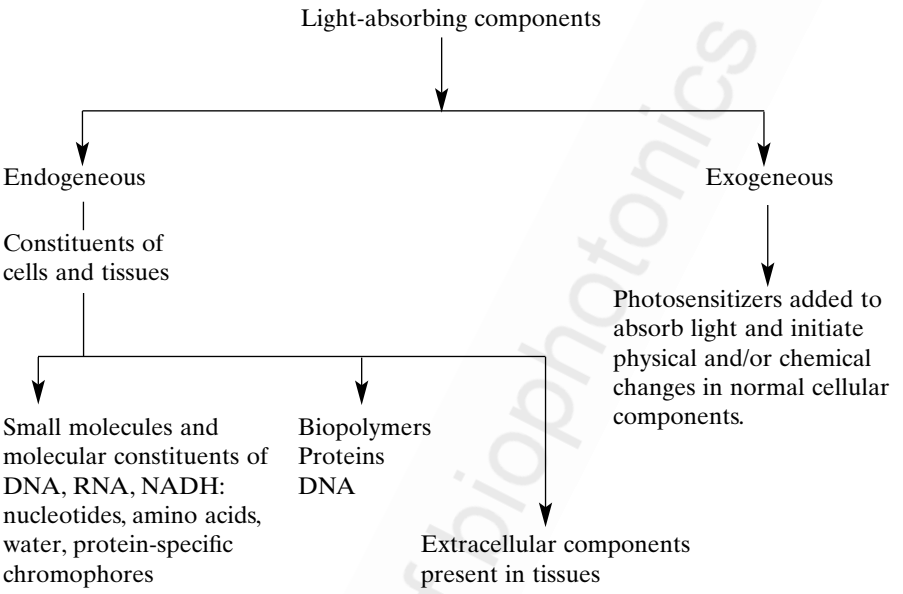

anism (attenuation of light transmission), the longer the wavelength of light, the deeper it would penetrate in a biological specimen. However, an upper wavelength limit of transmission is set up by absorptive losses in IR due to water absorption and absorption by the —CH and the —OH vibrational overtone bands. Bulk scattering becomes more pronounced in tissues and will be discussed in the next section.

In this section, light absorption by various components of the cell and the effects caused by light absorption will be discussed. Primary photoinduced cellular effects are produced by light absorption to induce transition between two electronic states (electronic or coupled electronic–vibrational [vibronic] transitions). Purely vibrational transitions (such as IR and Raman) are of significance only in structural identification and in conformational analysis.

In this section we discuss first the absorption by the various constituent molecules and biopolymers. Subsequently we discuss the various photochemical and photophysical processes induced by light absorption. Then we discuss the effects produced from light absorption by an exogenous chromophore added to the cell.

6.2.1 Light Absorption in Cells

Proteins are the most abundant chemical species in biological cells. They also are the most diversified chemical unit in living systems, from smaller-sized

enzymes to larger proteins and from colorless to highly colored systems. They also exhibit a diversity of functions, from carrying oxygen to providing a light-induced neurological response for vision.

The basic constituents (building blocks) of proteins are amino acids, which can be aliphatic or aromatic (containing benzene or fused benzene type π-electron structures; see Chapter 2). The aliphatic amino acids absorb the UV light of wavelengths shorter than 240 nm (Grossweimer and Smith, 1989). Colorless aromatic amino acids such as phenylalanine (Phe), tyrosine (Tyr), and tryptophan (Trp) absorb at wavelengths longer than 240 nm, but well below the visible. However, the absorption by a protein is not completely defined by those of the constituent amino acid residues. Protein bonding involving the polypeptide bonds and disulfide linkage also absorb and contribute to the overall absorption of a protein. Furthermore, a protein may contain a chromophore such as the heme group (in hemoglobin) and *cis*-retinal (in case of retinal protein), which provide strong absorption bands. Hemoglobin has absorption peaks around 280 nm, 420 nm, 540 nm, and 580 nm. Melanin, the basic pigment of skin, has a broad absorption, covering the entire visible region, but decreasing in magnitude with the increase of wavelength. These features are evident from Figure 6.1, which exhibits the absorption characteristics of oxyhemoglobin (HbO_2) and melanin.

The constituents of DNA and RNA are the nucleotides that contain carbohydrates and purine and pyrimide bases (A, C, T, G, and U discussed in Chapter 3). The absorption by carbohydrates is below 230 nm; the absorption by the carbohydrate groups generally does not produce any significant photophysical or photochemical effect. The purine and pyrimidine bases absorb light of wavelengths in the range of 230–300 nm. This absorption is mainly responsible for DNA damage. A cellular component, exhibiting absorption in the visible, is

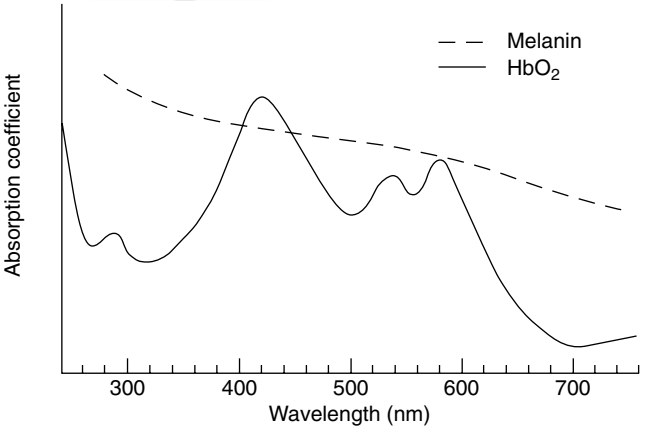

Figure 6.1. The absorption spectra of two important cellular constituents.

NADH, with absorption peaks at ~270 nm and 350 nm. Water does not have any bands from UV to near IR, but starts absorbing weakly above 1.3 μm, with more pronounced peaks at wavelengths ≥2.9 μm and very strong absorption at 10 μm, the wavelength of a CO_2 laser beam. Therefore, most cells exhibit very good transparency between 800 nm (0.8 μm) and 1.3 μm.

6.2.2 Light-Induced Cellular Processes

Cells exhibit a wide variety of photophysical, as well as photochemical, processes followed by light absorption. Some of these processes are shown in Table 6.2. A number of cellular constituents fluoresce when excited directly or excited by energy transfer from another constituent (Wagnieres et al., 1998). This fluorescence is called *endogenous fluorescence* or *autofluorescence*, and the emitting constituent is called an *endogenous fluorophore* (also called *fluorochrome*). As discussed in Chapter 4, fluorescence originates from an excited singlet state and has typical lifetimes in the range of 1–10 nsec. Phosphorescence, which is emission from an excited triplet (usually T_1), is generally not observed from cellular components.

Some of the fluorophores native to cells are NADH, flavins and aromatic amino acid constituents of proteins (e.g., tryptophan, tyrosine, phenylalanine). Various porphyrins and lipopigments such as ceroids and lipofuscins, which are end products of lipid metabolism, also fluoresce.

In addition, some important endogenous fluorophores are present in the extracellular structures of tissues. For example, collagen and elastin, present in the extracellular matrix (ECM), fluoresce as a result of cross-linking between amino acids. The absorption and emission spectra of some endogenous fluorophores are shown in Figure 6.2 (Katz and Alfano, 2000).

An important fluorescing protein that has received considerable attention during recent years for fluorescence-tagging of proteins is the green fluorescent protein (GFP) derived from jellyfish (Pepperkok and Shima, 2000; Hawes et al., 2000). In its native form, it absorbs at 395 nm and 475 nm with emission maximum in green, around 508. Intensive mutagenesis of the primary sequence has produced a wide variety of GFPs with broad spectral and biochemical properties. As shall be discussed in Chapter 8, the GFP and its variants have been utilized as multicolor fluorescent markers to be used as subcellular probes.

The thermal effects induced by light become more pronounced at the tissue level and will be discussed in the next section. Photochemical processes involving a chemical reaction in the excited state of a cellular constituent (or a chemical unit such as thymine in DNA) are varied, as exhibited in Table 6.2. Here are some examples (Grossweiner and Smith, 1989; Kochevar, 1995):

(i) *Photoaddition.* An important photoaddition process responsible for UV-induced molecular lesions in DNA is the photodimerization of thymine as illustrated below:

TABLE 6.2. Various Light-Induced Cellular Processes

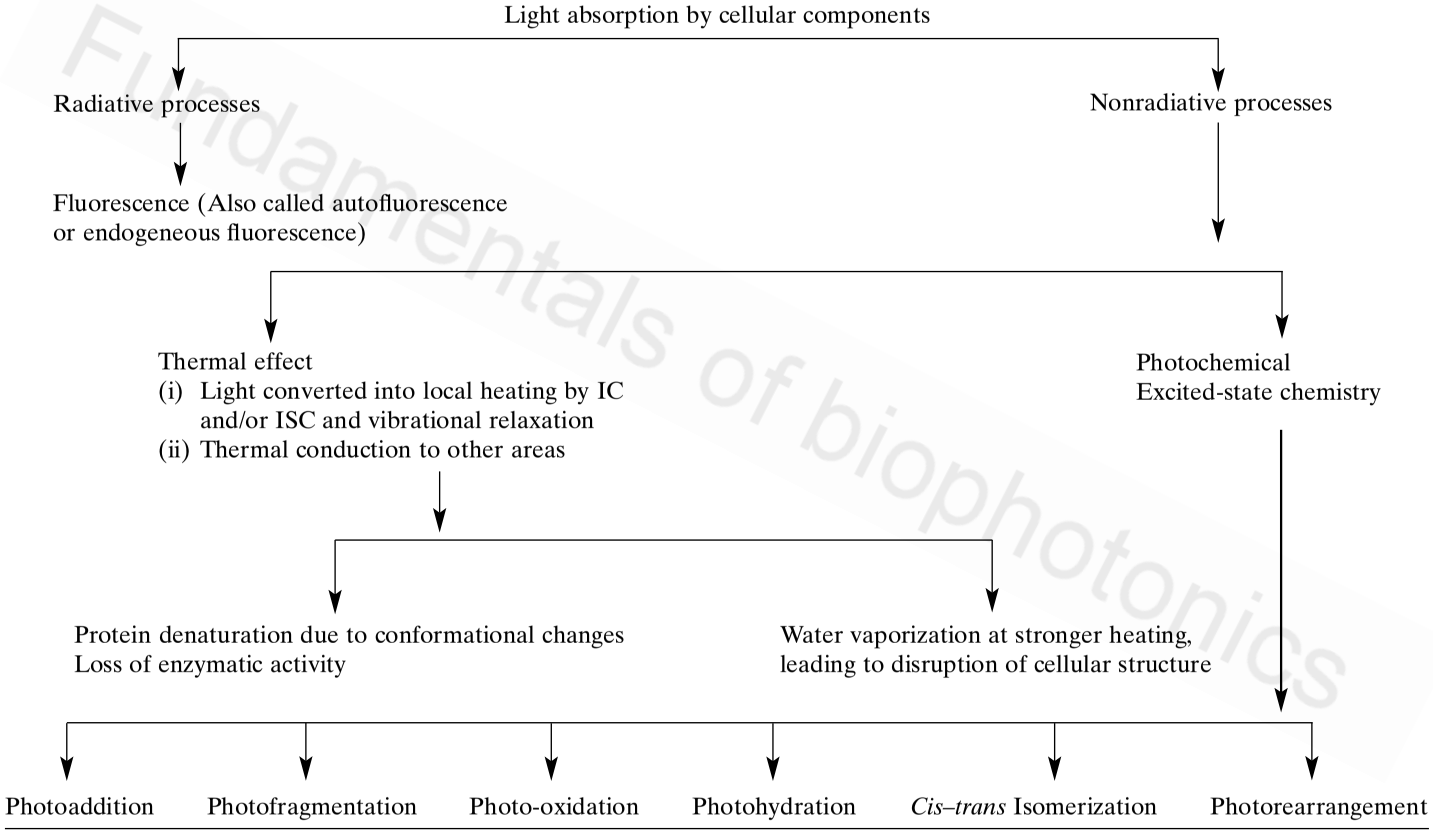

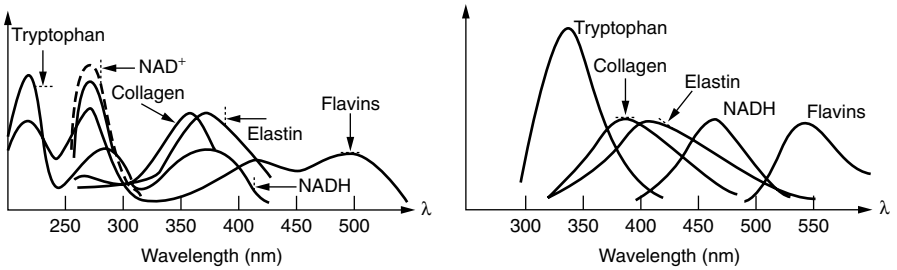

Figure 6.2. The absorption (*left*) and fluorescence (*right*) spectra of important tissue fluorophores. The *y* axes represent the absorbance (*left*) and fluorescence intensity (*right*) on a relative scale. (Reproduced with permission from Katz and Alfano, 2000.)

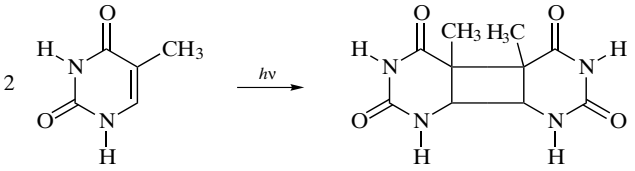

(6.1)

Another important photoaddition is that of cysteine (in protein) to thymine (in DNA), which can lead to photochemical cross-linking of DNA to protein as illustrated below:

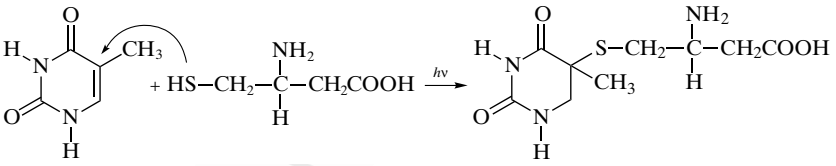

(6.2)

(ii) *Photofragmentation.* In a photofragmentation reaction the original molecule, when photoexcited, decomposes into smaller chemical fragments by the cleavage of a chemical bond. This type of reaction is very common in biomolecules when exposed to short wavelength UV light. An example is the photofragmentation of riboflavin as illustrated below:

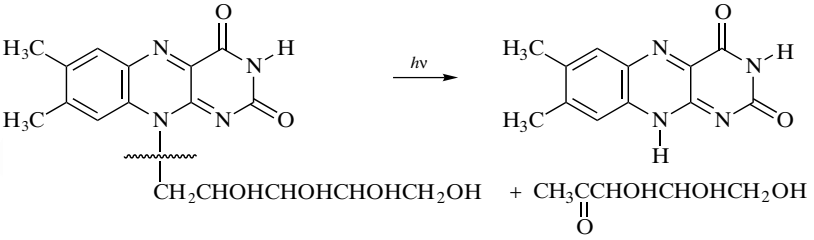

(6.3)

(iii) *Photooxidation.* Here the molecule, when excited, adds an oxygen molecule from the surroundings (a chemical process called oxidation). An example is the photooxidation of cholesterol:

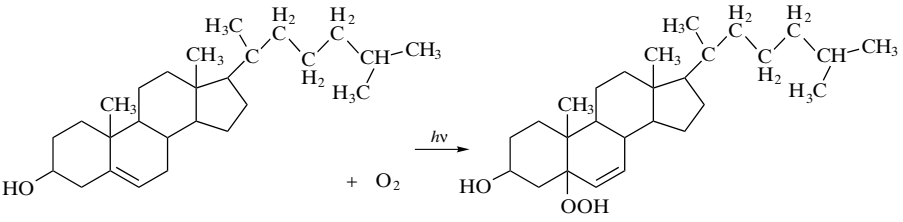

Cholesterol — 3β-Hydroxy-5α-hydroperosy-Δ^6-cholestene

(6.4)

(iv) *Photohydration.* This type of reaction is also responsible for creating lesions in DNA. In this reaction, an excited molecule adds a water molecule to produce a new product, as illustrated for uracil.

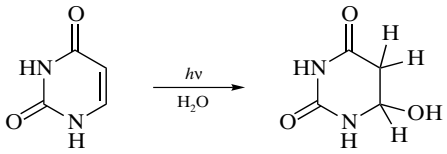

(6.5)

Uracil — 6-Hydroxy-5-hydrouracil

(v) *Photoisomerization.* Photoisomerization here specifically refers to the change in geometry or conformation of stereoisomers (discussed in Chapter 2). An important photoisomerization process responsible for retinal vision is that of 11-*cis*-retinal which upon excitation rotates by 180° around a double bond to produce a geometric isomer, the all-*trans*-retinal. This process is shown below:

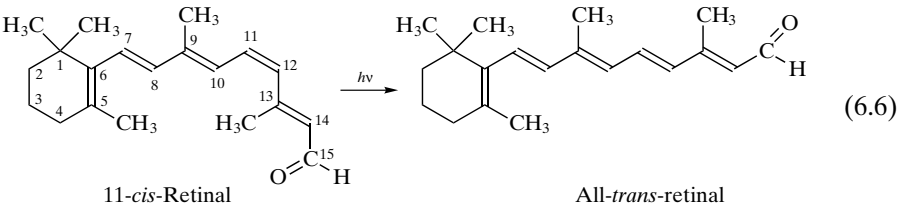

(6.6)

11-*cis*-Retinal — All-*trans*-retinal

(vi) *Photorearrangement.* In this photoinduced process the chemical formula of the molecule does not change, only a rearrangement of bonds occurs as illustrated for 7-dehydrocholesterol in skin which upon UV exposure produces vitamin D_3:

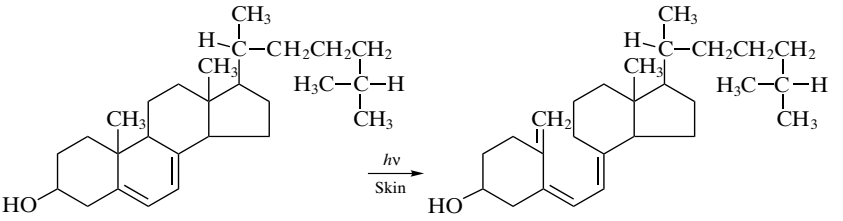

7-Dehydrocholesterol Vitamin D_3 (6.7)

Photochemistry of proteins is derived from those of its amino acid residues. In addition, important photochemical processes in proteins involve the splitting of the disulfide bridges. Furthermore, DNA–protein cross-linking involves the addition of thymine in DNA with cystine in protein. This addition process has been discussed above.

In the case of DNA, UV irradiation can also lead to the breaking of either one or both DNA strand and intra- and intermolecular DNA cross-linking. The photochemistry of RNA is very similar to that of DNA.

6.2.3 Photochemistry Induced by Exogenous Photosensitizers

There are some important photochemical reactions that are produced by light absorption in chemicals introduced in a cell (or a tissue). These are exogenous chromophores that perform the function of photosensitization—that is, sensitizing a photoprocess (Kochevar, 1995; Niemz, 1996). The mechanism for most photosensitization involves photoaddition and photooxidation. These processes have been discussed in the previous section. However, in the present context, these processes are initiated by light absorption by the exogenous photosensitizers.

In the photoaddition reaction, a photosensitizer, when excited by light absorption, covalently bonds to a constituent molecule of the cell. An important example is the photoaddition reaction between the photosensitizer, 8-methoxypsoralen (8-MOP) with a pyridine base in DNA as shown below (Kochevar, 1995).

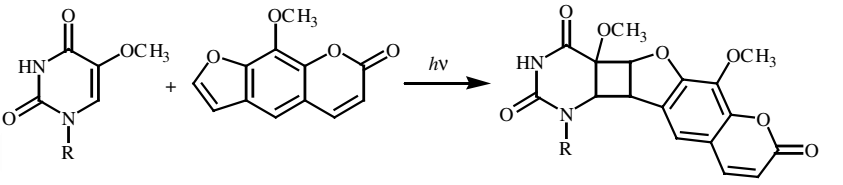

Thymine in DNA 8-Methoxypsoralen Cycloadduct (6.8)

This photochemical reaction occurs through the singlet excited state of 8-MOP. Because the singlet-state lifetime is short (in the nanosecond range), 8-MOP must be in a close proximity to a pyrimidine base. Therefore, the photoaddition is more likely to involve those 8-MOP molecules that are intercalated into the double-stranded DNA. This type of photoaddition reaction is supposed to be responsible for the phototoxicity of 8-MOP in human skin (Yang et al., 1989).

Photosensitized oxidation reactions involve a process in which the excited state of a photosensitizer produces a highly reactive oxygen specie such as an excited singlet oxygen ($^1O_2$), a superoxide anion (O_2^-), or a free radical (these are neutral chemical species with an unpaired electron, often represented by a dot as a superscript on the right-hand side) such as a hydroxyl radical ($OH^\bullet$). In fact, a photosensitized oxidation reaction often involves a chain reaction as shown below (Niemz, 1996):

(i) S_0 (photosensitizer) $\xrightarrow{h\nu}$ S_i (photosensitizer) $\longrightarrow$ T_1

(ii) T_1(photosensitizer) + T_0 (oxygen) $\longrightarrow$ S_1 (oxygen) + S_0 (photosensitizer)

(iii) S_1 (oxygen) + A cellular component $\longrightarrow$ Photooxidation of the cellular component

This photosensitized oxidation process forms the basis for light-activated cancer therapy, called *photodynamic therapy*, which is discussed in Chapter 12.

6.3 INTERACTION OF LIGHT WITH TISSUES

Nature of Optical Interactions. A tissue is a self-supporting bulk medium. In other words, unlike cells, which have to be supported in a medium (in an aqueous phase as *in vitro* specimen or in a tissue either as an *ex vivo* or an *in vivo* specimen), tissues do not need a medium. Tissues, therefore, behave like any bulk medium in which light propagation produces absorption, scattering, refraction, and reflection as discussed in Chapter 4 (Niemz, 1996). These four processes are shown in Figure 6.3. The reflection of light from a tissue is reflection from its surface. The greater the angle of incidence, the larger the reflection from the surface. Therefore, maximum light will be delivered to the tissue (penetrate the tissue), when it is incident on the tissue at 90° (the light beam is perpendicular to the tissue).

The absorption of light under weak illumination (such as under lamp or a CW laser source) is a linear absorption described by Beer–Lambert's law, discussed in Chapter 4. The absorption is due to various intracellular as well as extracellular constituents of the tissue.

However, the most pronounced effect in a tissue is scattering. A tissue is a highly scattering turbid medium. The turbidity or apparent nontransparency of a tissue is caused by multiple scattering from a very heterogeneous structure consisting of macromolecules, cell organelles, and a pool of water. This

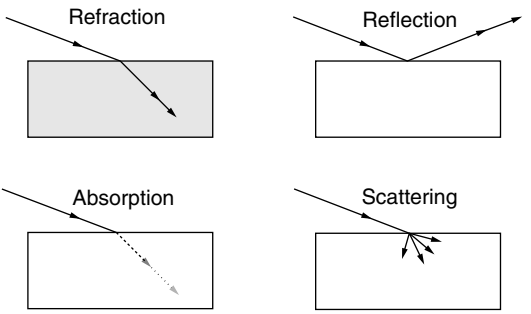

Figure 6.3. The four possible modes of interaction between light and tissue.

TABLE 6.3. The Various Light Scattering Processes in a Tissue

Light scattering

Elastic scattering

Incident and scattered photons are of the same frequency

Rayleigh scattering

- Scattering by particles of size smaller than the wavelength of light.
- Scattering depends on λ^{-4}, hence significantly more for blue compared to red light.
- Forward and backward scattering is the same.

Mie scattering

- Scattering of particles of size comparable to λ.
- Weaker wavelength dependence: λ^{-X} with $0.4 \leq X \leq 0.5$.
- Preferably forward scattering.

Inelastic scattering

Incident and scattered photons are of different frequencies

Brillouin scattering
The difference in energy generates acoustic phonons.

Raman scattering
The difference in energy generates a vibrational excitation in the molecule.

scattering leads to spreading of a collimated beam, resulting in a loss of its initial directionality as well as in defocusing (spread) of the light beam spot. The scattering process in a tissue is more complex and involves several mechanisms (Niemz, 1996). They are represented in Table 6.3.

The inelastic scattering in a biological tissue is weak. Brillouin scattering becomes significant only under the condition of generation of shockwaves discussed below. The acoustic phonons are ultrasonic frequency mechanical waves. Raman scattering in cells produces excitation of molecular vibrations, as discussed in Chapter 4. However, neither Rayleigh scattering nor Mie scattering completely describes the elastic scattering of light by tissue where photons are preferably scattered in the forward direction. The observed scattering shows a weaker wavelength dependence than that predicted by Rayleigh scattering but stronger than wavelength dependence predicted by Mie scattering. Other theories of scattering in a turbid medium (such as a tissue) have been proposed (Niemz, 1996). However, any detailed discussion of this subject is out of the scope of this book.

Raman scattering from tissues can provide valuable information on chemical and structural changes occurring as a result of diseases as well as due to mechanical deformations induced by aging or a prosthetic implant. Morris and co-workers have applied Raman spectroscopy to bone and teeth tissues. They have obtained spectra of both minerals (inorganic components) and proteins (organic components) of these tissues (Carden and Morris, 2000; Carden et al., 2003). In response to mechanical loading/deformation, they reported changes in the vibrational spectra in both the inorganic and organic components regions. Raman spectra taken at the edge of the indents revealed increases in the low-frequency component of the amide III band ($1250\,cm^{-1}$) and high-frequency component of the amide I band ($1665\,cm^{-1}$). These changes were interpreted as indicative of the rupture of collagen cross-links due to shear forces exerted by the indenter passing through the bone. More recently, Morris and co-workers have also applied Raman scattering for studying craniosynostosis (premature fusion of the skull bones at the sutures), which is the second most common birth defect in the face and skull (Tarnowski et al., submitted).

Like absorption, scattering creates a loss of intensity as the light propagates through a tissue. This loss is also described by an exponential function of the same nature as discussed for absorption in Chapter 4. Therefore, the total intensity attenuation in a tissue can be described as

$$I(z) = I_0 e^{-(\alpha + \alpha_s)z} \tag{6.9}$$

In this equation, $I(z)$ is the intensity at a depth z in the tissue; I_0 is the intensity when it enters the tissue, α = absorption coefficient, and α_s = scattering coefficient. Therefore, $\alpha + \alpha_s$ is the total optical loss. Another term used to describe the optical transparency of a tissue is the *optical penetration depth*, δ, which measures the distance z in the tissue after traveling which the intensity $I(z)$ drops to a fraction $1/e$ (= 0.37) of the incident value I_0. The term δ provides a measure of how deep light can penetrate into a tissue, and thus the extent of optical transparency of a tissue. From equation (6.9) one can find that the penetration depth δ is equal to $1/(\alpha + \alpha_s)$. The initial intensity I_0 is reduced to approximately 90% at a depth of 2δ in a tissue. In general, δ

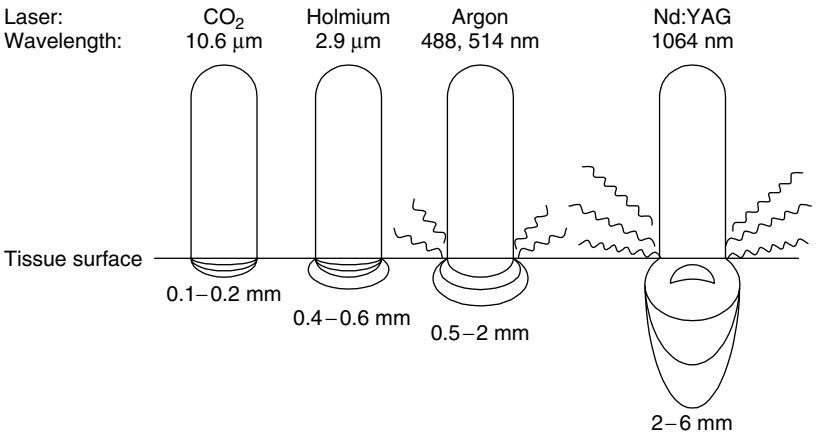

Figure 6.4. Penetration depths for commonly used laser wavelengths.

decreases with the vascularity (blood content) of a tissue. Furthermore, δ is significantly less for blue light than for red light and is the largest in the region 800–1300 nm. Figure 6.4 illustrates the penetration depths in a typical tissue for light of wavelengths of some commonly used lasers.

Measurement of Optical Properties of a Tissue. This subsection describes a method to determine reflection, absorption, and scattering properties of a tissue (Niemz, 1996). In a typical transmission experiment, one measures the transmission of a collimated beam (a laser source being the most convenient source) through a tissue of a finite length (the tissue specimen may be a dissected tissue). This method, in its simplest form, provides a total attenuation coefficient including optical losses from reflection, absorption, and scattering. In order to get information on each of these processes, a more sophisticated experimental arrangement has to be made which also takes into account the angular distribution of the scattered intensity. A commonly used experimental arrangement to simultaneously determine the reflectance, absorption, and scattering is that of double-integrating spheres first applied by Derbyshire et al. (1990) and Rol et al. (1990). The schematic of this experimental arrangement is shown in Figure 6.5.

In this method, two nearly identical spheres are located in front of and behind the tissue sample. These spheres have highly reflective coatings on their inner surface. Therefore, light-reaching detectors D_R and D_T are collected from all angles (hence the term *integrating spheres*). The first sphere integrates all the light that is either reflected or scattered backward from the sample. The light that is transmitted through the sample and scattered forward is detected by the second sphere at two ports. The port with detector D_T integrates all the forward scattering of the transmitted light, while the detector D_C measures the intensity of light in the forward direction of propagation. From these two

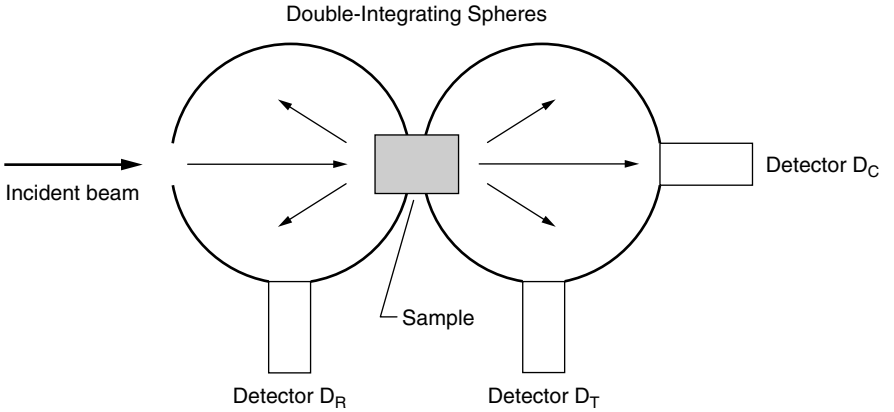

Figure 6.5. Schematics of an experimental arrangement utilizing a double-integrating sphere geometry for simultaneous measurement of reflection, scattering and absorption. The detectors D_C, D_T, and D_R at three different parts measure three quantities respectively: (i) transmitted coherent light that passes through the tissue in the direction of light propagation, (ii) transmitted diffuse intensity, and (iii) reflected diffuse intensity.

measurements one can separate the contributions due to scattering and absorption.

Light-Induced Processes in Tissues. Interaction of light with a tissue produces a variety of processes, some from its cellular and extracellular components and some derived from its bulk properties (Niemz, 1996). These processes are listed in Table 6.4. Each of these manifestations is briefly discussed below.

Autofluorescence. The autofluorescence subject has already been discussed in Section 6.2.2. Autofluorescence arises from the endogenous fluorophores that are present either as a cellular component or in the extracellular matrix. Any given tissue has in general a nonuniform distribution of many fluorophores that may also vary as a function of depth below the tissue surface. Therefore, the fluorescence spectrum measured at tissue surfaces may be different from that within the tissue from different layers. Furthermore, the autofluorescence may be different from a premalignant or malignant tissue compared to a normal tissue, thus providing a method for optically probing and even for early detection of cancer. Also metabolic changes induce changes in autofluorescence. For example, NADH is highly fluorescent, but its deprotonated form NAD^+ is not.

Photochemical Processes. The various photochemical processes in tissue components, initiated by absorption of light have been discussed above in

TABLE 6.4. Light-Induced Various Processes in Tissues

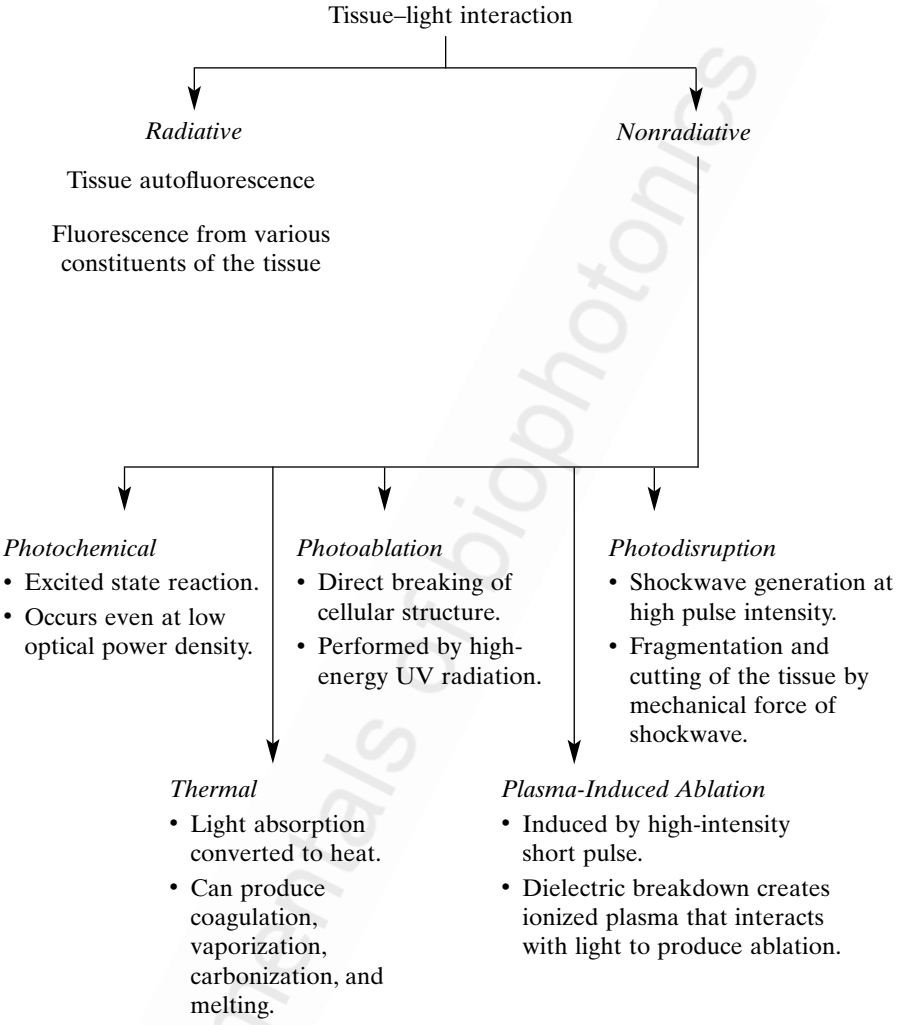

Section 6.2.2. These effects occur even at very low power densities (typically at $1\,W/cm^2$) when the absorption process is a simple one-photon absorption (linear absorption). These processes are dependent on fluence (irradiance) rather than intensity. Even though a conventional lamp source can be used for this purpose, one often uses a laser beam as a convenient light source. Recent interest has focused on nonlinear optical excitations such as multiphoton absorption, particularly two-photon absorption, discussed in Chapter 5, to induce photochemical processes, particularly photosensitzed oxidation in photodynamic therapy. The advantage offered by two-photon absorption is that the same photochemistry can be affected deeper inside the tissue, compared

to that induced by one-photon absorption which remains localized within microns of depth from the surface. One of the most important photochemical processes in tissues, from the biophotonics perspective, is the photosensitized oxidation discussed in Section 6.2.2. This subject will be further discussed in Chapter 12 on photodynamic therapy.

Thermal Effects. The thermal effects result from the conversion of the energy of light, absorbed in tissues, to heat through a combination of nonradiative processes such as internal conversion (IC), intersystem crossing (ISC), and vibrational relaxations. These topics have been discussed in Chapter 4. Thermal effects can be induced both by lamp as well as by CW and pulse laser sources and they are nonspecific; that is, they do not show a wavelength dependence, implying that no specific excited state need to be populated to create these effects. In the case of the use of a monochromatic laser beam, the choice of wavelength (absorption strength) and the duration of laser beam irradiance (pulse width, in the case of a pulse laser) may determine how the thermal effect manifests. The two important parameters are the peak value of the tissue temperature reached and the spread of the heating zone area in the tissue. The heating of an area in a tissue can produce four effects: (i) coagulation, (ii) vaporization, (iii) carbonization, and (iv) melting. For coagulation, the local temperature of a tissue has to reach at least 60°C, where the coagulated tissue becomes necrotic. Both CW (e.g., Nd:YAG) and pulse (e.g., Er:YAG) lasers have been used for different tissues. For a vaporization effect to manifest, the local temperature of a tissue has to reach 100°C, where water starts converting into steam, producing thermal ablation (or photothermal ablation) of the tissue. This ablation is a purely thermomechanical effect produced by the pressure buildup due to steam formation and is thus different from photoablation discussed below. In this process the tissue is torn open by the expansion of steam, leaving behind an ablation crater with lateral tissue damage. In a living tissue, the blood vessels can transport heat away from the ablation site, creating damage at other sites and thus the spread of the lateral damage. If one wishes to reduce the lateral thermal damage from thermal diffusion, one must ablate the tissue with a short pulse laser. Based on the thermal diffusion characteristics of biological tissues, it can be assumed that if the energy is deposited in the tissue in tens of microseconds, the thermal ablation remains primarily localized around the focal spot of the beam and the lateral thermal damage is minimized. However, the use of ultrashort and high-intensity pulses can lead to other complications such as nonlinear optical processes that may produce other effects.

Carbonization occurs when the tissue temperature reaches above 150°C, at which tissue chars, converting its organic constituents into carbon. This process has to be avoided because it is of no benefit and leads to irreparable damage of a tissue.

At sufficiently high power density from a pulse laser (generally in microseconds to nanoseconds), the local temperature of a tissue may reach above

its melting point. This type of process can be used for tissue welding and shall be further discussed in the chapter on tissue welding.

Photoablation. This is a process whereby the various cellular and extracellular components are photochemically decomposed by the action of an intense UV laser pulse. The result is the release of photofragmented species from a tissue, causing etching (or ablation). This ablation is localized within the beam spot and is thus very clean. Typical power densities are 10^7–10^{10} W/cm^2. A convenient UV laser source is an excimer laser that provides a number of lasing wavelengths in the range of 193–351 nm. The pulses from these lasers are typically 10–20 nsecs. This method is very useful for tissue contouring (sculpturing), such as in refractive corneal surgery. This topic is also covered later in Chapter 13, entitled Tissue Engineering with Light.

Plasma-Induced Ablation. When exposed to a power density of 10^{11} W/cm^2, the tissue experiences an electric field of 10^7 V/cm associated with the light. This field is considerably larger than the average coulombic attraction between the electrons and the nuclei (a subject covered in Chapter 2) and causes a dielectric breakdown of the tissue to create a very large free electron density (plasma) of ~10^{18} cm^3 in the focal volume of the laser beam in an extremely short period (less than hundreds of picoseconds). This high-density plasma strongly absorbs UV, visible, and IR light, which is called *optical breakdown* and leads to ablation.

Photodisruption. This effect occurs in soft tissues or fluids under high-intensity irradiation that produces plasma formation. At higher plasma energies, shock waves are generated in the tissue which disrupt the tissue structure by a mechanical impact. When a laser beam is focused below the tissue, cavitation occurs in soft tissues and fluids produced by cavitation bubbles that consist of gaseous vapors such as water vapor and CO_2. In contrast to a plasma-induced ablation, which remains spatially localized to the breakdown region, photodisruption involving shockwaves and cavitation effects spreads into adjacent tissues. For nanosecond pulses, the shockwave formation and its effects dominate over plasma-induced ablation. However, for shorter pulses both plasma-induced ablation and photodisruption may occur and it is not easy to distinguish between these two processes. Their application is described in Chapter 13.

Photodisruption has found a number of applications in minimally invasive surgery such as posterior capsulotomy of the lens, often needed after cataract surgery and laser-induced lithotripsy of urinary calculi.

6.4 PHOTOPROCESSES IN BIOPOLYMERS

Photoprocesses in biopolymers are excellent examples of how Nature involves biophotonics more efficiently to perform various biological functions. The

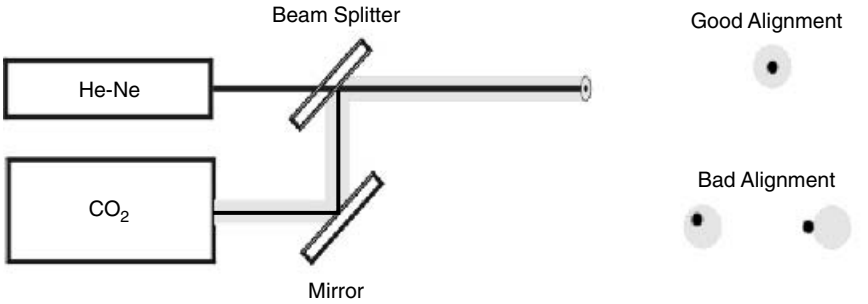

Figure 6.13. Articulated arm laser beam delivery with an aiming beam from an He–Ne laser.

6.5.4 Hollow Tube Waveguides

Another light delivery system involves a hollow tube made of a metal, ceramic, or plastic (Cossman et al., 1995). The inside wall of the tube is coated with a high reflector. The laser light is propagated down the tube by reflection from the inner wall. The advantage of using this type of plastic waveguide over an articulated arm is its semiflexibility. The plastic waveguides generally have an inner diameter of ~1 mm and an outer diameter of ~2 mm.

An important recent development in this area is the use of a photonic crystal waveguide. The photonics crystals are discussed in Chapters 9 and 16. An example of a photonic crystal is a multilayered medium that reflects (does not allow the propagation through it) light of a given wavelength range. Using an appropriately designed multilayered plastic hollow waveguide, one can make light within a given wavelength range to reflect from the inner walls with very high reflectivity.

6.6 *IN VIVO* SPECTROSCOPY

In vivo spectroscopy has emerged as a powerful technique for biomedical research covering a broad spectrum, from study of cellular and tissue structures, to biological functions, to early detection of cancer. The spectroscopic methods used have involved study of electronic absorption spectra by analysis of back-scattered light, Raman scattering, and fluorescence. Fluorescence spectroscopy has been the most widely used technique because of its sensitivity and specificity (Wagnieres et al., 1998; Brancoleon et al., 2001). For fluorescence studies, both endogenous fluorescence (autofluorescence) and exogenous fluorescence have been used.

Earlier reports focused on the use of optical absorption properties of tissues for clinical applications (Wilson and Jacques, 1990). An example is blood oximetry, which is widely used clinically to monitor continuously blood oxygenation with the help of an optical fiber probe as described in the previous

section. In this method the diffuse reflectance also collected by the fiber is analyzed based on the differences in the absorption bands of oxy- and deoxyhemoglobins. Diffuse reflectance from the skin can be used to monitor changes induced, for example, by the UV radiation. Endoscopic reflectance spectroscopy from mucosa of the gastrointestinal tract has been used to determine blood content and oxygenation (Leung et al., 1987).

6.7 OPTICAL BIOPSY

A major focus of *in vivo* spectroscopy has been to use it for early detection of cancer. Optical biopsy refers to detection of the cancerous state of a tissue using optical methods. This is an exciting area, offering the potential to use noninvasive or minimally invasive *in vivo* optical spectroscopic methods to identify a cancer at its various early stages and monitor its progression. One can envision that one day noninvasive optical spectroscopic methods would find routine usage in doctors' offices, clinics, and operating rooms for diagnosis of diseases, monitoring its progression and determining the efficacy of a medical treatment or procedure.

The basic principle utilized for the method of optical biopsy is that the emission and scattered light are strongly influenced by the composition and the cellular structures of tissues. The progression of a disease or cancer causes a change in the composition and the cellular structure of the affected tissues, producing a change in emission and scattering of light. Thus, the optical biopsy can be represented by the schematics of Figure 6.14 (Katz and Alfano, 1996).

The primary optical methods used in the past have been fluorescence and Raman spectroscopic techniques. The changes in tissue from a normal state to a cancerous state have been shown to alter the fluorescence and the Raman spectra. These methods have successfully differentiated normal tissues from those with breast, gynecological, colon, and prostate cancers.

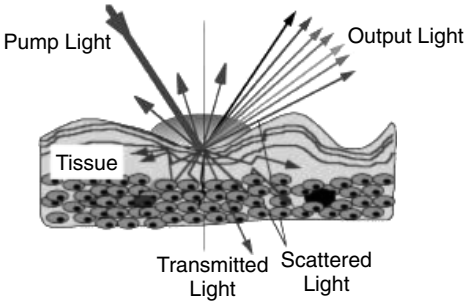

Figure 6.14. Schematics of various optical interactions with a tissue used for optical biopsy. (Reproduced with permission from Katz and Alfano, 1996.)

The benefits provided by optical biopsy are (Katz and Alfano, 1996) as follows:

- Optical biopsy is noninvasive or minimally invasive, utilizing endoscopic or needle based probes. Hence, removal of a tissue specimen is not required.
- The method provides rapid measurements. Hence, real-time measurements can be made.
- High spatial resolution offered by the optical methods provides the ability to detect small tumors.
- Optical biopsy provides the ability to detect precancerous conditions. This feature is derived from the presence of distinguishable spectral characteristics associated with molecular changes that manifest even before a cancer actually can be detected.

For fluorescence detection, endogenous fluorescence (autofluorescence) from a tissue is preferred over exogenous fluorescence (fluorescence from an added dye). The endogenous fluorescence is derived from a number of fluorophores that are constituents of a tissue or a cell. Examples of endogenous fluorophores are tryptophan, elastin, collagen, NADH, and flavin. The absorption and the fluorescence spectra of these molecules have been covered in Section 6.2 (Figure 6.2).

Alfano and co-workers were the first to use the fluorescence property of an animal tissue to study cancer (Alfano et al., 1984). Since then the area of optical biopsy has received a great deal of attention as is evidenced by a number of symposia held on optical biopsy (Alfano, 2002). Fluorescence measurements have used both laser excitation (e.g., 488 nm from an argon ion laser) and excitation (particularly in the UV region) from a xenon lamp. The optical biopsy studies have been extended both to *ex vivo* and *in vivo* human tissues. Furthermore, *in vivo* studies have utilized both endoscopic and needle-based probes to a variety of cancers, some of which are listed below (Alfano, private communications):

Endoscopic-Based Probes

- Stomach
- Colon
- Intestines
- Lungs
- Gynecological tract

Needle-Based Probes

- Breast
- Prostate
- Kidney

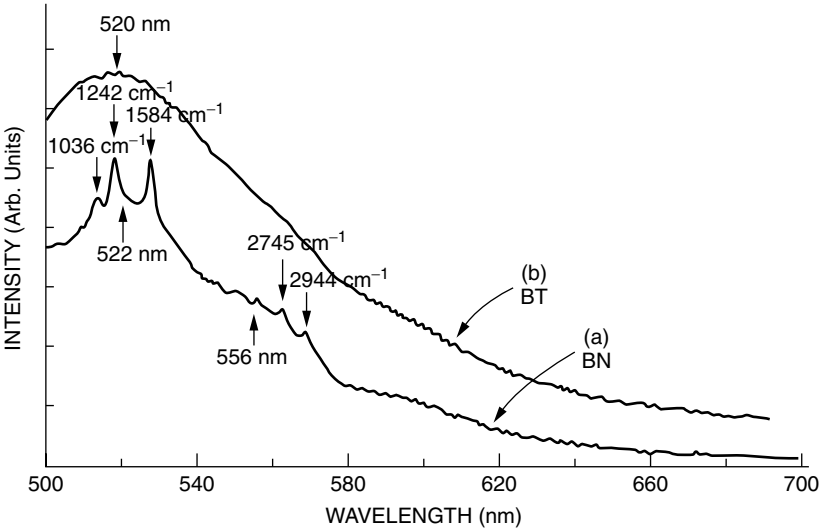

Figure 6.15. Fluorescence spectra of the normal breast (BN) and the tumor breast tissue (BT) excited at 488 nm. (Reproduced with permission from Alfano et al., 1989.)

In the endoscopic approach, large-diameter optical fibers coupled to an endoscope are used to excite and collect the emission. In needle-based probes, small-diameter optical fibers are mounted in stereotactic needles to provide high spatial resolution for *in vivo* examination of a breast or prostate tissue.

Alfano et al. (1989) used this method to show differences between the fluorescence and Raman spectra of normal and malignant tumor breast tissue. The observed fluorescence spectra of the normal breast tissue (BN) and that of a tumor breast tissue (BT), observed with excitation at 588 nm from an argon ion laser, is shown in Figure 6.15. The fluorescence is associated with flavins. The normal breast tissue also shows sharp Raman vibrational peaks in the region of 1000–1650 cm^{-1} associated with hemeproteins, lipids, hemoglobin, and porphysims. Frank et al. (1995) also reported the use of Raman spectroscopy to distinguish normal and diseased human breast tissues. The advantage of vibrational spectroscopy is that it provides detailed information relating to molecular structure and composition and, thus, can be used as a detailed signature associated with abnormality.

Another study is the use of *in vivo* autofluorescence spectroscopy of human bronchial tissue for early detection of lung cancer (Zellweeger et al., 2001). An optical fiber bundle was adapted to fit the biopsy channel of a standard flexible bronchoscope. Clear differences in the autofluorescence spectra were observed for the healthy, inflammatory, and early-cancerous lung tissue when excited at 405 nm *in vivo*.

The *in vivo* tissue autofluorescence also was used to distinguish normal skin tissue from nonmelanoma skin cancer (NMSC) (Brancoleon et al., 2001). They

reported that in both basal cell carcinomas and squamous cell carcinomas, the autofluorescence (endogenous fluorescence) at 380 nm due to tryptophan residues and excited at 295 nm was more intense in tumors than in the normal tissue, probably due to epidermal thickening and/or hyperproliferation. In contrast, the fluorescence intensity at ~480 nm produced by excitation at 350 nm and associated with cross-links of collagen and elastin in the dermis was found to be lower in tumors that in the surrounding normal tissue. The authors suggested this change to be due to degradation or erosions of the connective tissues due to enzymes released by the tumor.

Recently, a fiber-optic diagnostic analyzer with a trade name of Optical Biopsy System has been introduced by Spectra Science, Inc. of Minneapolis, Minnesota (FDA approved). It is used as an adjunct to lower gastrointestinal (GI) endoscopy for evaluation of polyps less than 1cm in diameter and can aid a physician to decide whether they should be removed. In this device, light is transmitted through a long fiber inserted in a colonoscope and is directed to a polyp. The autofluorescence from the polyp is collected back through the optical fiber.

Raman spectroscopy, particularly near-infrared FT-Raman (see Chapter 4), has been applied to *in vitro* studies of human breast, gynecological, and arterial tissues. The advantage of Raman spectroscopy is that it provides detailed information (with sharp vibrational transitions) relating to molecular structure and composition and, thus, can be used as a detailed signature associated with abnormality. The use of infrared excitation for Raman is advantageous because it reduces the probability of interference (background) from autofluorescence and provides deeper penetration in a tissue.

Alfano et al. (1991) used 1064 nm from a Nd:YAG laser to acquire the Raman spectra of a normal breast tissue, as well as of a benign and malignant tumor. These spectra in the region of 700–1900 cm^{-1} are shown in Figure 6.16. These different types of tissues exhibit differences in relative intensities and number of vibrational transitions.

Frank et al. (1995) also reported the usefulness of Raman spectroscopy to distinguish normal and diseased human breast tissues. More recently, Vo-Dinh et al. (2002) have used surface-enhanced Raman spectroscopy (Chapter 4) to detect cancer.

Other spectroscopic techniques used for optical biopsy are:

1. Optical coherence tomography, developed by Fujimoto and co-workers (Tearney et al., 1997). This optical technique, useful for bioimaging, is discussed in detail in Chapter 7. This technique of imaging was adapted to allow high-speed visualization of tissue in a living animal with a catheter endoscope, 1 mm in diameter.
2. Diffuse-reflectance measurements, developed by Alfano and co-workers (Yang et al., 2001). This method was used to obtain the absorption spectra of malignant and normal human breast tissues. The absorption in the wavelength ranges of 275–285 nm and 255–265 nm, which are

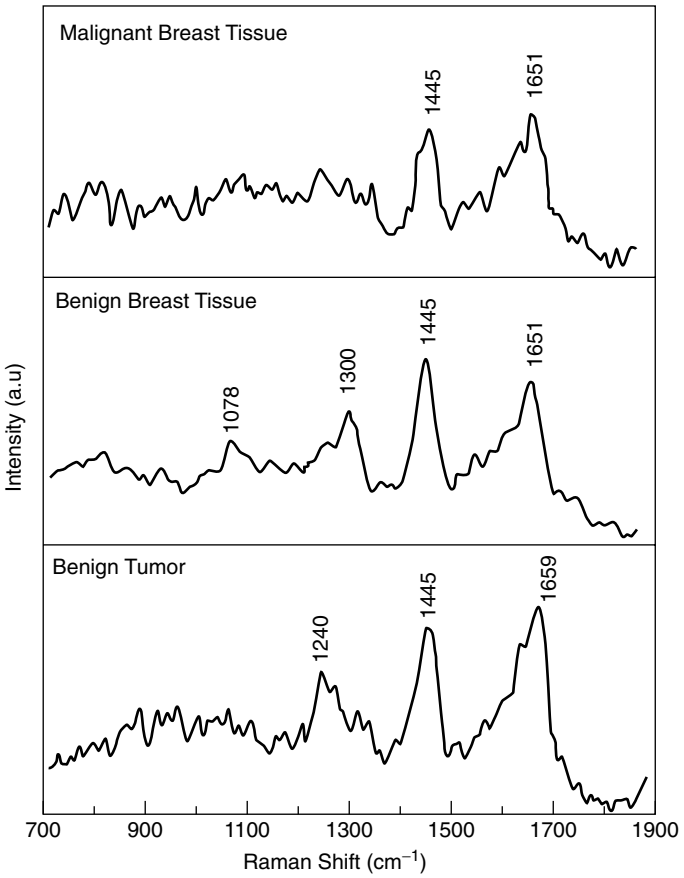

Figure 6.16. Raman spectra from normal (benign tissue), benign, and malignant breast tumors. (Reproduced with permission from Alfano et al., 1991.)

fingerprints of proteins and DNA components, revealed differences between the malignant, fibroadenoma, and normal breast tissues.

The applicability of autofluorescence and diffuse-reflectance spectroscopy for intraoperative detection of brain tumors was investigated in a clinical trail (Lin et al., 2001). The result suggested that brain tumors and infiltrating tumor regions can be effectively separated from normal brain tissues *in vivo* using a combination of these techniques.

6.8 SINGLE-MOLECULE DETECTION

Single-molecule detection is an exciting new frontier. The ability to detect a single molecule and study its structure and function provides the opportunity

to probe properties that are not available in measurements on an ensemble. A new journal, *Single Molecules*, published by Wiley-VCH in 2000, is dedicated to single-molecule spectroscopy and detection.

Fluorescence has been the spectroscopic method for single-molecule detection. Single-molecule fluorescence detection has been successfully extended to biological systems (Ha et al., 1996, 1999; Dickson et al., 1997). Excellent reviews of the applications of single-molecule detection to bioscience are by Ishii and Yanagida (2000) and Ishijima et al. (2001). Single-molecule detection has been used to study molecular motor functions, DNA transcription, enzymatic reactions, protein dynamics, and cell signaling. The single molecule detection permits one to understand the structure–function relation for individual biomolecules, as opposed to an ensemble average property that is obtained by measurements involving a large number of molecules.

The single-molecule detection utilizes fluorescence labeling of a biomolecule or a biopolymer. An ideal choice will be a fluorescent marker with the quantum efficiency (defined in Chapter 4), close to 1 so that maximum emission can be observed. Recent advances in the photoelectric detection system (conversion of an emitted photon to an electrical signal) have pushed the limit to single-photon detection, thus greatly facilitating this field. It is to be pointed out that single molecule detection does not always imply the observation of an isolated single molecule. The observation generally utilizes two approaches:

1. Detection in the dilution limit where the sample volume under optical observation consists of only one molecule or biomolecule.
2. Detection where a single biomolecule is attached to a microscopic bead which can be observed and tracked.

Manipulation of these biomolecules can be conducted by using a glass microneedle (Ishijima et al., 1996). Many studies, however, have used laser trapping of microbeads by optical tweezers, where a single molecule is attached to a microbead. Laser tweezers are discussed in Chapter 14. Therefore, single-molecule detection studies using optical trapping will be discussed there.

Fluorescence probes used for single-molecule detection are fluorescence lifetime, two-photon excitation, polarization arrisotropy, and fluorescence resonant energy transfer (FRET). Single-molecule fluorescence lifetime measurements have been greatly aided by the use of a technique called *time-correlated single-photon detection* (Lee et al., 2001). Microscopic techniques such as confocal microscopy and near-field microscopy, discussed in Chapter 7, have provided the capability to perform single-cell imaging of stained cells or cell aggregates. A two-channel confocal microscope with separated polarization detection pathways has been used by Hochstrasser and co-workers at the Regional Laser and Biotechnology Laboratories (RLBL) at University of Pennsylvania to study time-resolved fluorescence arrisotropy of single molecules. Using this technique, Hochstrasser and co-workers

simultaneously recorded single-molecule fluorescence in two-orthogonal polarizations, for free porphyrin cytochrome-c and Zn porphyrin cytochrome-c encapsulated in a glass (Mei et al., 2002). The fluorescence polarization anisotropy was shown to provide information on the orientational motions of these proteins and their interaction with the microenvironment surrounding them.

Zhuang et al. (2002) have studied the correlation between the structural dynamics and function of the hairpin ribozyme, a protein-independent catalytic RNA, by using fluorescence energy transfer. In this case they used the Cy3 dye as the energy donor and used the Cy5 dye as the energy acceptor, attached respectively to the 3′ and 5′ ends of the RzA strand of the ribozyme and studied fluorescence resonant energy transfer from Cy3 to Cy5. They found that this RNA enzyme exhibits a very complex structural dynamics with four docked (active) states of distinct stabilities and a strong memory effect. These observations would be difficult to obtain from an ensamble study because less stable conformational states are nonaccumulative. Thus, this result signifies the importance of single-molecule study in characterizing complex structural dynamics.

HIGHLIGHTS OF THE CHAPTER

- Photobiology deals with the interaction of light with complex, multistep biological processes, which can photo-induce physical, thermal, mechanical, and/or chemical effects.
- Light-absorbing components can be endogenous (cell and tissue constituents) or exogenous (photosensitizing dyes, staining components, etc).
- Transmission in biological specimen has an upper and lower cutoff of useable wavelength defined by scattering and absorptive losses.
- Most cells exhibit good transparency between 800 nm and 1300 nm.
- Light absorption in protein molecules is dictated by the characteristic absorption features of the constituent amino acids as well as the polypeptide bonds and disulfide linkages and by other chromophore that may be present.
- Absorption of light may cause radiative as well as nonradiative processes in endogenous molecules—that is, cellular constituents.
- Autofluorescence, a radiative process, is caused by the endogenous fluorophores—for example, NADH, flavins, tyrosine, porphyrins and lipopigments.
- Thermal nonradiative effects induced by light (e.g., protein denaturation and vaporization of water) are significant at the tissue level.
- Excited-state photochemical nonradiative processes include photoaddition, photofragmentation, photoxidation, photohydration, photoisomerization, and photorearrangement.

- Exogenous (added) photosensitizers can also induce photosensitization through photoaddition and photooxidation.
- Optical interactions in tissues occur in the form of refraction, reflection, absorption, and scattering.
- Scattering from tissues involves several different mechanisms: Rayleigh and Mie scattering (elastic) and Brillouin and Raman scattering (inelastic).
- Optical penetration depth δ, which is a measure of optical transparency, is the distance in a medium such that the light intensity becomes $1/e$ of the original intensity after traveling this distance.
- The experimental arrangement of double-integrating spheres can simultaneously determine the reflectance, absorption and scattering from a biological specimen.
- Interaction with light leads to radiative (autoflorescence) and nonradiative (photochemical, thermal, photoablation, plasma-induced ablation, and photodisruption) processes.
- Autofluorescence spectra provide a method of optical probing for detection of cancer, detection of metabolic changes, and so on.
- In photochemistry, recent focus is on nonlinear excitations such as two-photon absorption. It has the advantage of affecting the photochemistry at a much greater tissue depth than is possible in one-photon processes. This is advantageous in photodynamic therapy.
- Thermal effects include coagulation, vaporization, carbonization, and melting.
- Photoablation uses intense UV laser pulses (excimer laser) to photochemically decompose cellular and extracellular components and is very useful in tissue contouring.
- High-intensity irradiation leads to plasma formation, and shock waves are generated which disrupt the tissue structure (photodisruption). This has applications in minimally invasive surgery.
- The various methods of light delivery to specific regions of a biological specimen for *in vivo* spectroscopy are: free-space propagation with collimation, optical fiber delivery system e.g. medical endoscopes, articulated arm delivery system used for mid-infrared range, and hollow tube waveguides that offer some flexibility.
- Spectroscopic methods used for *in vivo* studies include electronic absorption through analysis of back-scattered light, Raman scattering, and fluorescence.
- *In vivo* spectroscopy and optical biopsy cover a broad spectrum of research such as study of cellular and tissue structures, biological functions, and early detection of cancer.

- The exciting new frontier of single-molecule detection and spectroscopy enables probing the structural and functional properties of individual biomolecules as opposed to ensemble averages. This has been used to study molecular motor functions, DNA transcription, protein dynamics, cell signaling, and so on.

REFERENCES

Adranov, A., and Frechet, J. M. J., Light-Harvesting Dendrimers, *Chem. Commun.* **18**, 1701–1710 (2000).

Agarwal, R., Krueger, B. P., Scholes, G. D., Yang, M., Yom, J., Mets, L., and Fleming, G. R., Ultrafast Energy Transfer in LHC-II Revealed by Three-Pulse Photon Echo Peak Shift Measurements, *J. Phys. Chem. B* **104**, 2908–2918 (2000).

Alfano, R. R., ed., Optical Biopsy IV, SPIE Proc. Vol. 4613, SPIE, Bellingham (2002).

Alfano, R. R., Liu, C. H., Sha, W. L., Zhu, H. R., Akins, D. L., Cleary, J., Prudente, R., and Celmer, E., Human Breast Tissue Studied by IR Fourier Transform Raman Spectroscopy, *Laser Life Sci.* **4**, 23–28 (1991).

Alfano, R. R., Pradham, A., Tang, G. C., and Wahl, S. J., Optical Spectroscopic Diagnosis of Cancer and Normal Breast Tissues, *J. Opt. Soc. Am. B.* **6**, 1015–1023 (1989).

Alfano, R. R., Tata, D. B., Cordero, J. J., Tomashefsky, P., Longo, F. W., and Alfano, M. A., Laser Induced Fluorescence Spectroscopy from Native Cancerous and Normal Tissues, *IEEE J. Quantum Electron*. **QE-20**, 1507–1511 (1984).

Brancoleon, L., Durkin, A. J., Tu, J. H., Menaker, G., Fallon, J. D, and Kellias, N., *In Vivo* Fluorescence Spectroscopy of Nonmelanoma Skin Cancer, *Photochem. Photobiol.* **73**, 178–183 (2001).

Carden, A., and Morris, M. D., Application of Vibrational Spectroscopy to the Study of Mineralized Tissues (Review), *J. Biomed. Opt.* **5**, 259–268 (2000).

Carden, A., Rajachar, R. M., Morris, M. D., Kohn, D. H., Ultrastructural Changes Accompanying the Mechanical Deformation of Bone Tissue: A Raman Imaging Study, *Calcif. Tissue Int.* **72**, in Press (2003).

Connelly, J. P., Müller, M. G., Hucke, M., Gatzen, G., Mullineaux, C. W., Ruban, A. V., Horton, P., and Holzwarth, A. R., Ultrafast Spectroscopy of Trimeric Light-Harvesting Complex II from Higher Plants, *J. Phys. Chem. B* **101**, 1902–1907 (1997).

Cossmann, P. H., Romano, V., Sporri, S., Alterman, H. J., Croitoru, N., Frenz, M., and Weber, H. P., Plastic Hollow Waveguides: Properties and Possibilities as a Flexible Radiation Delivery System for CO_2-Laser Radiation, *Lasers in Surgery and Medicine* **16**, 66–75 (1995).

Derbyshire, G. J., Bogden, D. K., and Unger, M., Thermally Induced Optical Property Changes in Myocardium at 1.06 Microns, *Lasers Surg. Med.* **10**, 28–34 (1990).

Dickson, R. M., Cubitt, A. B., Tsien, R. Y., and Meerner, W. E., On/Off Blinking and Switching Behavior of Single Molecules of Green Fluorescent Protein, *Nature* **388**, 355–358 (1997).

Frank, C. J., McCreery, R. L., Redd, D. C. B., Raman Spectroscopy of Normal and Diseased Human Breast Tissues, *Anal. Chem.* **67**, 777–783 (1995).

CHAPTER 7

Bioimaging: Principles and Techniques

Bioimaging using optical methods forms a major thrust of biophotonics. Optical bioimaging can be used to study a wide range of biological specimens, from cells to *ex vivo* tissue samples, to *in vivo* imaging of live objects. Optical bioimaging also covers a broad range of length scale, from submicron size viruses and bacteria, to macroscopic-sized live biological species. This chapter describes the basic principles and techniques used for optical bioimaging. Thus it is intended to provide the reader with the appropriate background for appreciating the various applications of optical bioimaging covered in the next chapter.

Optical bioimaging utilizes an optical contrast such as a difference in light transmission, reflection, and fluorescence between the region to be imaged and the surrounding region (background). The various optical principles involved and microscopic methods used to enhance these contrasts and utilize them for bioimaging are described.

Various types of fluorescence microscopic methods, currently in wide usage, are covered. An advantage offered by fluorescence microscopy is the use of laser beams to excite an illuminated point and scan the point of illumination to form the image. This is commonly called *laser scanning microscopy*. Confocal microscopy, which allows one to obtain images at different depths and thus reconstruct a three-dimensional image of a biological sample, is described.

Optical coherence tomography, which utilizes an interferometric method to enhance contrast in a reflection geometry and has emerged as a powerful technique for three-dimensional imaging of highly scattering biological media (such as a tooth), is discussed. Other types of microscopy described in this chapter are (i) near-field scanning microscopy (often abbreviated as NSOM), which allows one to obtain optical images at a resolution of ≤ 100 nm, much smaller than the wavelength of light itself, and (ii) total internal reflection fluorescence (TIRF) microscopy, which provides enhanced sensitivity to image and probe cellular environment close to a solid surface.

Introduction to Biophotonics, by Paras N. Prasad
ISBN: 0-471-28770-9

Other bioimaging techniques discussed are (i) spectral imaging, which provides information on spatial variation of spectra, (ii) fluorescence resonance energy transfer (FRET) imaging, which utilizies energy transfer from one fluorescent center to another to probe interactions, and (iii) fluorescence lifetime imaging microscopy (FLIM), which is used to obtain the spatial distribution of fluorescence lifetime and is a highly sensitive probe for the local environment of the fluorophore. These imaging methods offer multidimensional imaging to probe details of interactions and dynamical processes in biological systems.

Section 7.15 provides a discussion of nonlinear optical techniques used for bioimaging. These techniques have gained considerable popularity because of the ability to use short-pulse near-IR lasers that allow deeper penetration in biological materials with little collateral damage. Specifically covered in this section are second- and third-harmonic microscopies, two-photon microscopy and coherent anti-Stokes Raman scattering (CARS) microscopy.

The chapter concludes with a presentation of some future directions for further development in bioimaging. A list of commercial sources for various microscopes is also provided.

The contents of this chapter are developed using the following sources, which serve as excellent references on this subject:

Periasamy (2001): A comprehensive coverage of cellular imaging

Lacey (1999): Light microscopy in biology

Pawley (1995): Comprehensive coverage of confocal microscopy

Diaspro, ed. (2002): Coverage of foundations, applications, and advances in confocal and two-photon microscopy

Tearney and Bouma (2001): Coverage of optical coherence tomography

Pawslear and Moyer (1996): Coverage of theory, instrumentation, and applications of near-field microscopy

The following websites give extensive information on optical microscopy techniques including Java-based tutorials:

http://micro.magnet.fsu.edu

http://www.microscopyu.com

http://www.olympusmicro.com

The following periodic publications are convenient sources of updates in this field:

Journal of Bioimaging

Biophotonics International

Microscopy

BioTechniques

Journal of Biomedical Optics

7.1 BIOIMAGING: AN IMPORTANT BIOMEDICAL TOOL

Biomedical imaging has become one of the most relied-upon tools in healthcare for diagnosis and treatment of human diseases. The evolution of medical imaging from plain radiography (radioisotope imaging), to x-ray imaging, to computer-assisted tomography (CAT scans), to ultrasound imaging, and to magnetic resonance imaging (MRI) has led to revolutionary improvements in the quality of healthcare available today to our society. However, these techniques are largely focused on structural and anatomical imaging at the tissue or organ levels. In order to develop novel imaging techniques for early detection, screening, diagnosis, and image-guided treatment of life-threatening diseases and cancer, there is a clear need for extending imaging to the cellular and molecular biology levels. Only information at the molecular and cellular levels can lead to the detection of the early stages of the formation of a disease or cancer or early molecular changes during intervention or therapy.

The currently used medical techniques of x-ray imaging, radiography, CAT scans, ultrasound imaging, and MRI have a number of limitations. Some of these are:

- Harmful effects of ionizing radiations in the case of x-ray imaging and CAT scan
- Unsuitability of x-ray imaging for young patients and dense breasts, as well as its inability to distinguish between benign and malignant tumors
- Harmful radioactivity in radioisotope imaging
- Inability of MRI to provide specific chemical information and any dynamic information (changes occurring in real time response to a treatment or a stimulus)
- Inability of ultrasound to provide resolution smaller than millimeters as well as to distinguish between a benign and a malignant tumor

Optical imaging overcomes many of these deficiencies. Contrary to the perception based on the apparent opacity of skin, light, particularly in near-IR region, penetrates deep into the tissues as discussed in Chapter 6. Furthermore, by using a minimally invasive endoscope fiber delivery system, one can reach many organs and tissue sites for optical imaging. Thus, one can even think of an "optical body scanner" that a physician may use some day for early detection of a cancer or an infectious disease.

Optical imaging utilizes the spatial variation in the optical properties of a biospecie, whether a cell, a tissue, an organ, or an entire live object. The optical properties can be reflection, scattering, absorption, and fluorescence. Therefore, one can monitor spatial variation of transmission, reflection, or fluorescence to obtain an optical image. The use of lasers as an intense and convenient light source to generate an optical response, whether reflection, transmission, or emission, has considerably expanded the boundaries of optical imaging,

making it a most powerful technique for basic studies as well as for clinical diagnostics. Some of the benefits offered by optical imaging are:

- Not being harmful
- Imaging from size scale of 100 nm (using near field, to be discussed in Section 7.11) to macroscopic objects
- Multidimensional imaging using transmission, reflection, and fluorescence together with spectroscopic information
- Imaging of *in vitro*, *in vivo*, and *ex vivo* specimens
- Information on cellular processes and tissue chemistry by spectrally resolved and dynamic imaging
- Fluorescence imaging providing many parameters to monitor for detailed chemical and dynamical information. These parameters are:
  - Spectra
  - Quantum efficiency
  - Lifetime
  - Polarization
- Ability to combine optical imaging with other imaging techniques such as ultrasound
- Sensitivity and selectivity to image molecular events

The area of optical imaging is very rich, both in terms of the number of modalities and with regard to the range of its applications. It is also an area of very intense research worldwide because new methods of optical imaging, new, improved, and miniaturized instrumentations, and new applications are constantly emerging.

7.2 AN OVERVIEW OF OPTICAL IMAGING

A number of methods based on the optical properties monitored are used for imaging. These methods are summarized in Table 7.1.

Transillumination microscopic imaging utilizes a spatial variation of absorption and scattering in the microscopic and macroscopic structures of tissues. A tissue is a highly scattering medium. As the light propagates through a tissue, the transmitted light is comprised of three components: unscattered (or coherently scattered), weakly scattered, and multiply scattered light. These different components can be visualized by taking an example of a short pulse of laser light propagating through a tissue, as illustrated in Figure 7.1 (Gayen and Alfano, 1996).

The coherently scattered light, called the *ballistic photons*, propagate in the direction of the incoming beam. They, therefore, travel the shortest path and emerge first from the tissue. Ballistic photons carry maximum information on

TABLE 7.1. Optical Methods of Imaging

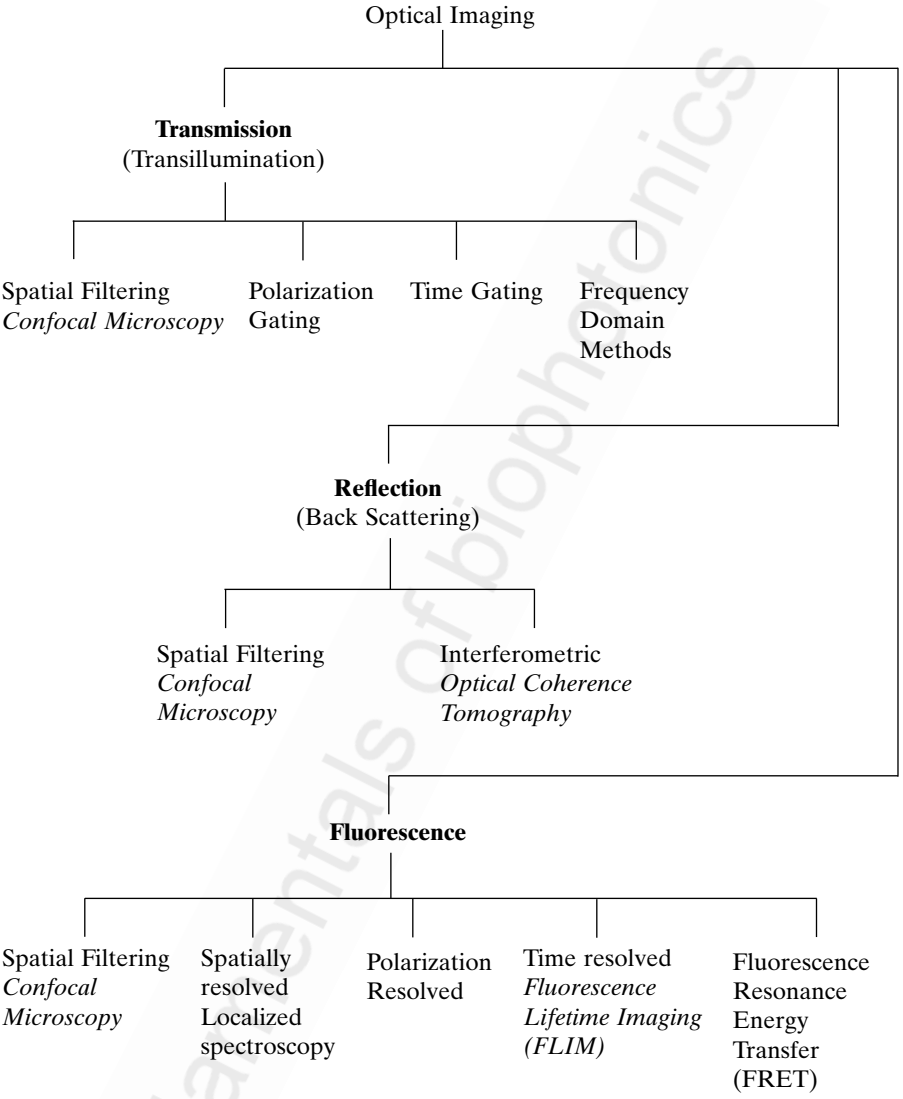

the internal structure of the tissue. The portions of light that scatter slightly more, but still in the forward direction, are called *snake photons* because of their wiggly trajectories in the forward direction. These photons are time-delayed with respect to the ballistic photons but still carry significant information on the scattering medium. However, most portions of the light beam undergo multiple scattering and travel long distances within the medium. They

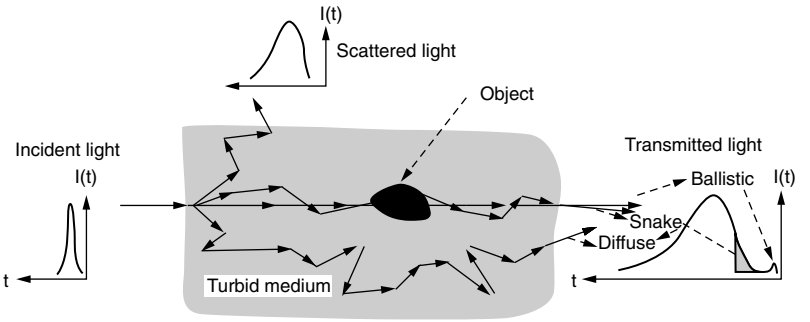

Figure 7.1. Propagation of a laser pulse through a turbid medium. (Reproduced with permission from Gayen and Alfano, 1996.)

emerge even later and are called *diffuse photons*. They carry little information on the microstructure of the tissue and have to be discriminated in order to image using ballistic and snake photons. Some of the commonly used methods to discriminate against the diffuse photons are listed in Table 7.1 and are briefly described below:

- *Spatial Filtering*. It is one of the simplest methods and relies on the fact that diffuse photons, undergoing multiple scattering, are more spread out and off-axis. Therefore, applying spatial filtering by using a transmitted light collection using an aperture (such as a small diameter fiber or a pinhole) provides rejection of a substantial amount of off-axis diffuse light. The most widely used microscope, a confocal microscope discussed later, uses a confocal aperture (pinhole) in the light collection path for spatial filtering. This confocal aperture in a confocal microscope is also used to enhance contrast and provide depth discrimination in reflection and fluorescence imaging.
- *Polarization Gating*. Here one utilizes a linearly polarized light. The transmitted ballistic and snake photons still retain much of the initial polarization, while the multiply scattered diffuse light are depolarized. Thus, by collecting the transmitted light through a polarizer allowing the transmission of light only with the polarizations parallel to the initial polarization, one can reject a significant portion of the diffuse light.
- *Time Gating*. This method utilizes a short laser pulse as the illumination source. The transmitted light is passed through an optical gate that opens and closes to allow transmission only of the ballistic and/or snake photons. Synchronization can be achieved by using a reference optical pulse that controls the opening and closing of the optical gate. A number of pulse gating techniques such as Kerr gate, nonlinear optical gate, and time-correlated single-photon counting are used. However, a detailed discussion of any of these methods is outside the scope of this book.

- *Frequency-Domain Methods*. In this method the time gating is transformed to intensity modulation in frequency domain (Lakowicz and Berndt, 1990). In this mode, the specimen is illuminated with an intensity-modulated beam from a CW laser, and the AC modulation amplitude and the phase shift of the transmitted signal are measured using methods such as heterodyning. One often uses the diffuse photon density wave description to analyze the transport of the modulated beam. In a sense, the situation here is analogous to the frequency domain measurement of fluorescence lifetime as described in Chapter 4, in which the temporal (time-resolved) information is obtained from the phase-shift information. The advantage of this method is that less expensive CW laser sources can be utilized. A limitation is that the readily available modulation frequency is only of a few hundred megahertz, which corresponds to time gating only with a few nanosecond resolution.

Reflection imaging collects the back-scattered light. Again, the coherently scattered light needs to be discriminated against the multiply scattered component. Two methods used are confocal and interferometric. The latter method has given rise to a very powerful microscopic technique called *optical coherence tomography* (OCT) for imaging of highly scattered tissues. This technique is discussed in detail in Section 7.9. In some cases, both confocal and OCT approaches are combined to enhance the discrimination against multiple-scattered light.

Fluorescence microscopy is the most widely used technique for optical bioimaging. It provides a most comprehensive and detailed probing of the structure and dynamics for *in vitro*, as well as *in vivo*, biological specimens of widely varying dimensions. The topic of fluorescence imaging is discussed in a separate section. Nonlinear optical methods have also recently emerged as extremely useful for bioimaging. Multiphoton-induced fluorescence microscopy is currently a very exciting new approach for bioimaging. Second-harmonic microscopy is also gaining popularity.

7.3 TRANSMISSION MICROSCOPY

7.3.1 Simple Microscope

A simple microscope is nothing but a single magnifying lens. The early design of a microscope had a single lens mounted on a metal plate with screws to move the specimen across the field of view and to focus its image. The concept of image formation by a lens is shown in Figure 7.2. A lens works by refraction and is shaped so that the light rays near the center are hardly refracted and those at the periphery are significantly refracted (Born and Wolf, 1999). A parallel beam of light passing through a convex lens is focused to a spot.

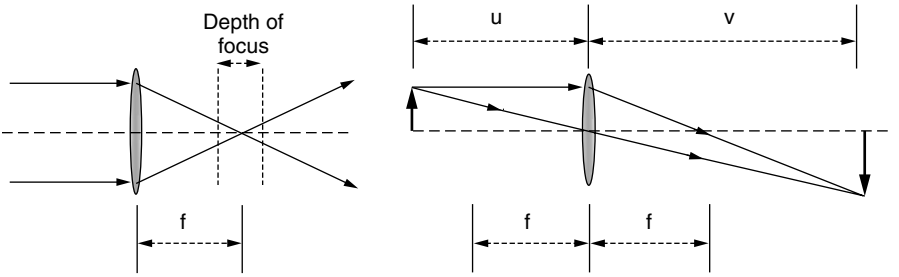

Figure 7.2. Ray tracing diagram showing the focusing action of a convex lens (*left*) and an image formation (*right*).

The distance from the center of the lens to the spot is known as the *focal length* of the lens (f). As shown in the figure, if an object is placed on one side of the lens at a distance u from it, a real image of that object is formed on the other side of the lens at a distance v. The image formed will be a magnified image, with magnification factor given by M = (image height) / (object height), which in turn is equal to the ratio of the image distance to the object distance (v/u). In a microscope, the object is placed in its focal plane and it forms a magnified image, which can either be observed by eyes or recorded by a camera. The object has to be placed close to the focal plane, within a short range known as the *depth of focus*, to obtain a sharp magnified image.

7.3.2 Compound Microscope

A compound microscope consists of a combination of lenses to significantly improve the magnification and functionality over a simple microscope. Figure 7.3 shows a compound microscope and its various components. Here, a magnified image of an object is produced by the objective lens that is again magnified by a second lens system (the ocular or eyepiece) for viewing. Thus, final magnification of the microscope is dependent on the magnifying power of the objective (lens) multiplied by the magnifying power of the eyepiece. Typical objective magnification powers range from 4× to 100×. Lower magnification objectives in a compound microscope are not commonly used because of spatial constraints of illumination (require special condensers for illumination), while higher magnification objectives are impractical due to their limited working distances.

Ocular magnification ranges are typically 8×–12×, though 10× oculars are most common. As a result, a standard microscope provides one with a final magnification range of ~40× up to ~1000×. Usually, a compound microscope contains many lenses to provide convenient illumination and to correct for different optical aberrations.

In a typical microscope, the objective lens projects an intermediate image of an object placed slightly off the front focal plane, onto a plane inside the

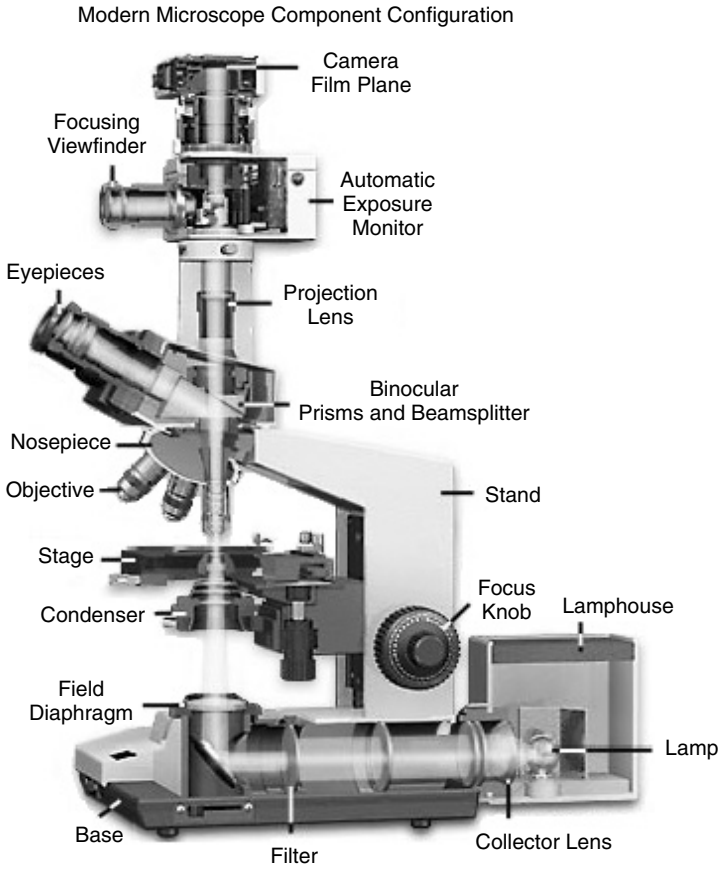

Figure 7.3. Schematic diagram of an upright transmission microscope. (Reproduced with permission from http://micro.magnet.fsu.edu/primer/anatomy/components.html.)

microscope. This intermediate image is then magnified and projected onto the retina by the eyepiece of the microscope. This type of microscope is called a *finite-tube-length microscope*, because it assumes a fixed path length between the objective and the eyepiece. But in most modern microscopes, a slightly different design is used to accommodate the introduction of different optical components, like a polarizer, inside the microscope, without affecting the image formation. In this design, the objective doesn't form an intermediate image, but an extra tube lens placed close to the eyepiece does the job of projecting the intermediate image. In this *infinity-corrected microscope*, there is a parallel beam of light in the space between the objective and the tube lens, whereby adding any other required optical component does not disturb the ray path. Figure 7.4 shows the optical ray path in these two variants of microscopes.

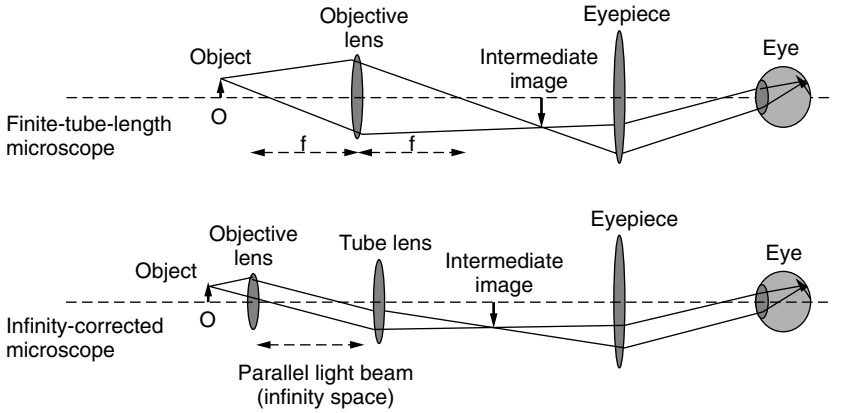

Figure 7.4. Schematic diagrams of optical ray paths in finite-tube-length microscope and in infinity-corrected microscope.

In a commonly used microscope, the sample plane is illuminated by a lamp through a set of collecting and condensing lenses and iris diaphragms. A proper illumination of the specimen observed under the microscope is critical for achieving a high-quality image through the eyepiece. The achievable resolution of a microscope depends not only on the objective lens used, but also on the way the sample is illuminated by its illumination system.

7.3.3 Kohler Illumination

One of the most commonly used illumination system in a transmission microscope is Kohler illumination, which provides an evenly illuminated field of view with a bright image, without glare and minimum heating of the specimen. Furthermore, as discussed below, it is important to have an illumination scheme where the sample is illuminated with a cone of light as wide as possible to achieve the best resolution possible. This feature is realized in the Kohler illumination scheme as shown in Figure 7.5. The light from the illuminating lamp, passing through a set of field diaphragms and lenses, simultaneously creates a uniformly illuminated field of view (parallel rays) while illuminating the specimen with a cone of light as wide as possible. The light pathways illustrated in Figure 7.5 are schematic representations of separate paths taken by the sample illuminating light rays and the image-forming light rays. Though in reality one cannot separate these two components, these diagrams help us to understand the process of uniform illumination and image formation.

As shown in Figure 7.5, the illuminating light ray path produces focused images of the lamp filament at the plane of the condenser aperture diaphragm, at the back focal plane of the objective, and at the eye point of the eyepiece.

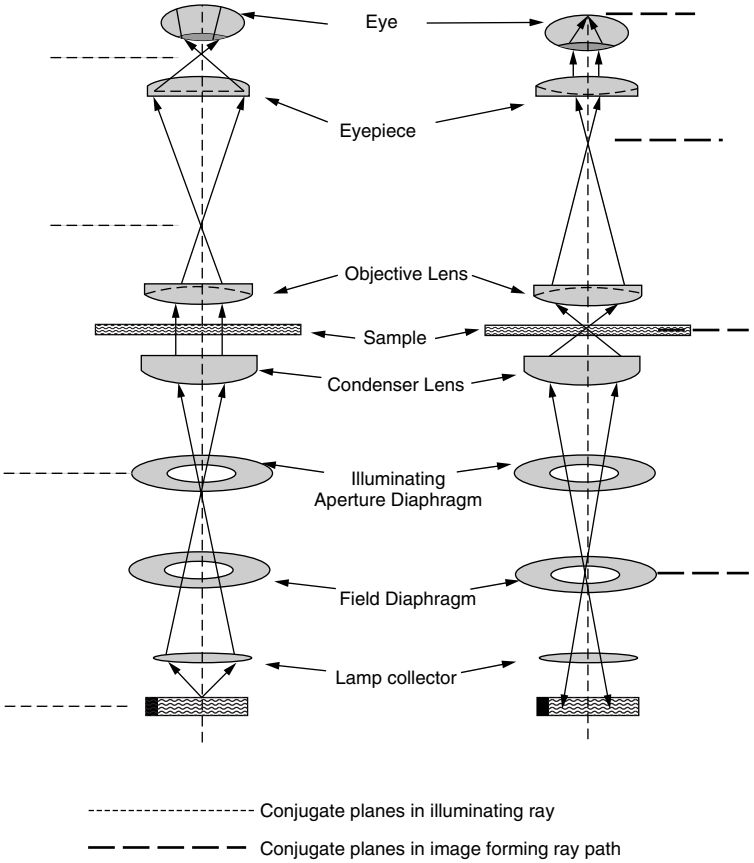

Figure 7.5. Schematic design for Kohler illumination.

These planes are called the *conjugate planes* of illuminating ray path. Conjugate planes in an optical system represent a set of planes such that an image focused on one plane is automatically focused on all other conjugate planes. The conjugate planes for image forming rays consist of the field diaphragm, the sample plane, the intermediate image plane and the retina of the eye. The field diaphragm and the condenser diaphragm are placed at the conjugate planes of image forming rays and illuminating rays, respectively. This allows independent controls over the angle, at which the sample is illuminated, and the intensity of illumination. A detailed description of Kohler illumination and Java-based tutorials on the effect of apertures in the microscopic illumination system can be found at the website http://micro.magnet.fsu.edu/primer/java/microscopy/transmitted/index.html.

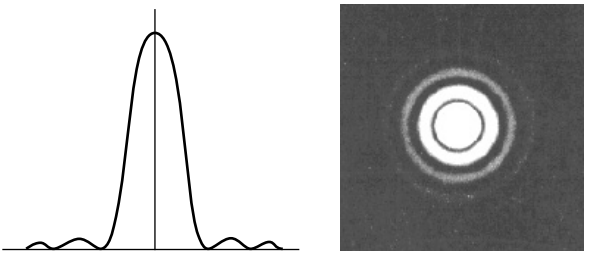

Figure 7.6. Intensity distribution and Airy disk formation.

7.3.4 Numerical Aperture and Resolution

The resolution of a microscope is its ability to distinguish between the smallest possible objects. This is directly related to the cone of light entering the objective from the sample. But, this optical resolution is limited by the diffraction of light occurring from the object, due to the wave nature of light. This principle can be understood by looking at a beam of light passing through a pinhole (Abbe, 1873; Born and Wolf, 1999). The image produced by the light passing through a pinhole and its intensity profile are shown below. This circular fringe pattern formation is known as the *Airy disk*. It looks like a negative target with a large bright central disk of light surrounded by a series of thin concentric circles of light of decreasing brightness as moving away from center (Figure 7.6). This effect is due to the diffraction of light emerging from the pinhole into multiple orders, which are represented by the concentric circles. The diffraction through pinholes has also been discussed in Chapter 2. While imaging small features in a sample using a microscope, a similar effect takes place. In order to get the entire information on these small features, the objective lens has to collect light of all these diffraction orders. Furthermore, the bigger the cone of light brought into the objective lens, the more of these diffraction orders can be collected by it, thus increasing the resolving power of the objective. As described below, this collection angle of the objective also determines the resolution of a microscope. This acceptance angle of light is quantified by a parameter called *numerical aperture* (NA) of the objective. The numerical aperture is defined as

$$\mathrm{NA} = n\sin(\theta) \tag{7.1}$$

Here n is the refractive index of the medium from which the light rays enter the objective and θ is the maximum angle at which the light rays enter the objective as shown in Figure 7.7. The bigger the cone of light that can be brought into the lens, the higher its numerical aperture. From the expression shown above, it is clear that the maximum NA aperture an objective can achieve is the refractive index of the medium (since the maximum value of a

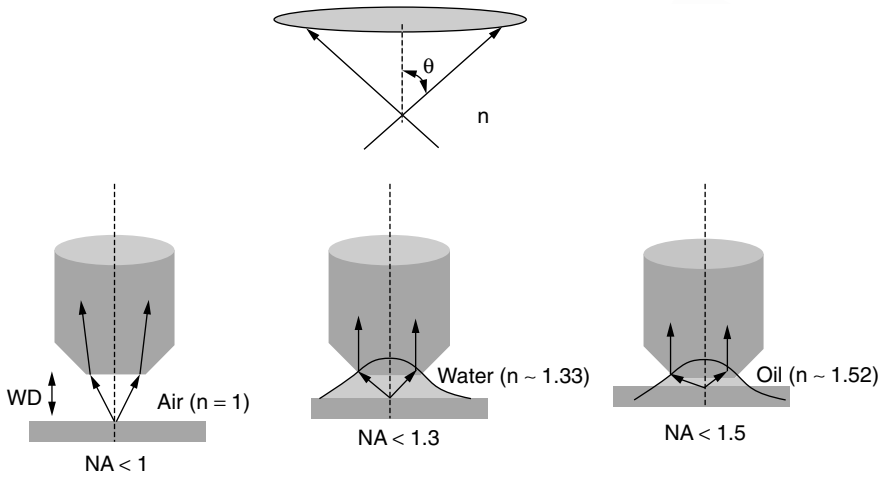

Figure 7.7. Numerical apertures for air, water, and oil as the media between the sample and the objective lenses.

sine function is 1). One way to improve the NA is to use an immersion medium with a higher refractive index than air. The most commonly used media for this purpose are water and oil. But, one thing to remember is that the use of higher NA objectives leads to a reduction of the working distance of the objective (distance between the objective and the sample). This behavior is also illustrated in Figure 7.7.

The resolution of an objective/microscope is defined as the distance, d, between two adjacent particles which still can be perceived as separate. Based on the limits of diffraction the resolution is given by Rayleigh's criteria (Born and Wolf, 1999) as

$$d = 1.22(\lambda/2\mathrm{NA})$$

Therefore, lenses with higher NA can give better resolution. In a transmission microscope, the numerical aperture of the objective, together with the NA of the condenser lens providing the illuminating light, determines the resolution. Thus, to achieve diffraction-limited resolution using a particular objective, the condenser must have an equal or higher NA. Furthermore, the magnification and the resolution of a microscope can be determined only by taking together into account the objective, the condenser, the eyepiece, and the illumination scheme used.

7.3.5 Optical Aberrations and Different Types of Objectives

The two major distortions or aberrations (Davidson and Abramowitz, 1999) in optical microscopy are (i) chromatic aberration which is due to the different

refractive indices of the glass optical element (such as a lens) for different wavelengths and (ii) geometrical or spherical aberrations due to the shape of the lens, in which the rays from the edges of the lens don't get focused at the same point where the axial rays focus. Both these aberrations can be corrected by using lens doublets consisting of two lenses made of materials of different refractive indices. Good-quality objectives may contain multiple lenses to compensate for these errors. These corrected objectives are named *achromatic* and *aspheric* objectives. Another aberration in optical microscopy is due to the field curvature (curved image plane) of the objective lens that produces a curved image. New objectives made of special fluorite glass are available which correct for most of these aberrations. Thus one can choose from different types of objective lenses such as achromat, Plan-achromat, Plan-apochromat, Plan-Fluor, and so on, depending on the application and degree of aberration correction needed.

7.3.6 Phase Contrast Microscopy

Phase contrast microscopy is one of the most commonly used optical microscopic techniques in biology. Many of the unstained biological samples like cells don't introduce any amplitude changes (by absorption or scattering) in the transmitted light and hence are difficult to observe under normal bright-field microscopy. Phase contrast microscopy or dark-field microscopy provides enhancement of contrast.

In this technique (Zernike, 1942; Abramowitz, 1987a), the phase and the amplitude differences between undiffracted and diffracted light are altered to produce favorable conditions for interference and contrast enhancement. In phase specimens, the direct zeroth-order (undiffracted) light passes through or around the specimen undeviated. However, the light diffracted by the specimen is not reduced in amplitude, but is slowed by the specimen because of the specimen's refractive index or thickness (or both). This diffracted light, lagging behind by approximately 1/4 wavelength, arrives at the image plane shifted in phase from the undeviated light by 90°. Introduction of a phase plate that introduces an additional l/4 phase difference between diffracted and undiffracted beams produces destructive interference between these two parts of the light. This interference can translate the phase difference into amplitude difference, which can be observed by eyes in a microscope. This is called *dark* or *positive phase* contrast, because the refractive object under observation appears dark in a bright background. For this, an annular ring is placed at the front focal plane of the condenser lens and a matching phase ring at the back focal plane of the objective, as shown in Figure 7.8.

7.3.7 Dark-Field Microscopy

Another technique commonly used for contrast enhancement is dark-field illumination (Abramowitz, 1987b; Davidson, 1999). In this case, the sample is

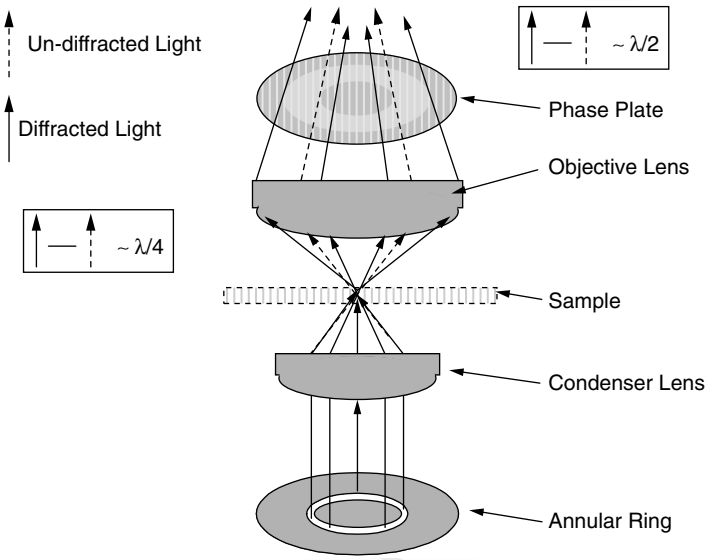

Figure 7.8. Optical schematics for phase contrast microscopy.

illuminated at an angle that cannot be accepted by the objective's aperture. In this case only the highly diffracted rays enter the objective. Hence only highly scattering or diffracting structures can be observed using this technique. Dark-field illumination requires blocking off the central light that ordinarily passes through and around the specimen, allowing only oblique rays from every angle to reach the specimen. This requires the use of special condensers that allow light rays emerging from the surface in all azimuths to form an inverted hollow cone of light with an apex centered in the sample plane. If no specimen is present and the numerical aperture of the condenser is greater than that of the objective, the oblique rays cross and all such rays miss entering the objective. In this case the field of view is dark. Because only the rays diffracted or refracted from the specimen reach the objective, this technique gives a high contrast image of the structures in the sample that diffract or refract the light.

7.3.8 Differential Interference Contrast Microscopy (DIC)

Differential interference contrast is a technique that converts specimen optical path gradients into amplitude differences that can be visualized as improved contrast in the image. This is accomplished by using a set of modified Wollaston prisms (Abramowitz, 1987b; Davidson, 1999). In this technique, living or stained specimens, which often yield poor images when viewed in bright-field illumination, are made clearly visible. Today there are several implementations of this design, which are collectively called *differential inter-*

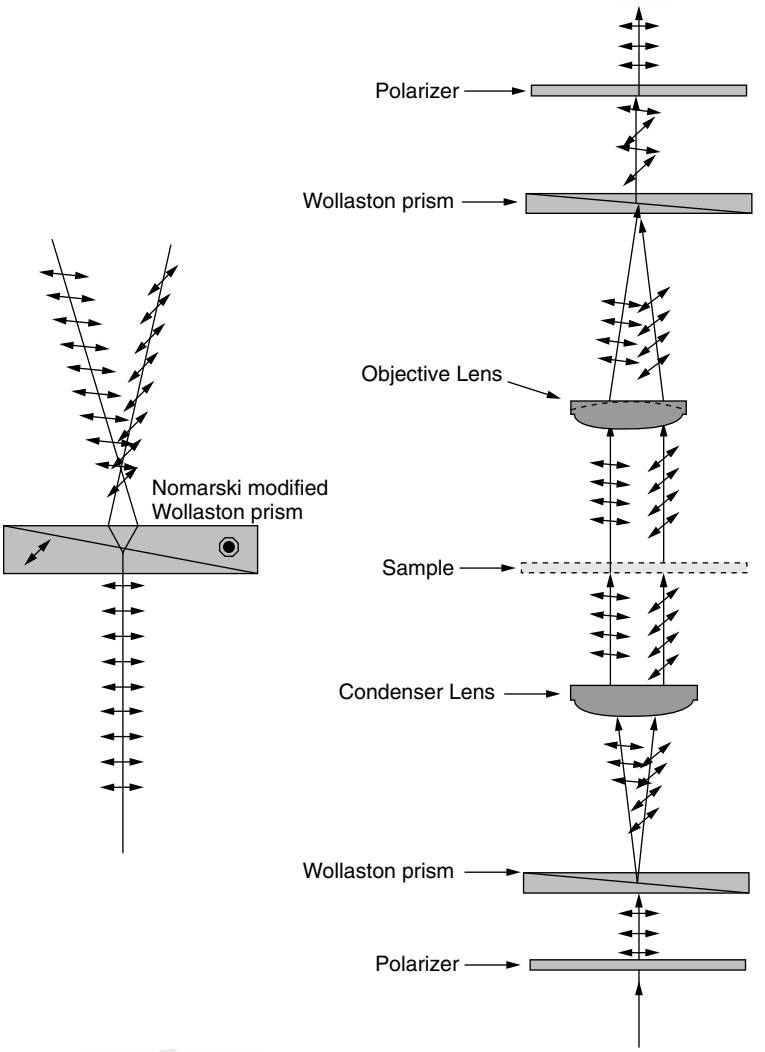

Figure 7.9. Principle of DIC microscope.

ference contrast (DIC), as shown in Figure 7.9. In transmitted light DIC, light from a lamp is passed through a polarizer located beneath the substage condenser, in a manner similar to polarized light microscopy. Next in the light path (but still beneath the condenser) is a modified Wollaston prism that is composed of two quartz wedges cemented together.

The plane-polarized light, oscillating only in one direction perpendicular to the propagation direction of the light beam, enters the Wollaston prism, which

splits the light into two rays oscillating perpendicular to each other. The split beams enter and pass through the specimen where their wave paths are altered in accordance with the specimen's varying thicknesses, slopes, and refractive indices. When the parallel beams enter the objective, they are focused above the rear focal plane where they enter a second modified Wollaston prism that combines the two beams at a defined distance outside of the prism itself. As a result of having traversed the specimen, the paths of the two beams are not of the same length (optical path difference) for different areas of the specimen. After passing through another polarizer (analyzer) above the upper Wollaston beam-combining prism, these two beams interfere to translate the path difference introduced by the objects in the sample plane, into intensity difference. When a white light source from a lamp is used for imaging, each color will have a different optical path-length difference, thereby producing a color contrast. This results in observing the object details in pseudo—3-D and in color contrast.

7.4 FLUORESCENCE MICROSCOPY

Fluorescence microscopy has emerged as a major technique for bioimaging. Fluorescence emission is dependent on specific wavelengths of excitation light, and the energy of excitation under one photon absorption is greater than the energy of emission (the wavelength of excitation light is shorter than the wavelength of emission light). Fluorescence has the advantage of providing a very high signal-to-noise ratio, which enables us to distinguish spatial distributions of even low concentration species. To utilize fluorescence, one can use endogenous fluorescence (autofluorescence) or one may label the specimen (a cell, a tissue, or a gel) with a suitable molecule (a fluorophore, also called fluorochrome) whose distribution will become evident after illumination. The fluorescence microscope is ideally suited for the detection of particular fluorochromes in cells and tissues.

The fluorescence microscope that is in wide use today follows the basic "epi-fluorescence excitation" design utilizing filters and a dichroic beam splitter. The object is illuminated with fluorescence excitation light through the same objective lens that collects the fluorescence signal for imaging. A beam splitter, which transmits or reflects light depending on its wavelength, is used to separate the excitation light from the fluorescence light. In the arrangement, shown in Figure 7.10, the shorter-wavelength excitation light is reflected while the longer-wavelength emitted light is transmitted by the splitter.

With the advent of different fluorochromes/fluorophores, specifically targeting different parts of the cells or probing different ion channel processes (e.g., Ca^{2++} indicators), the fluorescence microscopy has had a major impact in biology (See Chapter 8). The development of confocal microscopy, discussed in Section 7.7, has significantly expanded the scope of fluorescence microscopy.

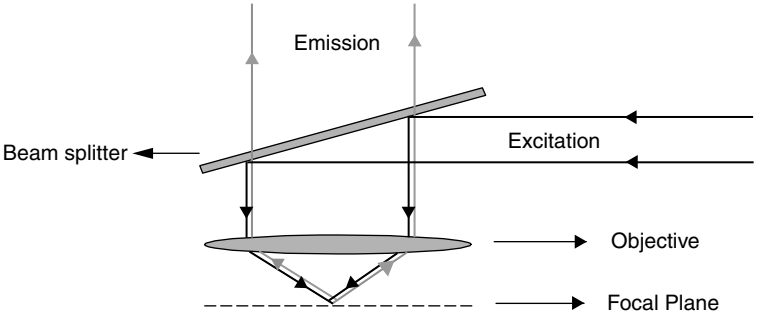

Figure 7.10. Basic principle of epi-fluorescence illumination. (See color figure.)

7.5 SCANNING MICROSCOPY

A primary problem with the fluorescence images that one observes or generates is that the out-of-focus regions of the sample appears as a "flare" in the object, reducing the signal-to-noise ratio substantially. Furthermore, during the imaging process, the entire sample is illuminated with high intensity excitation light, which can easily photooxidize (also known as photobleaching) the fluorochrome. As a means to eliminate both of these problems, it is possible to utilize a scanning optical microscope (Shepperd et al., 1978; Wilson et al., 1980) that permits observation of specimens at very high resolution, with comparatively low photooxidation of the fluorochrome.

A scanning optical microscope is designed to illuminate an object in a serial fashion, point by point, where a focused beam of light (from a laser) is scanned across the object rapidly in an X–Y raster pattern. The raster pattern is created by the repeated rotation of a beam deflecting galvanometric mirror assembly. Thus, a bright spot of light scans across an object and the image is generated point by point, in a raster format using a photomultiplier tube detection system. The intensity information is digitized and stored in a computer to generate the entire image of the scanned region. The resolution in scanning microscopy is limited by the spot size of the laser beam, which can approach the diffraction limit for the wavelength used.

Another approach to scanning microscopy is Nipkow disk microscopy (also known as tandem scanning microscopy). Instead of the point scanning techniques described above, Nipkow disk microscopy uses a spinning opaque disk perforated with multiple centrosymmetrical sets of holes (known as Nipkow disk) to illuminate the sample with multiple points (Petran et al., 1968, 1985). By rotating this disk, the entire sample area can be illuminated at high speeds, allowing real-time imaging or video rate imaging.

7.6 INVERTED AND UPRIGHT MICROSCOPES

The different types of transmission microscopy or fluorescence microscopy generally utilize a standard upright microscope in which light enters from the bottom and is viewed through the objective from the top. Alternatively, an inverted microscope can also be used in which the light source and the condenser are above the sample stage and the objective is below the stage.

For bioimaging, an inverted microscope offers certain advantages over an upright microscope. The main advantage of an inverted microscope is that gravity works in its favor. If the sample is something that will settle (or if the sample is at the bottom of a Petri dish), the settling will occur toward the objective in an inverted microscope, but away in an upright microscope. Thus settling objects are easier to image using an inverted microscope.

However, the design of an inverted microscope is more complex and the maximum magnification available is smaller than that for an upright microscope. All the options like phase contrast, DIC, or fluorescence imaging are available with an inverted microscope as well.

7.7 CONFOCAL MICROSCOPY

In a conventional wide-field microscope, thick specimens will produce an image that represents the sum of sharp image details from the in-focus region, combined with blurred images from all the out-of-focus regions. This effect does not significantly deteriorate images at low magnification (10× and below) where the depth of field is large. However, high-magnification objectives utilize high-numerical-aperture lenses that produce a limited depth of field, defined as the distance between the upper and the lower planes of the in-focus region. The area where sharp specimen focus is observed can be a micron or less at the highest numerical apertures. As a result, a specimen having a thickness greater than three to five microns will produce an image in which most of the light is contributed by the regions that are not in exact focus. The contribution from a blurred background reduces the contrast of the in-focus image.

Confocal microscopy overcomes this problem by introducing a confocal aperture (such as a pinhole) in the path of the image forming beam (fluorescence in case of fluorescence microscopy) to reject the out of focus contribution (Minsky, 1961).

In confocal microscopy, a point-like light source (laser) is focused by an objective onto a sample (Egger and Petran, 1967). The spatial extension of the focus spot on the sample is determined by the wavelength, the numerical aperture of the lens, and the quality of the image formation. The image spot is then focused through the same (or a second) lens onto an aperture (pinhole) and onto a detector. This pinhole is situated at a plane where the light from the

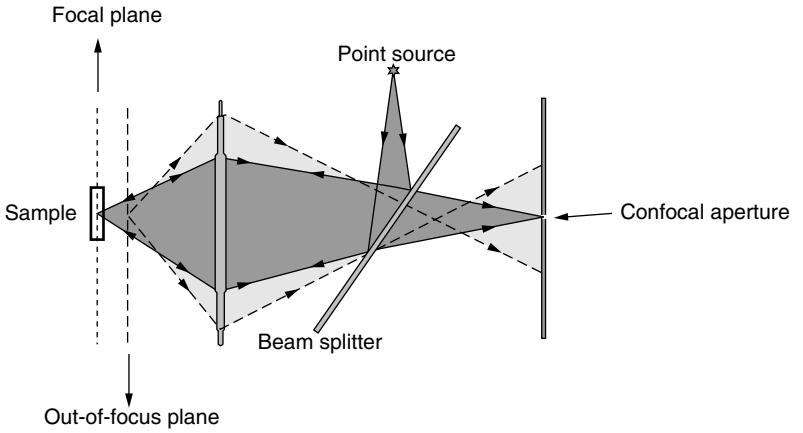

Figure 7.11. Ray path in confocal microscopy showing the out-of-focus rejection of the light from the sample by a confocal aperture.

in-focus part of the image converges to a point (i.e., at a conjugate focal plane). The principle utilized in a confocal microscope is shown in Figure 7.11.

Light from object planes above or below that of the focused image do not converge at the pinhole and hence is mostly blocked by it. Consequently, all out-of-focus optical background is removed from the image and the confocal image is basically an "optical section" of what could be a relatively thick object. The "thickness" of the optical section may approach the limit of resolution. However, in practice, the resolution in the z direction is somewhat greater: approximately 0.4–0.8 μm, depending on the excitation wavelength used. This value is dependent on multiple factors, such as the wavelength used and the size of the confocal aperture.

In order to build an image using the confocal principle, the focused spot of light is scanned across the specimen, either by scanning the laser beam (Brakenhoff, 1979; Brakenhoff et al., 1979) in a raster mode with a galvanometer mirror assembly (beam scanning) or by moving the sample stage (stage scanning) (Sheppard et al., 1978; Wilson et al., 1980). The stage scanning arrangement offers the advantage that the scanning beam is held stationary on the optical axis of the microscope, thus eliminating most aberrations introduced by lenses. For biological specimens, however, any movement of the specimen can cause wobble and distortion, resulting in a loss of resolution in the image. Therefore, bioimaging generally utilizes beam scanning with a galvanometer mirror assembly. To obtain a three-dimensional image, the focal plane is changed by translating the sample stage vertically, using a stepper motor or using a piezoelectric stage. The raster scanned data from each focal plane are obtained and stored in a computer, to reconstruct the 3D image of the sample. The principles of three-dimensional imaging in confocal microscopy has been discussed in detail by Gu (1996).

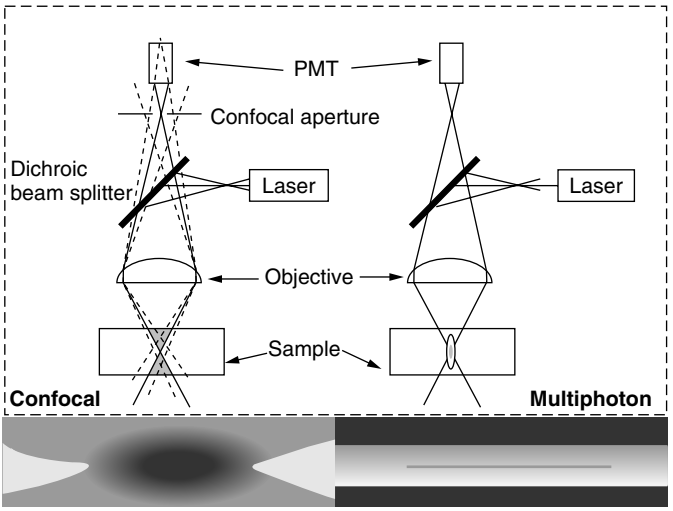

Figure 7.12. Confocal and multiphoton imaging. The bottom panel demonstrates the vertical cross section of the photo-bleached area in a sample. (Bottom panel reproduced with permission from Denk et al., 1995.)

Even though confocal microscopy provides a high-resolution optical sectioning capability, it has some inherent problems (Pawley, 1995). Since the confocal aperture reduces the fluorescence signal level, one needs a higher excitation power, which can increase the possibility of photobleaching. Furthermore, in single-photon confocal microscopy, linear excitation is used to obtain fluorescence. In this case the excitation of fluorescence occurs along the exciting cone of light, as shown in Figure 7.12, thus increasing the chance of photobleaching a large area. Another problem is that most fluorophores used for bioimaging are excited by one-photon absorption in the UV or blue light region. At these wavelengths, light is highly attenuated in a tissue, limiting the depth access. Some of these problems can be overcome (Konig, 2000) with the use of multiphoton excitation (also shown in Figure 7.12), which is described in the next section.

7.8 MULTIPHOTON MICROSCOPY

In multiphoton microscopy, a fluorophore (or fluorochrome) is excited by multiphoton absorption discussed in Chapter 5, and the resulting up-converted fluorescence (also discussed in Chapter 5) is used to obtain an image. Both two-photon and three-photon absorption-induced up-converted fluorescence have been used for multiphoton microscopy (Denk et al., 1990; Maiti et al., 1997). However, for practical reasons of three-photon absorption requiring extremely high peak power, only two-photon microscopy has emerged as a

powerful technique for bioimaging. Two-photon laser scanning microscopy (TPLSM) can use a red- and near-infrared-wavelength short pulse (picoseconds and femtoseconds) laser as the excitation source and produce fluorescence in the visible range. Therefore, two-photon microscopy extends the range of dynamic processes by opening the entire visible spectral range for simultaneous multicolor imaging (Bhawalkar et al., 1997). Two-photon excitation, as discussed in Chapter 5, involves a simultaneous absorption of two laser photons from a pulsed laser source, to achieve fluorescence at the desired wavelength. The transition probability for simultaneous two-photon absorption is proportional to the square of the instantaneous light intensity, hence necessitating the use of intense laser pulses. It is preferable to use ultra-short laser pulses (picosecond or femtosecond pulses from mode-locked lasers), whereby the average power can be kept very low to minimize any thermal damage of the cell or biological specimen. A Ti: Sapphire laser (See Chapter 5), which produces very short (~100 fs) pulses of light around 800 nm (at a rate of ~80-MHz repetition rate), with a very large peak power (50 kW), has been a popular choice for two-photon microscopy.

Merits of TPLSM

In TPLSM, which utilizes a tightly focused excitation beam, the region outside the focus has much less chance to be excited. This eliminates the substantial "out-of-focus" fluorescence, often induced by one-photon excitation when used without a confocal aperture. TPLSM thus provides an inherent optical sectioning ability without using any confocal aperture. Two-photon excitation can also greatly reduce photobleaching, becasuse only the region at the focused point can be excited. This feature is derived from the fact that two-photon excitation is quadratically dependent on the intensity and hence highly localized at the focal point at which the intensity is greater.

Compared to short wavelength excitation in the UV-visible range, longer wavelength excitation with near-IR light can penetrate much deeper into a tissue because of less scattering or absorption at a longer wavelength (see Chapter 6). The elimination of UV also improves the viability of a cell (or tissue) and permits more scans to obtain a better 3-D image. From the instrumentation perspective, converting a conventional scanning laser microscope to TPLSM is straightforward. One only needs to change few optical elements. The dichroic mirror is to be replaced by a mirror to reflect near-IR or red excitation wavelength.

In addition to the sectioning ability, less photo damage and a better penetration ability, the resolution is another factor in evaluating the potential of TPLSM. As discussed earlier in this chapter, the image resolution is determined by the objective lens and the diffraction of light by the specimen (Rayleigh criteria). When comparing two-photon excitation with one-photon

excitation of the same dye, two-photon excitation theoretically should yield worse resolution because it utilizes a significantly longer wavelength. However, other factors such as the out-of-focus fluorescence in one-photon excitation may come into play, affecting the achievable resolution. Generally, the strength of TPLSM does not lie in improvement of resolution, but in the other advantages described above.

7.9 OPTICAL COHERENCE TOMOGRAPHY

Optical coherence tomography (often abbreviated as OCT) is a new bioimaging technique that is rapidly growing in its applications (Tearney and Bouma, 2001). Already a number of clinical applications have been demonstrated in a widely diverse range of areas such as ophthalmology and dentistry (Huang et al., 1991; Brezinski et al., 1999; Schmitt et al., 1999). It is a reflection imaging technique similar to ultrasound imaging, except that light wave (usually in the near-IR to IR range) scattered from a specific tissue site is used to image. The sensitivity of the scattered light, as well as its selectivity from a specific back-scattering site, is achieved by using the interference between the back-scattered light and a reference beam. The OCT method of imaging is particularly suited for a highly scattering medium, such as a hard tissue. The interference between the propagating wavefronts of two light sources occurs when both wavefronts have well-defined coherence (phase relation) within the overlapping region. This well-defined coherence of a wavefront from a source is maintained within a distance called *coherence length*, as defined in Chapter 2. Therefore, if both the reference beam and the beam back-reflected from a scattering site are derived from the same light source, a well-defined interference pattern will be produced only if their path-length difference is within the coherence length. This behavior is shown in Figure 7.13.

A displacement of the reference beam produces the path-length difference between the light reflected from the reference mirror and the back-scattered ballistic photons (discussed in Section 7.2) from the scattering sample. In the case of a fully coherent source (such as a high-coherence laser source), the interference between the reference beam and the back-scattered beam can be maintained over a large path-length difference induced by reference mirror displacement. Thus no selectivity to back-scattering from a specific depth in the sample can be achieved in this case. The case on the right-hand side is for a low-coherence source (with a short coherence length). In this case the interference pattern between the reference beam and the back-scattered beam is produced only when their path difference is within the coherence length. In a three-dimensional scattering medium, at any given location of the reference beam mirror, only a given depth range (defined by the coherence length) of back-scattered light will interfere. Therefore, by scanning the reference mirror,

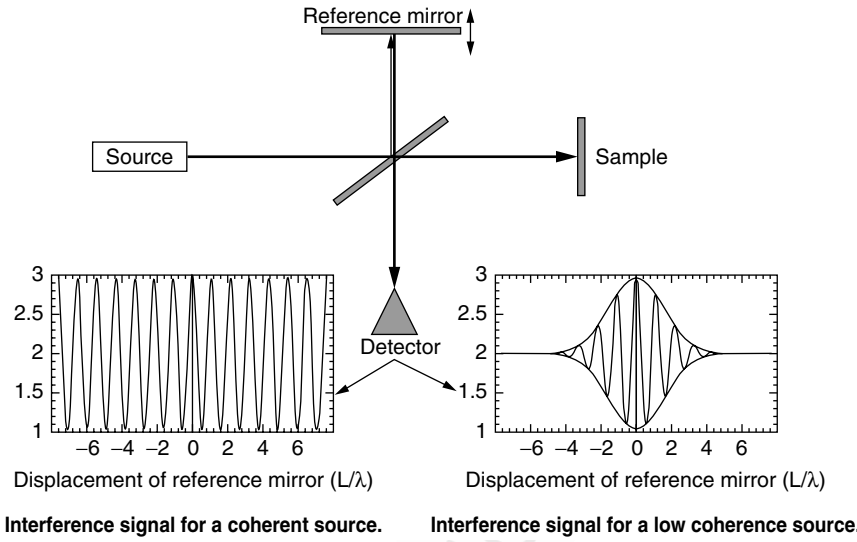

Figure 7.13. The interference signal as a function of the reference mirror displacement in case of a coherent source (e.g., laser) and a low-coherence source (e.g., SLD) are shown here.

one can achieve the depth discrimination. The interference patterns contain the information about the refractive index variation of the sample (tissue) which thus provides an optical image.

In OCT, the axial (depth) resolution is defined by the coherence length of the light source. The shorter the coherence length, the better the depth resolution. A broad-band light source will have a short coherence length (ΔL). Therefore, one often uses an incoherent but bright light source such as a superluminescent diode (SLD) or a laser with a poor coherence (such as a femtosecond laser source with a broad-band width associated with it). An example of a bench-top OCT setup designed at our Institute for Lasers, Photonics, and Biophotonics (ILPB) is shown in Figure 7.14 (Xu et al., 1999). Here an SLD (8 mW at 850 nm with 20-nm bandwidth) is used as a low-coherence source. A polarizing beam splitter splits the beam into the reference and the sample arms. A combination of wave plates and polarizers allows the control of intensity of light in both arms. A phase modulator, introduced in one arm to modulate the signal derived from interference between the reference and sample beams, allows phase-sensitive detection of the signal using a lock-in amplifier. The sample is mounted on an XYZ stage, and the 3-D image of the sample can be obtained by using computer-controlled scanning and data acquisition. In this setup, the depth resolution was further enhanced by introducing a confocal aperture and a lens in the front of the detector, which further reduced the background interferences.

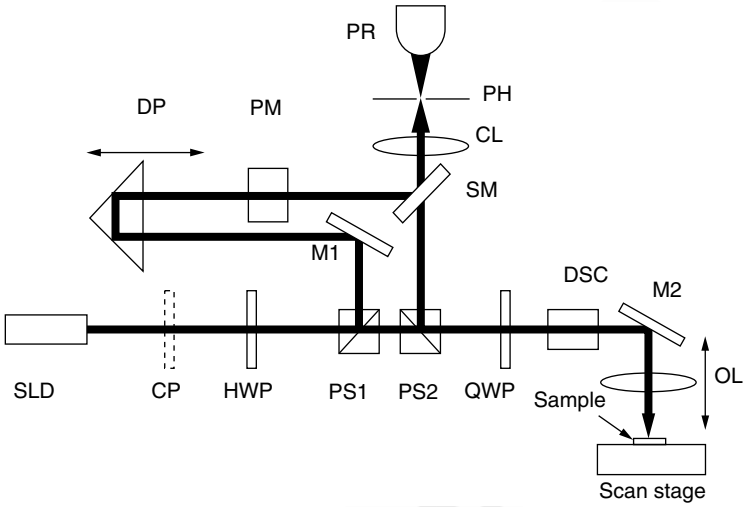

Figure 7.14. A table top OCT designed at the Institute for Lasers, Photonics, and Biophotonics (Buffalo) using an SLD light source. (Reproduced with permission from Xu et al., 1999).

The depth or axial resolution of this OCT is given by the FWHM of the round-trip coherence envelope, which is $\Delta L = 0.44\lambda^2/\Delta\lambda$ where $\Delta\lambda$ is the source bandwidth. The lateral resolution is given by the diffraction-limited spot size obtained by the focusing optics which is similar to that described in the previous section on confocal imaging. Fujimoto and co-workers (Swanson et al., 1993) developed a compact optical-fiber-based OCT setup as shown in Figure 7.15. In this arrangement, a dual-core fiber is used. One core of the fiber transmits the broad-band light source and splits it into the two arms: the sample probe and the reference. The other core of the fiber collects the back-scattered signal and reflected reference beam and combines to produce the interference.

Another variation of a fiber-based OCT has been used by Colston and others (Colston, 1998) for dental applications. The advantages of OCT and a comparison between OCT and confocal microscopy are presented below.

Advantages of OCT

High Resolution. Current OCT systems generally have resolutions of 4–20 μm compared to 110 μm for high-frequency ultrasound.

Real-Time Imaging. Imaging is at or near real time.

Catheter/Endoscopes. The fiber-based design allows relatively straightforward integration with small catheter/endoscopes.

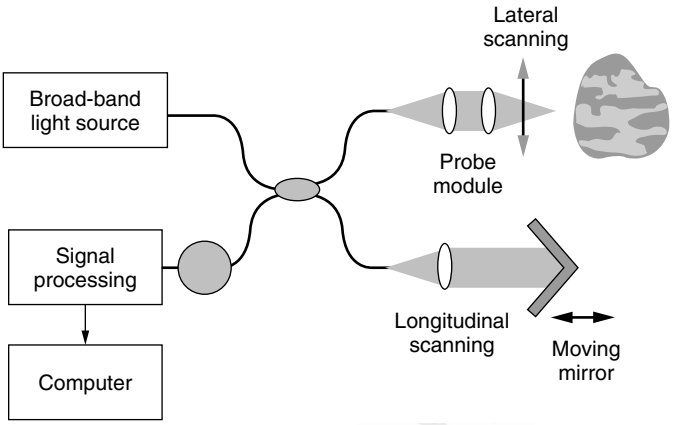

Figure 7.15. A fiber-based OCT. (Reproduced with permission from Swanson, et al., 1993).

Clinical Benefits

- Fiber-based OCT are compact, portable, and noncontact and can be combined with laser spectroscopy and Doppler velocimetry.

Comparison Between OCT and Confocal or Multiphoton Microscopy

Advantages

- Higher capability of imaging turbid medium (e.g., biological tissue).
- High depth resolution, even when the depth resolution of the objective is low.
- No need to use fluorescent stains or tags as in the case of confocal fluorescence or TPLSM.
- Compact compared to TPLSM setup (using SLD instead of Ti:sapphire laser as light source).

Disadvantage

- The depth resolution is lower than that for two-photon fluorescence or confocal microscopy with high magnification objective.

7.10 TOTAL INTERNAL REFLECTION FLUORESCENCE MICROSCOPY

Total internal reflection fluorescence microscopy, often abbreviated as TIRF microcopy, is best suited to image and probe a cellular environment within a

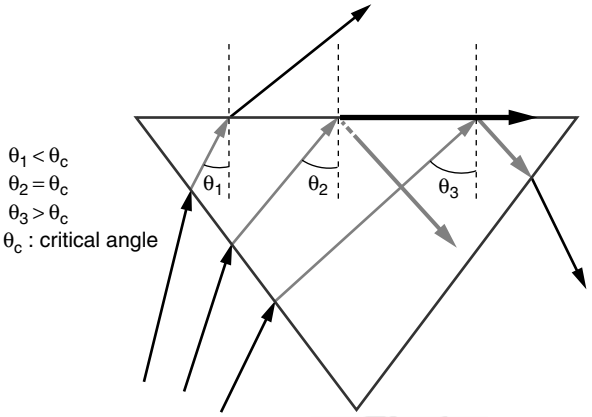

Figure 7.16. Principle of total internal reflection.

distance of 100 nm from a solid substrate. It relies on excitation of fluorescence in a thin zone of 100 nm from a solid substrate of refractive index higher than that of the cellular environment being imaged, by using the electromagnetic energy in the form of an evanescent wave. The concept of an evanescent wave can be understood by using the propagation of light through a prism of refractive index n_1 to the cellular environment of a lower refractive index n_2. At the interface, a refraction would occur at a small incidence angle. But when the angle of incidence exceeds a value θ_c, called the *critical angle*, the light beam is reflected from the interface as shown in Figure 7.16. This process is called *total internal reflection* (TIR). The critical angle θ_c is given by the equation

$$\theta_c = \sin^{-1}(n_2/n_1)$$

As shown in the figure, for incidence angle $>\theta_c$, the light is totally internally reflected back to the prism from the prism/cellular environment interface. The refractive index n_1 of a standard glass prism is about 1.52, while the refractive index n_2 of an intact cell interior can be as high as 1.38. The critical angle for these n_1 and n_2 parameters is 65°. For permeabilized, hemolyzed, or fixed cells, the n_2 value is that of an aqueous buffer which is 1.33, yielding a critical angle of 61°.

Even under the condition of TIR, a portion of the incident energy penetrates the prism surface and enters the cellular environment in contact with the prism surface. This penetrating light energy (or wave) is called an *evanescent wave* or an *evanescent field* (Figure 7.17). In contrast to a propagating mode (oscillating electromagnetic field with the propagation

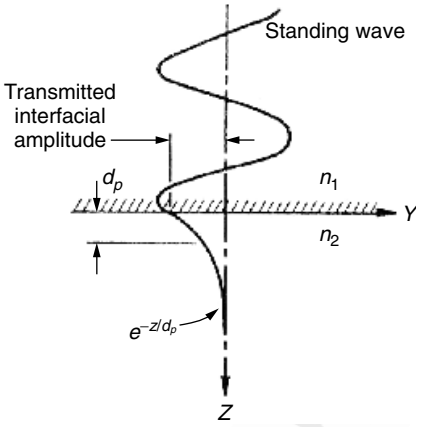

Figure 7.17. Evanescent wave extending beyond the guiding region and decaying exponentially. For waveguiding, $n_1 > n_2$, where n_2 is the refractive index of surrounding medium and n_1 is the refractive index of guiding region.

constant k, defined in Chapter 2, as a real quantity), an evanescent wave has a rapidly decaying electric field amplitude, with an imaginary propagation constant k. Therefore, its electric field amplitude E_z decays exponentially with distance z into the surrounding cellular medium of lower refractive index n_2 as

$$E_z = E_0 \exp(-z/d_p)$$

where E_0 is the electric field at the surface of the prism (solid substrate of higher refractive index). The parameter d_p, also called the *penetration depth*, is defined as the distance at which the electric field amplitude reduces to $1/e$ of E_0. The term d_p can be shown to be given as (Sutherland et al., 1984; Boisdé and Harmer, 1996).

$$d_p = \lambda \Big/ \left\{ 2\pi n_1 \left[\sin^2 \theta - (n_2/n_1)^2 \right]^{1/2} \right\}$$

Typically, the penetration depths d_p for the visible light are 50–100 nm. The evanescent wave energy can be absorbed by a fluorophore to generate fluorescence which can be used to image fluorescently labeled biological targets. However, because of the rapidly (exponentially) decaying nature of the evanescent field, only the fluorescently labeled biological specimen near the substrate (prism) surface generates fluorescence and can thus be imaged. The fluorophores that are further away in the bulk of the cellular medium are not excited. This feature allows one to obtain a high-quality image of the flu-

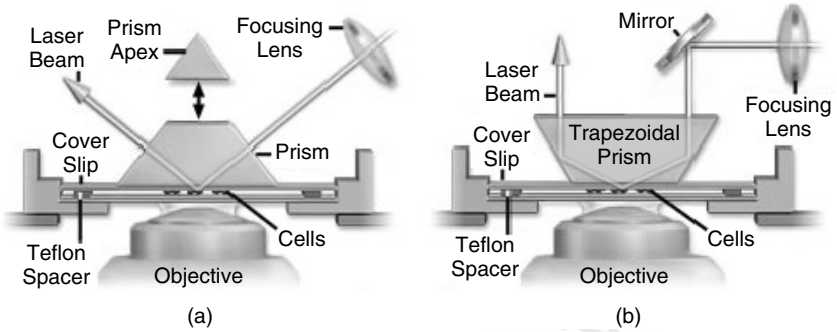

Figure 7.18. Inverted microscope TIP configuration. (Reproduced with permission from http://www.olympusmicro.com/primer/techniques/fluorescence/tirf/tirfconfiguration.html.)

orescently labeled biologic near the surface, with the following advantages (Axelrod, 2001):

- Very low background fluorescence
- No out-of-focus fluorescence
- Minimal exposure of cells to light in any other planes in the sample, except near the interface

The TIRF imaging offers a number of relative merits compared to the confocal microscopy. TIRF allows one to achieve a narrower depth of optical section (0.1 μm) compared to a typical value of 0.5 μm achieved in confocal microscopy. The illumination and hence the excitation are confined to a thin section (near the interface) in the case of TIRF, thus limiting any light-induced damage to cell viability. The TIRF microscopy is also much less expensive than the confocal microscopy, because one can use a standard microcope with TIRF attachment (or TIRF microscopy kits) available from a number of commercial sources.

Figure 7.18 shows two different prism based TIRF setups utilizing an inverted microscope. In Figure 7.18a, a prism is employed to achieve total internal reflection; the maximum incidence angle is obtained by introducing the laser beam from the horizontal direction. This arrangement is not compatible with conventional transmission imaging techniques. In Figure 7.18b, a trapezoidal prism is used and the incoming laser beam is vertical, so the total internal reflection area does not shift laterally when the prism is raised and lowered during specimen changes. In addition, transmission imaging techniques are compatible with this experimental design. Another approach is to utilize a hemispherical prism which permits continuous variation of the incidence angle over a wide range.

TIRF microscopy has been used for numerous applications that take advantage of the surface selectivity. Some of these are:

- Single-molecule fluorescence detection near a surface (Dickson et al., 1996; Vale et al., 1996; Ha et al., 1999; Sako et al., 2000)
- Study of binding of extracellular and intracellular proteins to cell surface receptors and artificial membranes (McKiernan et al., 1997; Sand et al., 1999; Lagerholm et al., 2000)

TIRF microscopy can be used with other optical imaging techniques such as fluorescence resonance energy transfer (FRET), fluorescence lifetime imaging (FLIM), fluorescence recovery after photobleaching (FRAP), and nonlinear optical imaging. FRET and FLIM are discussed in Sections 7.13 and 7.14. The TIRF microscopy can also utilize two-photon or multiphoton excitation of the fluorophores, similar to what was discussed above under two-photon laser scanning microscopy. Lakowicz and co-workers (Gryczynski et al., 1997) demonstrated two-photon excitation of a calcium probe Indo-1 using an evanescent wave.

7.11 NEAR-FIELD OPTICAL MICROSCOPY

Near-field optical microscopy is an optical technique that allows one to achieve a resolution of ≤100 nm, significantly better than permitted by the diffraction limit. As discussed in previous sections, the resolution of any optical imaging technique is limited by diffraction of light. The concept of using the near field for imaging was first discussed in 1928 by Synge, who suggested that by combining a subwavelength aperture to illuminate an object, together with a detector very close to the sample (<< one wavelength, or in the "near field"), high resolution could be obtained by a non-diffraction-limited process (Figure 7.19) (Synge, 1928). The implementation of this principle in practice (Ash, 1972; Pohl, 1984; Betzig and Trautman, 1992; Heinzelmann and Pohl, 1994) brought the field of near-field microscopy into existence. There are different variations

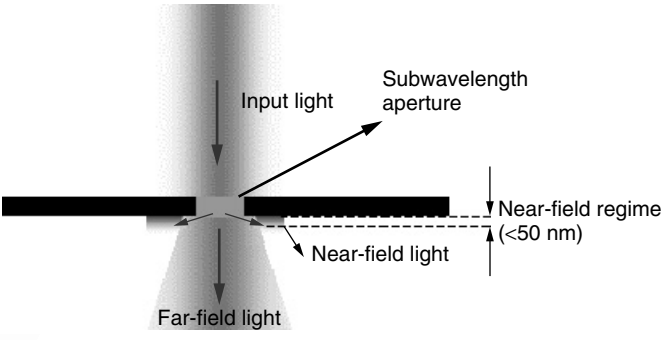

Figure 7.19. Principle of near-field microscopy.

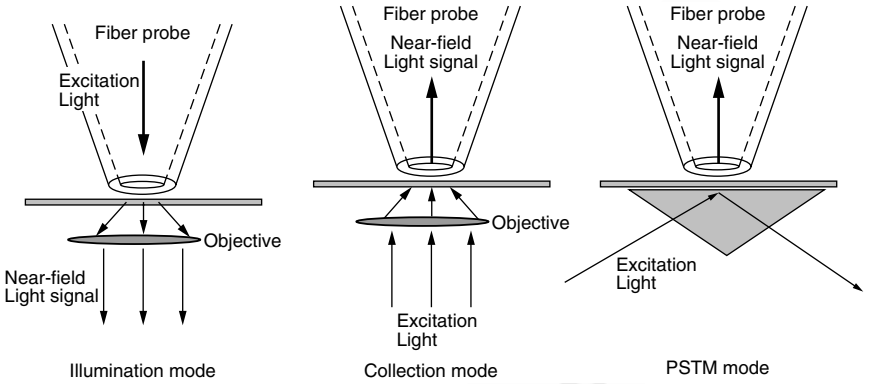

Figure 7.20. Different modes of near-field microscopy.

of this principle. One can illuminate the sample in the near field, but collect the signal in the far field or illuminate the sample in the far field while collecting the signal in the near field or do both in the near field. In almost all different methods, the most important component is the use of a subwavelength aperture that can be achieved by using a tapered optical fiber with a tip radius of <100 nm.

The most commonly used near-field probe consists of an optical fiber that is tapered and coated on the outside with a reflective aluminum coating. The tip of the fiber is typically about 50 nm. Light propagating through this fiber, either for excitation or for collection of emission, produces a resolution determined by the size of the fiber tip and the distance from the sample. The image is collected from point-to-point by scanning either the fiber tip or the sample stage. Hence the technique is called *near-field scanning microscopy* (NSOM) or *scanning near-field microscopy* (SNOM). Different modes of near-field microscopy are shown in Figure 7.20.

In illumination-mode NSOM, the excitation light is transmitted through the probe and illuminates the sample in the near field.

A typical setup used for near-field imaging is shown in Figure 7.21.

In collection-mode NSOM, the probe collects the optical response (transmitted or emitted light) in the near field. Another mode used in near-field imaging is photon scanning tunneling microscopy (PSTM) in which the sample is illuminated in a total internal reflection geometry using an evanescent wave (discussed in Section 7.10, but described here as due to photon tunneling); the emitted light is collected by a near-field optical probe.

The resolution in NSOM and PSTM is determined by two factors: the probe aperture (opening) size and the probe–sample distance. Because most samples exhibit some topography, it is important to keep the optical probe at a constant distance from the sample surface so that any change in the optical signal is attributed to a variation in the topographic feature, and not to variation in

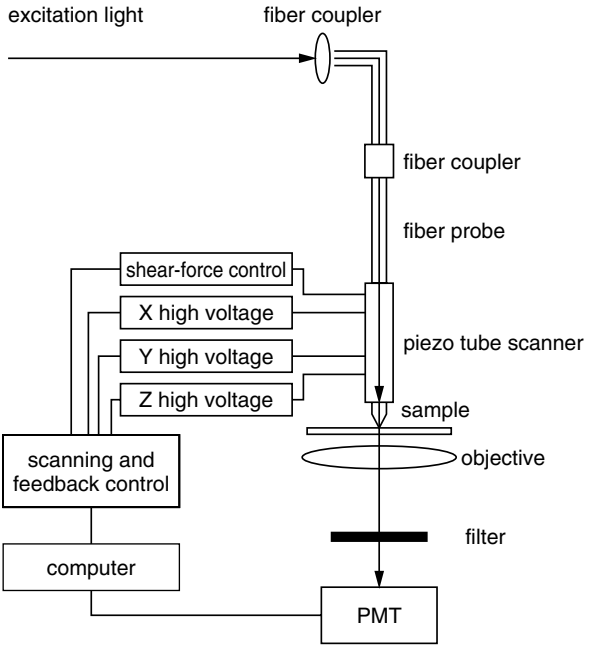

Figure 7.21. Typical instrumentation used for a near-field imaging setup. (Reproduced with permission from Shen et al., 2000.)

the probe–sample distance. A shear-force feedback technique can be used for distance regulation in cases of both conductive and nonconductive samples. In a shear-force feedback, the optical probe is attached to a tuning fork and oscillates laterally at its resonance frequency, with an amplitude of a few nanometers. As the probe approaches the sample surface, the probe–sample interaction dampens the amplitude and shifts the phase of the resonance. The change in the amplitude normally occurs over a range of 0–10 nm from the sample surface and is monotonic with the distance, which can be used in a feedback loop for distance regulation. The shear-force feedback can also be used to simultaneously obtain the topographic (AFM) image of the sample, to provide a monitoring reference for NSOM and PSTM. The applications of the near-field microscopy have ranged from single-molecule detection to biological imaging of viruses and bacteria (van Hulst, 1999; Hwang et al., 1998; Gheber et al., 1998; Subramanian et al., 2000).

7.12 SPECTRAL AND TIME-RESOLVED IMAGING

Discussions presented in the earlier sections of this chapter have focused on the types of microscopes used to provide spatial resolutions to probe structures down to subcellular levels. The optical probing methods utilized by them

have been transmission, reflection or fluorescence to image structural details. Polarization characteristics have been used to enhance phase contrast for high-contrast imaging.

To probe biological functions, merely spatial imaging of structures is not sufficient. One needs to combine this information with spectrally resolved and time-resolved imaging in order to probe structure and dynamics that can provide useful information on biological functions. This combination of spatial, spectral, and temporal resolution, coupled with polarization discrimination, constitutes the emerging powerful field of multidimensional imaging. This section deals with spectral and time-resolved imaging. They are primarily used in conjunction with fluorescence detection. Thus, these methods of imaging can be used with epifluorescence, confocal, near-field, or TIRF microscopic techniques discussed above, which utilize fluorescence detection. Vibrational spectral imaging has also been gaining popularity in the form of Raman Imaging and CARS (coherent anti-Stokes Raman scattering) imaging. CARS imaging is described in Section 7.15.

7.12.1 Spectral Imaging

In fluorescence-based optical imaging described above, spatial distribution of fluorescence intensity is used to determine structure and organization at the cell or tissue level. In other words, the detection simply is of the intensity level of fluorescence. Spectral imaging provides spectral information on the spatial variation of fluorescence spectra. In other words, one can also obtain information on the fluorescence spectra at a given spatial location. This feature permits simultaneous use of more than one fluorescent marker and maps their distribution in various biological sites (tissue locations, cell organelles, etc.). Thus, spatial distribution and localization of a specific drug or biologic in a cell or a tissue can selectively be studied. Furthermore, by monitoring spectral shift in the emission maximum (or a change in the emission spectral profile) of a fluorescent marker, one can obtain information about the local environment (interaction and dynamics). This is a useful information in terms of understanding physiological changes occurring in response to a biological function or in elucidating the molecular mechanism of a drug–organelle interaction. Some of the spectral wavelength selection techniques are described below.

7.12.2 Bandpass Filters

In the simple case of imaging using more than one fluorescent probes, where their fluorescence spectra are widely separated, one can simply use a set of bandpass filters (green filters, red filters, etc.) in the path of fluorescence collection and detection. These bandpass filters allow transmission in a specific wavelength region, in which fluorescence can be detected, while rejecting the

fluorescence from other regions. A number of choices exist such as interference transmission filters or dichroic mirrors. The simplicity and relatively low costs are the advantages offered by this method. The major disadvantage is that the system does not offer continuous tunability of wavelength selection and one has to use a mechanical method to introduce a specific filter in the fluorescence collection path (such as a rotating tray or filter wheel containing a set of filters).

7.12.3 Excitation Wavelength Selection

This method can be used when the fluorophores used have well-separated excitation spectra so that excitation at one wavelength generates fluorescence only from a particular fluorophore. A laser source providing a number of lasing lines (such as an argon–krypton laser) or a continuously tunable output over a broad range (such as a laser pumped OPO, described in Chapter 5), or a combination of lasers can be used for this purpose. The advantage, again, is the simplicity of the method, and there is no need to introduce any additional optical or mechanical element in the fluorescence collection (imaging) light path, thus providing minimal image degradation. However, this approach requires an achromatic objective lens to produce focusing of different excitation wavelengths at the same spot. Furthermore, this approach is limited because it involves the combination of only those fluorophores that have well-separated excitation spectra.

7.12.4 Acousto-Optic Tunable Filters

The use of acousto-optic tunable filters, often abbreviated as AOTF, for rapidly tunable multispectral imaging has been pioneered by Farkas and co-workers (Farkas, 2001; Wachman et al., 1997). AOTF are electronically controllable solid-state devices where a narrow spectral bandwidth is angularly deflected away (diffracted) from the incident beam by an acoustic frequency applied to AOTF. The central wavelength of the deflected light can be continuously tuned over a wide frequency range by the choice of the acoustic frequency, and the wavelength switching speed can be in tens of microseconds. The advantage of this approach is a fast switching speed, tunability of both the wavelength and the bandwidth, and control of the intensity of transmitted light.

The mechanism of AOTF involves the modulation of the refractive index by elasto-optic (or acousto-optic) effect in a certain crystal (acousto-optically active) when an acoustic wave is generated inside the crystal. The acoustic field is electronically generated by applying an rf field to a piezoelectric transducer bonded to one of the faces of the crystal. The periodic modulation of the refractive index acts as a grating to diffract certain wavelengths at an angle from the incident beam direction.

Image blur encountered using AOTF had limited the use of this technique in the past. Farkas and co-workers proposed a new transducer design, along

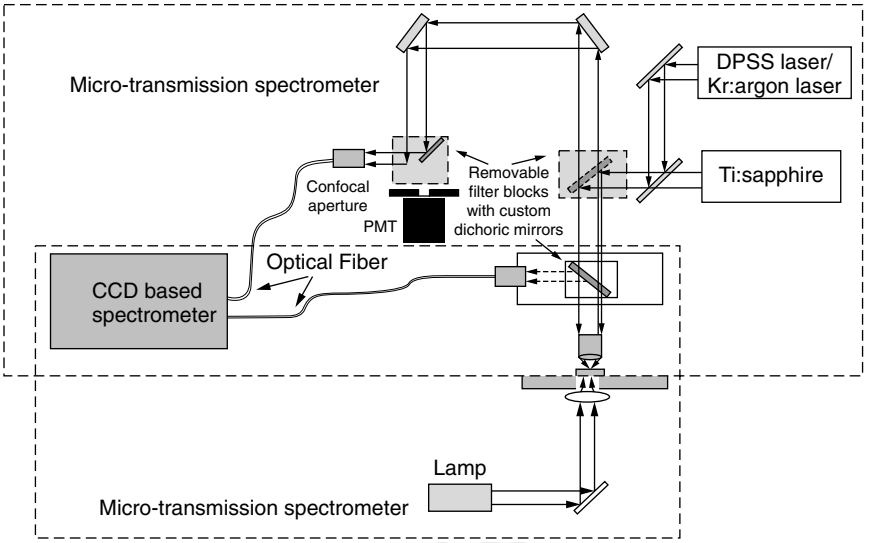

Figure 7.22. Schematics of experimental arrangement for obtaining fluorescence spectra from a specific biological site (e.g., organelle) using a CCD-coupled spectrograph. (Reproduced with permission from Pudavar et al., 2000.) (See color figure.)

with the use of two AOTFs in tandem, to provide out-of-band rejection that leads to an improvement of the image blur.

7.12.5 Localized Spectroscopy

Another approach is to use a spectrograph to analyze fluorescence from a specific point of the image plane (Masters et al., 1997; Wang et al., 2001). This approach, incorporated in the multiphoton confocal setup at our Institute for Lasers, Photonics, and Biophotonics is shown in Figure 7.22. The fluorescence is collected by the objective lens and, after the dichroic beam splitter, coupled into a fiber which also acts as a confocal aperture. The light is guided by the fiber to a spectrograph where the wavelengths are dispersed and detected by a CCD array. The CCD (charge coupled device) array is a multiarray detector where each array (pixel) detects a specific wavelength (or a narrow wavelength range). Therefore, the entire fluorescence spectrum can be simultaneously monitored.

7.13 FLUORESCENCE RESONANCE ENERGY TRANSFER (FRET) IMAGING

Fluorescence resonance energy transfer, abbreviated as FRET, is an example of spectral imaging that has emerged as a powerful technique for biomedical research. Its applications cover a broad range such as study of protein–protein interactions, calcium metabolism, protease activity, and high-throughput

screening assays (Herman et al., 2001; Periasamy, 2001). The fundamental principle involves the use of Förster excitation energy transfer from an excited molecule of higher energy (donor) to another molecule of lower excitation energy (acceptor). This energy transfer, discussed in Chapter 4, occurs nonradiatively through dipole–dipole interaction, showing a distance dependence of R^{-6}. It is maximized when there is a significant overlap of the emission spectrum of the donor with the absorption spectrum of the acceptor.

Thus, the interactions of cellular components with each other (such as protein–protein interactions) can be studied and quantified by labeling the two components with two appropriately chosen fluorophores that act as an excitation donor and an excitation acceptor, respectively. In FRET spectral imaging, the donor is selectively excited and the quenching of its emission, concomitant with a gain in the fluorescence of the acceptor, indicates appreciable interaction between the donor and the acceptor labeled cellular components, leading to donor-to-acceptor excitation energy transfer. Another variation of FRET imaging utilizes lifetime where a considerable shortening of the fluorescence lifetime of the donor implies an efficient FRET process. The lifetime imaging is discussed below in a separate section.

A popular choice of fluorophores for studying subcellular interactions has been various mutants of green fluorescent proteins (GFP) which now offer a choice of fluorescence covering the entire visible range. Thus, both the donor and the acceptor fluorophores can be chosen from this family. GFP is discussed in Chapter 8.

FRET imaging involves measuring the intensities of the donor emission (I_D) and the acceptor emission (I_A) and obtaining a spatial distribution of the ratio I_A/I_D. This approach is also known as *steady-state FRET imaging*. An important consideration in getting a FRET image with a high signal-to-noise ratio is using optical means (as described in the above sections) to spectrally discriminate the donor and the acceptor absorption and emission spectra. A simple approach is to use narrow bandpass filters that allow selective excitation only of the donor so that any emission from the acceptor results from the FRET process. Also, the choice of the filters to separate the donor and the acceptor emissions is very important. This spectral discrimination using an appropriate combination of filters reduces any spectral bleedthrough background.

Another important factor to enhance the quality of FRET imaging is the appropriate choice of the donor and the acceptor optimal concentrations. These optimal concentrations can be determined in a systematic study of the FRET signal as a function of concentration of one component (e.g., donor) while keeping the concentration of the other component (acceptor) at a fixed value.

7.14 FLUORESCENCE LIFETIME IMAGING MICROSCOPY (FLIM)

Fluorescence lifetime imaging microscopy, often abbreviated as FLIM, provides a spatial lifetime map of a fluorophore within a cell or a tissue (Tadrous,

2000; Bastiaens and Squire, 1999). The use of fluorescence lifetime of a fluorophore as an imaging contrast mechanism offers a number of advantages over steady-state fluorescence microscopy. First, the fluorescence lifetime is a highly sensitive probe of the local environment of the fluorophore. The temporal resolution obtained in this modality of imaging provides an opportunity to study the dynamic organization of a living system. For FRET imaging described above, FLIM provides an advantage to measure the energy transfer only by measuring the donor fluorophore lifetime, which is significantly affected (reduced) by energy transfer to an acceptor. FLIM also has the advantage that the fluorescence lifetimes are independent of the fluorescence intensity, concentration, and, to a larger extent, photobleaching of the fluorophore. Furthermore, there may be cases where a fluorophore may exhibit similar spectra, but significantly different lifetimes in different environments, as the lifetime is a more sensitive probe of the environment. FLIM has been used for many different types of imaging experiments using both one- and two-photon excitations. These include imaging using multiple fluorophore labeling, quantitative imaging of ion concentrations, quantitative imaging of oxygen, and energy transfer efficiency in FRET (Periasamy et al., 1996; French et al., 1997; Bastiaens and Squire, 1999; Lakowicz et al., 1992).

The two methods of measurements of lifetime are (i) the time domain method using a pulse laser excitation and (ii) the frequency domain method using phase information. These methods have already been discussed in Chapter 4. The simplest case is a single exponential decay of fluorescence intensity $I(t)$ given as

$$I(t) = I_o \exp(-t/\tau)$$

where τ is the fluorescence lifetime. In such a case, the time domain FLIM imaging involves obtaining the fluorescence images by applying a pulse excitation at two different time delays t_1 and t_2, using gated detector for a duration of ΔT, as shown in Figure 7.23. The accumulated emitted photons during the ΔT periods are measured by integrating the signal using a CCD camera and given as D_1 and D_2 for the two time delays. The single exponential decay can be shown to yield the following relation for the fluorescence lifetime:

$$\tau = (t_2 - t_1)/\ln(D_1/D_2)$$

Using this equation, one can then obtain the FLIM image. An advantage offered by the time-resolved measurement is that the background noise due to scattering (such as Raman scattering) can be eliminated. Scattering occurs almost instantaneously. Hence using a time delay between the excitation pulse and opening of the electronic gate to collect fluorescence (such as t_1, in Figure 7.23), one can eliminate background scattering. In the case of a more complicated decay of multiexponential nature, one has to obtain the fluorescence

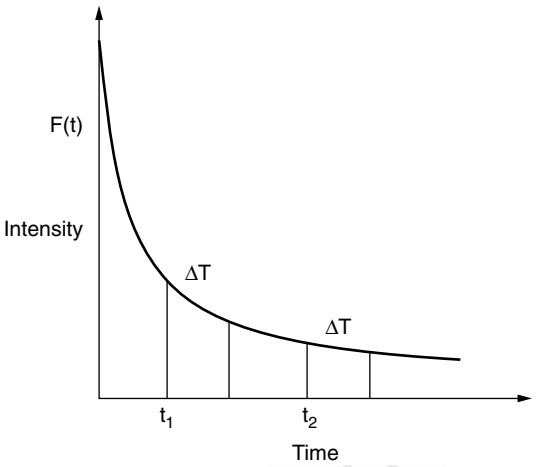

Figure 7.23. Exponential decay of fluorescence showing the sampling period T for two different delays t_1 and t_2.

signal at a number of delays to obtain the full decay curve and fit the curve to a double (or multiple) exponential.

In the frequency domain method, as described in Chapter 4, one utilizes a sinusoidally modulated light to excite fluorescence. Phase shift in fluorescence is measured to obtain lifetime information (Verneer et al., 2001). Measuring multiple lifetimes using a number of fluorophores simultaneously requires excitation with a sum of sinusoidally modulated signals with different frequencies. Thus, simultaneous detection of several fluorescently tagged biomolecules can be made and their individual interactions can be monitored. The fluorescence lifetimes of the fluorophores are in nanoseconds, enabling one to measure dynamical processes in cells and tissues. For example, activation state of proteins *in situ* can be investigated without any disruption of the cellular architecture.

FLIM is not only useful for cellular research, but is also an informative tool for the pharmacological and medical industries (Bastiaens and Squire, 1999). FLIM provides a detection platform for ultra-high throughput screening of drugs on their interactions with living cells. This technique is also well-suited to assess the early functional states of proteins implicated in the pathology of a diseased tissue.

7.15 NONLINEAR OPTICAL IMAGING

Nonlinear optical effects discussed in Chapter 5 can be used as a contrast mechanism for microscopic studies of biologics (Mertz, 2001). A clear advan-

tage of using the nonlinear optical effects is a gain in the spatial resolution due to a higher-order dependence on the excitation intensity. A number of nonlinear optical effects have been used for bioimaging. A very popular method in bioimaging is that of two-photon excitation. The two-photon excitation has already been discussed in the Section 7.8, on multiphoton microscopy. This nonlinear optical method has also been used in TIRF and near field microscopy. There has also been reports of using three-photon processes for microscopy (Schrader et al., 1997; Wokesin et al., 1996). In this case, a simultaneous absorption of three IR photons produces an up-converted emission in the visible. Recently, we reported (He et al., 2002) highly efficient three-photon excitation of visible fluorescence (λ^{max} = 550 nm) in a new fluorophore, abbreviated as APSS, by using a pump wavelength of 1.3 μm. The excitation is so efficient that one can create a population inversion to produce stimulated emission. At the wavelength of 1.3 μm, biological cells and tissues still exhibit very good transparency. Furthermore, emission at 550 nm can also be more efficiently collected compared to emission in blue, generated by three-photon excitation at ~1 μm. Therefore, the availability of highly efficient new three-photon fluorophores that can be excited in the IR around 1.3 μm can lead to further expansion of applications of three-photon microscopy.

This section covers other nonlinear optical techniques. Specifically, second-harmonic generation, third harmonic generation and coherent anti-Stoke Raman scattering methods and microscopy based on them are described here.

7.15.1 Second-Harmonic Microscopy

In this approach, the nonlinear optical process of second-harmonic generation is used to generate image contrast. As discussed in Chapter 5, second-harmonic generation is a second-order nonlinear optical process, generated in a noncentrosymmetric medium (Prasad and Williams, 1991), whereby a second-harmonic output at the frequency of 2ν (or wavelength of $\lambda/2$) is generated from an input beam of frequency ν. Therefore, it is an up-conversion process, just like two-photon excited emission. Also, like a two-photon process, second-harmonic generation is quadratically dependent on the input intensity. However, the second-harmonic microscopy offers the following features, different from the two-photon microscopy.

- Since second-harmonic generation dos not involve any absorption of light (see Chapter 5), no thermal damage or photobleaching occurs if a pump beam of wavelength outside the absorption band is selectively chosen. In contrast, the two-photon microscopy involves a two-photon absorption of light.
- Second-harmonic generation shows a symmetry selection, occurring only in an asymmetric medium such as an interface or an electric-field-induced

noncentresymmetric environment. Therefore, the second-harmonic microscopy is more useful for probing structures and functions of membranes and the membrane potential induced alignment of dipolar molecules in a membrane. A two-photon process does not readily select and probe asymmetry.

- The second-harmonic signal is obtained at exactly half the wavelength of the pump laser beam and is thus easy to discriminate against the pump beam and any autofluorescence. The two-photon excited emission, in contrast, is a broad fluorescence band.
- The second-harmonic microscopy can be used with nonfluorescent samples and tissues.

The disadvantage of the second-harmonic microscopy is that it is not as versatile as the two-photon microscopy, since the signal is generated only in an asymmetric medium.

Second-harmonic generation was first reported by Fine and Hansen (1971) in nearly transparent tissues. Freund et al. (1986) described a cross-beam steering second-harmonic microscopy with a transmission geometry to obtain detailed variation of collagenous filaments in a rat tail tendon. Alfano and co-workers have used second-harmonic imaging to probe structures of animal tissues (Guo et al., 1996, 1997) and have used 100-fsec pulses at 625 nm to map subsurface structure of animal tissues by using second-harmonic generation tomography noninvasively. In the tomography approach (like in OCT described earlier), the second-harmonic signal is obtained in a back-reflection geometry to build a three-dimensional layered structure map near the surface of a tissue. They suggested that second-harmonic imaging can be implemented with fiber optics and adapted to endoscopy for morphological evaluation in cardiology, gynecology, and gastrointestinal applications.

Lewis and co-workers have shown that second-harmonic generation can be a powerful method to probe membrane structure and measure membrane potential with a single-molecule sensitivity (Bouevetch et al., 1999; Peleg et al., 1999; Lewis et al., 1999). They used this method to probe membrane proteins and obtain functional imaging around selective sties and at single molecule level in biological membranes. For this imaging they used a donor–acceptor-type dye structure, discussed in Chapter 5 for second-order nonlinear optical effect, that undergoes internal charge transfer and can bind and orient in a lipid bilayer. These molecules respond to membrane potential by an electrochromic mechanism in which the field due to the membrane potential is sufficiently large due to a change in the induced dipole moment of the dye. Thus they produce a change in the generated second-harmonic signal. The membrane potential variation can be induced by changes in extracellular potassium concentrations.

Moreaux et al. (2001) have used second-harmonic generation to measure membrane separation and have shown that this method can be used to measure separations over ranges not accessible by FRET.

7.15.2 Third-Harmonic Microscopy

Third-harmonic generation is a third-order nonlinear optical process in which a fundamental pump beam of frequency ν (wavelength, λ) generates a coherent output at 3ν (wavelength, $\lambda/3$). Thus, an input beam at the fundamental wavelength of 1064 nm in the IR will generate an output at ~355 nm in the UV. Again, this process, unlike three-photon absorption, does not involve light absorption in the medium. In contrast to second-harmonic generation, third-harmonic generation does not have any symmetry requirement and can occur both in bulk and at surfaces. The molecular structural requirement for an organic substance to efficiently produce third-harmonic is only that it has extended conjugation of π electrons (Prasad and Williams, 1991). Thus third-harmonic microscopy can be used for both interface and bulk imaging.

The third-harmonic generation has been shown to have monolayer sensitivity and was used to study conformational changes in monolayer films prepared by the Langmuir–Blodgett technique (Berkovic et al., 1987, 1988).

The third-harmonic microscopy has been used to image biological samples (Yelin and Sieberberg, 1999; Müller et al., 1998). Yelin and Sieberberg used a synchronously pumped OPO with a 130-fsec pulse output at 1.5 μm, at a repetition rate of 80 MHz as the fundamental pump source. They showed that even though a high peak power was needed to generate the third-harmonic signal, the use of ultra-short femtosecond pulses allows one to use low average power (50 nW in their experiment). Using third-harmonic generation for laser scanning microscopy, the image is collected point by point. Yelin and Sieberberg imaged live neurons in a cell culture and obtained detailed images of organelles. In view of the high peak power needed (hundreds of GW/cm^2) for third-harmonic generation, combined with the danger of damaging the specimen under illumination with such high intensity pulses, it is not yet apparent how wide an application this nonlinear technique will find.

7.15.3 Coherent Anti-Stokes Raman Scattering (CARS) Microscopy

Coherent anti-Stokes Raman scattering (abbreviated as CARS) is a third-order nonlinear optical process that can produce a vibrational transition. This nonlinear optical process has been discussed in Chapter 5. For CARS, two optical beams of frequencies ν_p and ν_s interact in the sample to generate an anti-Stokes optical output at $\nu_{AS} = 2\nu_p - \nu_s$ in the phase-matched direction (a specific direction). The signal has an electronic contribution (from the electronic third-order nonlinear optical response), but is resonantly enhanced if $\nu_p - \nu_s$ coincides with the frequency of a Raman active molecular vibration (see Chapter 4). The molecular vibration involved in a CARS signal enhancement can then be used as a contrast mechanism for bioimaging. Since the first attempt of Duncan et al. (1982), CARS microscopy has attracted a great deal of attention in recent years (Zumbusch et al., 1999; Muller et al., 2000; Potma et al., 2000; Hashimoto et al., 2000; Cheng et al., 2001; Volker et al., 2002). Xie

and co-workers have made significant advances in the application of the laser scanning CARS microscopy to cell biology (Zumbusch et al., 1999; Cheng et al., 2001; Volkmer et al., 2001). The CARS microscopy provides a number of advantages, some of which are (Volker et al., 2001):

- Vibrational contrast in the CARS microscopy is inherent to the cellular species, thus requiring no endogenous or exogenous fluorophores that may be prone to photobleaching.
- CARS, being a coherent optical process (phase matching), offers much higher sensitivity than the spontaneous Raman process.
- CARS, being a nonlinear optical process, exhibits a nonlinear dependence on the pump intensity and, like in two-photon or other nonlinear microscopy described above, generates signals from the focal volume. This feature allows three-dimensional optical sectioning of thick samples to obtain a high-resolution three-dimensional image.
- CARS can provide chemical selectivity as different vibrational modes can be used for contrast.
- The CARS signal can be detected even in the presence of background autofluorescence, since a CARS signal is highly directional because of the phase-matching requirement.

CARS imaging is complicated by background signals derived from two sources: (i) the nonresonant electronic contributions that exist even when the Raman resonance condition is not met and (ii) electronic and Raman contributions from the solvent. The latter is particularly troublesome when using an aqueous medium as water generates a strong resonant CARS signal. Volker et al. (2001) have shown that by detecting CARS signal in the backward direction (which they call E-CARS) one can effectively suppress the solvent background and significantly increase the sensitivity of the CARS microscopy.

High-peak power lasers are needed to enhance the nonlinear optical process of CARS. At the same time it is necessary to maintain a narrow bandwidth of pulses in order to obtain good spectral resolution for selectively using a specific vibrational mode for resonance enhancement. Cheng et al. (2001) suggested the use of picosecond pulses instead of femtosecond pulses because the former allows one to achieve a better signal-to-background ratio (Cheng et al., 2001). Furthermore, to obtain and maintain overlap of two femtosecond laser pulses is much more difficult, in comparison with overlap to obtain and maintain of two picosecond pulses. The schematics of their experimental arrangement is shown in Figure 7.24. It utilizes two synchronized mode-locked Ti : sapphire lasers producing picosecond pulses at the 80-MHz repetition rate. The pump beam with frequency ν_p is tunable from 690 to 840 nm, while the Stokes beam with frequency ν_s is tunable from 770 to 900 nm. This arrangement allows one to cover the vibrational frequency range from 100 to 3400 cm^{-1}. They used this arrangement to obtain the CARS image of unstained human epithelial cells. The Raman band at 1570 cm^{-1}, arising from proteins and nucleic acid, was used.

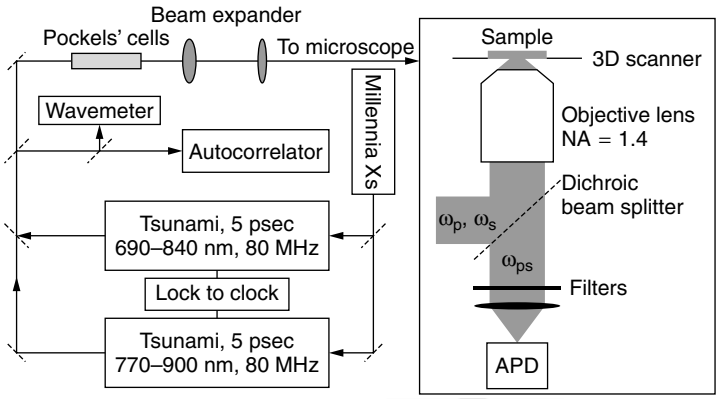

Figure 7.24. Schematics of a synchronized mode-locked picosecond Ti:sapphire laser system for backward detection CARS microscopy. Millenia is the diode-pumped Nd laser. Tsunami is the Ti:sapphire laser. (Reproduced with permission from Cheng, et al., 2001.)

7.16 FUTURE DIRECTIONS OF OPTICAL BIOIMAGING

7.16.1 Multifunctional Imaging

Each of the imaging techniques described in the previous sections has its own unique approach to imaging which can be suitable for obtaining certain biological information. But none of the techniques can be of universal use. For a comprehensive investigation of biological species and processes, one may require to use a combination of bioimaging methods, often at the same time. Integration of the various techniques is one of the evolving areas in bioimaging. Some modern confocal/multiphoton microscopes have the ability to provide simultaneous fluorescence, fluorescence lifetime imaging, and four-dimensional imaging (stack of three-dimensional images in different spectral region). Some of them can easily be adapted for polarization anisotropy imaging, Raman imaging, harmonic generation imaging, and so on, as well.

7.16.2 4Pi Imaging

Another technique, which is gaining popularity for high-resolution bioimaging is 4Pi imaging. In this technique, a standing wave is created in the sample plane, by the interference of two opposing wavefronts (Hell and Stelzer, 1992). In a 4Pi confocal microscope, two opposing high-NA objectives are used for illuminating and detecting the same point of a fluorescent sample. In such an arrangement with a coherent light source, an interference between the two light beams produce a standing wavefront, which in turn limits the volume of emission from the sample. In single-photon 4Pi imaging, even though the axial resolution is significantly improved, the lateral resolution is actually

degraded (Martínez-Corral, 2002). But with the introduction of two-photon 4Pi imaging (Nagorni and Hell, 2001), good axial and lateral resolution can be achieved.

7.16.3 Combination Microscopes

Another important development in this area is the integration of near-field and far-field techniques (confocal or multiphoton imaging) to increase the dynamical range of imaging. Switching between the near-field and the far-field modes (e.g., from confocal) in the same instrument can give high-resolution small-area scans as well as large-area far-field images. Some commercial systems combining a near-field microscope with a confocal microscope are already available in the market.

7.16.4 Miniaturized Microscopes

Most of the instruments or setups used for the above-described techniques are desktop instruments. In order to use them as regular diagnostic tools in the field, there is a need for miniature instrumentation. Current research in bioimaging is concerned with exploiting the developments in the MEMS (micro-electro-mechanical devices) technology to miniaturize many of these imaging setups (Dickensheets and Kino, 1998). There are few reports of a compact confocal microscope (Dickensheets and Kino, 1998) or OCT (Bouma et al., 2000; Tearney et al., 1997). Another important aim of this miniaturization effort is to develop catheter-based imaging inside a human body.

7.17 SOME COMMERCIAL SOURCES OF IMAGING INSTRUMENTS

Confocal Microscopy:

Biorad:	http://www.biorad.com
Leica Microsystems, Inc.:	http://www.llt.de/
Nikon:	http://www.nikonusa.com/
Olympus:	http://www.olympusamerica.com/seg_section/seg_confocal.asp
Optiscan Inc.:	http://www.optiscan.com/
Carl Zeiss Inc.:	http://www.zeiss.de/us/micro/home.nsf

Optical Coherence Tomography:

LightLab Imaging:	http://www.lightlabimaging.com/
Advanced Ophthalmic Devices:	http://www.humphrey.com/Systems/prod&sol.html

Near Field Imaging:

Thermomicroscopes:	http://www.tmmicro.com/
Nanonics Imaging Ltd.:	http://www.nanonics.co.il
WITec Wissenschaftliche:	http://www.witec.de
Triple-O Microscopy GmbH:	http://www.triple-o.de

HIGHLIGHTS OF THE CHAPTER

- Optical imaging utilizes spatial variation in the optical properties such as transmission, reflection, scattering, and fluorescence of a cell, a tissue, an organ, or a living object to generate an optical contrast for obtaining an optical image of the specimen.
- The light transmitted through a tissue, which is a highly scattering medium, is comprised of three components: unscattered ballistic photons, weakly scattered snake photons, and multiply scattered diffuse photons.
- Information about the internal structure of a tissue is carried by ballistic and snakes photons. They are discriminated from the diffuse photons by spatial filtering, polarization-gating and time-gating, and frequency domain methods and are then used to obtain images.
- A transmission microscope utilizes the spatial variation of absorption and scattering in a tissue to obtain images. A common example is a compound microscope.
- The most common illumination method for transmission microscopy is Kohler illumination, which uses a specialized optical arrangement.
- The magnification, M, of a microscope is defined as the ratio of the image and the object dimensions.
- The numerical aperture, NA, is related to the cone of the angle θ and the refractive index n of the medium from which light enters the objective lens as $\text{NA} = n \sin\theta$.
- The resolution of a microscope, defined as the minimum resolvable distance between two adjacent spots, is determined by the numerical aperture according to $d = 1.22(\lambda/2\text{NA})$.
- An objective lens with a higher NA also produces higher magnification, but provides shorter working distance between the specimen and the objective lens due to a tighter focus.
- The two types of distortions, called *optical aberrations*, encountered in optical imaging are (i) spherical aberrations, related to the shape of the lens in which rays refracted from the periphery of a lens do not focus at the same spot as those from near the center, and (ii) chromatic aberrations in which light of different wavelengths focus at different spots.
- Specially designed aspherical and achromatic lenses are commercially available which minimize the distortions.
- Phase-contrast microscopy utilizes changes in the phase of transmitted light, introduced by the biological sample, to obtain the image.
- Dark-field microscopy utilizes an angle of sample illumination at which only the highly diffracting structures can be imaged.
- Differential interference contrast microscopy (DIC) is based on optical interference techniques to convert the optical path difference, traveled by light passing through different parts of a specimen, to differences in intensities.

- Fluorescence microscopy utilizes either endogeneous fluorescence (autofluorescence) or fluorescence of an exogenous labeling (staining) fluorophore to obtain the image.
- Fluorescence microscopy provides the opportunity to utilize multiparameter control for imaging by using excitation wavelength, emission, lifetime and polarization selectivity. It is the most widely used method for bioimaging.
- Scanning microscopy which constructs an image using a serial, point-by-point illumination of the object provides the benefit of improved resolution with relatively low photodamage of the sample.
- Confocal microscopy is a popular imaging method, which utilizes a confocal aperture, such as a pinhole, to reduce the out-of-focus light from reaching the detector. It thus provides enhanced contrast and also the ability to obtain depth discrimination for three-dimensional imaging.
- Two-photon laser scanning microscopy (TPLSM) is gaining wide acceptance for fluoresence imaging. Here a two-photon excitation of the fluorophore using a near-IR pulsed laser source provides greater penetration in the tissue, more spatial localization, and less complication due to autofluorescence.
- Optical coherence tomography (OCT) is a refection imaging technique that utilizes back-scattered light from a tissue. Improved sensitivity in OCT is achieved by using interference between the back-scattered light and a reference beam.
- For a highly scattering dense medium, two-photon laser scanning microscopy and OCT are preferred techniques, with OCT having the advantage that no fluorescence labeling is required, but TPLSM generally provides better resolution.
- Total internal reflection fluorescence (TIRF) microscopy utilizes fluorescence excitation of the specimen, deposited on a solid surface, by an evanescent wave. This evanescent wave extends from the solid surface, when light is propagated on to the solid surface at a critical angle of total internal reflection. TIRF provides enhanced, sensitivity e to image and probes a cellular environment close to the solid surface.
- Near-field scanning optical microscopy (NSOM or SNOM) uses a tapered and metal-coated optical fiber with an optical opening of ~50 nm at the tip to excite a specimen and/or collect the transmitted, reflected, or fluorescence light signal, thus providing a resolution of <100 nm.
- Spectral imaging obtains information on spatial variation of spectra and provides information on the molecular mechanism of a biological function, a drug–organelle interaction, and so on.
- Fluorescence resonance energy transfer (FRET) imaging utilizes the ratio of fluorescence of an energy acceptor to that of the energy donor which is excited by light absorption and then transfers the excitation energy to the acceptor by the Forster energy transfer mechanism.

- FRET is useful in probing the interaction between cellular components such as protein–protein interactions or drug–binding-cell interactions.
- Fluorescence lifetime imaging (FLIM) maps the spatial distribution of the fluorescence lifetime. It serves as a sensitive probe of the local environment of a fluorophore and, thus, for the interactions and dynamics in a biological system.
- The nonlinear optical techniques of second-harmonic generation (SHG) and third-harmonic generator (THG) provide high spatial selectivity. Second-harmonic microscopy is very selective to interfaces and thus very suitable to probe interactions and dynamics at a membrane interface.
- The nonlinear optical techniques of coherent anti-Stokes Raman scattering (CARS) microscopy utilizes imaging by a coherent photon output generated at $2\nu_p - \nu_s$. The incident beams are at frequencies ν_p and ν_s, under the condition that $\nu_p - \nu_s$ corresponds to a Raman vibrational frequency of the molecule under illumination.
- CARS provides chemical information on the imaged region by mapping the spatial distribution of Raman vibrational spectra.

REFERENCES

Abbe, E., Beitrage zur Theorie des Mikroskops der microskopischen Wahrnehmung, *Schultzes Arch. Mikr. Anat*. **9**, 413–468 (1873).

Abramowitz, M., *Microscope Basics and Beyond*, Olympus Corporation Publishing, New York, 1987a.

Abramowitz, M., *Contrast Methods in Microscopy: Transmitted Light*, Olympus Corporation Publishing, New York, 1987b.

Abramowitz, M., *Fluorescence Microscopy: The Essentials*, Olympus America, New York, 1993.

Amos, W. B., White, J. G., Fordham, M., Use of Confocal Imaging in the Study of Biological Structures, *Appl. Opt*. **26**, 3239–3243 (1987).

Ash, E. A., Nicholls, G., Super-resolution aperture scanning microscope, *Nature* **237**, 510–513 (1972).

Axelrod, D., Total Internal Reflection Fluorescence Microscopy in A., Periasamy, ed. *Methods in Cellular Imaging*, Oxford University Press, Hong Kong, 2001, pp. 362–380.

Bastiaens, P. I. H., and Squire, A., Fluorescence Lifetime Imaging Microscopy: Spatial Resolution of Biochemical Processes in the Cell, *Trends Cell Biol.* **9**, 48–52 (1999).

Berkovic, G., Shen, Y. R., and Prasad, P. N., Third Harmonic Generation from Monolayer Films of a Conjugated Polymer, Poly-4-BCMV, *J. Chem. Phys*. **87**, 1897–1898 (1987).

Berkovic, G., Superfine, R., Guyot-Sinnoset, P., Shen, Y. R., and Prasad, P. N., A Study of Diacetylene Monomer and Polymer Monolayers Using Second- and Third-Harmonic Generation, *J. Opt. Soc. Am*. **135**, 668–673 (1988).

CHAPTER 9

Optical Biosensors

The field of biosensors has emerged as a topic of great interest because of the great need in medical diagnostics and, more recently, the worldwide concern of the threat of chemical and bioterrorism. The constant health danger posed by new strands of microbial organisms and spread of infectious diseases is another concern requiring biosensing for detecting and identifying them rapidly. Optical biosensors utilize optical techniques to detect and identify chemical or biological species. They offer a number of advantages such as the ability for principally remote sensing with high selectivity and specificity and the ability to use unique biorecognition schemes. The topic of optical biosensors is comprehensively covered in this chapter.

The objectives of this chapter are many. First, it describes the basic optical principles and the various techniques utilized in biosensing, which can be useful as a text for students or non-experts in this field. Second, the detailed coverage of the various optical biosensors, reported ongoing activities, and a list of commercially available optical biosensors can serve as a valuable reference source for researchers. Finally, some examples of opportunities for future developments, provided at the end of the chapter, are intended to stimulate the interest of a new researcher or one interested in expanding an ongoing research and development program in this field.

The two important components of biosensing, discussed in this chapter, are (i) a biorecognition element to detect chemical or biological species and (ii) a transduction mechanism which converts the physical or chemical response of biorecognition into an optical signal. The various types of biorecognition elements are discussed. This is followed by a coverage of the various principles of optical transduction and optical geometries utilized for biosensing. An important aspect of biosensing is to immobilize the biorecognition element to increase its local concentration in the sensor probe. The various physical and chemical methods utilized for this purpose are described.

The subsequent sections describe various types of optical biosensors that have been reported, some of which are already in practice. Specifically, these are fiber-optic biosensors, planar waveguide biosensors, evanescent wave

Introduction to Biophotonics, by Paras N. Prasad.
ISBN: 0-471-28770-9

biosensors, interferometric biosensors, and surface plasmon resonance (abbreviated as SPR) biosensors.

Some novel sensing methods reported recently are described in Section 9.9. Next is a discussion of future development opportunities in Section 9.10. The chapter concludes with Section 9.12, which provides a list of commercial available biosensors.

For further reading, suggested general references are:

Wolfbeis (1991): Covers fiber-optics-based chemical and biosensors

Boisdé and Harmer (1996): Covers optical fibers and waveguide-based sensors

Ramsay (1998): Covers commercial biosensors

Mehrvar et al. (2000): Covers trends and advances in fiber-optic biosensors

Ligler and Rowe-Taitt (2002): Provides comprehensive, up-to-date coverage of optical biosensors

9.1 BIOSENSORS: AN INTRODUCTION

Biosensors are analytical devices that can detect chemical or biological species or a microorganism. They can be used to monitor the changes in the *in vivo* concentrations of an endogenous specie as a function of a physiological change induced internally or by invasion of a microbe. Of even more recent interest is the use of biosensors to detect toxins, bacteria, and viruses because of the danger posed by chemical and biological terrorism. Biosensors thus find a wide range of applications:

- Clinical diagnostics
- Drug development
- Environmental monitoring (air, water, and soil)
- Food quality control

A biosensor in general utilizes a biological recognition element that senses the presence of an analyte (the specie to be detected) and creates a physical or chemical response that is converted by a transducer to a signal. The general function of a biosensor system is described in Figure 9.1. The sampling unit introduces an analyte into the detector and can be as simple as a circulator. The recognition element binds or reacts with a specific analyte, providing biodetection specificity. Enzymes, antibodies or even cells such as yeast or bacteria have been used as biorecognition elements. The principles of biorecognition are discussed in Section 9.2. Stimulation, in general, can be provided by optical, electric, or other kinds of force fields that extract a response as a result of biorecognition. The transduction process transforms the physical or chem-

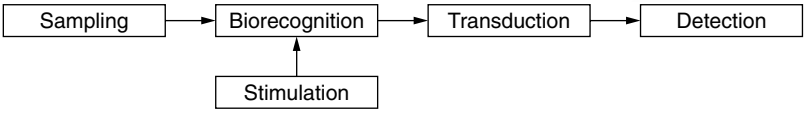

Figure 9.1. General scheme for biosensing.

ical response of biorecognition, in the presence of an external stimulation, into an optical or electrical signal that is then detected by the detection unit. The detection unit may include pattern recognition for identification of the analyte. In the most commonly used form of an optical biosensor, the stimulation is in the form of an optical input. The transduction process induces a change in the phase, amplitude, polarization, or frequency of the input light in response to the physical or chemical change produced by the biorecognition process. These processes are discussed in more detail in Section 9.2. Some of the other approaches use electrical stimulation to produce optical transduction (e.g., an electroluminescent sensor) or an optical stimulation to produce electrical transduction (e.g., a photovoltaic sensor).

The field of biosensors has been active over many decades. The earlier successes were sensors utilizing electrochemical response (Janata, 1989). This type of sensor still tends to dominate the current commercial market. However, progress in fiber optics and integrated optics (such as channel waveguides and surface plasmon waves) and the availability of microlasers (solid-state diode lasers) have made optical biosensors a very attractive alternative for many applications. An optical biosensor, in general, utilizes a change in the amplitude (intensity), phase, frequency or polarization of light created by a recognition element in response to a physiological change or the presence of a chemical or a biologic (e.g., microorganism). Enhancement of the sensitivity and selectivity of the optical response is achieved by immobilizing the biorecognition element (such as an antibody or an enzyme) on an optical element such as a fiber, a channel waveguide, or a surface plasmon propagation where light confinement produces a strong internal field or an evanescent (exponentially decaying; see Chapter 7, Section 7.7) external field. Thus, the main components of an optical biosensor are (i) a light source, (ii) an optical transmission medium (fiber, waveguide, etc.), (iii) immobilized biological recognition element (enzymes, antibodies or microbes), (iv) optical probes (such as a fluorescent marker) for transduction, and (v) an optical detection system.

Some of the advantages offered by an optical biosensor are:

- Selectivity and specificity
- Remote sensing
- Isolation from electromagnetic interference
- Fast, real-time measurements

- Multiple channels/multiparameters detection
- Compact design
- Minimally invasive for *in vivo* measurements
- Choice of optical components for biocompatibility
- Detailed chemical information on analytes

9.2 PRINCIPLES OF OPTICAL BIOSENSING

The two important principles involved in biosensing are biorecognition and optical transduction. They are discussed in this section together with the various geometries used for optical stimulation and collection of transduced optical response. A key step of immobilizing the biorecognition elements is discussed separately in Section 9.3.

9.2.1 Biorecognition

The biorecognition elements are biologics such as enzymes, antibodies, and even biological cells and microorganisms that selectively recognize an analyte. They are often immobilized to increase their local concentration near an optical sensing element and to allow them to be reused. Some of the molecular bioreceptors used for biorecognition in biosensitizing are described here.

Enzymes. The use of an enzyme as a biorecognition element utilizes its selectivity to bind with a specific reactant (substrate) and catalyze its conversion to a product. This enzyme–substrate-catalyzed reaction, also discussed in Chapter 3, is often represented as

$$\mathrm{E} + \mathrm{S} \rightleftharpoons \mathrm{ES} \rightarrow \mathrm{P}$$

In addition to providing selectivity, the reaction of certain analytes/substrates with enzymes can also provide optical transduction by producing a product that absorbs at a different wavelength (change in absorption), or is fluorescent (fluorescence sensor). Alternatively, the product of the enzyme-catalyzed reaction can interact with a dye (an optical sensing element such as a fluorescence marker) to produce an optical response.

Antibodies. Antibodies, as discussed in Chapter 3, are proteins that selectively bind with an antigen or hapten (analyte) because of their geometric (site) compatibility. Very often an antibody–antigen pair's selective association in terms of their conformational compatibility is represented as a lock (antibody) and key (antigen) combination, as shown in Figure 9.2. This specific physical association can also produce an optical response that can be intrinsic such as a change in the optical property of the antibody or the antigen

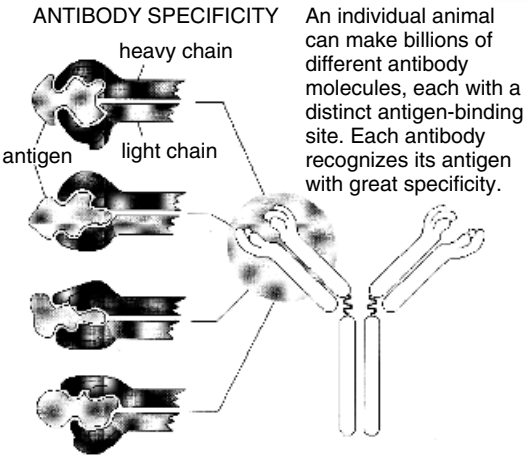

Figure 9.2. Schematic representation of antibody–antigen selective recognition. (Reproduced with permission from http://www.accessexcellence.org/AB/GG/antibodies.html)

as a result of association. Alternatively, an optical transducer (such as a fluorescent marker) can be used to tag the antibody or the antigen.

Lectins. Lectins are proteins that bind to oligosaccharides or single-sugar residues as well as to some glycoproteins such as immunoglobulins. Therefore, the lectins can act as biorecognition elements for these analytes. For example, concanavalin A in its A-form has been extensively used for its specific binding with α-D-mannose and α-D-glucose residues in a glucose sensor. In a glucose sensor utilizing concanavalin A, the lectin is immobilized on a sepharose film coated on the interior walls of a hollow fiber (Schultz et al., 1982; Boisdé and Harmer, 1996). Furthermore, it is liganded (conjugated) to dextran labeled with a fluorochrome, fluorescein-isothiocyanate (FITC). The glucose as an analyte diffusing through the hollow fiber displaces dextran from concanavalin A. The fluorescently labeled dextran then migrates to the area illuminated by light, being conducted through an inner solid optical fiber, to produce detectable fluorescence.

Neuroreceptors. These are neurologically active compounds such as insulin, other hormones and neurotransmitters that act as messengers via ligand interaction. They are also labeled with a fluorescent tag to produce an optical response through chemical transduction.

DNA/PNA. The specificity or complementary base pairing (that provides the basis for the DNA double-helical structure) can be exploited for recognition of base sequence in DNA and RNA (Kleinjung et al., 1998). An example is a DNA microarray (detailed coverage in Chapter 10) that consists of

micropatterns of single-stranded DNA or finite-size oligonucleotides immobilized on a plate. They act as biorecognition elements by forming hydrogen bonds with a specific single-stranded DNA or RNA having a complementary base sequence. This process of base-pairing to form a double-stranded DNA is called *hybridization* (see 8.5.4). Another example of biosensing utilizing the hybridization in DNA is provided by a molecular beacon sensor, discussed below.

Recently, remarkable sequence specificity has been reported using peptide nucleic acids (PNAs) as biorecognition elements (Wang, 1998; Hyrup and Nielsen, 1996). The PNAs provide the advantage of a neutral backbone and correct interbase spacing to ensure that the PNAs bind to their complementary sequence with higher affinities and with specificity comparable to oligonucleotides.

9.2.2 Optical Transduction

Optical biosensing utilizes a rich variety of optical manifestations, in response to the presence of an analyte, created by the recognition element in the presence of an optical stimulation. Table 9.1 lists some of the principal optical manifestations (transduction) used for biosensing. Phase change produced by a change in the real part of the refractive index manifests itself as (i) a change of polarization of a linearly polarized light, (ii) a change in the propagation characteristics, particularly in relation to a light-confining geometry such as a fiber or a planar channel waveguide, or (iii) a change in the optical field distribution, particularly at an interface. All these manifestations have been used for optical biosensing, as described below.

Amplitude change derived from absorption, reflection, or other transmission loss mechanisms produces changes in the intensity of the sensing light. Frequency changes associated with biosensing utilize (a) fluorescence where

TABLE 9.1. Various Optical Manifestations Used for Biosensing

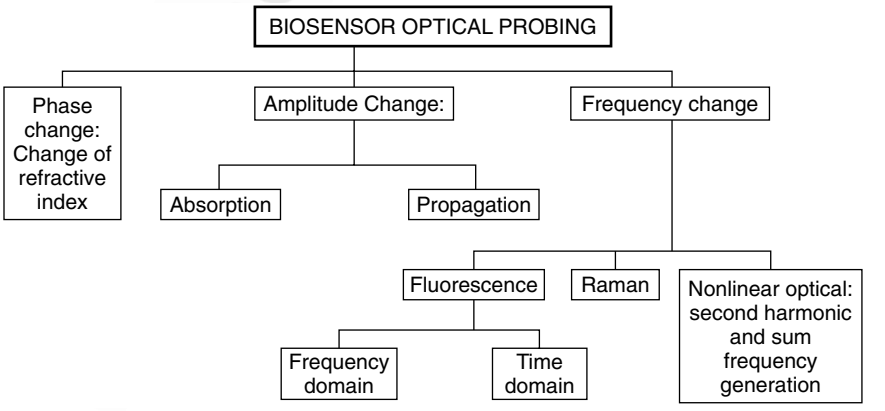

the optical signal generated is at a Stokes-shifted frequency from the exciting (absorbed) light, (b) Raman scattering, which is again Stokes-shifted, but now by vibrational excitation, (c) frequency shift by a nonlinear optical interaction mechanism such as second-harmonic generation. These effects were discussed in Chapters 4 and 5. For fluorescence sensors, one can use even an incoherent light source such as a light-emitting diode. However, for sensors utilizing Raman and second-harmonic generation, one needs a laser source.

9.2.3 Fluorescence Sensing

Direct Sensing. This type of sensing scheme utilizes a direct change in the fluorescence property as a result of the analyte binding with the biorecognition element (antibody or enzyme) or the production of a specie of a particular fluorescence property by a specific enzyme-catalyzed reaction. An example of this type of sensing is enzyme-catalyzed reactions that produce NADH. As discussed in Chapter 6, NAD^+ is nonfluorescent but NADH is fluorescent, with $\lambda_{ex}^{max} = 350\,nm$ and $\lambda_{em}^{max} = 450\,nm$. Therefore, dehydrogenase enzyme-catalyzed substrate reaction as

$$\text{Substrate} + NAD^+ \xrightarrow{\text{dehydrogenase}} \text{Product} + NADH$$

can be followed by monitoring the NADH fluorescence.

Indirect Sensing. Here an external dye, which may not be a part of the reaction but whose fluorescence property changes in response to biorecognition of an analyte, is used as a fluorescent tag for optical transduction.

An example of this type of biosensor is an ion-selective sensor that relies on the specific recognition of a specific ion. One example is that of a fluorescent dye conjugated to an enzyme, calmodulin, which recognizes and binds with Ca^{2+}. Figures 9.3 and 9.4 illustrate the principle and the response of Ca^{2+} binding to calmodulin on the fluorescence of the dye (producing a decrease in fluorescent intensity).

9.2.4 Fluorescence Energy Transfer Sensors

This scheme of fluorescence sensing involves an energy transfer that produces a change in the fluorescence of either the biorecognition element or the fluorescent marker (deSilva, 1997). The two main schemes used for biosensing utilizing this principle are shown in Figures 9.5 and 9.6.

A fluorescence resonance energy transfer (FRET) biosensor involves a donor and an acceptor group, with the electronic energy transfer between them being affected as a result of biorecognition. The biorecognition (such as antibody–antigen association) can lead to efficient electronic energy transfer from an excited donor group to an acceptor group that is highly fluorescent

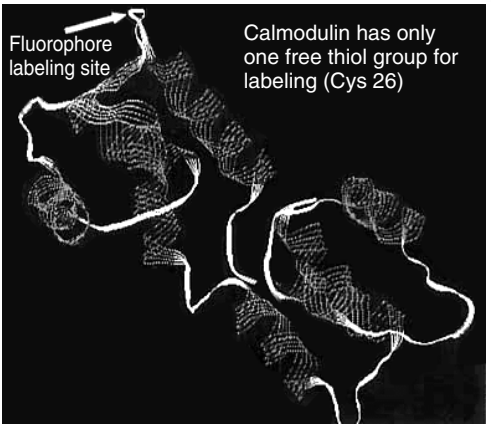

Figure 9.3. Calmodulin binding to Ca^{2+}, which produces conformational change in the enzyme structure. (Reproduced with permission from Watkins and Bright, 1998.)

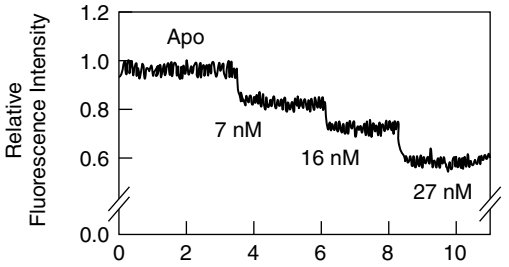

Figure 9.4. Decrease in fluorescence upon Ca^{2+} binding. (Reproduced with permission from Watkins and Bright, 1998.)

(or fluoresces at a different wavelength that is being detected). Alternatively, the facilitation or inhibition of energy transfer as a result of binding can affect the fluorescence of the donor group. In other words, the acceptor group acts as a fluorescence quencher. Another example of this type of sensing is the molecular beacon approach, discussed below. The energy level scheme dictates that the electronic excitation energy level of the donor is higher than that of the acceptor. Other requisites for an efficient fluorescence resonance energy transfer have been discussed previously in Chapter 7.

The scheme presented in Figure 9.6 utilizes the principle of photoinduced electron transfer. In this mechanism, the sensing unit consists of an electron donor group and an electron acceptor group. In the absence of the analyte, there is an efficient photoinduced electron transfer from the electron donor to the electron acceptor group when the acceptor is electronically excited. This results in quenching of the acceptor fluorescence. The appropriate energy level

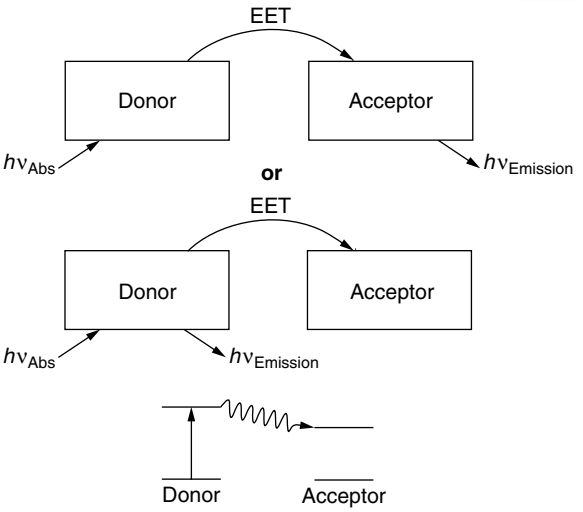

Figure 9.5. Fluorescence sensor utilizing fluorescence resonance energy transfer. EET represents electronic energy transfer. (Reproduced with permission from deSilva et al., 1997.)

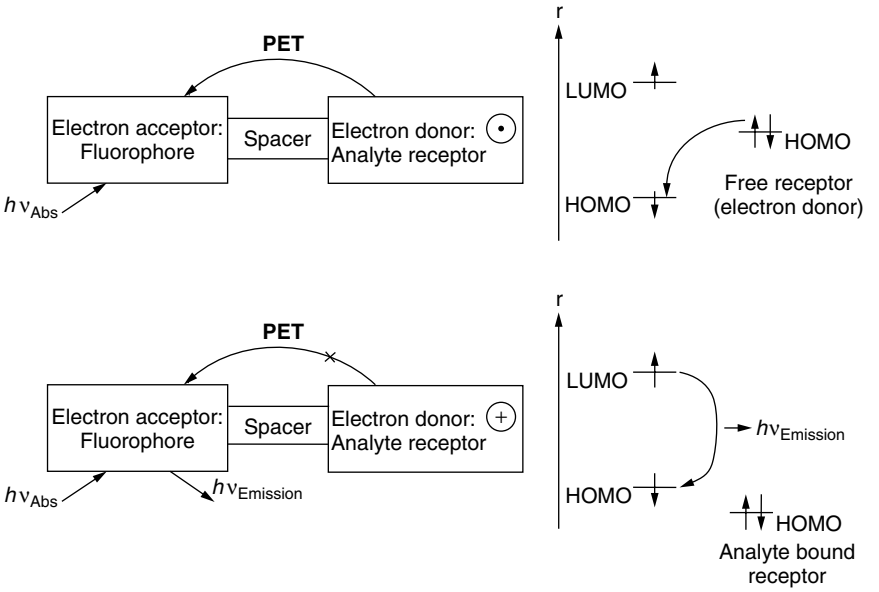

Figure 9.6. Fluorescence sensor utilizing photoinduced electron transfer (PET). (Reproduced with permission from deSilva et al., 1997.)

diagrams for this process are also shown in Figure 9.6. The HOMO (highest occupied molecular orbital, discussed in Chapter 2) energy level of the donor (when acting as a free receptor) is higher than that of the acceptor, permitting the photoinduced electron transfer when an electron is promoted from the HOMO to the LUMO (lowest unoccupied molecular orbital, discussed in Chapter 2) of the acceptor by optical absorption. When the electron donor group binds with an analyte or with a chemical product produced by the reaction of the analyte with the biorecognition element, it transfers the electron, thus transforming itself into a positively charged unit. Therefore, photoexcitation of the acceptor group now is unable to induce electron transfer from the donor to the acceptor group. Consequently, there is no quenching of the acceptor fluorescence. Therefore, the optical transduction here is the appearance of the acceptor fluorescence in the presence of an analyte. Figure 9.6 shows that the HOMO of the analyte-bound receptor (donor) is now lower than that of the electron acceptor.

9.2.5 Molecular Beacons

The molecular beacon approach is also based on the electronic energy transfer scheme between a fluorescent unit (Fl) and a fluorescent quencher (Q) (Tan et al., 2000). A molecular beacon consists of a loop and a stem. The loop structure involves a single-stranded oligonucleotide in a specific sequence. The stem usually consists of five to seven complementary base pairs. The two ends of the stem consist of a fluorophore (Fl) and a fluorescence quencher (Q). In the absence of the analyte, the stem is intact keeping the fluorophore and the quencher in close proximity and producing an efficient energy transfer, thus causing a quenching in the fluorescence of the fluorophore. In the presence of the analyte, the binding or biorecognition process forces the stem apart, thus increasing the distance between the fluorophore and the quencher sufficiently to inhibit the energy transfer. The result is restoration of the fluorophore fluorescence. This principle of operation is illustrated in Figure 9.7.

Molecular beacons have emerged recently as a new class of DNA, RNA, or PNA probes. Molecular beacons with a selected sequence of bases in the loop can be synthesized to detect the complementary DNA strand by hybridization (pairing up of complementary strands by hydrogen bonding), the hybridization forces the stem to open and restore the fluorescence of the fluorophore, as illustrated in Figure 9.8. In this study, a PNA–DNA hybrid probe was surface immobilized using biotin/streptavidin coupling. The hybridization with a single-stranded target DNA analyte opens the stem and produces fluorescence. A spectacular example of the molecular beacon approach is shown in Figure 9.9, where the molecular beacon loop consists of the oligonucleotide directed to the serine hydroxymethyltransferase pseudogene (SHMT-*ps1*). These studies confirmed those obtained using PCR that only primates possess this gene. As is clearly evident in Figure 9.9, fluorescent signal was obtained as the result of hybridization of the molecular beacon

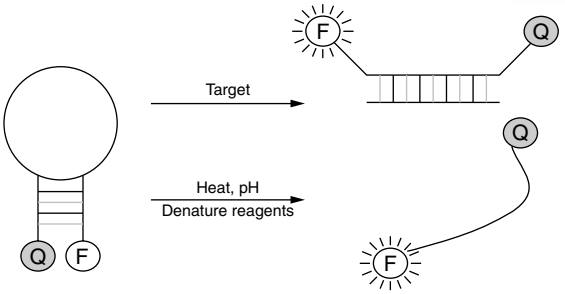

Figure 9.7. Molecular beacon approach for biosensing. Hybridization with the target DNA molecules of complementary sequence or unwinding with the increase of temperature, change of pH, or presence of denaturing agent produces an increase of fluorescence. (Reproduced with permission from Tan et al., 2000.)

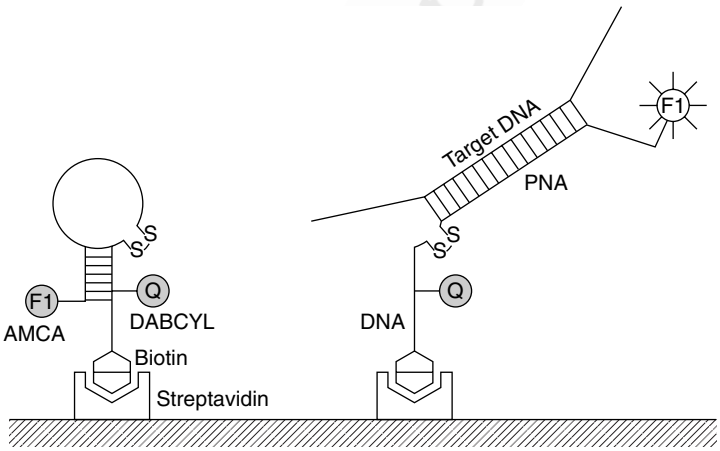

Figure 9.8. DNA probing by hybridization of the DNA unit/single-stranded (oligonucleotides) in the loop with a complementary sequence in the DNA analyte. (Reproduced with permission from Ortiz et al., 1998.)

probe with the target DNA obtained from primates (*H. sapiens, P. troglodytes, L. rosalia*). No signal was seen using nonprimate DNA (*V. varigegata, O. cunniculatus, O. aries*).

The molecular beacon approach has shown extremely high selectivity with single-base pair mismatch identification capability and suggests the prospect of studying biological processes in real time and *in vivo*.

9.2.6 Optical Geometries of Biosensing

A number of optical geometries have been used in the design of various optical biosensors. These geometries are listed in Table 9.2. The choice of any

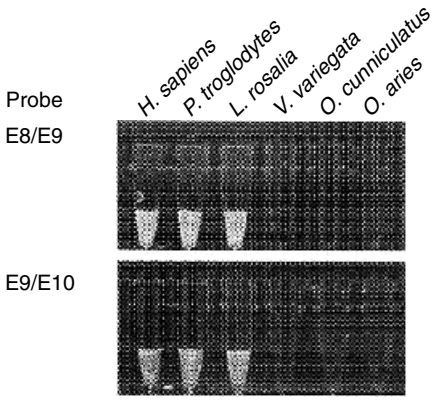

Figure 9.9. Molecular beacon fluorescence detection of pseudogene SHMT-*ps1* using two molecular beacon probes, E8/E10 and E9/E10. (Reproduced with permission from Devor, 2001.)

TABLE 9.2. Various Optical Geometries Used for Biosensors

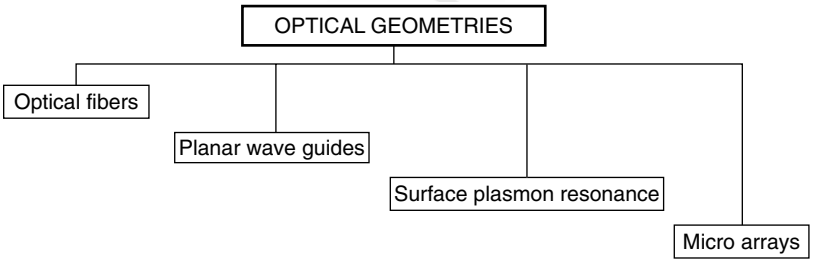

of these geometries is dependent on the nature of the analyte and the optical probing method used. A major consideration is enhancement of sensitivity and specificity. The guided wave geometries utilized in optical fibers and planar waveguide devices also provide an opportunity to use the evanescent waves that extend externally beyond the waveguiding region. As discussed in Chapter 7 (Section 7.7), the evanescent waves are nonpropagating optical fields whose strength decays exponentially as a function of distance away from the surface of the optical guiding region. The analyte/biorecognition element/optical probe at the interface between the biomedium and the guiding medium can interact with this evanescent field and produce an optical response. This evanescent wave can be utilized both for phase and amplitude modulation biosensors. The evanescent waves can be used to sense an analyte localized near the surface (by selectivity of the recognition element immobilized on the surface of an optical fiber, a planar waveguide or a surface plasmon resonance element). The surface plasmon geometry used for biosens-

ing is discussed in Section 9.8. The microarray geometry is covered in detail in Chapter 10.

9.3 SUPPORT FOR AND IMMOBILIZATION OF BIORECOGNITION ELEMENTS

The biorecognition elements are normally immobilized on a solid support, although in some cases a membrane or a solid support is simply used for physical confinement of the biorecognition unit to increase its local concentration in the region of biodetection. The solid supports are usually a membrane, a polymer, a copolymer, or a glass such as sol–gel processed glass. A biore-cognition element is immobilized on this solid support, either by a physical method (such as adsorption) or by chemical attachment. In some approaches, a biorecognition element is entrapped in the volume of a matrix (solid support) with controlled porosity, in which case the solid support also provides selectivity toward an analyte of certain size compatible with its pore dimension.

In the case of evanescent wave sensing, discussed below, the surface of a fiber or a waveguide itself acts as a solid support for the biorecognition element. Also in some optical fiber sensors, the distal end of the fiber itself acts as the solid support.

9.3.1 Immobilization

The various physical or chemical methods used to immobilize a biorecognition element (an enzyme, antibody, etc.) are discussed extensively in the literature (Boisdé and Harmer, 1996; Kuswandi et al., 2001). A brief discussion of this topic is presented here.

Physical Methods. The simplest physical method is containment within semipermeable membranes. A number of optical fiber sensors have utilized this technique. Another method calls for adsorption on a solid support. Depending on the nature of the biomolecule, either ionic, hydrophobic, or even van der Waal's forces can be used for selective adsorption. The adsorption is facilitated by preactivation of the surface. A simple approach used for dye adsorption involves immersing a polar cross-linked polymer or copolymer placed at the end of the optical fiber into dye solution and then washing off the unadsorbed dye (Boisdé and Harmer, 1996). A number of pH sensors utilize this method. Another solid support utilizing adsorption for immobilization involves microspheres whose surfaces are preactivated to enhance adsorption of the biorecognition element or a dye on the surface. For example, the glass microspheres can be treated with a silane to make it hydrophobic, allowing protein adsorption. The advantage of using microspheres is in maximizing the available surface area for adsorption. However, if the microspheres

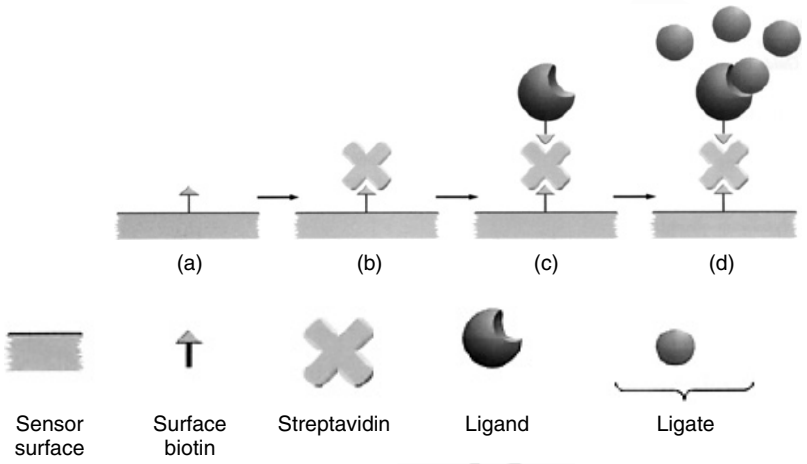

Figure 9.11. Biotin–avidin coupling scheme. (Reproduced with permission from Lowe et al., 1998.)

Another covalent attachment, frequently used in surface plasmon resonance (SPR) sensors, discussed in Section 9.8, requires immobilization of a biorecognition element on a gold surface. For this purpose, self-assembling of a monolayer formed from long-chain molecules with an —SH group at one end and an $—NH_2$ or a $—\overset{O}{\overset{\|}{C}}—$ group at the other end (Rogers, 2000) is used. The—SH group binds to the gold surface. The $—NH_2$ or $—\overset{O}{\overset{\|}{C}}—$ group at the other end can be used to couple to an enzyme or an antibody at multiple sites.

Cellulosic and polyacrylamide compounds, carboxylic-acid-modified polyvinyl chloride (PVC), and polystyrenes can be surface functionalized to bind with proteins (Boisdé and Harmer, 1996). For example, polystyrenes can be chloromethylated, sulfonated, and halogenated to bind with an indicator containing an —OH group.

9.4 FIBER-OPTIC BIOSENSORS

Fiber-optic biosensors are the most widely studied optical biosensors and have been a subject of extensive investigation over more than two decades. A number of excellent recent references describe fiber-optic based biosensors, their applications, and current status (Wolfbeis, 1991; Boisdé and Harmer, 1996; Mehrvar et al., 2000). Fiber-optic biosensors offer a number of advantages. Some of these are listed here:

- Optical fiber technology is now highly developed, providing optical fibers with many characteristics such as single-mode fibers, polarization pre-

serving fibers, and multimode fibers. This topic was discussed earlier in Chapter 6 under light delivery systems. The availability of these well-defined characteristics has led to the application of optical fibers in biosensing based on all the principles listed in Table 9.1.

- Optical fibers also provide a number of convenient geometries such as a single core fiber, a dual core fiber, a Y-junction fiber, and fiber bundles, offering flexibility to make them compatible to a specific need. The single fiber configuration provides the advantage of compactness (small sample volume). It is also more efficient as the overlap between the incident light probe and the collected (returned) optical response is maximized. On the other hand, a fiber bundle yields a higher optical throughput, thus providing an opportunity to use inexpensive nonlaser sources and detection systems.
- Use of a longer-length fiber provides a gain in interaction length or surface area for multiple analyte detection. Using the evanescent wave coupling, one can utilize a longer interaction length of a fiber by simply increasing its length. One can also use different segments of the same optical fiber, by appropriate labeling, to probe different analytes, thus providing an opportunity for multianalyte detection.
- Optical fibers also offer compatibilities with catheters or endoscopes for *in vivo* biosensing. Thus, one can use minimally invasive optical biosensing methods to measure *in vivo* blood flow, glucose content, and so on.

A number of classification schemes have been used for fiber-optic biosensors. One scheme classifies fiber-optic sensors into extrinsic or intrinsic. In an extrinsic fiber-optic sensor, the optic fiber simply is used as a transmission channel to take light to and from the sensing elements. In an intrinsic sensor, the fiber itself acts as a sensing element (transduction) because one or more of the physical properties of the optical fiber changes in response to the presence of an analyte. Another scheme is based on whether a direct or indirect (indicator-based) sensing scheme is used. In the case of a direct fiber-optic sensor (sometimes abbreviated as FOS), the intrinsic optical properties of the analyte are measured, while in the case of an indirect sensor, optical properties (absorbance, fluorescence) of an immobilized indicator dye, label, or optically detectable bioprobe is monitored.

As discussed earlier, a fiber-optic biosensor can utilize an amplitude change, in which case it is called an *intensity-modulated sensor*. Alternatively, it can utilize a phase change, in which case it is called a *phase-modulated sensor*. A phase-modulated sensor utilizes interferometric techniques such as a Mach–Zehnder interferometer, which involves two fibers: a reference fiber and a sensing fiber. In the presence of an analyte, the basic optical parameter of the sensing fiber is changed, creating a phase difference between the light traveling through the two fibers, resulting in a change in the optical interference signal.

For intensity modulation even an incoherent light source such as a light-emitting diode (LED) can be used. In contrast, phase-modulated interferometric sensors require high-coherence single-mode lasers.

In its most basic form, an intensity-modulated fiber-optic sensor as well as a fluorescence fiber-optic sensor utilizes optical fibers of various types, the tip of which contains an immobilized biological recognition element such as an enzyme or an antibody. The different configurations of optical fiber geometries and immobilization scheme used are shown in Figures 9.12 through 9.14.

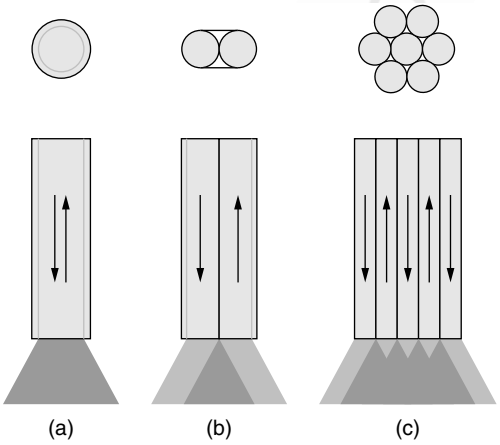

Figure 9.12. Different types of optical fiber configurations used for sensing. (Reproduced by permission of The Royal Society of Chemistry; Kuswandi et al., 2001.)

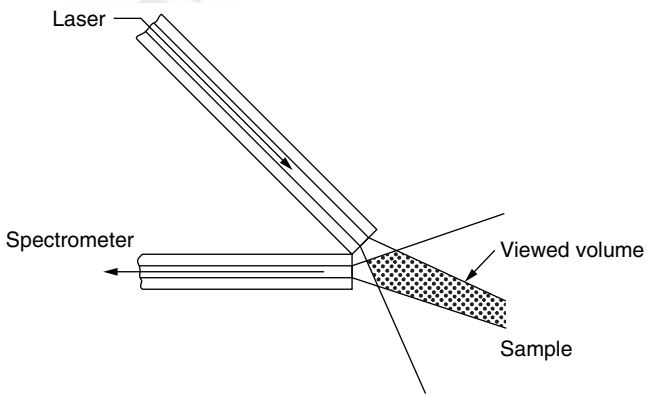

Figure 9.13. Double optical fiber terminal. (Reproduced with permission from CRC Press; Wolfbeis, 1991.)

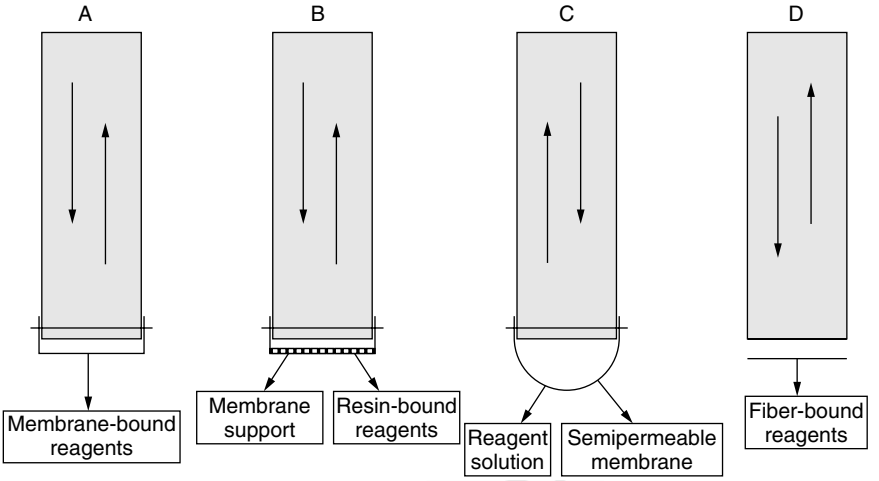

Figure 9.14. Various approaches of the sensing layers (immobilization of the recognition element) in fiber-optic sensing. (Reproduced by permission of The Royal Society of Chemistry; Kuswandi et al., 2001.)

The sensing layer containing the biorecognition element also can serve as a biochemical transduction system that produces a change in its optical property upon interaction with the analyte. As shown in Figure 9.14, the transduction reagent can be immobilized directly on a membrane held against the optical fiber (A), can be in a solid particulate form supported on the fiber end by a membrane (B), can be a liquid reagent confined near the fiber end by a semipermeable membrane (C), or can be bonded to the fiber itself (D).

A simple example is a urea sensor, depicted in Figure 9.15 (Abdel-Latif et al., 1990). Urea in the presence of urease, splits as ammonium and bicarbonate. Due to the production of ammonium, there is a change in the pH of the reagent. This results in a change in the spectral properties of the pH indicator. In the sensor shown above, urease and bromothyl blue are held at one of the fiber by a semipermeable membrane. The ammonium production changes the pH. The pH-sensitive dye changes its color when the pH of the surrounding environment changes. A similar pH-sensitive dye can be used for glucose sensing. In this case, a pH-sensitive dye along with a glucose biorecognition element (an enzyme: glucose oxidase) is held at one end of the optical fiber by a semipermeable membrane. The oxidation of glucose, which is catalyzed by glucose oxidase by the enzyme–substrate binding mechanism, consumes oxygen and produces protons (H^+), thereby changing the pH of the solution. The pH-sensitive dye changes its color (absorption) when the pH of the surrounding environment changes. Thus, by measuring the absorbance (absorption spectrum) using the light out (light returning in the optical fiber), one can get information on the glucose concentration.

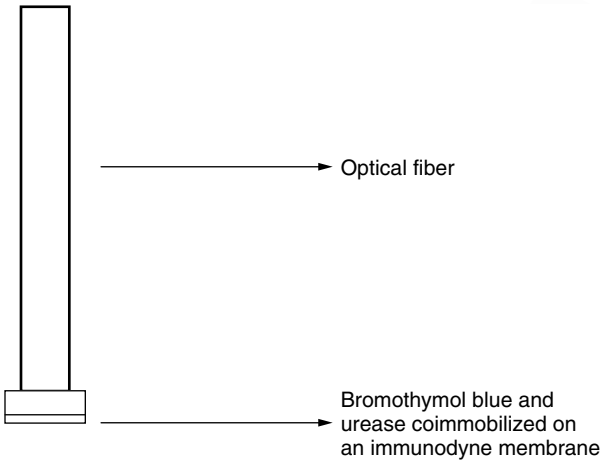

Figure 9.15. A fiber-optic urea sensor utilizing a pH-sensitive dye. (Reproduced with permission from Abdel-Latif et al., 1990.)

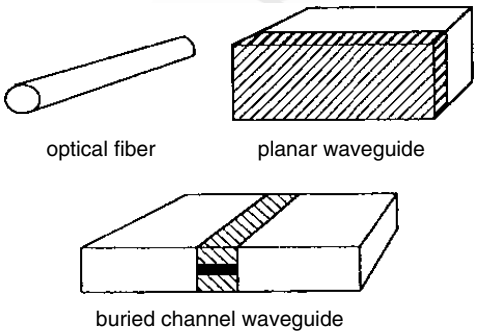

Figure 9.16. Typical examples of optical waveguides.

9.5 PLANAR WAVEGUIDE BIOSENSORS

Like optical fibers, planar waveguides are media in which the propagation of an optical waveguide is confined in a dimension comparable to the wavelength of light. Planar waveguides were discussed in Chapter 7 in the section on total internal reflection fluorescence (TIRF) imaging. However, for the sake of clarity, they are represented here in Figure 9.16.

As pointed out earlier (Chapter 6), a fiber is a waveguide in which the optical propagation is confined in two dimensions. In a planar waveguide the confinement is in one dimension (the thickness of the film). The film guiding the wave, again, is typically of the dimensions of $\sim 1\,\mu m$.

A channel waveguide actually produces two-dimensional confinement (height and width) and is quite analogous to a fiber. The three important techniques for coupling light into a planar waveguide are (i) prism coupling, (ii) grating coupling, and (iii) end-fire coupling.

An excellent recent review on planar waveguide sensors is provided by Sapsford et al. (2002) and by the book by Boisdé and Harmer (1996). Just like an optical fiber sensor, a planar waveguide utilizes immobilization of the biorecognition element on its surface. Most planar waveguide sensors are evanescent wave sensors, described in Section 9.6. The advantage of a planar waveguide sensor is that it allows the immobilization of multiple biorecognition elements, thus providing the prospect for multianalyte detection using a single substrate. This approach utilizes patterns of immobilized biomolecules. A number of techniques have been used to create such a patterned structure (Blawas and Reichert, 1998; Sapsford et al., 2002). Photolithography has been used to produce patterns of protein (Bhatia et al., 1992, 1993). Another approach utilizes photopatterning of a polymer surface by photoablation (Schwarz et al., 1998). Ink jet printing technology has also been used to pattern antibodies or the protein, avidin, in 200-μm-diameter spots on the surface of polystyrene films (Silzel et al., 1998).

Most planar waveguide sensors have been used in the fluorescence detection mode using evanescent wave excitation as described in the Section 9.6. When the dimensions of the waveguide are comparable to optical wavelength ($\leq$1 μm), the wave propagation is described in terms of concepts of integrated optics in which a continuous field distribution along the propagation path exists. In such a case, the waveguide is often referred to as an *integrated optical waveguide* (IOW). If the dimensions (width) of the waveguide are considerably thicker (100 μm), classical ray-optics describing total internal reflection of rays from the boundaries of the waveguide is used. Therefore, the waveguide is often referred to as an *internal reflection element* (IRE). In this case, the fluorescence sensing method utilizing an immobilized biorecognition system on the surface of the waveguide is referred to as total internal reflection fluorescence (TIRF) sensing. TIRF has also been discussed in Section 7.10 of Chapter 7 in the context of bioimaging. In the TIRF sensing, the waveguide surface produces a series of sensing "hot spots" along the planar surface from where the light beam is reflected. These discrete regions of high intensity can be used as sensing regions. However, it may be preferable to have a uniform field distribution achieved by reducing the waveguiding dimensions.

Many different kinds of materials have been used for waveguides. They include silica glass, polystyrene, and Ta_2O_5 (Sapsford et al., 2002). Depending on the material used, different surface chemistry approaches have been used to immobilize a molecule on the surface of a waveguide. In the case of a silica glass, silanization has been used. The avidin–biotin binding approach has been extensively used in general for various waveguides. These methods have been described in Section 9.3. More details are provided in the review by Sapsford et al. (2002).

As discussed earlier, a principal advantage of using a planar waveguide geometry is patterning for simultaneous multichannel multianalyte detection. In these approaches, a patterned array of a series of biorecognition elements is immobilized on the surface of a planar waveguide. Various analytes, fluorescently labeled with different fluorophores, are flowed over the surface of the waveguide. Then the pattern of fluorescent biorecognition : analyte complexes is detected. Image analysis software then can be used to correlate the position of a particular fluorescence signal with the identity of a specific analyte. An approach using patterning of captured biomolecules using flow cells is schematically represented in Figure 9.17, which is taken from the work of Feldstein et al. (1999). In this approach, a multichannel flow cell was pressed onto a planar waveguide surface and each channel was filled with a solution of the biomolecule. Then the sample and a fluorescent-tagged antibody were passed over the waveguide surface perpendicular to the immobilized biomolecule channel using another flow cell. Further advances have been made recently using automated fluidic systems and automated image analysis programs to develop a fully automated array sensor (Feldstein et al., 2000; Rowe-Taitt et al., 2000a).

Wadkins et al. (1998) used a scheme, shown in Figure 9.18, that used patterned antibody channels. They demonstrated the detection of *Y. pestis* F1 in clinical fluids such as whole blood, plasma, urine, saliva, and nasal secretion.

In another approach, Zeller et al. (2000) developed a TIRF system in which the planar waveguide consisted of multiplanar single pad sensing units. Each of the single pads had its own laser light input, coupling of fluorescence emission to the detector, and background suppression. In one example, they demonstrated a two-pad sensing device in which one pad was modified with mouse IgG while the other was modified with rabbit IgG. Other work in this direction is by Silzel et al. (1998), Plowman et al. (1999), and Rowe-Taitt et al. (2000b).

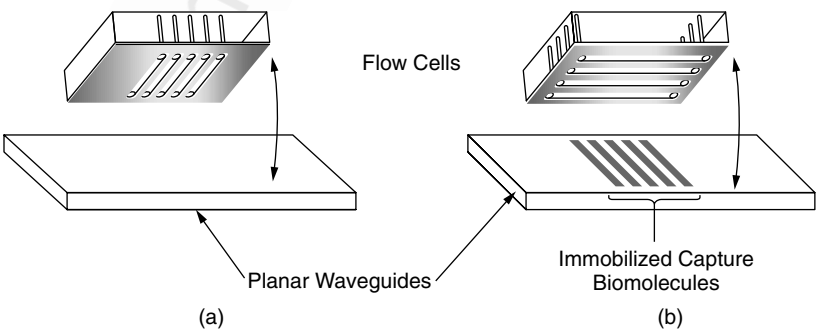

Figure 9.17. Patterning of capture biomolecules using flow cells. (Reproduced with permission from Feldstein et al., 1999.)

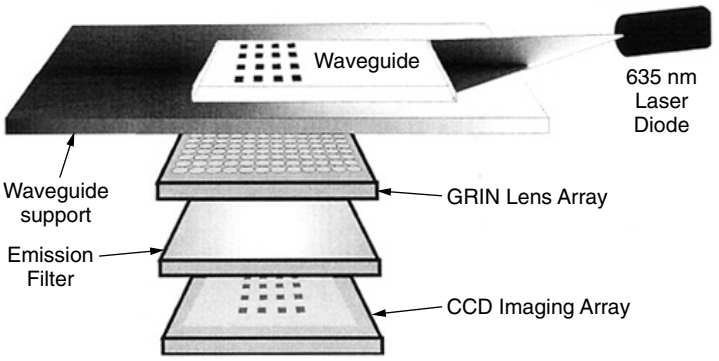

Figure 9.18. Array biosensors developed by Ligler, Golden, and co-workers at the Naval Research Laboratory. (Reproduced with permission from Wadkins et al., 1998.)

Hug et al. (2001) have proposed another method, which they call optical waveguide lightmode spectroscopy (OWLS), that is based on measurements of the effective refractive index of a thin layer above a waveguide. This thin layer can be due to whole cells. The effective refractive index of this adsorbate layer is dependent on the nature of adhesion and the cell and determines the coupling angle of light of a given polarization (TE or TM) into the planar waveguide. They used this approach to monitor the adhesion behavior of anchorage-dependent cells such as fibroblasts.

9.6 EVANESCENT WAVE BIOSENSORS

Evanescent wave sensors utilize the interaction with the electromagnetic field (evanescent wave) that extends away from the surface of the light guiding medium, whether a planar waveguide, a channel waveguide, or a fiber (Rowe-Taitt and Ligler, 2002; Boisdé and Harmer, 1996). In other words, these sensors rely on the light that is not confined within the waveguide itself, but penetrates into the surrounding medium of lower refractive index (cladding or air or into a surface immobilized biorecognition element) and thus senses the chemical environment on the surface of the waveguide (or fiber). In contrast to a propagating mode (oscillating electromagnetic field with the propagation constant k, defined in Chapter 2, as a real quantity), an evanescent wave has a rapidly decaying electric field amplitude, with an imaginary propagation constant k. The topic of evanescence has already been covered in detail in Chapter 7, Section 7.7.

Evanescent wave biosensing can utilize a number of optical transduction mechanisms, as illustrated in Table 9.4. In frequency conversion techniques, the fluorescence excitation has been used extensively both in a planar waveguide and in a fiber geometry. In this sensing scheme, the fluorescence is gen-

TABLE 9.4. Evanescent Wave Sensing

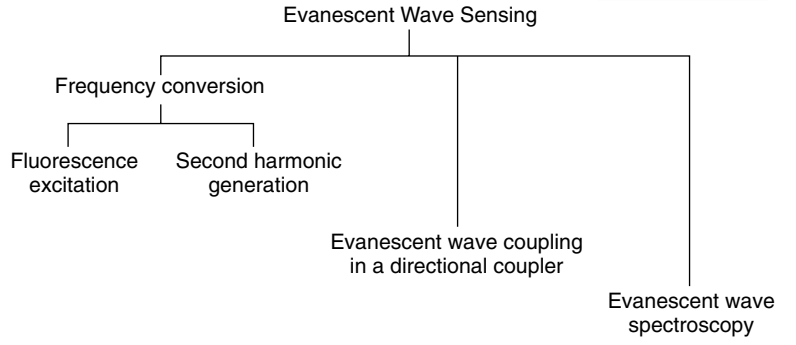

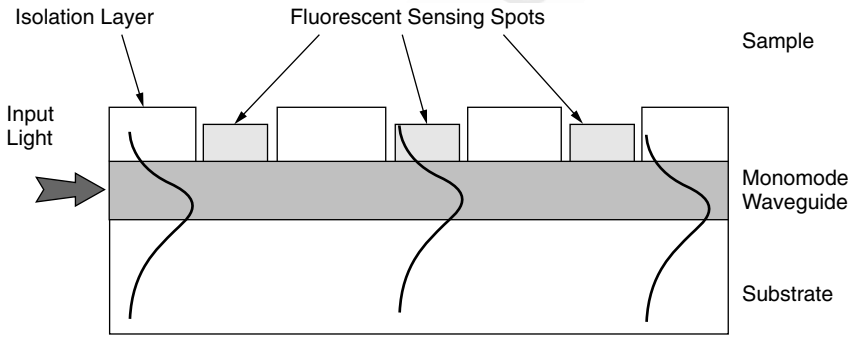

Figure 9.19. A fluorescence sensing scheme using a monomode planar waveguide. (Reproduced with permission from http://barolo.ipc.uni-tuebingen.de/projects/riana/summary/james.html).

erated from the analyte (antigen) specifically binding with a biorecognition element (antibody) which is immobilized on the surface of the waveguide or a fiber. Alternatively, the biorecognition element can be entrapped in a sol–gel film coated on the surface of the waveguide or the optical fiber. Even though the fluorescence is radiated isotropically in all directions, it is the fluorescence from the molecules close to the surface which couples into the waveguide (or fiber) and is detected for sensing.

A fluorescence sensing scheme using a monomode planar waveguide is shown in Figure 9.19. The idea is to excite with the evanescent field as well as to detect the fluorescence. Isolation layers (windows) are drawn on the surface of the waveguide, leaving a certain area of the waveguide surface exposed. This is achieved by rf spluttering with silica. The areas left exposed on the surface form the sensing spots of the sensor. These sensing spots form the regions of interaction with the analyte. If appropriate fluorophores are posi-

tioned in these sensing spots, then the evanescent wave protuding from the waveguide will excite the fluorophores to induce fluorescence.

In the case of a cladded fiber-optic probe, the amount of evanescent power is related to the fraction (f_e) of light power, P_{clad}, in the cladding region compared to the total power, P_t. It is defined as

$$f_e = (P_{\text{clad}}/P_t) = 1 - (P_{\text{core}}/P_t)$$

where P_{core} is the power in the core of the fiber. A crucial factor determining f_e is the V number of the optical fiber, which is defined as

$$V = (2\pi r/\lambda)(n_1^2 - n_2^2)^{1/2}$$

where r is the radius of the optical fiber, n_1 is the refractive index of the fiber, and n_2 is the refractive index of the surrounding medium or cladding layer. The fraction f_e decreases with the increasing V number (i.e., for a greater difference between n_1 and n_2 or larger r). In contrast, the efficiency of coupling of fluorescence emission from the surface back into the fiber increases with an increase in the V number (Thompson, 1991).

In order to enhance the interaction of the evanescent wave with the sensing layer containing a fluorescent marker, optical fibers with unclad, partially clad, and D-shaped forms have been used (Rowe-Taitt and Ligler, 2002). The D fibers are fibers in which the cladding from one-half of the fiber is removed, exposing that half to the sensing layer. In a partially cladded region, a major problem is V-number mismatch between the cladded region and the uncladded region. This can happen if the refractive index of the cladding layer is different from the medium surrounding the declad sensing region. This V mismatch creates light loss; particularly the fluorescence emission from the decladded sensing region is not guided into the core but enters the cladding layer and is therefore not transmitted to the detector. Approaches used to reduce the V-number mismatch are based on decreasing the radius of the fiber. The various geometries used for this purpose are shown in Figure 9.20.

Evanescent wave coupling sensors involve coupling between two channel waveguides or fibers that are close enough so that their evanescent fields overlap and couple them. The coupling is analogous to two coupled oscilla-

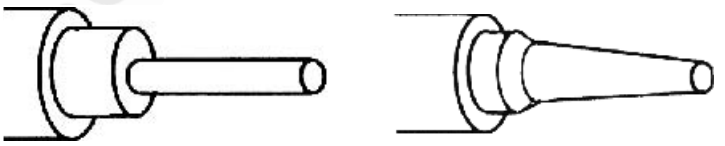

Figure 9.20. (A) Step-tapered core fiber. (B) Continuously tapered fiber.

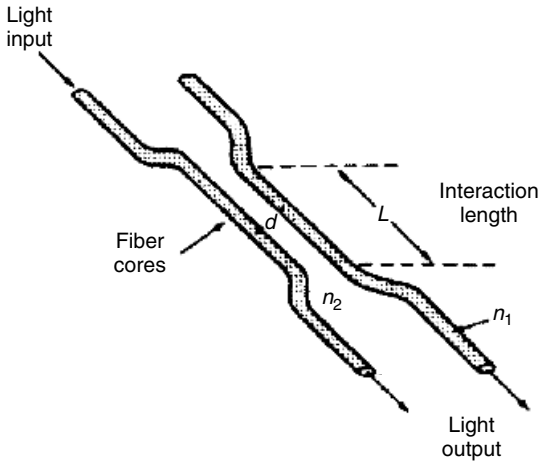

Figure 9.21. Evanescent wave coupled fiber-optic sensor. (Reproduced with permission from CRC Press; Wolfbeis, 1991.)

tors. It is, in fact, a phase sensing device that is highly sensitive to a change in the refractive index of the region between the two guides. An example of an evanescent wave coupled sensor is shown in Figure 9.21, where a pair of optical fibers are simply brought together.

When light is launched in one fiber, the overlap of the evanescent wave field with that of the adjacent fiber leads to a power transfer into the second fiber. The power transfers back and forth between the two fibers with a periodicity determined by the coupling constant between them that is strongly dependent on the refractive index. Therefore, when the refractive index between them changes as a result of biosensing the power transfer conditions change, resulting in a change of the intensity of light exiting one of the fibers. One specific case is when the length of the coupling region is half of a characteristic length called the *beat length*; then the light launched in one fiber is completely transferred to the other fiber. The biorecognition element in this case is immobilized in the region of evanescent wave overlap. The analyte binding changes the refractive index, thus changing the coupling condition whereby the same length now does not meet the condition of complete transfer. Therefore, the power transfer to the second fiber decreases.

In evanescent wave spectroscopic sensors, the interaction of the evanescent wave with the sensing layer is used to get spectroscopic information on the analyte binding (Boisdé and Harmer, 1996). The spectroscopic information can be on the IR (vibrational) or UV-visible (electronic) absorption band or the Raman spectroscopic transitions. Recent studies have used near-IR and FT–IR spectroscopic approaches. Silver halide fibers have been used for obtaining spectral information in the region 2–20 μm. Also, uncladded chalcogenide fibers and sapphire fibers have been utilized.

where M is the modulation factor and $\Delta\Phi$ is the relative phase shift between the two arms. If the initial conditions are adjusted so that the relative phase shift $\Delta\Phi$ is zero, the binding of an analyte to the sensing layer on the sample arm channel waveguide introduces an additional phase shift $\Delta\Phi_{sens}$, given as (Heideman and Lambeck, 1999)

$$\Delta\Phi_{sens} = (2\pi/\lambda)L_{int}\Delta N$$

where L_{int} is the "interaction length" of the guided wave with the analyte, λ is the wavelength, and ΔN is the change in the effective index in the evanescent field.

Integrated-optic Mach–Zehnder interferometric sensors utilizing a planar waveguide geometry have been used for many applications. Some examples are glucose sensor (Liu et al., 1992), immunosensor (Brecht et al., 1992), and sensors for pesticide determination (Schipper et al., 1995).

9.8 SURFACE PLASMON RESONANCE BIOSENSORS

Surface plasmon resonance (often abbreviated as SPR) sensors are, perhaps, the most extensively utilized optical biosensors that are also commercially sold by a number of companies as discussed below in Section 9.11. There are a number of excellent reviews on this subject (Liedberg et al., 1995; Schuck, 1997; Homola et al., 1999; Myszka and Rich, 2000). The SPR technique has been utilized for a variety of biosensing methods, from biochemical detection such as of glucose and urea, to immunosensing for immunoassays (for protein hormones, drugs, steroids, immunoglobulins, viruses, whole bacteria, and bacterial antigens), to DNA binding assays, to real-time kinetics of drugs binding to therapeutic targets. Spangler et al. (2001) have compared the performance of a commercial SPR sensor with that of a quartz crystal microbalance for detection of *E. coli* heat-labile enterotoxin.

In principle, the SPR technique is an extension of evanescent wave sensing, described in Section 9.6, except that a planar waveguide is replaced by a metal–dielectric interface. Surface plasmons are electromagnetic waves that propagate along the interface between a metal and a dielectric material such as organic films (Wallis and Stegeman, 1986). Since the surface plasmons propagate in the frequency and wave-vector ranges for which no light propagation is allowed in either of the two media, no direct excitation of surface plasmons is possible. The most commonly used method to generate a surface plasmon wave is attenuated total reflection (ATR).

The Kretschmann configuration of ATR is widely used to excite surface plasmons (Wallis and Stegeman, 1986). This configuration is shown in Figure 9.23. A microscopic slide is coated with a thin film of metal (usually a 400- to 500-Å-thick gold or silver film by vacuum deposition). Then a biosensing layer containing an immobilized biorecognition element can be coated on the metal

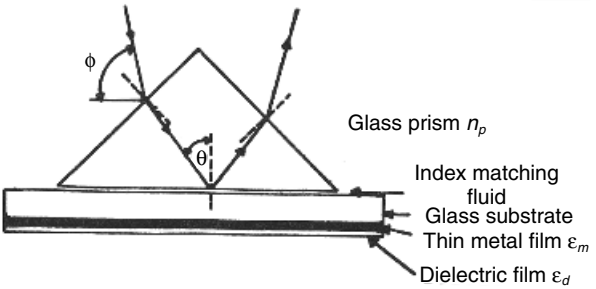

Figure 9.23. Kretschmann (ATR) geometry used to excite surface plasmons (Prasad, 1988).

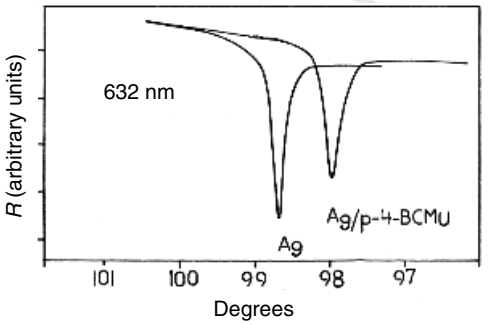

Figure 9.24. Surface plasmon resonance curves. The left-hand-side curve is for just the silver film (labeled Ag); the right-hand-side curve shows the curve (labeled Ag/p-4-BCMU) shifted on the deposition of a monolayer Langmuir–Blodgett film of poly-4-BCMU on the silver film (Prasad, 1988).

surface. The microscopic slide is now coupled to a prism through an index-matching fluid or a polymer layer. A p-polarized laser beam (or light from a light-emitting diode) is incident at the prism. The reflection of the laser beam is monitored. At a certain θ_{sp}, the electromagnetic wave couples to the interface as a surface plasmon. At the same time, an evanescent field propagates away from the interface, which extends to about 100 nm above and below the metal surface. At this angle the ATR signal drops. This dip in reflectivity is shown by the left-hand-side curve in Figure 9.24. The angle is determined by the relationship

$$k_{sp} = kn_p \sin\theta_{sp}$$

where k_{sp} is the wave vector of the surface plasmon, k is the wave vector of the bulk electromagnetic wave, and n_p is the refractive index of the prism. The surface plasmon wave vector k_{sp} is given by

$$k_{\mathrm{sp}} = (\omega/c)[(\varepsilon_m \varepsilon_d)/(\varepsilon_m + \varepsilon_d)]^{1/2}$$

where ω is the optical frequency, c is the speed of light, and ε_m and ε_d are the relative dielectric constants of the metal and the dielectric, respectively, which are of opposite signs. In the case of a bare metal film, ε_d (or square of the refractive index for a dielectric) is the dielectric constant of air and the dip in reflectivity occurs at one angle. In the case of metal coated with the sensing layer, this angle shifts. Upon binding with an analyte, a further shift of the SPR coupling angle occurs. Figure 9.24 also shows as an illustration the shift in the coupling angle on deposition of a monolayer Langmuir–Blodgett film of a diacetylene, poly-4-BCMU. The shifted SPR curve curve is shown on the right-hand side in Figure 9.24 (Prasad, 1988).

In this experiment one can measure the angle for the reflectivity minimum, the minimum value of reflectivity, and the width of the resonance curves. These observables are used for a computer fit of the resonance curve using a least-squares fitting procedure with the Fresnel reflection formulas, which yields three parameters: the real and the imaginary parts of the refractive index and the thickness of the sensing layer. The experiment involves the study of angular shift (change in θ_{sp}) as a function of analyte binding.

From the above equations, one can see that the change $\delta\theta$ in the surface plasmon resonance angle (the angle corresponding to minimum reflectivity; for simplicity the subscript sp is dropped) caused by changes $\delta\varepsilon_m$ and $\delta\varepsilon_d$ in the dielectric constants of the metal and the covering film, respectively, is given by (Nunzi and Ricard, 1984)

$$\cot\theta\,\delta\theta = (2\varepsilon_m \varepsilon_d (\varepsilon_m + \varepsilon_d))^{-1}(\varepsilon_m{}^2 + \delta\varepsilon_d + \varepsilon_d{}^2 \delta\varepsilon_m)$$

Since $|\varepsilon_m| \gg |\varepsilon_d|$, the change in θ is much more sensitive to a change in ε_d (i.e., of the sensing layer) than to a change in ε_m. Therefore, this method appears to be ideally suited to obtain $\delta\varepsilon_d$ (or a change in the refractive index) as a, function of analyte binding to the sensing layer. Another way to visualize the high sensitivity of SPR to variations in the optical properties of the dielectric above the metal is to consider the strength of the evanescent field in the dielectric, which is an order of magnitude higher than that in a typical evanescent wave sensor utilizing an optical waveguide as described above. The magnitude of the change in θ can be quantitatively related to the amount of analyte binding or to the extent of a chemical change in the sensing layer.

In an SPR sensor, the change $\delta\varepsilon_d$ (and hence $\delta\theta$) (such as in antibody–antigen reactions) that can be induced is independent of wavelength. However, in some cases such as for various immobilized chromophores, the change in ε_d is at specific wavelengths. In SPR biosensors the immobilized probe is usually attached to a sensor chip with a thin layer of metal. In an SPR sensor, the sensing response is a change in the refractive index of

the sensing layer containing ligands (e.g., antibodies) upon analyte binding which is measured as a change, $\delta\theta$, in the coupling angle. In commercial SPR sensors, this change in the coupling angle is measured by a CCD or photodiode array using a convergent light beam, rather than scanning the angle as described above. This arrangement, as shown in Figure 9.25, permits real-time monitoring of the ligand–analyte binding to obtain kinetics of association and dissociation. To get this information, the sample solution containing the analyte flows over the sensor chip containing the ligand. During the association phase, the analyte binds with the ligand immobilized on the sensor chip, generating an increase in response (amount of shift of the coupling angle). The magnitude of the response ($\delta\theta$) levels off over the time as an equilibrium condition between the free and the bound analyte is reached. To monitor dissociation, the flow switches to that of a running buffer which washes out the analyte (leading to dissociation of it from the ligand). During the dissociation, the magnitude of the response decreases. The generated response curve for the association and dissociation cycle is often called a *sensorgram*. The association process is also shown in Figure 9.25 as an inset on the right-hand side.

A wide variety of surface chemistries have been used to provide functionality to minimize nonspecific binding of ligands to the gold surface. Some of these are (Homola et al., 1999)

- Streptavidin monolayer immobilized onto a gold film with biotin which can further be functionalized with biotinylated biomolecules.

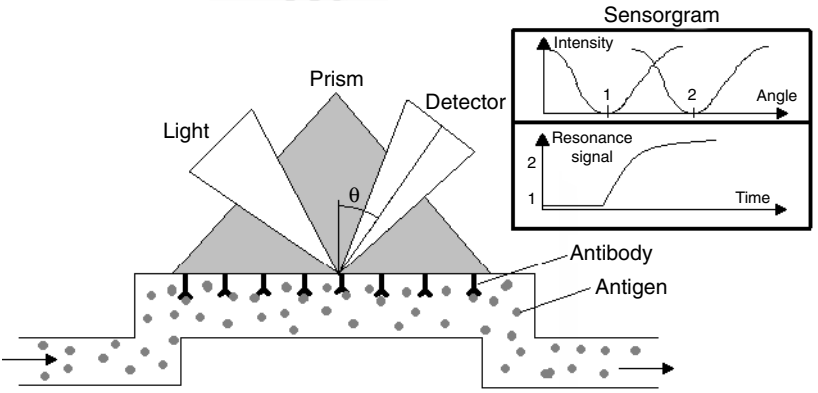

Figure 9.25. Surface plasmon resonance sensor schematic utilizing a CCD or photodiode array (*left*). The inset on the right-hand side shows the sensorgram. The top in the inset shows a shift in the SPR curve from 1 to 2 upon binding with the analyte. The bottom curve is obtained by monitoring the SPR signal at the shifted coupling angle as a function of time when the analyte is introduced. (Reproduced from http://chem.ch.huji.ac.il/~eugeniik/spr.htm.)

- A self-assembled monolayer (SAM) of thiol molecules such as 16-thiohexadecanol. The thiol group attaches to the gold surface. The tail can be bound to the ligands forming a monolayer of ligand molecules.
- An SAM layer covalently bonded to a dextran layer using epichlorohydrin. After treating dextran with iodoacetic acid, the resulting carboxylic group can be used to immobilize the ligands.
- Gold surface coated by a plasma polymerized thin film onto which the ligands can be immobilized via an amino group.

SPR sensors offer several distinct advantages, such as:

- No labeling (such as by a fluorescent marker) required, thus allowing for the analysis of a wide range of biomolecular systems.
- Real-time monitoring permitted, thereby providing rapid and quantitative information on kinetics of binding.
- Small amounts of materials required for typical analysis.

9.9 SOME RECENT NOVEL SENSING METHODS

Photonic Crystals Sensors. Photonic crystals are ordered dielectric arrays that diffract light at wavelengths determined by the lattice spacing between the arrays and the average refractive index of a structure (Carlson and Asher, 1984; Asher, 1986; John, 1987; Yablonovitch, 1987). One example of a photonic crystal is a closely packed colloidal array as shown in Figure 9.26. This crystal was prepared at our Institute, using 200-nm polystyrene spheres. These spheres were floated, as a suspension, over a patterned template where they settled to form a highly ordered array (Markowicz and Prasad, unpublished).

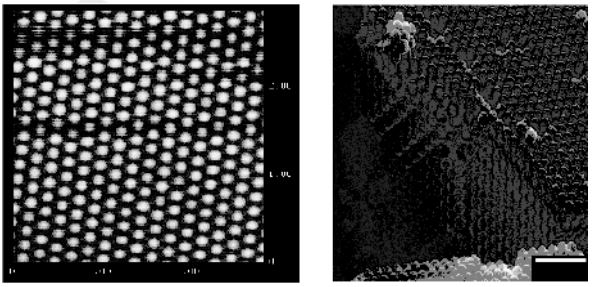

Figure 9.26. Close packing of colloidal nanospheres to form a photonic crystal of close-packed colloidal array. (*Left*) Atomic force microscope (AFM) image of the surface layer. (*Right*) Scanning electron microscope (SEM) image of a cross section (Markowicz and Prasad, unpublished).

CHAPTER 12

Light-Activated Therapy: Photodynamic Therapy

An important area of biophotonics is use of light for therapy and treatment. This chapter and Chapter 13 provide examples of the use of light for therapy and medical procedures. Chapter 12 covers the area of light-activated therapy, specifically the use of light to activate a photosensitizer that eventually leads to the destruction of cancer or a diseased cell. This procedure is called *photodynamic therapy* (abbreviated as PDT) and constitutes a multidisciplinary area that has witnessed considerable growth in activities worldwide. Treatment of certain types of cancer using photodynamic therapy is already approved in the United States by the Food and Drug Administration as well as in other countries by equivalent agencies. Therefore, this chapter can be useful not only for researchers but also for clinicians and practicing oncologists.

The basic principles utilized in photodynamic therapy are introduced. The nature of the photosensitizers, also called PDT drugs, plays an important role in determining the conditions and effectiveness of PDT. The various types of photosensitizers are described. Another section is devoted to the various applications of PDT, which are very diverse.

A very active area of investigation is the understanding of the mechanism of photodynamic action. This topic is covered in Section 12.4. Section 12.5 provides information on various light sources along with some examples of required light dosage and modes of light delivery for PDT. A new area of interest is the use of nonlinear optical techniques such as two-photon photodynamic therapy that show promise for the treatment of deeper tumors. This topic is covered in Section 12.6.

The chapter concludes with a discussion of current research and future directions in Section 12.7. This discussion is subjective, reflecting the views of this author. Nonetheless, it clearly illustrates that opportunities are manyfold and multidisciplinary: for chemists, physicists, engineers, biologists, and practicing clinicians.

For further reading, suggested general references are:

Introduction to Biophotonics, by Paras N. Prasad.
ISBN: 0-471-28770-9

Henderson and Doughtery (1992): Covers basic principles and clinical applications of PDT

Fisher et al. (1996): Covers clinical and preclinical PDT

12.1 PHOTODYNAMIC THERAPY: BASIC PRINCIPLES

Photodynamic therapy (PDT) has emerged as a promising treatment of cancer and other diseases utilizing activation of an external chemical agent, called a photosensitizer or PDT drug, by light. This drug is administered either intravenously or topically to the malignant site as in the case of certain skin cancers. Then light of a specific wavelength, which can be absorbed by the PDT photosensitizer, is applied. The PDT drug absorbs this light, producing reactive oxygen species that can destroy the tumor. This type of process induced by a photosensitizer was discussed briefly in Chapter 6.

The key steps involved in photodynamic therapy are shown in Figure 12.1. They are:

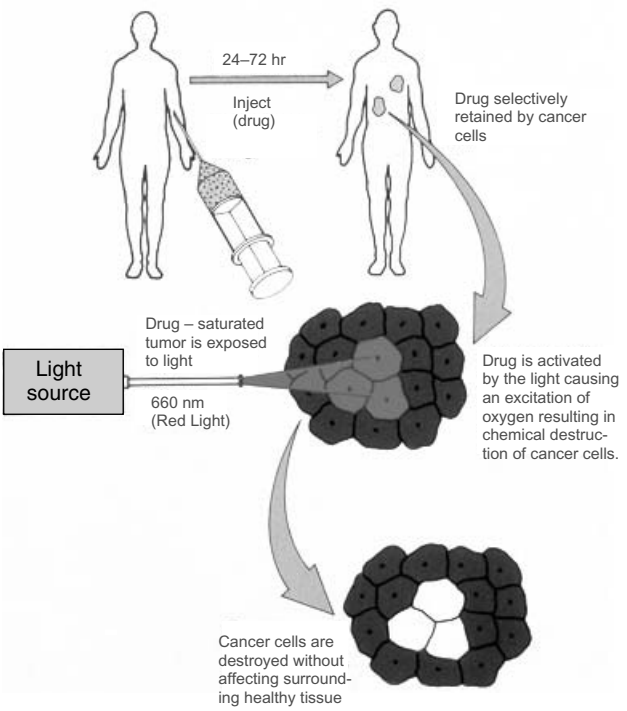

Figure 12.1. The steps of photodynamic therapy with a specific PDT drug.

- Administration of the PDT drug
- Selective longer retention of the PDT drug by the malignant tissue
- Delivery of light, generally laser light, to the malignant tissue site
- Light absorption by the PDT drug to produce highly reactive oxygen species that destroy cancer cells with minimal damage to surrounding healthy cells
- Clearing of the drug after PDT to reduce sunlight sensitivity

As indicated above, PDT relies on the greater affinity of the PDT drug for malignant cells. When a PDT drug is administered, both normal and malignant cells absorb the drug. However, after a certain waiting period ranging from hours to days, the concentration of the PDT drug in the normal cell is significantly reduced. Recent studies with tumor-targeting agents attached to the PDT drug have shown that their waiting period can be reduced to a matter of a few hours. In contrast, the malignant cells still retain this drug, thus producing a selective localization of this drug in the malignant tissue site. At this stage, light of an appropriate wavelength is applied to activate the PDT drug, which then leads to selective destruction of the malignant tissue by a photochemical mechanism (nonthermal, thus no significant local heating). In the case of cancer in an internal organ such as a lung, light is administered using a minimally invasive approach involving a flexible fiber-optic delivery endoscopic system. In the case of a superficial skin cancer, a direct illumination method can be used. Since coherence property of light is not required, any light source such as a lamp or a laser beam can be used. However, to achieve the desired power density at the required wavelength, a laser beam is often used as a convenient source for this treatment. The use of a laser beam also facilitates fiber-optic delivery.

The light activation process of a PDT drug is initiated by the absorption of light to produce an excited singlet state (S_1 or often written as $^1P^*$, where P* represents the excited photosensitizer), which then populates a long-lived triplet state T_1 (or $^3P^*$) by intersystem crossing. These terms and processes have been defined in Chapter 4. It is the long-lived triplet state that predominantly generates the reactive oxygen species. Two types of processes have been proposed to produce reactive species that oxidize the cellular components (hence, produce photooxidation) (Ochsner, 1997). These are described in Table 12.1.

A type I process generates reactive free radicals, peroxides, and superoxides by electron or hydrogen transfer reaction with water or with a biomolecule to produce a cytotoxic result. For the sake of simplicity, Table 12.1 only shows the generation of peroxides (H_2O_2) and the hydroxyl radical ($^{\bullet}OH$). In a type II process the excited triplet state of the photosensitizer reacts with the oxygen in the tissue and converts the oxygen molecule from the normal triplet state form to a highly reactive excited singlet-state form. It is the type II

TABLE 12.1. Mechanism of Photodynamic Photooxidation

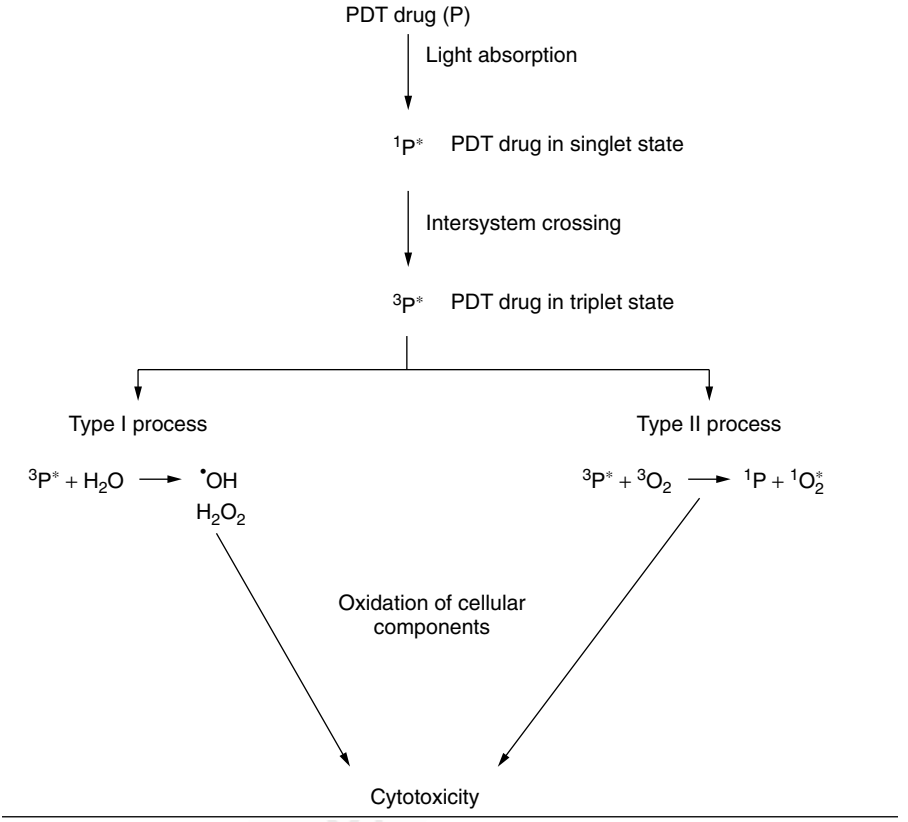

process that is generally accepted as the major pathway for photodynamic therapy—that is, the destruction of malignant cells.

The generation of singlet oxygen by an excited PDT photosensitizer can be detected spectroscopically or by chemical methods. The spectroscopic method utilizes the observation of phosphorescence emissions at ~1290 nm involving the transition from the excited singlet state of oxygen to its triplet ground state. Figure 12.2 shows the phosphorescence from singlet oxygen that is generated by a PDT drug, HPPH. This photosensitizer, discussed in Section 12.2, is being investigated at our Institute, in collaboration with the Roswell Park Cancer Institute (where it was developed).

The chemical method relies on the bleaching of absorption of a known singlet oxygen quencher such as 9,10-anthracenedipropionic acid (ADPA) (Bhawalkar et al., 1997). The absorption of ADPA at 400 nm is bleached (considerably reduced) by reaction with singlet oxygen.

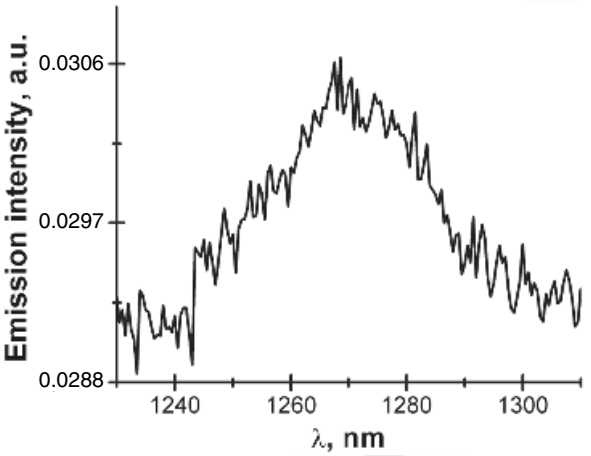

Figure 12.2. Phosphorescence from the lowest excited singlet state of oxygen generated by a photoexcited PDT drug, HPPH.

12.2 PHOTOSENSITIZERS FOR PHOTODYNAMIC THERAPY

A suitable choice of a PDT drug as a photosensitizer requires the following:

- The photosensitizer must have the ability to selectively accumulate in cancerous and precancerous tissues. In other words, while it is eliminated from normal tissue, it is retained in cancerous tissues and precancerous cells. Alternatively, the photosensitizer must target specific cancer cells.
- From the point of view of localization in tumors, the best sensitizers are those that are hydrophobic in order for them to penetrate cell membranes most readily. However, if they are to be administered intravenously, the sensitizers should be at least partially water-soluble and thus also hydrophilic to disperse in the bloodstream. Therefore, combining the two requirements, it is preferable to make the photosensitizers amphiphilic by chemically modifying a fundamentally hydrophobic PDT drug, by attaching polar residues such as amino acids, sugars, and nucleotides.
- The sensitizer should absorb significantly at a wavelength in the region of maximum transparency of biological tissues. This transparency region has been discussed in detail in Chapter 6. This choice will allow light to penetrate deeper in the tissue to activate a PDT drug, localized in malignant tissues which are deep, if the PDT drug absorbs at a long wavelength. However, wavelengths longer than 900 nm are energetically too low to provide the energy needed for excitation of triplet oxygen to its singlet state.

- The photosensitizer should exhibit minimum toxicity in the dark in order for light activation of the drug to produce maximum benefits without side effects derived from any inherent toxicity.
- The photosensitizer should have a high quantum yield of triplet-state formation and a long triplet lifetime. In other words, the nonradiative intersystem crossing from the excited singlet state of the photosensitizer to its excited triplet state should be efficient compared to the direct radiative transition (fluorescence) from the excited singlet. A longer triplet lifetime enhances the chance of producing a cytotoxic reagent or a cytotoxic reaction from this excited state.
- The photosensitizer should not aggregate since that can reduce the extinction coefficient and shorten the lifetime and quantum yield of the excited triplet state. Aggregated forms of the photosensitizer can also affect its pharmacokinetics and biodistribution.
- The photosensitizer should be rapidly excreted from the body. This will produce low systemic toxicity and will reduce sunlight sensitivity following PDT treatment.

12.2.1 Porphyrin Derivatives

The first group of photosensitizers used in clinical PDT were hematoporphyrin derivatives. The structure of hematoporphyrin is shown in Structure 12.1. Photofrin® (porfimer sodium), a PDT drug approved by the U.S. Food and Drug Administration as well as by other regulatory agencies throughout the world for the treatment of a variety of malignant tumors (see Figure 12.3), is obtained from hematoporphyrin by treatment with acids. Photofrin® actually is a complex mixture consisting of various derivatives as well as dimeric and

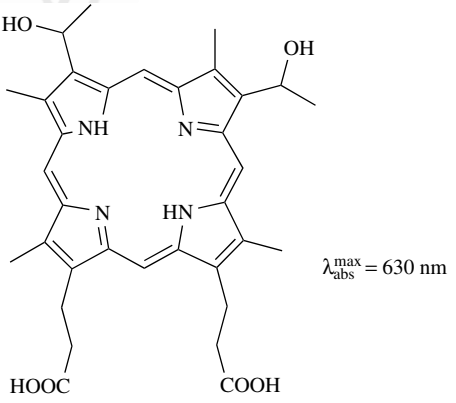

Structure 12.1. Structure of hematoporphyrin.

accompanied by immunosuppressive effects that aid in long-term tumor control.

The role of inflammation in the host's response to PDT seems to vary with different photosensitizers (e.g., Photofrin® versus HPPH, being of more importance in the former). The inflammation processes are involved in the concentration of the immune response in the area of need. Inflammation occurs in response to infection or tissue damage. As a result, collateral damage to cells by the inflammatory processes has an additive effect in tumor destruction. This collateral damage has a significant role in tumor destruction in PDT using Photofrin®, but plays less of a role in treatment with HPPH. Despite activation of many common components of inflammation (e.g., neutrophil and vascular adhesion molecules activation), the mode of cell death in PDT (necrosis, apoptosis, mixed response) may alter the role played by inflammation. In other models, the effects of mediators of inflammation [e.g., interleukin 6 (IL-6)] may either enhance, inhibit, or have no effect on the PDT response, depending on the model studied. IL-6 has a wide range of effects on many organ systems in regard to the initiation of inflammatory processes. PDT stimulation of the release of this cytokine would significantly enhance the role of inflammation in the destruction of the tumor and/or the immune response to specific tumor antigens.

12.5 LIGHT IRRADIATION FOR PHOTODYNAMIC THERAPY

12.5.1 Light Source

As discussed in Section 12.1, the PDT treatment using photoexcitation of the photosensitizer by linear absorption (as opposed to excitation by a nonlinear, two-photon absorption) does not require a high-peak power or a coherent light source. For this reason, incandescent filament lamps (tungsten) and arc lamps (xenon or mercury) were used in early clinical studies and continue to play a useful role. However, lasers are becoming more of a standard light source for most PDT studies and clinical applications (Fisher et al., 1996). The two practical advantages offered by a laser PDT are:

- The laser's ability to serve as a monochromatic source for selective and efficient excitation of a specific photosensitizer
- The efficiency and ease of coupling of a laser beam into fibers, making it ideal for insertion in flexible endoscopes and for interstitial use

For the excitation of PDT drugs photosensitized at 665 nm (such as Photofrin® and HPPH), a popular source has been a dye laser with rhodamine B as the lasing medium. A dye laser can be pumped by an argon-ion laser (a gas laser)

or an intracavity KTP-doubled Nd:Vanadate laser (a solid-state laser), both producing a CW dye laser output in the range of 1–4 W. This is the typical power range requirement for most PDT applications. Pulse laser sources providing high repetition rates in the kilohertz range have also been used. These are gold vapor lasers, copper vapor laser-pumped dye lasers, and quasi-CW Q-switched Nd:YAG laser-pumped dye lasers.

Solid-state diode lasers are, perhaps, the choice of the future. These lasers already produce CW and quasi-CW powers in the range of 1–4 W with a single emitter source in the range of 780–850 nm. A diode bar containing an array of diode emitters can produce powers in excess of 100 W. Diode lasers are thus ready to serve as a suitable light source with new PDT drugs that can be activated at these longer wavelengths. However, the available diode lasers operating at 630 nm which meet the PDT power requirement are expensive. An additional consideration is that it is likely that future PDT applications will utilize near-infrared laser sources to treat subcutaneous cancerous tumors. These are areas of future development of laser technology for PDT applications.

Other laser sources for PDT applications at longer wavelengths are tunable solid-state lasers, such as (i) the Ti:sapphire laser (Ti:$A1_2O_3$), which covers the wavelength range of 690–1100 nm, and (ii) the Alexandrite lasers covering the range 720–800 nm. These solid-state lasers were discussed in Chapter 5.

Another new source for future applications may utilize optical frequency generation by optical parametric oscillation (OPO) and parametric amplification. This approach also provides a broad-band tunability and was discussed in Chapter 5.

A few studies have been reported that compare the efficacies of CW laser sources with those of pulse laser sources for PDT. It appears that both types of lasers can be used for PDT. As long as the peak power is not too high (as encountered with a short-pulse, high-intensity laser), as in the case for a high repetition rate quasi-CW laser source, the results obtained from this type of pulse laser and a CW laser source are biologically equivalent for the same irradiance and power densities.

12.5.2 Laser Dosimetry

The appropriate light dose for a specific PDT treatment is determined by the size, location, and type of tumor. The light dose requirements for Photofrin® using 630-nm excitation are as follows (Fisher et al., 1996; Dougherty et al., 1998):

- *Radiant Exposure*: 25–500 J/cm^2 for surface treatment; 100–400 J/cm^2 for interstitial applications
- *Maximum Irradiance*: 200 mW/cm^2 for surface treatment; 400 mw/cm^2 for interstitial applications
- *Typical Output Power*: 1–2 W

The power requirements are not expected to be less for the new generation of PDT photosensitizers, because the primary focus has been on increasing the wavelength of excitation to achieve deeper penetration.

12.5.3 Light Delivery

In determining an appropriate light delivery mode, some of the considerations are as follows (Fisher et al., 1996):

- Compatibility of the light source with other clinical instrumentations such as endoscopes and stereotactic devices
- Ability to continuously monitor light output and light dosimetry
- Ability to tailor spatial distribution of light to match the tumor shape and size in individual patients

In an optical fiber delivery system, a more uniform irradiation is obtained by fitting a microlens to the fiber for forward surface illumination (Doiron, 1991). For an interstitial laser irradiation needed for treating thicker lesions and tumors, the fiber can be directly inserted into the tumor mass, either by point insertion or inside a needle using a flat-cut fiber tip. Typically, the fiber will have a spherical or cylindrical diffusing tip. If more than one site needs to be irradiated, one can surgically implant translucent nylon catheters for subsequent laser treatments. For treatment of a tumor in an internal organ such as a lung, light is delivered through a flexible bronchoscope.

A major focus of current PDT studies from a light source perspective is the incorporation of light monitoring and dosimetry instruments into clinical delivery systems to gain information from each patient. This will also provide real-time information during the PDT procedure. Direct measurement of the PDT drug concentration, for example, can be obtained from quantitative fluorometry or reflectance spectrophotometry. Studies are also being conducted to provide methods for *in vivo* measurements of singlet oxygen production, which is generally accepted as a mechanism for destruction of a tumor. One such method utilizes the emission of singlet oxygen at 1270 nm (Gormann and Rodgers, 1992, see Figure 12.2). However, a severe limitation to this approach of detection is the relatively short lifetime (microseconds) of singlet oxygen.

12.6 TWO-PHOTON PHOTODYNAMIC THERAPY

As discussed in Section 12.2 on photosensitizers, currently most photosensitizers in clinical applications are being photoactivated using a light source in the range 630–690 nm. At this wavelength, the tissue penetration (defined by $1/e$ loss of intensity; see Chapter 6) is about 2–4 mm and the photodynamic effect is generally seen up to 2–3 times deeper than that. As a result, the largest attainable depth of PDT-induced cellular changes could reach up to 15 mm,

but in most cases it is much less than half of that. For this reason, the increase of light penetration is considered to be an important factor in increasing the clinical efficacy of PDT. This is one of the focuses of current research. One approach is the design of new photosensitizers that absorb at longer wavelengths, as discussed in Section 12.2. Another approach is the use of two-photon absorption to photoactivate the photosensitizer. This two-photon process was discussed in Chapter 5. However, even two-photon PDT may prove ineffective beyond 1 to 2-cm penetration due to the large amount of scattering in some tissue types.

The spectral window for transmission through tissue lies around 800–1000 nm, which is in the near-infrared region. Such wavelengths may be used for excitation of the photosensitizer by using two-photon absorption. The idea of using two-photon excitation for PDT has been proposed by many investigators (Stiel et al., 1994; Lenz, 1994; Bhawalkar et al., 1997). However, the two-photon absorption cross-section of existing photosensitizers has been too small to be of practical significance until very recently (Karotki et al., 2001). The intensities required for direct two-photon excitation of these photosensitizers may cause damage to healthy tissues. Using efficient two-photon pumped upconverting dyes in conjunction with a PDT photosensitizer, at the Institute of Lasers, Photonics, and Biophotonics we have proposed a novel approach to PDT using infrared laser light for treatment (Bhawalkar et al., 1997). In this approach, an efficient two-photon absorbing dye is excited by short laser pulses. The dye molecule transfers the energy to the photosensitizer that is in proximity to it (or covalently bonded to it). The photosensitizer is thus excited to the singlet state from which the same sequence of energy transfer occurs as described earlier to produce the singlet oxygen.

The initial two-photon absorption of the dye molecules requires high-intensity IR laser pulses. These can be easily generated by ultra-short pulse lasers even with relatively low pulse energy. An example of such a laser is a typical mode-locked Ti:sapphire laser, which can produce 4-nJ pulses of about 70-fsec duration. This corresponds to a peak power of $5\,\mathrm{MW\,cm^{-2}}$ in a 2-mm-diameter beam. The low pulse energy is highly desirable because it minimizes thermal side effects. An added advantage of using two-photon absorption arises from the quadratic dependence of the efficiency of such a process on the incident light. Therefore, the photodynamic effect is restricted to a small area around the focal point. Such spatial selectivity is important in many treatments such as PDT of brain cancers.

Preliminary studies were conducted at the Institute of Lasers, Photonics, and Biophotonics (Bhawalkar et al., 1997) as an initial assessment of the potential value of two-photon-induced PDT. To test the concept of the cascading energy transfer process in the photochemical generation of singlet oxygen, a new two-photon absorbing red dye, ASPS (*trans*-4-[*P*-(*N*-ethyl-*N*-hydroxyethylamino)styryl]-*N*-butansulfonpyridinum), and a well-known porphyrin photosensitizer ($TPPS_4$, obtained from Logan, UT) were selected. The

fluorescence emission from three cuvettes irradiated with 1064-nm laser pulses from a Q-switched Nd:YAG laser was monitored in a fluorometer. One cuvette contained a solution of the dye alone, the second contained a solution of $TPPS_4$, and the third contained a mixture of both ASPS and $TPPS_4$ in solution. The dye solution showed a strong two-photon-induced fluorescence with a peak at around 610 nm while the $TPPS_4$ solution showed no detectable two-photon-induced fluorescence. The mixture of the two compounds showed, in addition to the characteristic emission spectrum of the dye, a new fluorescence peak at 653 nm which is the characteristic peak of $TPPS_4$. This is evidence of an energy transfer from the dye to the porphyrin. To further determine if the excited photosensitizer could generate singlet oxygen in the presence of atmospheric oxygen, a singlet oxygen-detecting compound was used. ADPA (9,10-anthracenedipropionic acid) is an excellent singlet oxygen quencher and a reaction with singlet oxygen leads to a bleaching of its 400-nm absorption band. This compound was added to the three cuvettes, and the solutions were exposed to IR pulses for several hours. Every hour, a sample from each cuvette was removed and its absorbance was measured. The cuvettes containing ADPA and the dye did not show any bleaching, nor did the ADPA and the porphyrin. However, in the cuvette containing the mixture, the absorbance at 400 nm was found to be steadily decreasing with each sample. This clearly indicated an increasing concentration of singlet oxygen during the exposure period. On repeating the observations with argon bubbled into the mixture, the bleaching was significantly lower.

A preliminary test of the feasibility of the two-photon process as an *in vivo* light source (at 500 nm) was performed in DBA (strain designation) mice with auxiliary SMT-F tumors, in collaboration with the PDT Center headed by Dr. Thomas J. Dougherty at the Roswell Park Cancer Institute in Buffalo. The treatment included APSS as the two-photon absorbing dye and Photofrin® as the photosensitizer. Immediately upon administering the mixture, the tumor area was illuminated with an unfocused train of 800-nm pulses from a mode-locked Ti:sapphire laser oscillator. The pulse duration was 90 fsec and the average power in the beam was 300 mW. The tumor was flat at 24 hours post-illumination, while the control group of Photofrin® plus light showed some hemorrhage and the light-alone control showed some edema (abnormal accumulation of serous fluid in the body). Additional unpublished studies at our Institute showed that APSS was nontoxic to mice.

Two-photon photodynamic therapy is currently an active area of both *in vitro* and *in vivo* studies, however, at the current time there have been no FDA-approved two-photon PDT protocols for cancer treatment.

12.7 CURRENT RESEARCH AND FUTURE DIRECTIONS

The field of photodynamic therapy is truly multidisciplinary, providing exciting opportunities for biomedical researchers, chemists, physicists, engineers,

and practicing oncologists. Some areas of current activities offering prospects for future research are listed here. The selection of these areas is based partly on the author's personal views and partly on ongoing activities at the Photodynamic Therapy Center at Roswell Park Cancer Institute (courtesy of Dr. Janet Morgan). These selected areas are discussed in the following sections.

Molecular and Cellular Mechanisms of PDT. The fundamental nature of the photosensitizer structure and its photoactivity and the importance of its subcellular drug localization and photoaction are topics that are still not fully understood and are under intensive investigation. Various chemical, analytical, and spectroscopic probes are being used to understand the molecular and cellular mechanisms of PDT.

Effect of PDT on Cytokine Gene Expression and Immune Response. The subjects of intensive studies include (i) immune suppression after cutaneous PDT, (ii) immune potentiation after tumor PDT on other tumors, (iii) molecular mechanisms of regulation of some of the cytokines involved in potentiation, and (iv) different gene expression models, with different photosensitizers.

Tissue Oxygen Level Limitation. An important limitation of PDT utilizing photosensitizers that act by a type II process (Section 12.1) producing singlet oxygen is that the oxygen level is depleted both by consumption of singlet oxygen in a photoinduced chemical reaction and by vascular damage, leading to the shrinkage of its radius. This effect limits further therapy for producing direct tumor cell killing. This limitation is being addressed in a number of ways:

1. Adjusting the light fluence rate to slow oxygen consumption sufficiently so that the tumor tissue oxygen level can be maintained at the necessary level. A useful method has been the delivery of light in fractions, such as very short (20–50 sec) light and dark intervals, which allows reoxygenation during dark periods.
2. Providing PDT treatment in oxygen-enriched conditions (such as in a hyperbaric oxygen chamber)
3. Developing oxygen-independent photosensitizers that utilize free radicals (such as hydroxyl groups) as the active agent. However, these photosensitizers are not very efficient because one can only use each photosensitizer molecule once.

New Photosensitizers. Further acceptance of photodynamic therapy, increasing its efficacy, reducing side effects, and broadening the scope of its applications are crucially dependent upon the development of new photosensitizers. This provides unique opportunities for chemists. Some areas of opportunities are:

- One-photon PDT sensitizers that operate in the near IR ($\lambda > 800\,\text{nm}$)
- Efficient multiphoton-absorbing photosensitizers
- Dendrimers carrying multiple photosensitizers
- Targeting photosensitizers that carry an antibody, small proteins or peptides, sugars, and so on
- Oxygen-independent sensitizers
- Amphiphilic photosensitizers

The benefits of these types of photosensitizers have been discussed at various sections in this chapter. For example, it has recently been shown that porphyrins can be designed and synthesized with dramatically enhanced two-photon cross sections (up to two orders of magnitude enhancement) (Karotki et al., 2001). These new materials have also exhibited very efficient singlet oxygen production in *in vitro* studies.

Enhanced Transport of PDT Drugs. The more efficient transport of a photosensitizer into a tumor tissue can increase the efficacy of PDT treatment and shorten the waiting period. A highly active area of research is the use of various methods as well as chemical conjugation with various carrying units to enhance the transport of the sensitizer (Konan et al., 2002). For example, transdermal transport of amino levulinic acid, ALA, a PDT pro-drug for protoporphyrin IX, can be enhanced severalfold by electroporation as compared to topical application. Electroporation is a technique whereby pulsed electrical stimulation of the skin results in the opening of the interdermal spaces (spaces between the cells), allowing for more efficient transport of the sensitizer into the tissue. Another approach is to attach an imaging reagent conjugated to a small peptide that can bind to over-expressed receptor sites on the tumor.

Enhanced Drug Delivery to Tumors by Low-Dose PDT. Subcurative PDT for tumors can make the tumor vasculature highly permeable to large molecules. The subclinical dose disrupts the tumor vasculature as a result of cell destruction and/or activation of inflammatory processes. The result is increased permeability to large molecules, toxic drugs such as doxorubicin that are encapsulated and delivered locally after application of PDT (Henderson and Dougherty, 1992).

New Light Sources. In order for PDT to gain wide acceptance by the medical community, there is a need for lasers that are compact, low cost, user-friendly, and relatively maintenance-free. Furthermore, the need to activate more than one photosensitizer requires a multiwavelength laser source. New-generation diode lasers, other solid-state lasers, and optical parametric oscillators offer great opportunities for laser physicists and engineers. Looking

futuristically, one can even think of implantable high-fluence diode light sources and low-fluence attachable device "patches" for long treatment.

Real-Time Monitoring of PDT. There is a real need for further development of techniques that will allow real-time monitoring of the parameters that determine PDT action. Some of these parameters are photosensitizer tissue concentration, photobleaching rates, blood flow, and oxygen pressure in tissue (pO_2). These types of studies will provide insights into ways to enhance treatment effectiveness and selectivity.

HIGHLIGHTS OF THE CHAPTER

- Photodynamic therapy, abbreviated as PDT, utilizes light, often laser light, to destroy cancerous or diseased cells and tissues.
- Photodynamic therapy involves selective light absorption by an external chemical agent, called a *photosensitizer* or a *PDT drug*.
- The PDT drug, when administered either intravenously or topically, has the property of producing selective longer retention by the malignant (or diseased) tissue.
- The mechanisms of PDT action can involve either of two processes, often labeled as Type I and Type II. They both involve the formation of excited triplet state of the PDT drug by intersystem crossing from the excited singlet state generated by light absorption.
- In the Type I process, the excited triplet state of the PDT drug generates highly reactive radicals, peroxides, and superoxides by photochemistry, which then destroy the cancer cells by oxidation.
- In the Type II process, the PDT drug in its excited triplet state interacts with an oxygen molecule in its ground triplet state to produce a highly reactive excited singlet form of oxygen, which is a powerful oxidant that destroys the cancer cell. The Type II process is believed to be the major pathway for PDT.
- Treatment of certain types of cancers using PDT is already in clinical practice.
- Most of the PDT drugs are porphyrin derivatives. Photofrin®, a complex mixture of various porphyrin derivatives and containing dimeric and oligomeric fractions, is FDA-approved and being used for treatment of a variety of malignant tumors.
- Other PDT drugs being investigated are phthalocyanines, naphthocyanines, chlorins, and tetraphyrins that absorb at longer wavelengths (in the red), providing a better penetration in tissues to allow for treatment of deeper tumors. This is an area of intense research activity.

- Multibranched dendritic photosensitizers provide the opportunity to utilize different modes of actions and different wavelength of activation by simultaneously incorporating multiple sets of photosensitizers.
- Besides cancer treatment, PDT also is useful for the treatment of a number of diseases such as cardiovascular disease, psoriasis, rheumatoid arthritis, and age-related macular degeneration.
- The three principal mechanisms proposed for the destruction of cells and tissues by photodynemic therapy are (i) cell damage by targeting of a specific organelle by a particular photosensitizer, (ii) vascular damage induced by PDT action, and (iii) PDT-induced immunological response.
- Even though PDT does not require a coherent light source, a CW laser source provides a convenient source of light with concentrated energy at the wavelength of absorption of the PDT drug. Also, a laser source can readily be coupled with a wide variety of light delivery systems and endoscopic devices.
- Two-photon photodynamic therapy is a new area where the light activation of a PDT drug is achieved by two-photon absorption of near-IR photons using a short pulse laser source. This approach shows the promise of treating deeper tumors using greater tissue penetration by near IR light.
- Some areas of intense current research and future directions are (i) improving the understanding of molecular and cellular mechanisms of PDT and (ii) developing new photosensitizers, activatable by linear (one-photon) absorption in the near IR and those with the ability to be efficiently excited by two-photon absorption.
- Some other areas of future direction are (i) development of carriers conjugated to PDT drug for enhanced transport and efficient targeting of specific sites (or organelles) and (ii) development of *in vivo* techniques for real-time monitoring of PDT action.

REFERENCES

Battah, S. H., Chee, C.-E., Nakanishi, H., Gerscher, S., MacRobert, A. J., and Edwards, C., Synthesis and Biological Studies of 5-Aminolevulinic Acid-Containing Dendrimers for Photodynamic Therapy, *Bioconjugate Chem.* **12**, 980–988 (2001).

Bhawalkar, J. D., Kumar, N. D., Zhao, C.-F., and Prasad, P. N., Two-Photon Photodynamic Therapy, *J. Clin. Laser Med. Surg.* **15**, 201–204 (1997).

Bonnett, R., White, R. D., Winfield, V. J., and Berenbaum, M. C., Hydroporphyrins of the *meso*-tetra(hydroxyphenyl)porphyrin Series as Tumor Photosensitizers, *Biochem. J.* **261**, 277–280 (1989).

Colussi, V. C., Feyes, D. K., Mulivhill, J. W. et al., Phthalocyanine 4 (Pc4) Photodynamic Therapy of Human OVCAR-3 Tumor Xenografts, *Photochem. Photobiol.* **69**, 236–241 (1999).

CHAPTER 13

Tissue Engineering with Light

Lasers have emerged as powerful tools for tissue engineering. Tissue engineering with light utilizes various types of light–tissue interactions discussed in Chapter 6. Consequently, some readers may find it helpful to revisit Chapter 6. Chapter 13 also has sufficient medical focus to be useful to medical practitioners as well.

This chapter covers three main types of laser-based tissue engineering: (i) tissue contouring and restructuring, (ii) tissue welding, and (iii) tissue regeneration. Two specific examples of tissue contouring and restructuring covered in this chapter are used in dermatology and ophthalmology. Dermatological applications discussed here are (i) the treatment of vascular malformations, such as port-wine stains, (ii) the removal of pigment lesions and tattoos, (iii) skin resurfacing (wrinkle removal), and (iv) hair removal. Appropriate lasers used for these applications are presented.

The ophthalmic applications covered are (i) repair of blockage, leaky blood vessels, or tears in the retina using photocoagulation, (ii) refractory surgery to reshape the cornea for vision correction using the procedures of photorefractive keratectomy (PRK), laser *in situ* keratomileusis (LASIK), and laser thermal keratoplasty (LTK), and (iii) photodisruptive cutting during posterior capsulotomy in post-cataract surgery. These procedures are defined, and there is a discussion of their respective underlying principles of laser–tissue interactions. Lasers commonly used for these procedures also are described.

The section on laser welding of tissues discusses how lasers are used to join or bond tissues. Also described are the three types of welding: (i) direct welding, (ii) laser soldering, and (iii) dye-enhanced laser soldering.

Laser tissue regeneration is a relatively new area; recent work suggests that laser treatment can effect tissue regeneration to repair tissue damage in an injury. Some results from studies in this area conducted at our Institute are presented.

A major impetus to the area of laser-based tissue engineering has been provided by developments in laser technology. Wide availability of ultra-short pulsed lasers (e.g., Ti:sapphire lasers discussed in Chapter 5) from a number

Introduction to Biophotonics, by Paras N. Prasad.
ISBN: 0-471-28770-9

of commercial sources has opened up new opportunity for more precise laser surgery with very little collateral damage. Hence, an emerging field is "femtolaser surgery," which employs femtosecond pulses to cut or ablate tissues.

This chapter concludes with a brief discussion of future directions. This section provides examples of the author's views on multidisciplinary opportunities that exist for future research and development in the area of tissue engineering with light.

The following references are suggested for further reading on the topics covered in this chapter:

- Puliafito, C. A., ed., *Laser Surgery and Medicine: Principles and Practice*, Wiley-Liss, New York, 1996.
- Alster, T. S., *Manual of Cutaneous Laser Technique*, Lippincott-Raven, Philadelphia, 1997.
- Goldman, M. P., and Fitzpatrick, R. D., *Cutaneous Laser Surgery*, Mosby, St. Louis, 1994.
- Reiss, S. M., Laser Tissue Welding: The Leap from the Lab to the Clinical Setting, *Biophotonics International*, **March**, 36–41 (2001).
- Talmor, M., et al., Laser–Tissue Welding, *Archives of Facial Plastic Surgery* **3**, 207–213 (2001).

13.1 TISSUE ENGINEERING AND LIGHT ACTIVATION

Tissue engineering is a field of bioengineering that recently has seen an immense amount of growth. It covers a broad spectrum including biocompatible artificial implants, tissue regeneration, tissue welding and soldering, and tissue restructuring and contouring. It is a multidisciplinary field that has resulted in the development of materials by chemists and material scientists, fabrication of engineering tools by engineers, determination of biocompatibility and reduced risk of dysfunction by biomedical research, and skills of implementation by surgeons. A vast number of approaches and procedures are being applied to tissue engineering.

The objective of this chapter, however, is significantly focused. It deals only with tissue engineering that utilizes light, which is generally produced by a laser. Lasers have emerged as promising tools for tissue engineering. The principles that drive these applications utilize various types of laser–tissue interactions discussed in Chapter 6 on photobiology. The scope of applications of lasers for tissue engineering is outlined in Table 13.1.

Lasers also are commonly used in general and other surgeries. Although these applications also can fall under the broad definition of tissue restructuring and tissue engineering, they will not be covered here. A good general reference covering many aspects of tissue engineering using lasers may be found in the book *Laser Surgery and Medicine: Principles and Practice*, edited

TABLE 13.1. Lasers Applied for Various Types of Tissue Engineering

Laser Based Tissue Engineering		
Tissue contouring and restructuring: Use of lasers to ablate, shape or change pigmentation of a tissue	Tissue welding: Laser induced welding and soldering to fuse tissues, repair a tear, or inhibit vascular growth	Tissue generation: Laser activation or incision to stimulate new tissue generation

by Puliafito (1996). The two main areas of laser activated tissue contouring and restructuring briefly discussed here deal with (i) dermatological applications in plastic and cosmetic surgeries and (ii) ophthalmic applications. These applications in current practice and represent a rapidly growing market (Alora and Anderson, 2000). They are covered in Section 13.2. The development of new, compact and cost-effective solid-state lasers, advancements in new protocols, and pre- and post-treatment regimens will lead to further demand of these laser-based plastic, cosmetic, and ophthalmic applications by both physicians and patients.

Another active area falling within the general scope of tissue restructuring is laser angioplasty (a cardiac procedure that dilates and unblocks atherosclerotic plaque from the walls of arterial vessels and often involves the placement of a mesh stent to prevent the vessels from closing again) (Deckelbaum, 1996). Fiber optics can be utilized to transmit laser radiation anywhere in the cardiovascular system accessible by an optical fiber. The laser is then used to vaporize obstructing atherosclerotic plaque (the thickening of arterial vessels with cholesterol buildup). Another approach is laser balloon angioplasty. With laser angioplasty, the laser beam heats the vessel wall during balloon angioplasty to improve the vessel remodeling induced by balloon dilation. Laser angioplasty may be particularly useful for treating chronic coronary artery occlusions and diffuse atheroscleric disease. The lasers used for this are a pulsed xenon chloride eximer laser operating in the UV at 308 nm or a pulsed holmium laser emitting in the infrared at 2.0–2.1 μm.

Some other applications of laser ablations include:

- *Otolaryngology*: A CO_2 laser is often used to create intense localized heating of the target tissue to vaporize both extra- and intracellular water, producing coagulative necrosis and soft tissue retraction or fusion.
- *Dentistry*: Lasers have been used for ablation of both soft and hard tissues. Soft tissue procedures have focused on incising and excising materials from the mucosa and gingiva in the oral cavity using a variety of lasers such as CO_2, Nd:Yag, Ho:Yag, and argon lasers. Er lasers with a wavelength in the 2.79- to 2.94-μm range have been used for cutting

dental tissues (drilling and preparation of cavities) as well as for removing dental materials.

Laser tissue welding is a developing biotechnology that looks promising for applications in practically all surgeries (Bass and Treat, 1996). Laser tissue welding utilizes the energy from the laser beam to join or bond tissues. The absorbed laser energy can produce alterations in the molecular structure of the tissues to induce bonding between neighboring tissue structures. Since the laser tissue-welding process is a noncontact and nonmechanical method, it is ideally suited for cases where suturing and stapling is difficult. The surgical requirements for tissue welding are to produce stronger welding strength while minimizing tissue thermal injury. To achieve these goals, current efforts are focused on developing new techniques using low laser energy and reduced energy absorption to produce localized thermal transmissions. The following approaches are being used (Xie et al., 2001):

- Use of a short pulse laser and thermal feedback to limit energy output
- Selection of laser wavelength to limit absorption in the tissue
- Application of solders and chromophores activated by lasers to increase bonding strength

However, clinical acceptability of laser tissue welding is limited by concerns about the stability of the weld strength (tensile strength, burst strength) and the difficulties in controlling the process. Laser tissue welding is covered in Section 13.3.

Recent studies at our Institute also show some promise in using lasers to promote the generation of new tissues in incisions. This topic is covered in Section 13.4.

Ultra-short pulse lasers promote nonthermal laser tissue interactions, primarily by the mechanism of photodisruption (discussed in Chapter 6), thus reducing the undesirable effect of collateral damage by a thermal mechanism. Interest in the use of these lasers has grown rapidly with the availability of femtosecond pulsed lasers, giving rise to a new field of femtolaser surgery. This topic is covered in Section 13.5.

13.2 LASER TISSUE CONTOURING AND RESTRUCTURING

The two specific applications discussed here are for the use of lasers in dermatologic and ophthalmologic procedures. The theory of selective photothermolysis, introduced by Anderson and Parrish in 1981, is the basis for much advancement in dermatological lasers (Anderson and Parrish, 1983). It allows for highly localized destruction of light absorbing "targets" in skin, with minimal damage to the surrounding tissue. To achieve selective photother-

molysis, an appropriate wavelength, exposure duration, and sufficient fluence are necessary. Various targets absorb at different wavelengths, and the wavelength of the laser should be absorbed more by the target structure than by the surrounding structures. Light absorbed in the target structure is converted to heat, which begins to diffuse away immediately. In general, the exposure duration should be shorter than or about equal to the thermal relaxation time of the target. Clinically, selective photothermolysis involves ensuring that a maximum tissue-damaging temperature occurs only in the desired tissue targets. When treating dermal targets (blood vessels, tattoos, hair, etc.), light must pass through the epidermis. Epidermal injury is the most frequent side effect in these settings.

Some of the dermatological applications include:

1. *The Treatment of Vascular Malformations (e.g., Cutaneous Port-Wine Stains of Sturge–Weber Syndrome).* Here, the target chromophore is oxyhemoglobin. Laser light is absorbed by hemoglobin and is converted into heat, which damages the endothelium and the surrounding vessel wall. This is followed by thrombosis (a blockage of a blood vessel) and vasculitis (an inflammatory disease of the vessels). As the removal of the abnormal venules (or small veins that serve as collecting channels for adjacent capillaries) occurs, the lesion regresses into a more normally colored skin area.
2. *Removal of Pigmented Lesions and Tattoos.* In this case the target chromophore is melanin or tattoo pigment. Laser light causes extremely rapid heating of melanin or tattoo pigment granules. This fractures these submicrometer particles and kills the cells that contain them. Figure 13.1 illustrates the clinical results of tattoo removal using a laser beam.
3. *Resurfacing.* The target chromophore here is water. A superficial layer of skin is ablated in wrinkle removal. The laser deposits energy in the

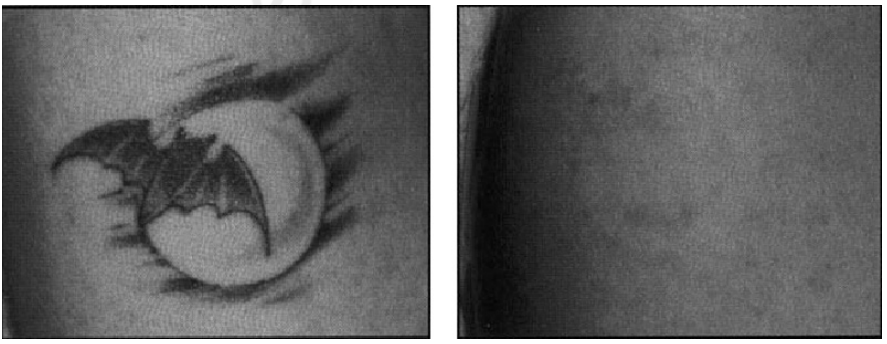

Figure 13.1. Tattoo removal using laser technology. Four treatments with Q-switched frequency doubled Nd:YAG laser (532-nm green) removed the tattoo. (Reproduced with permission from Hogan, 2000.)

upper 1 μm (Er:YAG laser) or 20 μm (CO_2 laser) skin because of the strong absorption of energy by water. This typically leaves 0.05–1 mm of residual thermal damage, which also achieves hemostasis. Lasers have also been used effectively for ablation of warts, actinic cheilitis, and other benign epidermal lesions.

4. *Hair Removal.* The target chromophore is follicular melanin. Selective photothermolysis of the hair follicles is achieved without damaging the skin. It is unknown at present whether the bulge, dermal papilla (nonvascular core elevations of tissues associated with irritation or immunological challenge), or both have to be destroyed to achieve permanent hair removal. Also, it is currently debatable if the hair removal achieved is permanent.

Table 13.2 lists the dermatological applications of skin resurfacing (a more popular form being wrinkle removal), hair removal, and tattoo removal. The lasers and their parameters used for these procedures are also listed.

Ophthalmic applications of lasers are some of the oldest medical applications going back more than three decades. New laser applications and techniques are being implemented in an exciting fashion and cover a broad range of ophthalmic problems. Ophthalmic applications utilize a number of laser–tissue interaction mechanisms discussed in Chapter 6, where the structure and function of the human eye is also discussed. The ophthalmic applications that correct medical conditions fall into two categories:

1. *Use of Visible or Near-Visible Infrared Laser Wavelengths to Treat Retinal Disease or Glaucoma.* Examples are: (i) diabetic retinopathy associated with capillary nonperfusion or swelling caused by leaking microaneurysms, (ii) retinal vein occlusions that block ocular blood drainage causing retinal hemorrhage, ischemia, and swelling, (iii) age-related macular degeneration (discussed in Chapter 12, which discusses photodynamic therapy), which, in the wet-type neovascular tissue, invades normal retina, producing macular edema and hemorrhage, (iv) retinal tears, which can occur as a part of aging, as a complication following cataract surgery or from an eye injury (tears allow vitreous liquids to leak beneath the retina, lifting the retinal photoreceptors away from their vascular blood supply and supporting eye structures), and (v) glaucoma, which may be treated by producing a channel in iris structures or shrinkage of drainage tissues in order to facilitate lowering of eye pressure.
2. *Use of Nonvisible Wavelengths for Refractive Surgery to Reshape the Cornea for Vision Correction.* Lasers are now routinely used to correct for myopia (near-sightedness) with two techniques: photorefractive keratectomy (PRK) and laser *in situ* keratomileusis (LASIK). In these procedures, a pulsed laser beam flattens the cornea by removing more tissue from the center of the cornea than from its midzone. The result of

TABLE 13.2. Dermatological Applications of Lasers

Procedure	Skin Resurfacing		Hair removal				Tattoo Removal	
Commonly used lasers	CO_2 laser	Er:YAG laser	Alexandrite laser	Diode laser	Nd:YAG laser	Ruby laser	Q-switched frequency-doubled Nd:YAG laser	Q-switched alexandrite laser
Wavelength	10.6 µm	2.94 µm	0.755 µm	0.81 µm	1.064 µm	0.694 µm	0.532 µm	0.752 µm
Pulse duration	800 µsec	0.3–10 msec	2–20 msec	0.2–1 sec	10–50 msec	3 msec	10–80 nsec	50 nsec
Fluence (energy)	3.5–6.5 J/cm^2 (0.250–0.4 J)	5–8 J/cm^2 (1–1.5 J)	25–40 J/cm^2	23–115 J/cm^2	90–187 J/cm^2	10–60 J/cm^2	6–10 J/cm^2	2.5–6 J/cm^2
General references and websites	1, 4		2–4				4–6	

1. http://www.lasersurgery.com/laser_resurfacing_aging_and_scars.html.
2. Goldberg, D. J., Unwanted Hair: Evaluation and Treatment with Lasers and Light Source Technology, *Adv. Dermatol.* **14**, 223–248 (1999).
3. Goldberg, D. J., ed., *Laser Hair Removal*, Dunitz, London, 2000.
4. Alora, M. B. T., and Anderson, R. R., Recent Developments in Cutaneous Lasers, *Lasers Surg. Med.* **26**, 108–118 (2000).
5. http://www.bli.uci.edu/medical/laserskinsurfacing.html.
6. http://www.bmezine.com/tattoo/tr/iqp1.html.

flattening of the cornea is that the focus of the eye moves farther back toward its desired spot on the retina and corrects the vision for distance. As discussed below, PRK and LASIK use the same laser system and the same interaction mechanism to achieve the same goal. However, there is a major difference. In PRK, the epithelial (outer) layer of the cornea first is removed by a mechanical (soft brush) or chemical (alcohol) means or even by using a laser beam (transepithelial ablation). The laser beam then is used to ablate and reshape the cornea. A soft contact lens is used as a bandage and is placed over the eye to help the epithelial layer grow back. This generally takes 3–5 days. In LASIK, the ophthalmologist creates a hinged flap of the cornea approximately 125 μm in thickness using a specialized cutting blade mounted on a vacuum device. The cutting tool, known as a microkeratome, is then removed, thereby exposing the underlying corneal tissue to ultraviolet ablation of the desired degree. Finally, the corneal flap is returned to its original position. PRK and LASIK have also been used to a much lesser extent for hyperopia (far-sightedness). A new method, also now approved by the Food and Drug Administration in the United States, for the treatment of hyperopia and presbyopia (loss of near-focusing ability due to aging), which affect many people over 40 years of age, is laser thermal keratoplasty (LTK). With LTK, the laser is utilized to shrink the cornea, causing its central part to become steeper. Unlike PRK and LASIK, LTK does not involve ablation of any corneal tissue. It utilizes the application of concentric rings of laser energy to gently heat the cornea and steepen its curvature.

Other ophthalmic applications of the laser are for posterior capsulotomy in post-cataract surgery or cutting strands of vitreous in the posterior segment of the eye. In capsulotomy, a laser beam is used to open a hole in the membrane to correct for the opacity of the membrane, which may occur after cataract surgery. As stated above, a number of laser–tissue interaction mechanisms play a role in these treatments. Table 13.3 lists these mechanisms.

TABLE 13.3. Various Laser-Tissue Interaction Mechanisms for Ophthalmic Applications

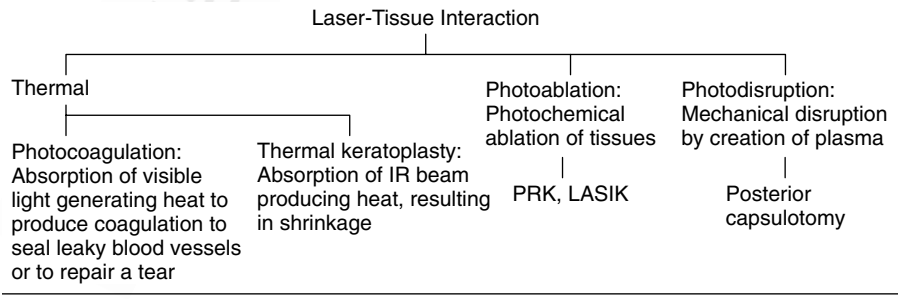

Table 13.4 provides the information on the types of lasers and their characteristics for some of these treatments.

13.3 LASER TISSUE WELDING

Laser tissue welding employs the process of using laser energy to join or bond tissues. Currently, the tissues welded by this technique are soft tissues. The approaches to join or bond tissues are listed in Table 13.5.

Laser tissue welding was first demonstrated by Jain and Gorisch (1979), who used Nd:YAG laser light to seal rat arteries. Subsequent studies suggested that laser interaction could be used to heat a tissue sufficiently to denature proteins (collagens) in the tissue surfaces to form new connecting structures (Jain, 1984; Schober et al., 1986). Most early studies of laser tissue welding employed CO_2 lasers. The use of the CO_2 laser relied on water, the largest constituent of most tissues, absorbing strongly at its wavelength (10.6 μm). This strong absorption leads to a shorter optical penetration depth (~13 μm), limiting its use to extremely thin tissues. Also, under a CW laser exposure, lateral spread of heating produces a large zone of injury.

Other lasers employed for laser tissue welding are argon-ion and Nd:YAG, which produce deeper and more uniform tissue heating than that achieved by using a CO_2 laser. In the case of the Nd:YAG laser, the 1.320-μm laser output has been used, because at this wavelength both water and hemoglobin absorb. Pulsed lasers have the appeal that they can minimize collateral thermal damage. However, the choice of laser wavelength and exposure parameters (energy, pulse duration, etc.) is clearly dependent on the tissue absorption, optical penetration depth, and the thermal relaxation time in the tissues to be welded. The optical penetration depth clearly has to be matched with the extent of the thickness to be welded to provide uniform heating.

The laser soldering technique utilizes laser light to fuse a proteineous solder to the tissue surface, thereby providing greater bond strength with less collateral damage compared to direct welding. Blood was the first material used as a solder. Subsequently, egg-white albumin followed by other proteins such as those derived from blood fibrinogen and other albumins were used a solder substitutes.

Dye-enhanced soldering was introduced to take advantage of the strong absorption of light by the selected dye and the efficient conversion of light into heat by the dye dispersed in the solder. This method also provided the benefit that an appropriate dye can be selected to match its absorption peak with the particular laser wavelength utilized. This method has allowed the ability to use the more common and relatively inexpensive 808-nm diode laser with the help of a biocompatible dye, indocyanine green (ICG) (Oz et al., 1990; Chivers, 2000). In yet another approach, a polymer scaffold doped with serum albumin and ICG was used (McNally et al., 2000). They found that the

TABLE 13.4. Ophthalmic Laser Procedures and Lasers Used with the Appropriate Specifications

Procedure	Laser Photocoagulation			Laser Thermal Keratoplasty (LTK)	Laser-Assisted *In Situ* Keratomileusis (LASIK)
Commonly used lasers	Argon ion laser	Krypton ion laser	Laser diode	Ho:YAG laser	ArF excimer laser
Wavelength	514.5 nm	647 nm	810 nm	2.1 μm	193 nm
Operation regime (pulse duration)	CW (0.1–1.0 sec)	CW (up to 10 sec)	CW (up to 2 sec)	Pulse (0.25–1 sec)	Pulse (15–25 nsec)
Power (energy)	0.05–0.2 W	0.3–0.5 W	2 W	20 mJ	50–250 mJ
General references and websites	1, 2			3–5	6–8

1. http://www.eyecenters.com/brochures/frames/laserfr.htm.
2. De Roo-Merritt, L., Lasers in Medicine: Treatment of Retinopathy of Prematurity, *Neonatal Netw.* **19**(1):21–26 (2000).
3. http://www.emedicine.com/oph/topic660.htm.
4. http://www.eyemdlink.com/EyeProcedure.asp?EyeProcedureID = 76.
5. Bower, K. S., Weichel, E. D., and Kim, T. J., Overview of Refractive Surgery, *Am. Fam. Physician* **64**:1183–90 (2001).
6. http://www.fda.gov/cdrh/LASIK/what.htm.
7. Roger, F. S., and Shamik, B., II., PRK and LASIK Are the Treatments of Choice, *Surv. Ophthalmol.* **43**(2):157–159 (1998).
8. http://www.lasik1.com.

TABLE 13.5. The Approaches for Tissue Bonding

Tissue Bonding		
Direct Welding of Tissues:	Laser Soldering:	Dye-enhanced Laser Soldering:
Local heating to ~60ºC–80ºC By laser energy absorption (photothermolysis) to denature collagen, uncoiling their native triple helical structure and producing collagen bonding	Use of proteineous Solder at the surfaces to be joined followed by application of laser light to selectively heat the solder and seal it to the surrounding tissue	A dye absorbing at the laser wavelength of soldering added to the solder to enhance selective absorption and subsequent heating of the solder and not of the nontarget tissue

addition of the polymer membrane improved the weld strength and provided better flexibility compared to the use of albumin protein solder alone. The polymer scaffold makes the solder sufficiently flexible, allowing it to wrap around the tissue. Solders can be used for applications other than tissue bonding. Laser-assisted tissue sealing (LATS) can be used to seal bleeding surfaces for hemostasis (blood clotting). Anastomoses (sites where blood vessels have been rejoined surgically) that leak can be sealed and made impermeable.

Laser welding or soldering can be used endoscopically and laparoscopically to extend the range of its applications to cases where sutures or staples cannot be used. Other advantages are:

- Microsurgery
- Reduced inflammation
- Faster healing
- Watertight seal
- Ease and speed of application

Applications of laser welding and soldering have been diverse (Bass and Treat, 1996):

- *Cardiovascular Surgery*: Primary vascular anastomosis; sealing to reduce blood loss in vascular surgery
- *Thoracic Surgery*: Sealing of air leaks after lung biopsy or wedge resection; sealing of the bronchial stump
- *Dermatology*: Skin closure with improved cosmesis and faster healing
- *Gynecology*: Repair of fallopian tubes
- *Neurosurgery*: Welding and repair of peripheral nerves
- *Ophthalmology*: Laser solder closure of incisions in the sclera and cornea
- *Urology*: Closure of ureter, ureteroneocystostomy, urethra, and bladder. [Most urinary tract closures must be watertight to prevent leakage of

urine, reducing the subsequent development of infection or fistula (i.e., blind sac) formation.]

13.4 LASER TISSUE REGENERATION

Laser-induced tissue regeneration is an exciting prospect to repair tissue damage after an injury. Since the early report of low-level light therapy for wound healing (Mester et al., 1971), there have been numerous reports of effects of light on wound healing and tissue regeneration (Basford, 1996). Many investigators report visible and IR radiation at relatively low fluences (irradiation densities) of 1–4 J/cm^2 stimulates capillary growth and granulation of tissue formation (Basford, 1986). However, these reports have not gone uncontested. Variability of experimental models, fluences, wavelengths, and other parameters have compounded the problem and lead to seemingly contradictory results.

At our own Institute, studies have focused on the prospect of laser-induced tissue regeneration. The following hypotheses were used to explore the prospect of laser-induced tissue regeneration:

- Postoperative wound healing begins with blood clot formation.
- Blood clot directs scar tissue formation.
- There is an absence of blood clot formation after laser ablation.
- Absence of clot may allow for regeneration of native tissue.

The following method was used to study any tissue regeneration:

- Bilateral surgical defects (3 mm × 3 mm × 3 mm) were created in the gluteal muscles of hamsters (*Mesocricetus auratus*).
- Each subject received one laser wound and a contralateral scalpel wound.
- Subjects were injected with BrDU (800 mg/kg) throughout the postoperative phase.
- Subjects were sacrificed and the wounds harvested for both histological and immunohistochemical analysis.

The results obtained yielded the following observations:

17 DAYS AFTER SURGERY

Laser	Scalpel
Disorganized myotubules	Fibrous (scar) tissue
BrDU incorporated into myoblasts	No BrDU incorporation

The incorporation of BrDU clearly suggests the growth of fresh tissue, thus providing the exciting prospect of laser-induced tissue regeneration. Further

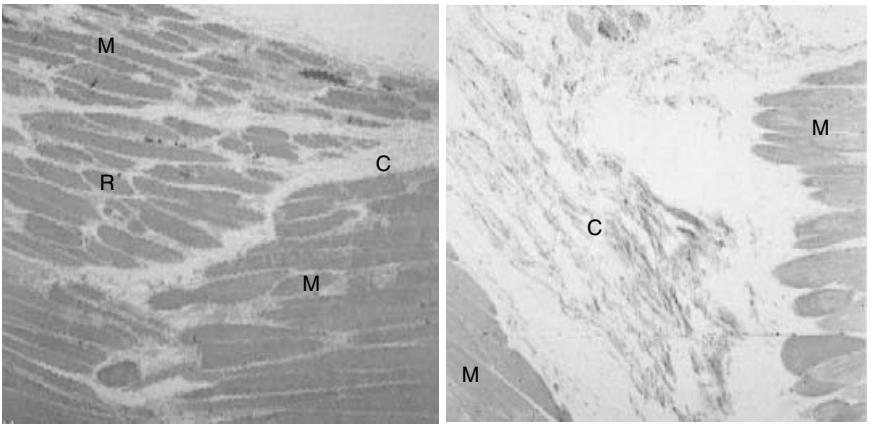

Figure 13.2. Muscle regeneration following laser excision of a $3 \times 3 \times 3$-mm section of tissue; C, connective (scar) tissue; R, regenerated muscle tissue; and M, muscle tissue. (a) Regeneration of muscle tissue after laser excision; (b) scar formation after scalpel excision (Kingsbury, Liebow, Bergey, and Prasad, unpublished results).

studies are warranted to firmly establish tissue regeneration using this procedure. This conclusion was confirmed histologically, as is shown in Figure 13.2. After H&E (hematoxylin & eosin) staining, regenerated muscle cells are clearly evident in the laser excised region. The contralateral component of muscle, excised with a scalpel, shows only connective or scar tissue in the excised region.

13.5 FEMTOLASER SURGERY

An area of growing interest is the use of ultra-short pulsed (femtoseconds) lasers for surgery and tissue ablation (Juhasz et al., 2002). The advantages offered by these ultra-short pulses are that cuts or ablations can be made more precisely, with very little collateral damage. The mechanism of laser–tissue interactions that occur using ultra-short laser pulses is also different from the photothermal and photoablation mechanisms discussed above because they pertain to tissue contouring and welding. The high peak power of the ultra-short pulses lead to photodisruption, discussed in Chapter 6. The mechanism of photodisruption involves laser-induced optical breakdown (LIOB), in which a strongly focused short-duration pulse generates a high-intensity electric field and leads to efficient multiphoton ionization and subsequent avalanche ionization to produce a hot microplasma. This hot microplasma expands with supersonic velocity, displacing (ablating or cutting) the surrounding tissue. Since the displacement is adiabatic (i.e., it occurs on a time scale short compared to the local thermal diffusion time), the effect of abla-

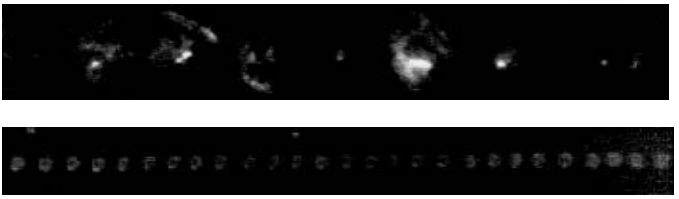

Figure 13.3. Laser tissue ablation using lasers of two different pulse widths. Top: pulse width of 200 ps; bottom: pulse width of 80 fs. (Reproduced with permission from http://www.eecs.umich.edu/CUOS/Medical/Photodisruption.html.)

tion or cutting is spatially confined and any spread due to thermal damage is also confined. The wide availability of mode-locked Ti:sapphire lasers producing ~100-fesec pulses at ~800 nm has provided much of the impetus for using them for femtolaser surgery or tissue ablation. Figure 13.3 shows the results of tissue ablation produced by two different sources: (a) a laser with 200-psec pulse width and (b) a laser with 80-fsec pulse width. These results are from the Center of Ultrafast Optical Science at the University of Michigan.

For these studies, the beams were focused to a circular spot and scanned across the sample. The spot separation is the same in both cases, but the ablation process takes place in an uncontrolled way in the case of the picosecond pulses, and the ablated domains are large. The femtosecond laser pulses, on the other hand, produce reproducible cuts that are spatially confined.

An advantage of using the photodisruption mechanism resulting from femtosecond pulses is that no specific absorbing target such as a pigment or a dye is required. Thus, a tissue that is totally transparent at the wavelength of the laser can be cut or ablated at any specific location in 3-D space. For this reason, a major application has been for refractive surgery involving the cornea. Four surgical procedures using laser surgery techniques approved by the Food and Drug Administration in the United States include (Juhasz et al., 2002):

- Corneal flap creation for LASIK
- Anterior lamellar corneal transplantation
- Keratomileusis
- Channel creation for corneal implants

A microkeratome has traditionally been used in LASIK for cutting a corneal flap to expose the internal corneal layers (stroma) for subsequent excimer laser ablation, as discussed in Section 13.2. However, flap creation with microkeratomes also produces a majority of the intraoperative and postoperative LASIK complications. Using femtosecond laser pulses, a flap is created by scanning a spiral pattern of laser pulses at the appropriate depth. This provides a greater control of precision and reliability as well as improved safety

and performance. The process also provides a highly precise control of flap parameters such as flap thickness, diameter, hinge position and angle, and entry cut angle.

Anterior lamellar corneal transplantation involves the replacement of diseased or damaged superficial corneal tissue using tissue obtained from a cadaver donor eye. The femtolaser surgery allows the recipient and donor corneas to be cut with a high degree of accuracy, ensuring a proper fit of the donor corneal graft in the recipient bed. In addition, femtolasers provide local tissue sealing to improve stability and healing at the donor and recipient tissue interfaces.

Other ophthalmic applications of femtolaser surgery currently being investigated include treatment of glaucoma; preparation of corneal tissue for LASIK surgery precuts for the placement of implants for presbyopia; and photodisrutpion of the lens for cataract surgery. Nonophthalmic applications include dermatological and neurosurgical procedures.

13.6 FUTURE DIRECTIONS

Some examples of future directions of tissue engineering with light include:

Computer-Aided Tissue Engineering. Development of appropriate hardware and software to control the precision of tissue ablation or welding and surgery will build the confidence of both the doctor and the patient. The computer-aided systems will also provide a monitoring and feedback mechanism to achieve the desired result with minimal collateral damage. Introduction of robotics is a promising opportunity in this area. Laser safety issues may also be addressed using computer-aided systems and robotics, making these systems more user-friendly. Therefore, this area is definitely projected for a future growth opportunity (Sun and Lal, 2002).

New Laser Solders and Dyes to Assist Soldering. New biocompatible materials for tissue bonding will broaden the scope and applicability of tissue bonding. A major emphasis is to use light activation at the wavelengths and outputs provided by inexpensive diode lasers. For example, McNally et al. (1999) have reported the use of solid protein solder strips containing indocyanine green dye that strongly absorbs at the commonly available GaAlAs diode laser wavelength of ~800 nm for peripheral nerve repair.

Mechanism of Tissue Ablation and Welding. Even though there is a general consensus on the primary mechanisms of the procedures presented above, there appears to be suggestions that other molecular processes are occurring during laser–tissue interactions. Improved techniques to monitor molecular changes in real time will be of significant value and thus enhance the efficacy of a given treatment.

Femtolaser Technology. As is discussed in Section 13.5, femtolasers will emerge as a powerful surgical and tissue engineering tool. Femtolasers are still at a level of technology and require great care and maintenance from a highly skilled technician. Furthermore, they are expensive. The technology is, however, rapidly developing with a major motivation derived from the potential applications of a femtosecond fiber laser to telecommunications. These 1.55-μm femtosecond fiber lasers, when frequency doubled to produce ~777.5-nm output, will be suitable for the frequency range provided by the current mode-locked Ti:sapphire lasers. The development of applications in telecommunication may also bring down the price of a fiber-based femtolaser, while providing a convenient and flexible laser source for integration with other medical instruments at the same time.

HIGHLIGHTS OF THE CHAPTER

- Laser light provides a new dimension for tissue engineering, covering a broad spectrum of usage, such as (i) tissue contouring and restructuring, (ii) tissue welding and soldering, and (iii) tissue regeneration.
- Tissue contouring and restructuring utilize lasers to ablate or shape a tissue or change the pigmentation of tissue.
- One major application of tissue contouring and restructuring is in dermatology. Here, lasers are now routinely used for (i) treatment of vascular malformation, such as port-wine stain, (ii) removal of pigmented lesions and tattoos, (iii) skin resurfacing (wrinkle removal), and (iv) hair removal.
- Dermatological applications use the process of selective photothermolysis, which utilizes highly localized distribution of light absorbing "targets" in the skin, with minimal damage to the surrounding tissue.
- The second major application of tissue contouring and restructuring is in ophthalmology. Some principal examples are (i) repair of blockage, leaky blood vessels, or tears in the retina, (ii) refractive surgery to reshape the cornea for vision correction, and (iii) posterior capsulotomy in post-cataract surgery.
- Photocoagulation is used to repair blockage of leaky blood vessels or tears in the retina. This is accomplished by using the heat generated by light absorption to produce coagulation.
- Photorefractive keratectomy (PRK) used to correct near-sightedness involves (i) removing the outer layer of the cornea and (ii) ablating the cornea with a laser beam to appropriately reshape it. The process of photochemical ablation with ultra-short laser pulses in the UV is utilized.
- Laser *in situ* keratomileusis (LASIK) involves the opening of a flap of the top layer of the cornea, laser ablating the underlying tissue to reshape

the cornea, and returning the corneal flap to its original position. Again, the process of photochemical ablation with a UV laser is utilized.

- Laser thermal keratoplasty (LTK) is a new procedure that utilizes heat produced by the absorption of an IR laser beam to shrink the cornea in such a way as to cause steepening of the central part of the cornea. This type of restructuring corrects for the loss of near focusing due to aging.
- Another ophthalmic application is posterior capsulotomy in post-cataract surgery, where to correct opacity that may occur after cataract surgery a photodisruption mechanism is used to open a hole in the membrane that has formed on the implanted lens.
- The three approaches used for tissue welding are (i) direct welding of tissues, (ii) laser soldering, and (iii) dye-enhanced soldering.
- Direct welding of tissues uses lasers to locally heat tissue to a temperature that denatures collagen and forms a collagen bond.
- Laser soldering utilizes a proteineous solder at the surfaces to be joined. Laser light selectively heats the solder, sealing it to the surrounding tissue.
- The dye-enhanced soldering procedure adds a dye, with enhanced absorption at the laser wavelength used for soldering, to the solder to enhance selective heating at the soldering point.
- Laser tissue regeneration, an area in an early stage of development, deals with the prospect of using lasers to effect tissue regeneration for repairing tissue damage from an injury.
- Preliminary studies conducted at our Institute provide indications of tissue regeneration in a tissue operated on (cut) with laser surgery.
- Femtolaser surgery is a new field that utilizes femtosecond laser pulses to cut or ablate a tissue segment with great precision and with very little collateral damage.
- The field of tissue engineering with light offers potential for further research and development through the continued exploration of the underlying mechanisms of laser engineering, computer-aided tissue engineering and the search for new types of laser soldering materials.

REFERENCES

Alora, M. B. T., and Anderson, R. R., Recent Developments in Cutaneous Lasers, *Lasers Surg. Med.* **26**, 108–118 (2000).

Alster, T. S., *Manual of Cutaneous Laser Technique*, Lippincott-Raven, Philadelphia, 1997.

Anderson, R. R., and Parrish, J. A., Selective Photothermolysis: Precise Microsurgery by Selective Absorption of Pulsed Radiation, *Science* **220**, 524–527 (1983).

Basford, J. R., Low-Energy Laser Treatment of Pain and Wounds: Hype, Hope, or Hokum?, *Mayo Clinic. Proc.* **61**, 671–675 (1986).

CHAPTER 14

Laser Tweezers and Laser Scissors

Lasers are useful tools for micromanipulation of biological specimens. This chapter covers two types of laser micromanipulations: laser tweezers for optical trapping and laser scissors for microdissection.

The principle of laser optical trapping using a laser beam has been explained using minimal amounts of theoretical discussion. Readers finding the concept still difficult to grasp may simply assume that submicron to micron size objects can be trapped in a focused laser beam spot, and then they can move on to appreciate the various biological applications of laser tweezers. These applications span a large number of areas.

This chapter also provides a detailed discussion of the design of a laser tweezer. Readers interested in building their own laser tweezers will find this section quite useful. Also presented are variations on laser tweezer techniques, such as using them as optical stretchers or as tools for the simultaneous, multiple trapping of many biological species.

Laser scissors function on the principle of photoablation, which is discussed in Chapter 6. They can be used to punch a hole in a cell membrane to allow the injection of a drug or genetic material. A more popular application is microdisscetion, used to excise a single cell or pure cell population from a tissue specimen. The two approaches used to capture the dissected portion—laser pressure catapulting (LPC) and laser capture microdissection (LCM)—are discussed in this chapter.

A vast, diverse number of applications in fundamental research cover the understanding of single biomolecule (DNA and protein) structure, function, and interactions (e.g., protein–protein interactions). Examples of these applications are provided. Selected practical applications of laser tweezers and scissors to genomics, proteomics, plant biology, and reproductive medicine are presented.

The chapter also includes a discussion of future directions of research and applications. A list of some commercial sources of these laser microtools is also given.

Introduction to Biophotonics, by Paras N. Prasad.
ISBN: 0-471-28770-9

A highly recommended book for further reading is by Greulich (1999). Some websites on laser micromanipulation are:

Harvard University:	http://www.lightforce.harvard.edu/tweezer
UMEA, Sweden:	http://www.phys.umu.se/laser/
Beckman Laser Institute:	www.bli.uci.edu

14.1 NEW BIOLOGICAL TOOLS FOR MICROMANIPULATION BY LIGHT

Imagine the following:

- Grasping a biological cell, noninvasively, by using a focused laser beam, holding it in place, and moving or stretching it.
- Holding an egg by one laser beam and bringing a sperm trapped in another beam for fertilizing the egg.
- Drilling a microhole in a cell to inject molecules for manipulation and control of intracellular activities, without permanently damaging the plasma membrane which then seals within a fraction of a second.
- Performing microsurgery using a laser as a scalpel to cut a portion of the intracellular structure (an organelle or a DNA segment) and to modify the structure and function of a cell without affecting the cell viability.

It may have appeared as science fiction at one time. These types of micromanipulation are now routinely conducted in many laboratories around the world. Laser tweezers and laser scissors are two different micromanipulation tools that can be independently used or used in combination. As discussed in Chapter 2, light as photon particles carries momentum, a property that is utilized for the operation of laser tweezers. Light is also a carrier of energy as energy packets called *quanta*; it is the energy aspect of light that is used in laser scissor action. When an electromagnetic wave interacts with a small particle, it can exchange energy and momentum with the particle. The force exerted on the particle is equal to the momentum transferred per unit time. The force exerted by an optical tweezer is on the order of piconewtons (10^{-12} N). It is too weak to manipulate macroscopic-sized objects but is large enough to manipulate individual particles on a cellular level. The force is distributed over most of the area of the particle, so fragile and delicate objects can be manipulated without causing damage. Near-infrared laser beams can manipulate cells without damaging them, because cells do not absorb at these wavelengths.

Laser tweezers, also known as *optical tweezers* or *optical traps*, utilize the principle of trapping small particles/biological cells in the waist of a focused continuous-wave (CW) laser beam based on the gradient force derived from

a change in the momentum of light. The wavelength of the laser beam (usually 1064 nm) is chosen from the region of optical transparency of the particle so that no exchange of energy (absorption of light) occurs. The particle/cell thus trapped in the optical beam can be moved around by moving the laser focal spot, hence the name optical tweezers as if the particle is picked up by a tweezer to manipulate its position. The development of optical tweezers is credited to the pioneering work of Ashkin et al. (Ashkin and Dziedzic, 1985; Ashkin et al., 1986). The first report of trapping and manipulating a living biological cell in a laser beam without harming it was also by Ashkin et al. (1987). Since then, optical tweezers have come a long way to be recognized as an important tool for biological micromanipulation. Current applications range from basic studies of biophysics and biochemistry at the single cell level to medical applications in blood cell analysis and *in vitro* fertilization (Greulich, 1999; Berns, 1998; Mehta et al., 1998; Strick et al., 2001). There is even a suggestion of the use of optical tweezers in early detection of cancer based on changes in viscoelastic properties of cells. Laser tweezers have provided much of the impetus for the study of single molecule biophysics, an area of considerable current interest.

A laser tweezer offers a number of benefits over a traditional mechanical micromanipulator. Some of these are:

- It does not involve any mechanical contact that can introduce a risk of contamination.
- It is a noninvasive method of manipulation that does not cause any damage to living cells. Thus a living cell can be optically trapped and manipulated without affecting its survivability.
- Subcellular organelles in a living cell can be manipulated (repositioned) without opening the membrane as required by other biological methods.
- Optical trapping has provided unprecedented capabilities to measure different forces in biology, down to the level of piconewtons, thus permitting one to correlate these forces with specific biological functions.
- Ability to use laser tweezers to mechanically unzip DNA can provide important applications to genomics by speeding up the sequencing of nucleotides.

An extension of laser tweezers or optical tweezers is an optical stretcher that utilizes placing of an object (e.g., biological cell) between two opposed, nonfocused laser beams to produce stretching of the cell along the axis of the beam (Guck et al., 2001).

The history of laser scissors is even older. Berns and Round (1970) showed that lasers can be used to microdissect cells. Other terms used for laser scissors are laser microscapel, laser microbeam, and laser microdissection unit. Laser scissors are convenient microtools for performing microscopic surgery on tissue specimen, cells, and molecules.

In contrast to laser tweezers with focused IR continuous wave laser beam, laser scissors utilize short pulses of high irradiance at a wavelength at which a tissue specimen or its cellular component absorbs. Typically, it can be a nanosecond, subnanosecond, or even a femtosecond solid-state laser with the output in a visible or UV spectral range. Often it is a UV laser source such as a nitrogen laser (337 nm). The absorbed energy produces the scissor action by photoablation to conduct delicate microsurgery on a tissue, a cell, or its organelle. In a more general sense, the laser scissor action has been used to include a broad range of action from pricking a hole in a cell, to ablating a portion of it. As explained in Chapter 6, the photoablation process involves a photochemical process of breaking of chemical bonds without generating heat. However, photodisruption involving a mechanical disruption produced by microplasma-induced shockwaves has also been used for microdissection. Therefore, the use of the term *laser scissors*, which literally implies a cutting action, may be confusing. This is why alternate terms such as laser microbeams, laser microdissection, and optoinjection are also used to represent different laser functions.

Laser scissors provide precision and selectivity compared to an invasive mechanical device. Compared to a regular scalpel, laser scissors provide the ability to act on dimensions as small as 0.25 μm in diameter. It can, therefore, be used to produce changes in a chromosome by cutting a portion of it while it is still deep within a living cell.

Laser scissors can be used to cut a micron-size hole in a membrane that seals within a fraction of a second. Exogenous species can be inserted in a cell through these holes without permanently damaging the membranes. This feature provides a convenient approach for genetic manipulation of cells.

The term *laser microdissection* is often used to refer to excise a portion of a tissue specimen to obtain clean (uncontaminated) tissue samples, or to separate tumor cells from precancerous neoplasm and supporting stroma.

Another term is *optoinjection*, which refers to a process in which a pulse laser beam pricks a hole in a cell to load it with exogenous molecules, without any visible damage to the cell and with high survival rates (Tsukakoshi et al., 1984; Krasieva et al., 1998; Rink et al., 1996). Yet another term used is *optoporation*, which implies pore production through optical means (Berns, 1998; Krasieva et al., 1998; Lee et al., 1997; Soughayer et al., 2000). This process refers to laser-induced transient permeabilization of a membrane to again allow entrance of exogenous species into selected cells.

The research groups of Gruelich and Berns pioneered applications involving the combined powers of laser tweezers and laser scissors. They utilized an Nd:YAG laser tweezer to bring two human myeloma cells close together, then used a pulsed UV nitrogen laser scissor to cut the adjoining membranes to fuse the two cells (Gruerlich, 1999; Berns, 1998). The two cells merged into a single hybrid cell containing the genomes of both. Greulich's group utilized a UV laser scissor and an optical tweezer combination for manipulation of pieces of chromosomes for gene isolation (Seeger et al., 1991).

Over the past decade the usage of laser tweezers and laser microbeams (scissors) have expanded considerably at a rapid pace. It is expected that new developments in laser micromanipulation as well as new applications will continue to emerge. The range of applications, already demonstrated, covers both fundamental research at single cell and subcellular level and in biotechnology. Some of these are listed here (*source*: www.PALM-microlaser.com). Selected examples of applications will be presented in somewhat more detail in a later section.

AREAS OF APPLICATIONS OF LASER MICROMANIPULATION

Biology	
Microsurgery	Basic studies in cell biology
Cell fusion	Plant breeding
Force measurements	Food engineering
Cell sorting	Patch-clamp studies
Bacteria separation	Cloning
Genetics	
Fetal cell capture	Cytogenetic analysis
Chromosome preparation, microinjection	Genetic engineering
Prenatal diagnosis	Gene therapy
Neuroscience	
Single-neuron capture	Analysis of neuronal disorders
Microinjection	Study of nerve stimulation processes
Expanding artificial dendrites	Patch-clamp studies
Microsurgery	
Molecular Medicine	
Single-cell capture	Diagnosis of diseases
Microinjection	Gene therapy
Cell fusion	Immunology
Analysis of cancer	
Pharmacy	
Preparation of pure samples	DNA array
Trapping of cells	Chip technology
Laser microinjection	Gene therapy
Capture of living cells	Genetic engineering
Drug screening and design	Tumor banking

Biotechnology	
Separation of single cells, yeast, bacteria	Genetic engineering
Gene analysis	Cloning studies
Reproductive Medicine	
Laser zona drilling	*In vitro* fertilization
Sperm trapping	Embryo hatching
Polarbody extrusion	Preimplantation diagnosis
Blastomere biopsy	Embryo development
Blastomere fusion	
Forensic	
Selective isolation of suspect material	Fingerprinting Analysis
DNA isolation	Genetic database of suspects

14.2 PRINCIPLE OF LASER TWEEZER ACTION

Laser tweezers utilize trapping of small particles in a focused laser beam. The principle of optical trapping of small particles by laser is based on the forces arising from a change in the momentum of the light itself. With lasers one can make these forces large enough to accelerate, decelerate, deflect, guide, and even trap small particles. This is a direct consequence of the high intensities and high-intensity gradients achievable with continuous-wave (CW) coherent light beams. Laser trapping and manipulation techniques apply to particles as diverse as atoms, large molecules, and small dielectric spheres in size ranges of tens of nanometers, and they even apply to biological particles such as viruses, single living cells, and organelles within cells.

A satisfactory explanation for large-particle trapping can be obtained using geometrical optics. For this, let us place a spherical particle with refractive index greater than of surrounding medium in the laser beam with a wavelength λ, much smaller than the radius r of the particle. Additionally, the laser beam is focused to a spot with a diameter comparable to the wavelength.

Optical trapping is based on the fact that photons have linear momentum. It changes when a photon changes direction, as when crossing an interface between two media of different refractive index. Since the total momentum is conserved, the difference between the initial and the final momentum of a photon is transferred to the particle and is responsible for appearance of the force acting on the sphere. The force equation is

$$F = \frac{\Delta P}{\Delta t} \tag{14.1}$$

where F is the force, ΔP is the change in momentum, and Δt is the change in time.

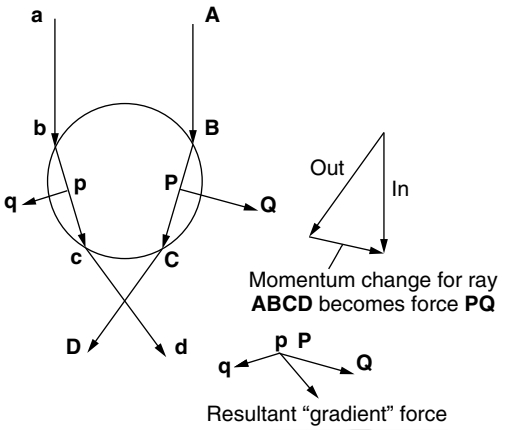

Figure 14.1. Force diagram for a sphere in a beam containing a power density gradient represented by two rays of unequal power.

The description provided here is based on an article by Ulanowski (2001). In Figure 14.1, a photon traveling along the path **abcd** imparts momentum to a spherical particle at **b** and **c**. The result is shown as a vector **pq**. Similarly, two photons in the path **ABCD** of a stronger ray transfer momentum at **B** and **C**, the resultant being the twice-longer vector **PQ**. From this we see that the sphere is forced toward the region of more intense light in the beam axis. This force is called the *gradient force*. Figure 14.2 shows the balance of force vectors for a particle positioned below the focal point of a focused beam directed downwards. We can see that the resultant force draws the particle upwards along the direction of propagation of the beam. This is the unexpected result, since a particle can be pulled toward the source of light against radiation pressure.

There is another force (not shown in Figure 14.1) present in such an experimental setup. This force appears since some light is reflected off the particle and is often called *scattering force*. This force is one reason why trapping is carried out on particles suspended not in air but in a liquid such as water so that the difference in the refractive indices between the particle and the immediate surround is less, thus resulting in smaller reflectivity. In this case the particle undergoes a smaller scattering force.

There is also the gravity force acting on the particle which, together with the scattering force, makes the sphere reside in equilibrium, a little beyond the focal point.

According to the size of the particle compared to the wavelength, different models of trapping interactions are used. For the $r \ll \lambda$ the Rayleigh model, for $r < \lambda$ the electromagnetic (EM) model, and for $r > \lambda$ the Ray-Optics (RO) model can be used. Since most biological cells are in the RO regime, the RO

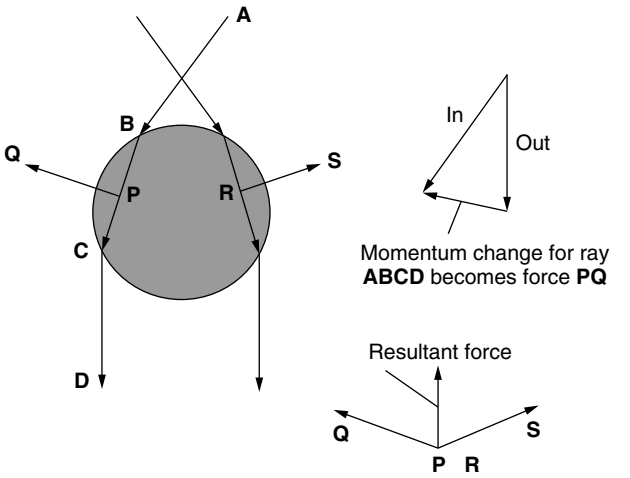

Figure 14.2. Balance of force vectors for a spherical particle positioned below the focal point of a focused beam. The resultant force pulls the particle upward.

model can be used to describe trapping of cells. In this case the forces F_{scatter} and F_{gradient} are given by (Ashkin, 1992)

$$F = \frac{\Delta P}{\Delta t} = F_{\text{scatter}} = n_m P Q_s / c$$
$$= n_m P / c \left\{ 1 + R\cos 2\Theta - \frac{T^2[\cos(2\Theta - 2\varepsilon) + R\cos 2\Theta]}{1 + R^2 + 2R\cos 2\varepsilon} \right\} \tag{14.2}$$

and

$$F = \frac{\Delta P}{\Delta t} = F_{\text{gradient}} = n_m P Q_g / c$$
$$= n_m P / c \left\{ R\sin 2\Theta - \frac{T^2[\sin(2\Theta - 2\varepsilon) + R\sin 2\Theta]}{1 + R^2 + 2R\cos 2\varepsilon} \right\} \tag{14.3}$$

where n_m, P, c, θ, and ε are refractive index of the medium, power, speed of light, angle of incidence, and angle of refraction, respectively. R and T are the Fresnel coefficients of reflection and refraction. Q is a dimensionless angle-dependent factor, different for both the scattering and the gradient forces.

Using the above formula and the Fresnel coefficients, the scattering and the gradient forces can be calculated for a beam coming perpendicular at a spherical polystyrene particle in water. They are: $F_{\text{scattering}} = 2.45 \times 10^{-12}$ N and $F_{\text{gradient}} = 3.18 \times 10^{-12}$ N. For this calculation it has been assumed that $\lambda = 1.064\,\mu$m, $P = 100$ mW, and the diameter r of the polystyrene sphere is $5\,\mu$m. Such a size is typical of many living cells. The force diagram for polystyrene

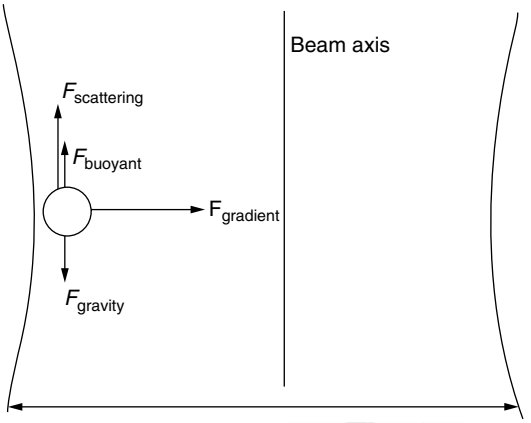

Figure 14.3. The force diagram for polystyrene particle. The arrow lengths are proportional to the magnitude of the forces.

particle is shown in Figure 14.3. The restoring gradient force is larger than the scattering force, and the gravitational force is balanced by the buoyancy force. Therefore, the polystyrene particle of radius 5 μm can be trapped by the laser beam.

14.3 DESIGN OF A LASER TWEEZER

Block (1998) provides a good description of the construction of optical tweezers. The single-beam optical trapping system used at our Institute for Lasers, Photonics, and Biophotonics is described here as an example of a basic design for a laser tweezer. The optic layout of this laser trap unit is shown in Figure 14.4. The main components of an optical trap used in this design are as follows:

1. *A Microscope (Either Upright or Inverted) with a High-Numerical-Aperture Objective Lens.* Some typical specifications are: NA 1.25–1.40, magnification 40–100×. The displayed configuration uses a Nikon TE200 inverted microscope with a 1.30-NA oil-immersion, 100× magnification objective lens. The high-numerical aperture allows for a tight focusing of the laser beam to generate a high-intensity gradient (and, thus, a large gradient force). Furthermore, for studies utilizing fluorescence imaging, this microscope can be either an epi-fluorescence or a confocal microscope system. To combine the optical trap and the epifluorescence mode in our case, the Nikon TE200 microscope design is modified by inserting mirror M_3, which permits us to introduce the trapping laser beam. The beam is introduced as a parallel beam by the use of lens L_2, reflected by mirrors M_3 and M_4 and, subsequently, focused on the specimen by lens L_3. The mirrors M_3 and M_4 were designed to transmit and to

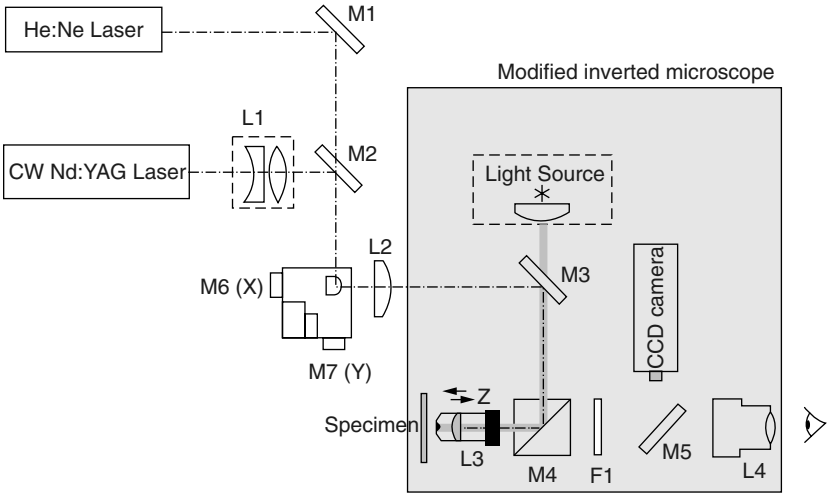

Figure 14.4. Single-beam optical trapping system.

reflect respectively the light from a mercury lamp (labeled as light source in Figure 14.4). The mercury lamp source can be used either for reflection mode (viewing) or for luminescence mode (imaging). All microscope functions are computer-controlled. The option of a CCD-TV camera port permits video viewing of microscope images and monitoring of optical trapping.

2. *A CW Laser Source that Provides Wavelengths at Which Biological Samples Are Transparent.* Based on the optical transparencies of cells; the near-IR region covering 700–1300 nm are used for optical trapping. CW lasers with powers in the range of several hundred milliwatts to several watts are utilized which can provide intensities in the range of 10^6–10^8 W/cm^2. Suitable choices are Nd : YAG at 1064 nm, Nd : YLF at 1047 nm, Ti : sapphire in the range 695–1100 nm, and various diode lasers, generally in the range 800–900 nm (where they are available with highest power). In order to produce the steepest gradient force, a laser beam with the TEM_{00} mode is used. Such high-quality mode structures can easily be achieved from diode bar-pumped Nd : YAG lasers and Nd : YAG laser second-harmonic-pumped Ti : sapphire lasers. However, in the case of diode lasers, which produce elliptical beams, special optical beam correction is required to make the beam circular. A diode-pumped continuous-wave Nd : YAG TEM_{00} laser was used for optical trapping in the configuration represented by Figure 14.4. A coincident red beam from a low-power He : Ne laser was used as the aiming beam.

3. *Beam Steering to Realize a Movable Trap*. A number of methods used to realize a movable trap for manipulation of trapped particles are shown in Figure 14.5. Figure 14.5 also shows the scheme of Figure 14.4, which uses an *x*–*y* galvano-head and a microscope objective lens on a movable mount. In

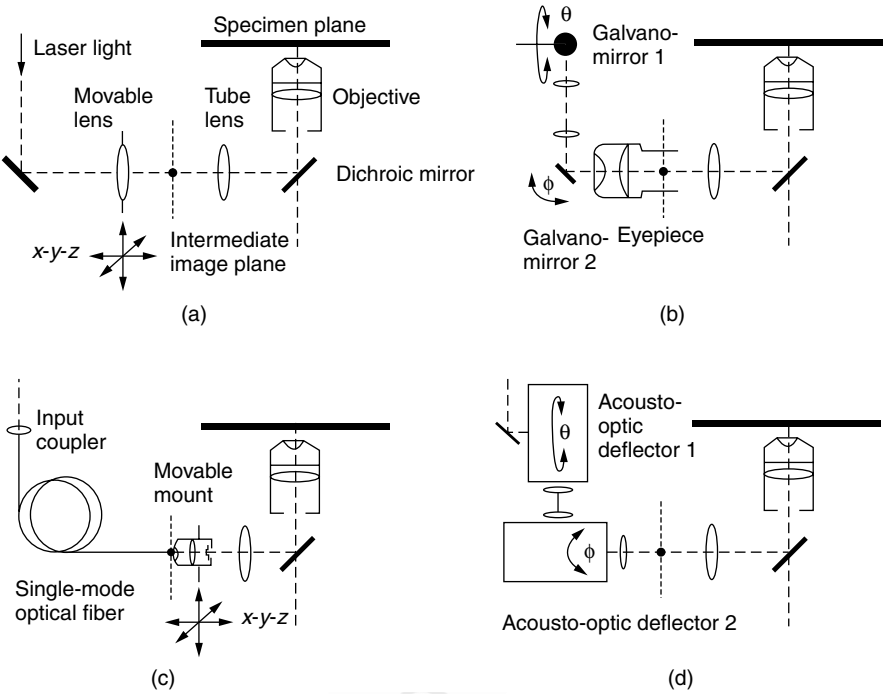

Figure 14.5. Four ways to scan the position of the laser spot in an optical trap in the object plane: (a) Translating the movable lens; (b) rotating galvanometer mirrors; (c) translating the end of an optical fiber; and (d) deflecting the beam with an acousto-optic deflector (AOD). (Reproduced with permission from Svoboda and Block, 1994.)

Figure 14.4, the in-plane x–y position of the laser focus (hence the optical trap) is controlled by the use of deflection from a set of galvano-mirrors M_6 and M_7. The z position of the laser focus is adjusted by piezoelectric displacement of microscope objective lens L_3.

Certain experiments require simultaneous use of more than one optical trap (Fallman and Axner, 1997). For two traps, a single laser beam can be split in two, utilizing a polarizing beam splitter (Misawa et al., 1992). A more flexible scheme to produce multiple optical traps utilizes time-sharing of the same beam among a set of positions in the specimen plane. This feature is achieved by rapidly scanning the beam focus position back and forth among the desired set of positions (Visscher et al., 1993). When the light is scanned sufficiently quickly, such as by using galvo-deflection or an acousto-optic deflector, the optical traps formed behave similar to what would be formed under steady illumination.

Figure 14.6 shows the schematics of a dual-beam trap produced by splitting a laser beam (Visscher et al., 1996). This design utilizes a polarized beam from

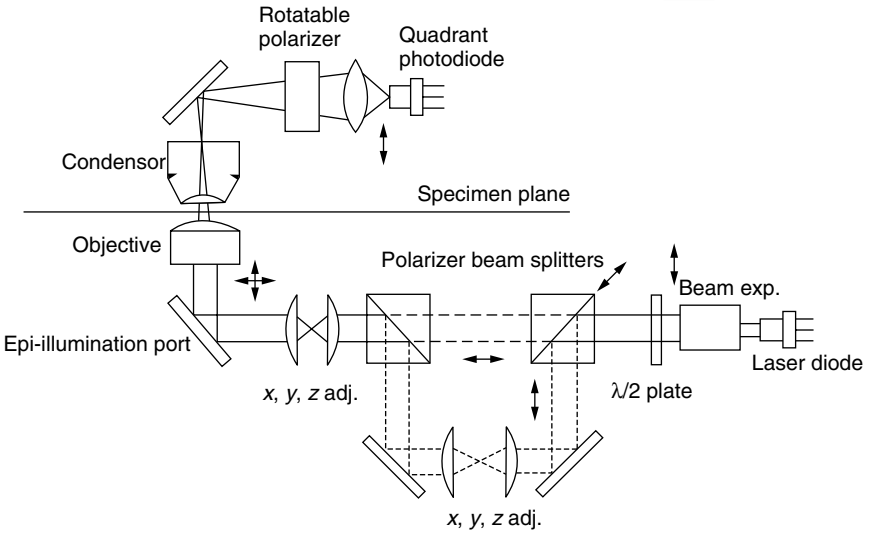

Figure 14.6. Schematic of a dual-beam optical trap.

an 830-nm diode laser which is expanded three times and passed through a half waveplate. The rotation of this half wave plate is used to alter the power split between the two orthogonally polarized trapping beams that are produced by a polarizing beam-splitting cube. The beam reflected by the first polarizing cube then passes through a pair of lenses forming a 1:1 telescope in which the first lens is movable in the x, y, and z directions. This allows adjustment of the position of the optical trap, formed by this beam, with respect to the trap formed by the horizontally polarized beam which is transmitted by the first cube. Both beams are subsequently combined together using a second polarizing beam-splitting cube and then pass through a second 1:1 telescope consisting of a movable first lens which is used to jointly adjust the position of both optical traps.

Another design of a dual-beam optical trap is shown in Figure 14.7. The unit utilizes the optical trap shown in Figure 14.4. Here thin-film polarizers P_1–P_3 are used to split and to combine the beam of a Nd:YAG laser. One beam, with selected s polarization, is reflected from thin-film polarizers P_1, P_2, and P_3. Subsequently, it is focused on the specimen by a combination of optical components L_2, M_7, M_9, and L_3. This beam forms a fixed x–y plane optical trap because it dos not incorporate the galvano-mirrors M_{10} and M_{11}. Another beam, with selected p polarization, passes through polarizer P_1 and is reflected from mirror M_4 as well as from galvano-mirrors M_{10} and M_{11}. Then it passes through polarizer P_3 and is subsequently focused onto the specimen, where it forms an optical trap movable in the x–y plane. Both trapping beams can be controlled in the z direction. This dual-trap arrangement permits the flexibil-

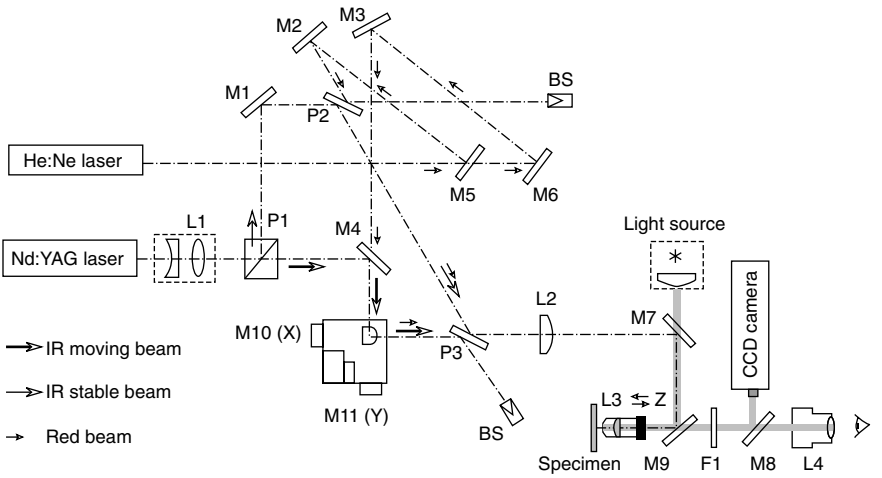

Figure 14.7. Optic layout of dual beam optical trap.

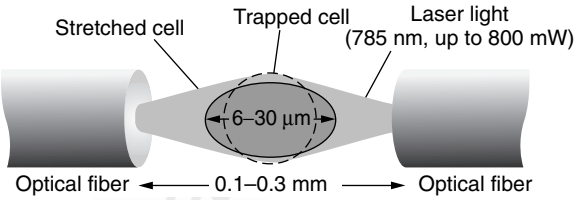

Figure 14.8. Schematic of the stretching of a cell trapped in an optical stretcher. (Reproduced with permission from Guck et al., 2001.)

ities of keeping one biological object in a fixed trap and manipulating another object using the movable trap.

A variation of optical trapping is the concept of an *optical stretcher* for micromanipulation of cells (Guck et al., 2001). An optical stretcher utilizes trapping of a cell between two opposed, nonfocused laser beams. The schematic is shown in Figure 14.8. This arrangement utilizes counterpropagating nonfocused laser beams and generates additive surface forces that produce stretching of a trapped cell along the axis of the beams. This optical stretcher can be used to measure viscoelastic properties of cells, with sensitivity sufficient to distinguish between different individual cytoskeletal phenotypes. Guck et al. (2001) used this type of optical stretcher to deform human erythrocytes and mouse fibroblasts.

The bottom picture shows single cells and the homogeneous cell area from the membrane-mounted tissue.

14.6.2 Laser Capture Microdissection (LCM)

This approach was developed at the National Institutes of Health (Emmert-Buck et al., 1996; Best and Emmert-Buck, 2001) and is now commercialized as a product, PixCell II by Arcturus Engineering of Mountain View, California (Roberts, 2002). LCM is performed using a tissue section of 5- to 10-μm thickness that has been preserved either by freezing or by fixation followed by paraffin embedding. A 100-μm-thick ethylene vinyl acetate (EVA) film, which has been impregnated with an infrared absorbing dye, is attached to a rigid 6-mm laser cap. It is lowered exactly opposite to the area of tissue section to be harvested and acts as a transfer film. This schematic is shown in Figure 14.16. A pulsed near-infrared beam, usually of duration less than 5 msec, is directed through the cap. The membrane absorbs the energy from the IR beam due to the presence of the IR absorbing dye, raising its temperature momentarily to 90°C and consequently melting it when it adheres to the underlying tissue. By adjusting the laser beam spot size (for example, between 7.5, 15, and 30 μm), one can select a single cell or a group of cells with one laser pulse. Furthermore, by moving the laser spot around on the tissue with the help of a joystick, one can select multiple sites of the same tissue with the same cap. When the cell selection is finished, the cap can be lifted off the tissue pulling off the cells attached to the membrane. The EVA films can be dissolved under the effect of lysis buffer to release the cells. Since the duration of the pulse is short, there is minimal transfer of thermal energy to the tissue, thereby reducing the danger of damage to the tissue and extracted cells.

14.7 SELECTED EXAMPLES OF APPLICATIONS

14.7.1 Manipulation of Single DNA Molecules

The use of laser tweezers has provided valuable insight into determining the forces that keep the DNA molecule in a randomly coiled configuration. Laser tweezers have also been successfully used to study DNA–protein interaction, gene transcription, and enzymatic degradation of DNA, all at the single molecule level. In these studies, one or both ends of a fluorescently labeled DNA chain is attached to a polystyrene microbead. For this purpose, one couples a biotin group at the end of the DNA chain which is then conjugated to commercially available avidin-coated polystyrene microbeads (typically of diameter ~1 μm). In the case where only one end of DNA is attached to the microbead, one can apply a viscous drag force using a hydrodynamic flow to stretch the DNA chain. If both ends of DNA have a microbead attached, one can use laser tweezers at each end to pull the DNA simultaneously from both

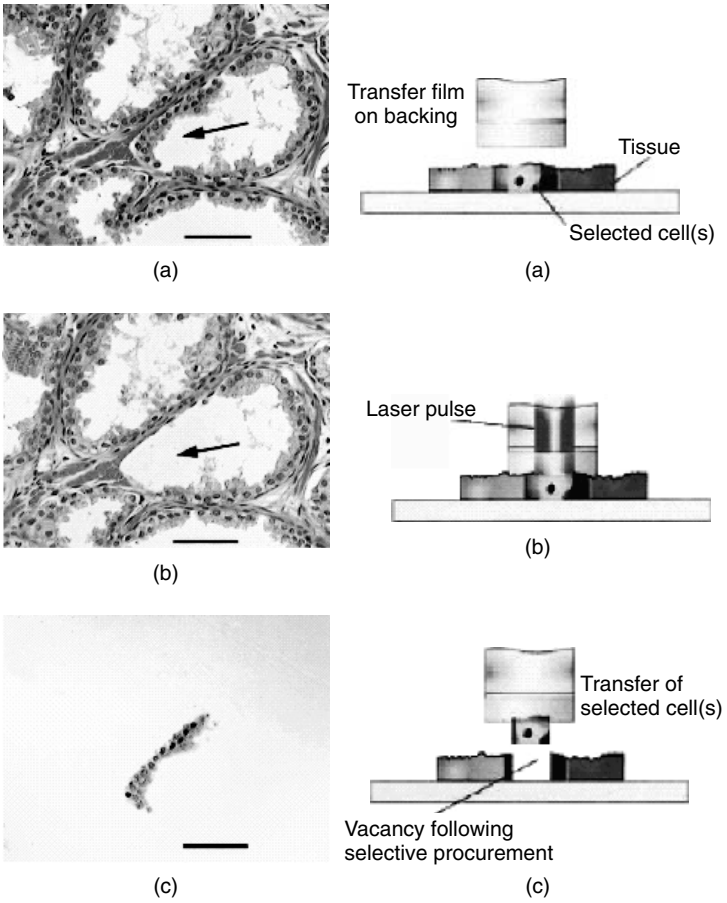

Figure 14.16. Schematic of laser capture microdissection (LCM). *Right*: Fixed, stained, microscopic tissue cells of interest are selected using LCM and transferred onto the area of the polymer surface activated by the laser beam. *Left*: Visualization of LCM-procured cells. Target region designated by arrow. (a) Before LCM. (b) Tissue after LCM; two shots. Note the vacancy left by the removal of selected cells. The bar represents 30 μm. (c) Epithelial cells transferred to cap surface. (Reproduced with permission from Simone at al., 2000.)

sides. The group of Chu (Perkins et al., 1995) used a laser tweezer to hold one end of a DNA molecule and used the hydrodynamic force from a flowing liquid to extend a 64.5-μm-long DNA molecule with increasing fluid velocity of flows. Figure 14.17 shows this extension at a number of flow velocities. These are fluorescence microscopic images.

The experimental result appeared to fit the force field elongation theory of Schurr and Smith (1990). The unstressed end (not attached to the bead) exhibits a disorder (k) expected at the free end. As the hydrodynamic force

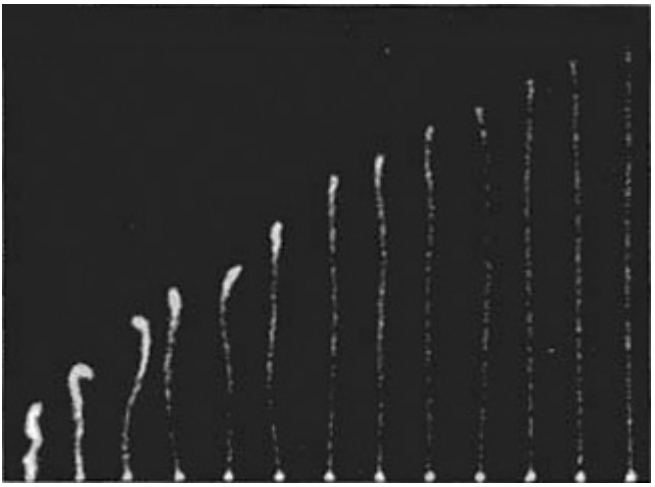

Figure 14.17. Use of hydrodynamic flow to stretch a DNA molecule held at the end coupled to a microbead using a laser tweezer. (Reproduced with permission from Perkins et al., 1995.)

field is increased, it increases elongation and decreases the size of k. When the flow is stopped, the DNA molecule relaxes to revert back to its condensed, more globular form, allowing one to follow this motion by time-resolved fluorescence microscopy (Perkins et al., 1994). Their result reveals that the relaxation is exponential, with a relaxation time dependent on the total length of the molecule.

Optical tweezers can be used as picotensiometers where displacement from the trapping center with nanometer accuracy can be calibrated in terms of force with piconewton accuracy for force measurements. This method has been used to measure forces involved in DNA stretching (Smith et al., 1996; Wang et al., 1997). Meiners and Quake (2000) have extended the range of force measurements to femtonewton sensitivity, using a dual optical-trap-based force spectroscopic technique. They have used this method to study thermal fluctuations of a single DNA molecule.

An important application of laser tweezers has been in the study of biochemistry at the single-molecule limit. An example is in the study of the force exerted by a single molecule of the enzyme, RNA polymerase, during gene transcription (Yin et al., 1995). For this investigation, the RNA polymerase was attached to the surface of a cover glass of a flow cell. In the presence of DNA and other components essential for *in vitro* transcription, the RNA polymerase catches a DNA molecule, pulls it through its active site, and synthesizes RNA with a sequence, complementary to that of the segment of DNA just read. The RNA falls off the polymerase as the transcription is completed when the DNA signals a stop codon. One end of the DNA molecule is coupled

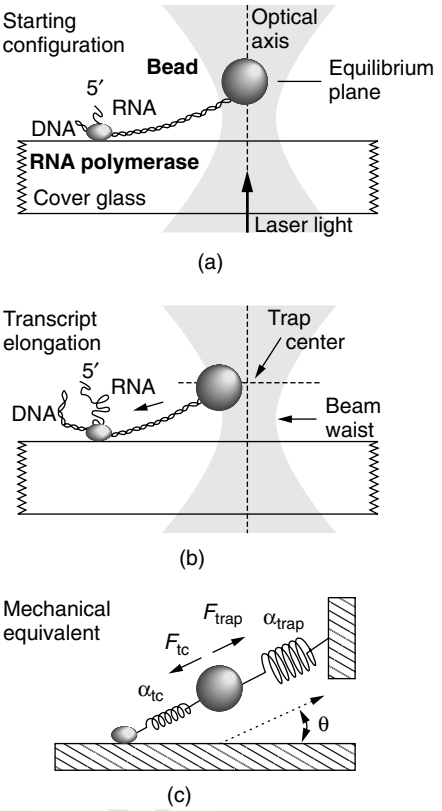

Figure 14.18. Schematic of the optical trapping experiment for the RNA polymerase produced gene transcription. (Reproduced with permission from Yin et al., 1995.)

to a polystyrene microbead (diameter ~0.5 μm). In the experiment by Yin et al. (1995), when the RNA polymerase catches the DNA molecule during transcription, the bead is pulled. The microbead is held in the center of the beam of an optical tweezer (using relatively low laser power of 25 mW at 1.06 μm) which has been calibrated to measure forces. Thus the pull exerted by RNA polymerase on the DNA from the optical trapping region can be measured by the displacement of the microbead and the stiffness of the optical trap. The position of the bead was measured with resolution in nanometers using interferometry. A schematic of this process is shown in Figure 14.18. The result of this measurement showed that *E. coli* RNA polymerase can provide a force up to 14 pN. Compared to it, the maximum force exerted by a typical motor protein is only 6 pN. The obvious conclusion is that enzyme transcription through DNA is a more stringent process than proteins driving a muscle. This optical trapping study of gene transcription also yielded information on the efficiency with which chemical energy is converted into mechanical energy.

The mechanical energy produced during the insertion of each nucleotide into the nascent RNA is simply force multiplied by the distance, the latter being 0.34 nm. The chemical energy released by one reaction step is known from other measurements. The measurement of mechanical energy using the optical trapping study yielded a chemical-to-mechanical energy conversion rate of up to 42%, which compares quite favorably with that of up to 60% for motor proteins. Another interesting observation was that DNA does not run smoothly through the active sites of the enzyme, exhibiting a frictional behavior.

Baumann et al. (2000) used optical tweezers to study the elastic response of single plasmid and lambda phase DNA molecules in the presence of various concentrations of trivalent cations which provoke DNA condensation in the bulk. They investigated the dependence of a single-molecule condensation on ionic conditions and the extent of stretching. The facilitation of DNA condensation in the presence of a certain multivalent ion is thought to arise from attractive lateral interactions between the adjacent helices produced upon binding a critical amount of multivalent cations. Their finding that intramolecular condensation occurs only when the DNA molecule is sufficiently relaxed to form intramolecular loops provides support for a lateral interaction rather than an elastic buckling mechanism.

Hirano et al. (2002) reported another approach for manipulation of single-coiled DNA molecules. This method does not require any prior chemical modification of DNA (biotin–avidin coupling) to attach it to a microbead. In their approach, a bead cluster is formed using laser trapping that can then be manipulated to capture a single native DNA molecule. The bead cluster was then used to drag the end of a single DNA molecule.

14.7.2 Molecular Motors

Molecular motors are special enzymes that catalyze a chemical reaction such as hydrolysis of ATP, capture the free energy released by the reaction, and use it to perform a mechanical work such as muscle contraction. An example of such a motor enzyme is kinesin, which binds to subcellular organelles such as chromosomes and transports them through the cytoplasm by pulling them along microtubules. Optical trapping has been used to study the process of movement of kinosin from site to site on the microtubule lattice (Visscher et al., 1999). In this work, they used a molecular force clamp method utilizing a feedback-driven optical trap, capable of maintaining a constant load (force) on a single kinosin molecule. The kinosin molecule is composed of two heavy chains, each consisting of a force generating a globular domain head (hence double-headed), a long α-helical coil, and a tail portion that is a small globular C-terminal domain. Microtubules are cylinders comprised of parallel protofilaments that are linear polymers of α- and β-tubulin dimers.

Visscher et al. (1999) used a kinosin-coated silica bead (diameter ~0.5 μm) that trapped in a focused 1064-nm beam from a Nd:YVO_4 laser using the objective lens of an inverted microscope. The trap position within the speci-

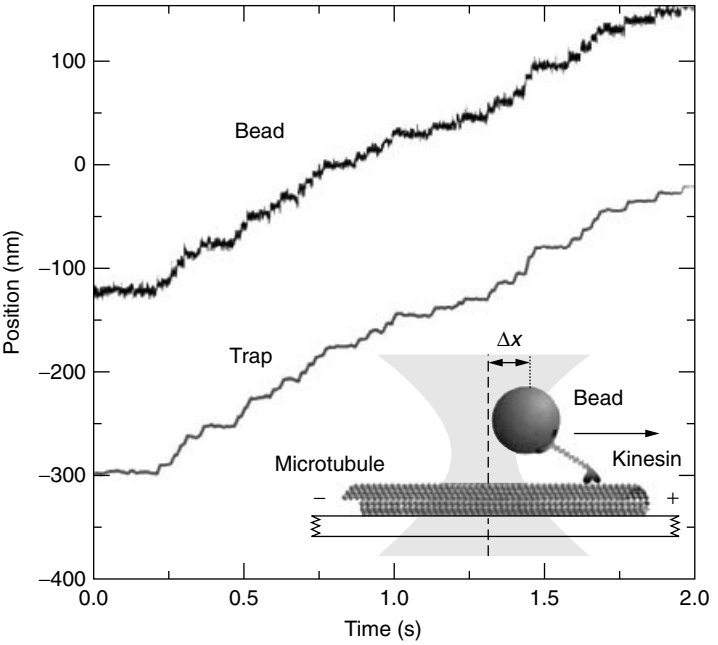

Figure 14.19. Schematic of the experimental geometry, which includes position measurement for kinosin-driven bead movement and the corresponding optical trap displacements at an ATP concentration of 2 mM. (Reproduced with permission from Visscher et al., 1999.)

men plane was specified using two digitally computer-controlled acousto-optic deflectors. The bead positions were determined by focusing a low-power He–Ne laser beam onto the optically trapped kinosin-coated silica bead and measuring the deflected light in a plane conjugate to the back focal plane of the microscope condenser, using a quadrant photodiode arrangement (Visscher et al., 1996).

The schematics of the experimental geometry and the results are shown in Figure 14.19. The results indicate kinosin stepping tightly coupled to ATP hydrolysis over a wide range of forces. A single hydrolysis produces kinosin movement along a microtubule with an 8-nm step that coincides with the α, β-tubulin dimer repeat unit. The progressive movement of kinosin was explained by a hand-over-hand mechanism in which one head remains bound to the microtubule, while the other detaches and moves forward.

14.7.3 Protein–Protein Interactions

Optical trapping has also been used to characterize individual intermolecular bonds in proteins and thus investigate protein–protein interactions (Stout, 2001). Figure 14.20 shows the schematics of the experimental arrangement

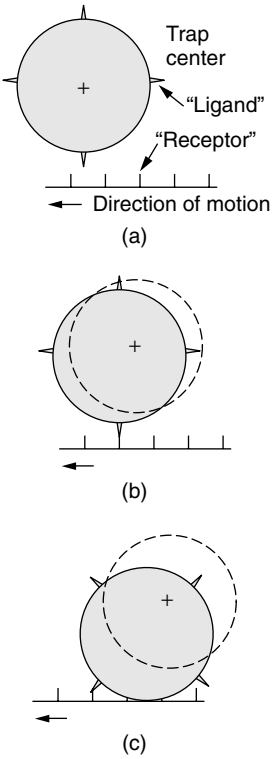

Figure 14.20. (a) A microbead coated with a small number of IgG held a short distance above a moving substrate coated with receptor molecules; (b) the binding of the bead with the surface produces bead movement away from the optical trap center with the same velocity as the moving surface; (c) as the bead moves away from the trap center it pivots, making contact with the surface which produces an additional normal force. (Reproduced with permission from Stout, 2001.)

used by Stout. A polystyrene microsphere, coated with immunoglobulin G (IgG), is held in a force-calibrated optical trap. A flat substrate is sparsely coated with a receptor protein (staphylococcus protein A [SpA]). The IgG-coated microsphere, as a probe, is held in contact with the substrate using a stationary optical trap to allow for protein–substrate binding. Then the substrate is scanned. This movement produces a lateral displacement of the microbead due to the pull exerted on the surface coated protein, now bound to the substrate, through protein–protein interaction. This displacement of the probe is monitored through an x–y position detector. The bound probe (microsphere) moves with the substrate until the force applied by the optical trap overcomes the bond between the probe and the substrate. The rupture of this bond allows the optical trap to pull back the probe to the trap center. This geometry of utilizing interaction between the probe and the surface

allows a fivefold enhancement of the force applied by the optical trap due to the substrate acting as a lever. Thus, this optical trapping method allows a laser tweezer to be used to access rupture forces up to 200 pN, as opposed to the regular upper limit of 50 pN. The experiment yielded a median single-bond rupture force from 25 to 44 pN for IgG from four mammalian species, which is in general agreement with predictions based on free energies of association obtained from solution equilibrium constants.

14.7.4 Laser Microbeams for Genomics and Proteomics

Laser microtools can be of significant value for genomics and proteomics in molecular profiling of cancer and other genetically based diseases. As discussed above, laser microbeam microdissection (LMM) coupled with laser pressure catapulting (LPC) or laser capture microdissection (LCM) allows isolation of a single cell, as well as a small number of specific cells from an archival tissue in a noncontact mode.Thus laser microdissection can be used to extract specific cell populations such as normal cells, precancerous cells, and invasive cancer cells. The purity of these specific cells then can permit one to compare and identify tumor suppressor genes as well as novel transcriptions and proteins that change in neoplastic cells (Best and Emmert-Buck, 2001; Maitra et al., 2002).

Genetic changes manifested in multistep progression of cancer can involve gain of mutation in dominant oncogenes, or loss of a function by delection, mutation, or methylation in repressive tumor suppressor genes. This loss of supressor gene function in a tumor is called *loss of heterozygosity* (LOH) (Gillespie et al., 2000). Laser microdissection has made a significant contribution to applications of LOH analysis to cancer studies because virtually pure populations of tumor cells or preneoplastic foci necessary for LOH analysis can be isolated without contamination even by a few unwanted cells. The LOH analysis has proved valuable in the mapping of tumor suppressor genes, localization of putative chromosomal "hot spots," and the study of sequential genetic changes in preneoplastic lesions. LCM in conjunction with fluorescence *in situ* hybridization (FISH, discussed in Chapter 8) demonstrated LOH on chromosome sp21 in prostate cancer. Loss of the dematin gene was observed, leading to dysregulation of cell shape (Lutchman et al., 2000). Study of preneoplastic lesions has revealed that genetic alterations in cancers actually starts in histologically "benign" tissue.

LCM used in conjunction with polymerase chain reaction (PCR) such as reverse transcriptase-PCR (RTPCR) provides an opportunity to study only a few hundred cells. The advantage is that even microscopic preneoplastic lesions can be studied. In addition to LOH analysis, other studies have been performed using laser microdissection. They include X-chromosome inactivation analysis to access clonality, single-strand conformation polymorphism (SSCP) analysis for mutations in critical genes, comparative genomic hybridization (CGH), and the analysis of promoter hypermethylation.

Microdissected cells have been used to obtain differential gene expression which is a useful parameter to differentiate tumors from their normal cells. Methods to study gene expression include expressed sequence tag (EST) sequencing, differential display, subtractive hybridization, serial analysis of gene expression (SAGE), and cDNA microarray technique. The microarray technology has been discussed in Chapter 10. LCM has been used to generate cDNA libraries for a number of cancers. These data can be accessed at the NIH Cancer Genomic Anatomy Project (CGAP) website (http://cgap.nci.nih.gov/). The cDNA libraries can be used for identification of novel genes that are either overexpressed or underexpressed in the multistage pathogenesis of cancer, which can eventually lead to genetic profiling of individual patient samples to customize treatment on an individual basis.

Laser microdissection for molecular profiling of global protein patterns will play an important role because it is crucial for protein analysis and differentiation to obtain pure populations of tumor cells and their preneoplastic lesions. Identification of proteins dysregulated during cancer progression will be valuable in formulating treatment and developing intervention strategies.

LCM has been used in conjunction with high-resolution two-dimensional polyacrylamide gel electrophoresis (2-D PAGE), a technique used to analyze populations of proteins in different cell types to resolve more than 600 proteins or their isoforms and identify dysregulated products in cancer cells. Sequencing of the altered peptide products unique to the tumor population can be used to identify novel tumor-specific alterations. For example, proteomic analysis of microdissected prostate cancers and benign prostatic epithelium revealed six differentially expressed proteins (Ornstein et al., 2000). Microdissected specimen of colon cancer has shown increased levels of gelatinase and cathepsin B, both implicated in cancer invasion and metastasis (Emmert-Buck et al., 1994).

To conclude, it can be envisioned that the use of a rapid microdissection technique, together with biomolecule amplification protocols, can provide more sensitive detection and database integration which can become a standard practice for cancer diagnostics. The molecular profile information on DNA, RNA, and protein alterations can lead to diseases management as well as to design of optimal, low-risk, and patient-tailored treatment.

14.7.5 Laser Manipulation in Plant Biology

Laser manipulation may hold promise for plant breeding. Many plant cells are transparent, thereby permitting the use of laser microtools to access subcellular structures such as mitochondria and chloroplasts. Furthermore, plant cells such as rapeseed cells contain subcellular organelles which are mobile and thus can be pulled through the cell with a high spatial control (Greulich, 1999).

Laser microinjection of genes is particularly suited for plant cells. The reason is that for plant cells, such as rapeseed cells, glass capillaries used for

microinjection are either too thick and damage the cell or are sufficiently fine but too fragile to penetrate the rigid plant cells. Laser microinjection has been utilized to inject foreign genes into individual cells in suspension. Bacterial glucuronidase (GUS) reporter gene is a promoter of cauliflower mosaic virus. It has been shown that when GUS DNA is laser-microinjected into some selected cells of the embryo, an appearance of a blue color indicates successful expression of GUS. Thus the gene becomes active in its new host cell.

Photosynthesis in plants take place in the organelle's chloroplasts, which are 5–10 μm in diameter (see Chapter 6). Foreign genes have succesfully been injected into the chloroplast by opening a hole in the membrane using a single laser shot, which would close one second after the laser treatment (Weber et al., 1990).

14.7.6 Laser Micromanipulation for Reproduction Medicine

Laser micromanipulation may one day provide benefits in assisting *in vitro* fertilization at fertility clinics. Human infertility can often be overcome by simply performing sperm–egg fusion externally in a reaction tube. The problem of infertility is often mechanical, derived from the surrounding of a mammalian egg by a highly viscous envelope called *zona pellucida*, which can not be penetrated by the sperm cells. By laser zona drilling (LZD) to produce a micron-sized hole in the zona pellucida, this viscous barrier can be opened for a sperm to penetrate and fertilize the egg. This process can occur in the normal course, or it can be assisted by using a laser tweezer to trap the sperm and lead it to the site of the hole in the egg produced by LZD. The procedure thus is completely noncontact and has been used by a number of researchers (Clement-Sengewald et al., 1997). Figure 14.21 schematically represents this process. This procedure has been shown to produce significant improvement in fertilization when the sperm density is low.

Using 50- to 60 4 μJ pulses (337 nm) of 3-nsec duration, a straight channel could be driven into the zona pellucida. For this operation, the egg cell did not have to be fixed by a micromanipulator; that is, it was essentially a suspension procedure. An insemination was judged to be successful when the egg cell divided. Table 14.1 summarizes the major results of this study. At high sperm density, there is no significant difference between conventional *in vitro* fertilization and the laser zona drilling technique. However, at low sperm density, the effect is significant, with a 58% success rate while using the laser-supported technique as compared to 33% for the nonlaser technique. The very low success rate (18%) of subzonal insemination is not explained.

Another occasional cause of infertility is the low mobility of a sperm cell. Again, the use of laser tweezers can overcome the problem of low mobility. A major concern in this case is whether there is any adverse effect on the velocity of a sperm after optically trapping it for some time. The results of a study (König et al., 1995) show that it is dependent on the wavelength as well as on the trapping period. The 760-nm light appeared to cause much higher damage

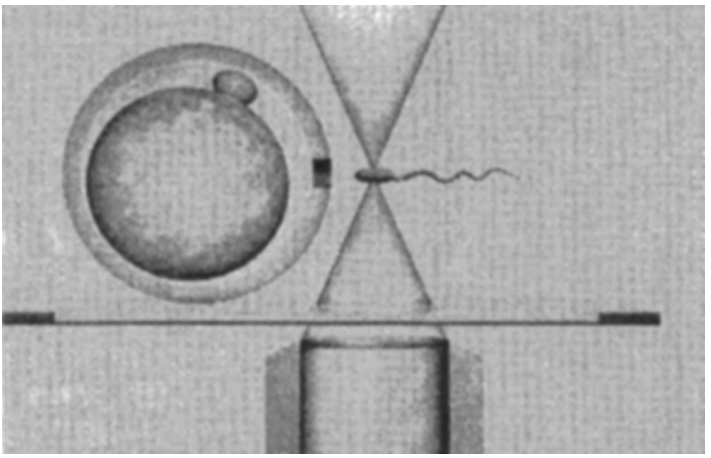

Figure 14.21. Schematic of laser zona drilling combined with laser tweezer capture of the sperm cell to bring it to the hole in the zona. (Reproduced with permission from Clement-Sengewald et al., 1997.)

TABLE 14.1. Success Rates in Mouse Gametes Using Different Types of Fertilization Techniques

Technique	Sperm Density	Cells Treated	Successfully Fertilized	Percent Success
Nonlaser IVF	Normal	85	45	53
Laser zona drilling	Normal	124	74	60
Nonlaser IVF	Low	63	21	33
Laser zona drilling	Low	40	23	58
Subzonal insemination	Low	22	4	18

than that produced by the 800-nm light. The longer trapping duration appears to increase the sperm cell damage.

14.8 FUTURE DIRECTIONS

Laser micromanipulation will continue to receive worldwide attention from fundamental researchers trying to understand single-molecule biochemistry and biofunction. It is receiving increasing attention for genomics and proteomics. Clinical interest in utilizing microdissection for cancer diagnostics and combined use of microdissection and optical trapping for genetic manipulation and fertilization may also see a growth. This field may also receive an impetus from laser developments, making them more efficient, user-friendly,

reliable, cost-effective, and compact. Some of the current activities defining future directions are outlined here.

14.8.1 Technology of Laser Manipulation

New physical/chemical processes for more efficient laser trapping and more effective laser microdissection are likely to emerge. Agayan et al. (2002) have shown theoretically that by selecting an optical trapping wavelength near the resonance absorption, a 50-fold enhancement in trapping forces can be realized together with increased specificity.

A new approach to produce a stable optical trap is by Zemanek et al. (1999), who demonstrated optical trapping of nanoparticles and microparticles by a Gaussian standing wave. The standing wave was produced under a microscope objective as a result of interference between an incoming laser beam and a beam reflected from a microscope slide coated with reflective dielectric layers. Three-dimensional trapping of nanoparticles (100-nm polystyrene spheres) and one or several vertically aligned micro-objects (5-μm polystyrene spheres, yeast cells) was achieved by use of even highly aberrated beams or objectives with low numerical apertures.

The modern combination of optical multitrap, microdissection, and far-field confocal (Raman) microscope function in one unit could open up new possibilities for biophotonics.

For laser microdissection, the use of ultra-short femtosecond laser pulses is being investigated. The femtosecond pulses can enhance the probability of multiphonon processes as very intense fields but at very low average powers. These pulses could produce a much precise microdissection with considerably reduced collateral damage. As the prices for femtosecond laser systems come down, they would become affordable to be widely utilized for laser microdissection.

14.8.2 Single Molecule Biofunctions

The use of optical trapping to manipulate single molecules and perform biophysical and biochemical studies will remain an area of growing interest. As sensitive spectroscopic detection techniques are emerging for single-molecule analysis, their application will lead to the study of DNA–protein and protein–protein interactions as well as to the monitoring of subcellular functions at a single biomolecule level. Xie et al. (2002) used a low-powered diode laser at 785 nm to both trap and excite Raman spectra of single biological cells in solution. As mentioned above, a combination of the advantages of NIR Raman spectroscopy and optical tweezers for the characterization of single biological cells with a low-power semiconductor laser provides high sensitivity, making it possible to obtain Raman spectra from single living red blood cells (RBCs) or yeast cells placed in an optical trap.

TABLE 14.2. Commercial Sources of Laser Microtools

Company	Product	Function	Website
Arturus Engineering, Hercules, CA, USA	Pixcell II	Laser capture microdissection	www.arcture.com
Bio-Rad Laboratories, Hercules, CA, USA	Clonis	IR laser microdissection	www.microscopy.bio-rad.com
Cell Robotics, Albuquerque, NM, USA	Pro 300	Laser microdissection using UV laser	www.cellrobotics.com
	Laser Tweezers©	IR or NIR for trappingr	
Leica Microsystems, Wetzler, Germany	Leica AS LMD	Laser microdissection using UV beam	www.leica-microsysystems.com
P.A.L.M. Microlaser Technologies, Bernried, Germany	PALM Microbeam	Laser pressure catapulting	www.palm-microlaser.com
	PALM Microtweezers	IR or NIR for trapping	
MMI AG Heidelberg, Germany	μ-CUT	Laser microdissection using UV laser	www.mmi-micro.com
ARRYX, Inc., Chicago, IL, USA	ARRYX BioRyx™ 200 SYSTEM	Holographic optical trapping (multiple beam) system to independently manipulate large numbers of microobjects simultaneously	www.arryx.com

14.9 COMMERCIALLY AVAILABLE LASER MICROTOOLS

A number of companies sell laser microdissection systems and laser tweezers. Table 14.2 lists some of them. However, it should be kept in mind that they exist at the time of writing of this book. It is very likely that this list can change significantly quickly, making Table 14.2 rather obsolete. Nonetheless, it may serve as a starting point for those looking to acquire a commercial system. It also is a demonstration that the activities and interests in the use of laser microtools are sufficiently advanced to recognize business opportunities in commercializing them.

HIGHLIGHTS OF THE CHAPTER

- Laser tweezers are microtools used to trap biological cells or micron-sized particles in the focused laser beam spot of a continuous-wave laser.

CHAPTER 15

Nanotechnology for Biophotonics: Bionanophotonics

Some describe us as living in an era of Nanomania where there is a general euphoria about nanoscale science and technology. The fusion of nanoscience and nanotechnology with biomedical research has also broadly impacted biotechnology. The subject covered in this chapter, however, is more focused, dealing with the interface between biomedical science and technology and nanophotonics, hence the term *bionanophotonics*. Nanophotonics is an emerging field that describes nanoscale optical science and technology.

Specifically, this chapter discusses the use of nanoparticles for optical bioimaging, optical diagnostics, and light-guided and activated therapy. Section 15.2 describes the power of nanochemistry to produce the various nanoparticles and tailor their structures and functions for biomedical applications. Specific examples provided for bioimaging are two classes of nanoparticle emitters. One consists of semiconductor nanoparticles, also known as *quantum dots*, whose luminescence wavelength is dependent on the size and the nature of the semiconductors. These nanoparticle emitters can be judiciously selected to cover the visible to the IR spectral range. They can also be surface-functionalized to be dispersable in biological media as well as to be conjugated to various biomolecules.

Another class of nanoparticle emitters for bioimaging consists of up-converting nanophores comprised of rare-earth ions in a crystalline host. They convert near-IR and IR radiation, which can penetrate deeper into a tissue, to emissions in the visible range by utilizing the process of sequential multiphoton absorption. In addition to bioimaging, the up-converting nanophores can also allow treatment of deeper tumors by using them for multiphoton photodynamic therapy described in Chapter 12. The use of metallic nanoparticles and nanorods for biosensing is described in Section 15.5.

The next two sections, 15.6 and 15.7, describe the use of a nanoparticles platform, for intracellular diagnostic and targeted drug delivery. Section 15.6 discusses the PEBBLE nanosensors approach for monitoring intercellular

Introduction to Biophotonics, by Paras N. Prasad.
ISBN: 0-471-28770-9

activities. Section 15.7 discusses the use of nanoclinics, which are thin silica shells (packaging various probes for diagnostics and agents for external activation) and are surface-functionalized with carrier groups to target specific biological sites such as cancer cells.

The chapter concludes with a discussion of future directions of research and development in bionanophotonics. For further reading, the following reviews are recommended:

Shen et al. (2000): A feature review article on nanophotonics

Murray et al. (2002): A review on synthesis and characterization of nanocrystals

15.1 THE INTERFACE OF BIOSCIENCE, NANOTECHNOLOGY, AND PHOTONICS

Imagine nanosubmarines navigating through our bloodstreams and destroying nasty viruses and bacteria. Imagine nanorobots hunting for cancer cells throughout our body, finding them, then reprogramming or destroying them. A subject of science fiction at one time has now been transformed into a future vision showing promise to materialize. The fusion of nanoscience and nanotechnology into biomedical research has brought in a true revolution that is broadly impacting biotechnology. New terms such as *nanobioscience*, *nanobiotechnology*, and *nanomedicine* have come into existence and gained wide acceptance.

Table 15.1 lists some nanotechnology frontiers in bioscience. The content of this chapter, however, is more focused on the applications of nanophotonics in biomedical science and technology. Nanophotonics is an emerging field that deals with optical interactions on a scale much smaller than the wavelength of light used (Shen et al., 2000). The three major areas of nanophotonics are shown in Table 15.2.

Nanoscale confinement of radiation is achieved in a near-field geometry. This allows one to break diffraction barriers and obtain optical resolution to less than 100 nm. Near-field microscopy, discussed in Chapter 7, is becoming a powerful biomedical research tool to probe structure and functions of submicron dimension biological species such as bacteria. Nanoscale confinement of matter is achieved by producing nanoparticles, nanomers, nanodomains, and nanocomposites. The nanosize manipulation of molecular architecture and morphology provides a powerful approach to control the electronic and optical properties of a material. An example is a semiconductor quantum dot, a nanoparticle whose electronic band gap and thus the emission wavelength are strongly dependent on its size. Nanoscale control of the local structure in a nanocomposite, consisting of many domains and separated only on the nanometer scale, provides an opportunity to manipulate excited-state dynamics and electronic energy transfer from one domain to another.

TABLE 15.1. Nanotechnology Frontiers in Bioscience

Biophysics	**Structural Biology**
Nanomechanics	Protein folding, design
Optical traps	"Rational" drug/ligand design
Flexible-probe methods	Novel and improved methods
Single-molecule methods	**Computational Biology**
FRET	Protein folding, design
New labels	"Rational" drug/ligand design
New reporters	Bioinformatic design, regulation
New imaging, microscopies	**Biotronics—Biomolecules on Chips**
Scanned-probe	DNA and protein nanotrays
Combinations	Sensors, detectors, diagnostics
	Labs-on-a-chip
Biochemistry	**Biofabrication**
Single-molecule enzymology	Nanoparticle delivery systems
Single-molecule kinetics	Biomaterials, tissue engineering
Single-molecule sequencing	Implants, prosthetics

Source: Steven Block from http:/grants.nih.gov/grants/becon/becon_symposia.htm.

TABLE 15.2. Three Major Areas of Nanophotonics

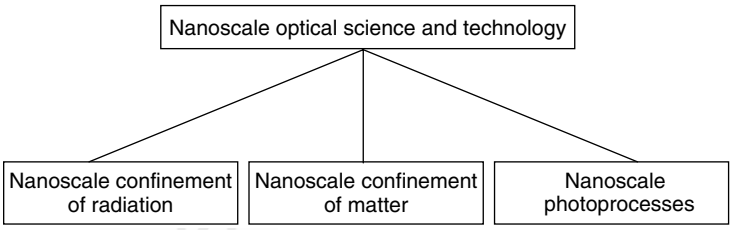

Such nanostructured materials can provide significant benefits in FRET imaging and in flow cytometry, the topics already covered in Chapters 8 and 11, respectively.

Nanoscale photoprocesses such as photopolymerization provide opportunities for nanoscale photofabrication. Near-field lithography can be used to produce nanoarrays for DNA or protein detection. The advantage over the microarray technology, discussed in Chapter 10, is the higher density of arrays obtainable using near-field lithography, thus allowing one to use small quantities of samples. This is a tremendous benefit for protein analysis in the case when the amount of protein produced is very minute and, as discussed in Chapter 10, there is no equivalent of DNA PCR amplification for proteins to enhance the detection.

The applications of nanophotonics to biomedical research and biotechnology range from biosensing, to optical diagnostics, to light activated therapy. Nanoparticles provide a highly useful platform for intracellular optical diagnostics and targeted therapy. The area of usage of nanoparticles for drug delivery has seen considerable growth. This chapter presents some selected examples of nanotechnology and applications to biophotonics.

A great deal of information can be obtained from visiting various websites on the Internet. Some selected examples of these websites are:

- National Nanotechnology Initiative—http://www.nano.gov
- Engines of Creation—http://www.foresight.org/EOC
- Stanford Nanofabrication Facility—http://www-snf.stanford.edu
- Cornell Nanofabrication Facility—http://www.cnf.cornell.edu
- NIH conference on nanotechnology and biomedicine—http://www.masimax.com/becon/index.html
- University at Buffalo Biophotonics and Nanophotonics Program—http://www.biophotonics.buffalo.edu

15.2 NANOCHEMISTRY

Nanochemistry is an active new field that deals with confinement of chemical reactions on nanometer length scale to produce chemical products that are of nanometer dimensions (generally in the range of 1–100 nm) (Murray et al., 2000). The challenge is to be able to use chemical approaches that would reproducibly provide a precise control of composition, size, and shape of the nano-objects formed. These nanomaterials exhibit new electronic, optical, and other physical properties that depend on their composition, size, and shape. Nanoscale chemistry also provides an opportunity to design and fabricate hierarchically built multilayer nanostructures to incorporate multifunctionality at nanoscale.

Nanochemistry offers the following capabilities:

- Preparation of nanoparticles of a wide range of metals, semiconductors, glasses, and polymers
- Preparation of multilayer, core-shell-type nanoparticles
- Nanopatterning of surfaces, surface functionalization, and self-assembling of structures on this patterned template
- Organization of nanoparticles into periodic or aperiodic functional structures
- *In situ* fabrication of nanoscale probes, sensors, and devices

Photobleaching and thermally induced degradation are the problems commonly encountered in laser dyes that reduce the operational lifetime of a dye. By encapsulation of a dye within the silica shell, where silica is chemically and thermally inert, photobleaching and photodegradation of the dye can also be minimized. This advantage has been demonstrated in our work. Another advantage of using silica is the introduction of a specific surface functionality, which can be obtained by modifying the surface hydroxyls on the silica surface with amines, thiols, carboxyls, and methacrylate. This modification can facilitate the incorporation of these nanoparticles into nonpolar solvents, glasses, and polymeric matrixes.

Competitive reaction chemistry (CRC) has also been utilized to prepare various sulfide and selenide nanocrystals (e.g., CdS, CdSe) (Herron et al., 1990). In the initiation phase of the synthesis, a solution containing cadmium ions, generated from cadmium acetate, is introduced into a solution containing S^{2-} and RS^{-} (RS^{-} represents an organic thiol anion) in the form of sodium sulfide and *p*-thiocresol, respectively, to create small nanocrystals of CdS. Once they are formed, a propagation step of nanocrystal growth competes with the growth terminating reaction of the thiolate with the surface of the nanocrystal. It has also been shown that although being covalently bonded to the surface of CdS nanocrystals, the thiocresol species are dislocated by additional sulfide ions, allowing for further growth of the cluster. However, once a sulfide ion has been incorporated into a given cluster, it cannot be replaced by a thiolate ion. Through this process the nanocrystals are allowed to grow until the supply of S^{2-} has been exhausted.

The above examples of nanocrystal formation are, clearly, examples of the "bottom-up" approach—that is, building naonobjects from smaller objects (molecules). On the other hand, examples of a "top-down" approach may be found in two-photon-induced photochemistry. Using near-field propagation of a femtosecond pulse laser beam at 800 nm (pulse with very high peak power to induce efficient two-photon excitation), Shen et al. (2000) successfully achieved two-photon induced photochemistry to produce structures of the dimension of 70 nm. The high spatial localization using two-photon excitation reduces the diameter of photofabrications to 70 nm, whereas single-photon excitation leads to 120-nm-size photopolymerized structures. Conventional photolithographic structures are much larger than this.

15.3 SEMICONDUCTOR QUANTUM DOTS FOR BIOIMAGING

Quantum dots (also frequently abbreviated as Qdots) are nanocrystals of semiconductors that exhibit quantum confinement effects, once their dimensions get smaller than a characteristic length, called the *Bohr's radius*. This Bohr's radius is a specific property of an individual semiconductor and can be equated with the electron–hole distance in an exciton that might be formed in the bulk semiconductor. For example, it is 2.5 nm for CdS. Below this length

scale the band gap (the gap between the electron occupied energy level, similar to HOMO, and the empty level, similar to LUMO, which are discussed in Chapter 2) is size-dependent. The physical picture can be visualized in terms of the simple concept of particle in a box, discussed in Chapter 2. As the length of the box (quantum confinement size of the particle) decreases, the band gap (the energy level separation) increases. In other words, as the particle size decreases below the Bohr's radius, the absorption, and, subsequently, the emission wavelengths of the nanoparticles shift to a shorter wavelength (toward UV). The quantum dots, therefore, offer themselves as fluorophores where the emission wavelength can be tuned by selecting appropriate-size nanocrystals (Bruchez et al., 1998; Chan and Nie, 1998). By appropriate selection of the materials (e.g., CdS, CdSe, etc.) and the size of their nanocrystals, a wide spectral range of emission can be covered for bioimaging. Also, a significantly broad range of emission covered by many sizes of nanocrystals of a given material can be excited at the same wavelength. The typical line widths are 20–30 nm, thus relatively narrow, which helps if one wants to use the quantum dots more effectively for multispectral imaging. Compared to organic fluorophores, the major advantages offered by quantum dots for bioimaging are:

- Quantum dot emissions are considerably narrower compared to organic fluorophores, which exhibit broad emissions. Thus, the complication in simultaneous quantitative multichannel detection posed by cross-talks between different detection channels, derived from spectral overlap, is significantly reduced.
- The lifetime of emission is longer (hundreds of nanoseconds) compared to that of organic fluorophores, thus allowing one to utilize time-gated detection to suppress autofluorescence, which has a considerably shorter lifetime.
- The quantum dots do not readily photobleach.
- They are not subject to microbial attack.

A major problem in the use of quantum dots for bioimaging is the reduced emission efficiency due to the high surface area of the nanocrystal. A number of groups as well as new start-up companies are addressing this issue.

Alivisatos and co-workers (Bruchez et al., 1998) used a core-shell structure in which a shell of another semiconductor (ZnS) with a larger band gap encapsulated the core of a narrower band-gap semiconductor (CdSe). This encapsulation produced confinement of the excitation to the core and eliminated the surface-induced nonradiative relaxation pathways to enhance the emission efficiency of the core quantum dot.

Figure 15.4 illustrates the different emission colors obtainable from the quantum dots of a number of materials of different sizes. It illustrates the spectral tunability as well as the narrow line width of luminescence obtainable from quantum dots.

Figure 15.4. (A) Size- and material-dependent emission spectra of several surfactant-coated semiconductor nanocrystals in a variety of sizes. The first five from right represent different sizes of CdSe nanocrystals with diameters of 2.1, 2.4, 3.1, 3.6, and 4.6 nm (from right to left). The next three from right is of InP nanocrystals with diameters of 3.0, 3.5, and 4.6 nm. The IR emitters are InAs nanocrystals with diameters of 2.8, 3.6, 4.6, and 6.0 nm. (B) A true-color image of a series of silica-coated core (CdSe)-shell (ZnS or CdS) nanocrystal probes in aqueous buffer, all illuminated simultaneously with a handheld ultraviolet lamp. (Reproduced with permission from Bruchez et al., 1998.)

To make the quantum dots water-dispersable, Alivisatos and co-workers (Bruchez et al., 1998) added a layer of silica onto the core-shell structure. The silica encapsulated core-shell of nanocrystals were soluble and stable in water or buffered solutions. They also exhibited a fair fluorescence quantum yield (up to 21%). Alivisatos' group demonstrated these nanocrystals for biological staining by fluorescently labeling 3T3 mouse fibroblast cells using two different-sized CdSe–CdS core-shell quantum dots encapsulated in a silica cell.

Nie's group (Chan and Nie, 1998) covalently bonded the quantum dots to biomolecules (such as proteins) for use in ultrasensitive biological detection. Their approach utilized coupling to mercaptoacetic acid through sulfur binding, which also solubilizes the quantum dots in an aqueous medium. Then the acid group is attached to a protein through an amide linkage (Chapter 3). The mercaptoacetic acid layer is also expected to reduce passive protein adsorption on the quantum dots.

A schematic of the ZnS-capped CdSe quantum dots covalently coupled to a protein by mercaptoacetic acid is shown in Figure 15.5. The work of Nie's group showed that the optical properties of the quantum dots did not change after conjugations and solubilization. They also reported that the Qdot emission was 100 times as stable as that of the common organic dye rhodamine 6G

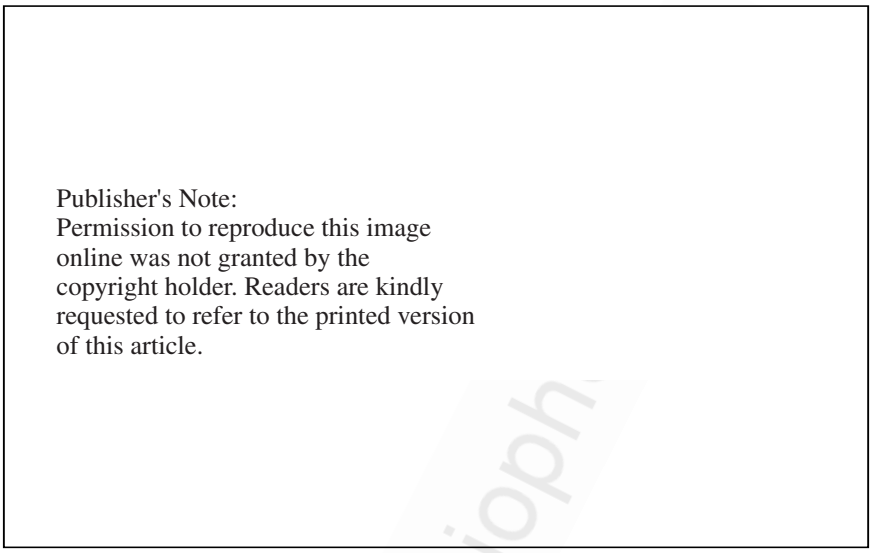

Figure 15.5. Schematics of a ZnS-capped CdSe quantum dot covalently coupled to a protein by mercaptoacetic acid. (Reproduced with permission from Chan and Nie, 1998.)

against photobleaching. They also demonstrated that the protein-attached Qdots were biocompatible *in vitro* as well as with living cells. For this they used transferrin-Qdot bioconjugates. Cultured HeLa cells were incubated with mercapto-Qdots as control and with transferrin-QD bioconjugates. Only the transferrin-Qdot bioconjugates were transported into the cell, as evidenced by emission from the stained cells, indicating receptor-mediated endocytosis. This result was taken as evidence that the attached transferrin molecules were still active and were recognized by the receptors on the cell surface.

Akerman et al. (2002) showed that ZnS-capped CdSe Qdots coated with a lung-targeting peptide accumulate in the lungs of mice after intravenous injection, whereas two other peptides directed Qdots to blood vessels or lymphatic vessels in tumors.

Bawendi and co-workers (Mattoussi et al., 2000) utilized a chimeric fusion protein to electrostatically bind it to the oppositely charged surface of capped colloidal core-shell-type CdSe–ZnS quantum dots to produce a bioconjugate. They suggested that this approach provided all the advantages of lipoic acid capped quantum dots (such as photochemical stability, size-dependent emission covering a broad spectral range, and aqueous compatibility) and at the same time yielded a facile electrostatic conjugation of a bioactive protein. In their approach, they capped the CdSe–ZnS nanocrystals, first with alkyl-COOH capping reagents. Adjusting the pH (basic) of an aqueous dispersion produces the quantum dots with negative charges (—COO^- groups). The use

of an engineered bifunctional recombinant protein consisting of a positive-charge domain leads to the formation of a bioconjugate by electrostatic attraction.

Thiol-terminated DNA segments (20–25 mers) have also been immobilized on mercaptopropionic acid capped CdSe–ZnS nanocrystals (Mitchell et al., 1999).

Nie's group (Han et al., 2001) has proposed the use of a porous microbead of polystyrene to capture quantum dots in specific quantities and in a wide range of colors and intensities. They demonstrated the application to DNA analysis by preparing microbeads of three different colors and attaching them to strips of genetic materials, each color corresponding with a specific DNA sequence. They then were used to probe complementary pieces of genetic material in a DNA mixture. The basics of this approach have already been discussed in Chapter 10.

15.4 METALLIC NANOPARTICLES AND NANORODS FOR BIOSENSING

Other types of materials used for biosensing are in the form of metal nanoparticles and nanorods. Storhoff and Mirkin (1999) linked a single-stranded DNA, modified with a thiol group at one terminal, to a gold nanoparticle ~15 nm in diameter via strong gold–sulfur interactions, discussed in Chapter 9. The 15-nm-diameter gold particles exhibit well-defined surface plasmon resonance, a topic also discussed in Chapter 9. Due to this resonance, the individual gold particles, even when attached to DNA, exhibit a burgundy-red color. When this DNA attached to the gold particle hybridizes with the complementary DNA in the test sample, the duplex formation leads to aggregation of the nanoparticles, shifting the surface plasmon resonance and, thus, the color to blue black. The reason for the shift is that the plasmon band is very sensitive to the interparticle distance as well as to the aggregate size.

15.5 UP-CONVERTING NANOPHORES

Another group of nanoparticles useful for bioimaging as well as for light activation of therapy is that of rare-earth-ion-doped oxide nanoparticles (Holm et al., 2002). The rare-earth ions are well known to produce IR to visible up-conversion by a number of mechanisms as shown in Figure 15.6. These up-conversion processes in rare-earth ions, like the two-photon absorption in organics, discussed in Chapter 5 and in Chapters 7 and 8 (two-photon bioimaging), are quadratically dependent on the excitation intensity. Thus, they provide better spatial resolution. They produce background-free (practically no autofluorescence) detection, because the excitation source is in the near-IR (generally 974-nm laser diodes). An advantage offered by these nanopar-

The two-photon dye is able to absorb one photon (with a wavelength of 400 nm) or two photons (with a wavelength of 800 nm) by direct two-photon absorption. The selective interaction and internalization of these nanoclinics with cells was visualized using two-photon laser scanning microscopy, allowing for real-time observation of the uptake of nanoclinics (Bergey et al., 2003). Two different types of particles were used in this study: LH–RH-positive (surface-coupled) and LH–RH-negative (spacer arm only). A suspension of nanoclinics was added to adherent (KB) oral epithelial carcinoma cells (LH–RH receptor positive), and uptake was observed using laser scanning microscopy. The time-dependent uptake of the LH–RH-positive nanoclinics by LH–RH receptor bearing cells was identified. A similar accumulation was not observed in LH–RH-negative nanoclinics studies or LH–RH-positive nanoclinics incubated with receptor-negative cells (UCI-107). Thus, targeting of LH–RH receptor-specific cancer cells and the specific effects of the nanoclinics were demonstrated.

The multifunctional nanoclinics containing the magnetic Fe_2O_3 nanoparticles also produced a new discovery for targeted therapy, a new effect that to our knowledge has not previously been reported, that being the selective lysing of cancer cells in a dc magnetic field using magnetic nanoclinics. Magnetic probes or particles have been investigated as a potential alternative treatment for cancer. Studies have demonstrated that the hyperthermic effect generated by magnetic particles coupled to a high-frequency ac magnetic field (requiring tremendous power) could be used as an alternate or adjuvant to current therapeutic approaches for cancer treatment. This hyperthermic effect (heat produced by the relaxation of magnetic energy of the magnetic material) was shown to effectively destroy tumor tissue surrounding the probes or particles. This approach resulted in reduction of the tumor size by hyperthermic effect when the particles were directly injected into the tissue and were exposed to an alternating magnetic field. However, no targeted therapy using a dc magnetic field has been reported previously, to our knowledge. Our work demonstrated the use of a dc magnetic field at a strength typically achievable by magnetic resonance imaging (MRI) systems for selectively destroying cancer cells. AFM studies together with a detailed study of magnetization behavior suggest mechanical disruption of the cellular structure by alignment of the nanoclinic.

15.8 FUTURE DIRECTIONS

The nanotechnology field is undergoing phenomenal growth. A primary impetus has been a major increase in funding for this field worldwide, such as the National Nanotechnology Initiative in the United States. It is beyond the limited scope of this book to cover all the new directions being pursued or to project all the prospects. Therefore, only some examples of future directions are presented here.

New Nanocrystals: Silicon Nanoparticles. The development of new semiconductor nanoparticles as efficient, inexpensive, stable, and tunable luminescent probes for biological staining and diagnostics is one future direction. In this regard, silicon and germanium nanoparticles appear to be promising.

Silicon nanoparticles had been produced by both top-down and bottom-up approaches. Nanoscale silicon has been extensively studied since 1990, when visible luminescence from porous silicon was first reported (Canham, 1990). Porous silicon contains a skeleton of crystalline nanostructures and is produced by electrochemically etching bulk silicon (which does not luminesce). Nanoparticles have been produced in a top-down fashion by many groups by using ultrasound to disperse porous silicon into various solvents, as first suggested by Heinrich et al. (1992). Bottom-up production methods have included both liquid phase methods (Holmes et al., 2001) and laser-induced decomposition of gas-phase species (Ehbrecht et al., 1995). At our Institute, such production methods are being used to generate silicon nanoparticles that emit at wavelengths throughout the visible spectrum.

An advantage of using silicon is that, through a controlled oxidation process, a thin shell of silica can be created on a silicon nanocrystal. This silica shell can then be functionalized to attach to DNA or to target specific biospecies as discussed earlier in this chapter.

Up-Converting Nanophores for Photodynamic Therapy. This subject, already discussed in Section 15.5, holds considerable promise for the treatment of tumors. The challenges are many. First, the up-conversion efficiency of these nanophores still needs to be improved. There appears to be an inverse relation between the efficiency of up-conversion and the size of nanocrystals. For more efficient up-conversion, one thus needs larger particles. However, larger particles cannot enter the cell through endocytosis. An appropriate balance of these two factors, together with the development of new host media for rare-earth ions to increase their up-conversion efficiency, has to be found.

Another area of investigation is real-time imaging and spectroscopy to determine the efficacy of photodynamic therapy. In the case of PDT drugs operating with singlet oxygen production, the singlet oxygen production can be monitored by its emission at ~900 nm.

In Vivo *Studies.* There are very few *in vivo* studies reported with the application of nanoparticles. This is an area that will attract a great deal of attention. The biocompatibility of the nanoparticles and nanoprobes, as well as their long-term toxicity, has to be studied.

Nanoarrays. The development of nanoarray technology for DNA and proteins is another future direction. Nanoarrays show promise for high-density analysis as well as for work with minute quantities of specimen. The challenges for biophotonics will be the use of optical methods to fabricate nanoarrays

and to be able to use fluorescence detection for DNA or protein binding at nanodomains. Near-field lithography and fluorescence detection using simultaneous control of multiple-fiber probes need to be developed. This offers an opportunity for engineering development. Vo-Dinh et al. (2001) have reported nanosensors and biochips for single-cell analysis.

BIONEMS. The most active areas emerging from the fusion of biomedical technology with nanotechnology are nanoelectromechanical systems (NEMS) and nanofluidics. The NEMS devices for biotechnology are also sometimes labeled as BIONEMS. The NEMS devices are nanoscale analogues of micro-electro-mechanical systems (MEMS). MEMS and NEMS act to convert mechanical energy to electrical or optical signals, and vice versa. The mechanical–optical signal interconversion devices are also sometimes called optical MEMS and optical NEMS. In the case of biotechnology, MEMS and NEMS have been used in a broader sense to include micro- and nanosize motors, actuators, and even sensors. Although most of the NEMS devices utilize the well-developed fabrication process for semiconductors, plastics MEMS and NEMS provide future opportunities because of the structural flexibility offered by plastics.

HIGHLIGHTS OF THE CHAPTER

- Bionanophotonics refers to research and applications that involve both biomedical sciences and nanophotonics.
- Nanophotonics involves light–matter interactions on nanoscale. It is another exciting frontier dealing with nanoscale optical science and technology.
- Nanoscale light–matter interactions can be manifested in two ways: (i) by confining the light on nanoscale with the use of a near-field geometry such as that in near-field microscopy, discussed in Chapters 7 and 8, and (ii) by confining the matter on nanoscale by using nanoparticles and nanodomains.
- Nanochemistry involves the use of confined chemical reactions to produce nanoscale materials, such as nanoparticles and nanostructures.
- Nanoparticles can be produced by nanochemistry, by confining a chemical reaction within a reverse micelle. It consists of molecules with hydrophilic heads and hydrophobic tails that are self-organized around a water droplet.
- Multilayered particles can be produced subsequent to nanoparticle formation by additional multiple steps invoking various appropriate chemistries.
- Competitive reaction chemistry (CRC) is another nanochemistry approach to produce nanoparticles; here, conditions are chosen for the

reactants to initially combine and form particles, but particle growth is limited by some competing reaction.

- Quantum dots are nanoparticles in which electrons and holes are confined in a semiconductor whose size is smaller than a characteristic length called the *Bohr radius*.
- The luminescence band width in a quantum dot is very narrow and the wavelength of the peak emission depends strongly on the size of the nanoparticle.
- Three advantages of typical quantum dots over dyes in bioimaging applications are that (1) they exhibit longer lifetimes (hence their emission can be separated from any autofluorescence), (2) they do not readily photobleach, and (3) they are insensitive to microbial attack.
- Because of their large surface-to-volume ratios, the optical and chemical properties of quantum dots depend strongly on their surface characteristics.
- Semiconductor nanoparticles capped with shells as silica or other semiconductors have been used for biological labeling and imaging.
- Metallic nanoparticles and nanorods have also been used in biosensing.
- Oxide nanoparticles doped with rare-earth ions exhibit emission that generally is long-lived phosphorescence. Hence they are sometimes referred to as *nanophores*.
- Up-converting nanophores are those that produce up-converted visible emission when excited by an IR radiation. The up-conversion involves sequential absorption of multiphotons; hence a continuous-wave IR laser can induce visible emission.
- These nanophores are useful for bioimaging and also show promise for use in multiphoton photodynamic therapy, to reach deep tumors.
- PEBBLE is an acronym for probe encapsulated by biologically localized embedding and refers to sensor molecules entrapped in an inert nanoparticle. These devices are advantageous because cells and the indicator dyes are protected from each other. Also, multiple sensing mechanisms can be combined onto one particle.
- Nanoclinics are surface functionalized silica nanoshells that encapsulate probes as well as externally activatable drugs or therapeutic agents. They have shown to be capable of targeting specific cancer cells.
- Magnetic nanoclinics appear to be capable of destroying cancer cells in the presence of a dc magnetic field.
- Future work in the field of bionanophotonics will include the development of new nanoparticles, the usage of up-converting nanophores in photodynamic therapy, the conduction of nanoparticle-based *in-vivo* studies, the development of nanoarrays that might replace modern-day microarrays; and the fabrication of plastic-based bionanoelectromechanical devices (BioNEMS).